

STANDARD MODEL NATURALNESS FROM
DARK VORTICES AND CODIMENSION-2
BRANEWORLDS

STANDARD MODEL NATURALNESS FROM DARK VORTICES
AND CODIMENSION-2 BRANEWORLDS

BY
ROSS DIENER, B.SC., M.SC.

A Thesis
Submitted to the School of Graduate Studies
in Partial Fulfilment of the Requirements
for the Degree
Doctor of Philosophy

McMaster University

© Copyright by Ross Diener, December 2015

DOCTOR OF PHILOSOPHY (2015)
(Physics & Astronomy)

McMaster University
Hamilton, Ontario, Canada

TITLE: Standard Model Naturalness from Dark Vortices and
Codimension-2 Braneworlds

AUTHOR: Ross Diener, B.Sc. (Ottawa), M.Sc. (Waterloo)

SUPERVISOR: Professor Cliff P. Burgess

NUMBER OF PAGES: xxi, 332

Abstract

There are numerous models of new physics that posit extra dimensions with characteristic length scale much larger than the inverse TeV scale. These so-called models of large extra dimensions can be used to confront the hierarchy problems that plague the standard models of particle physics and cosmology, as the usual arguments about hierarchy problems can be evaded if there are new physics scales and new dynamics in the extra dimensions. This thesis investigates a class of 6D models where the size of the two extra dimensions is exponentially sensitive to the value of a bulk zero mode, allowing a large hierarchy of scales to be generated if the zero mode is stabilized at a modestly large value. In general, scale invariance in the bulk forces the zero mode potential to have a runaway (or flat) form, so localized brane sources are added to the system which explicitly break the scale invariance and stabilize the zero mode. Brane physics can be chosen so that this stabilization naturally happens at values that give micron-sized extra dimensions, as desired in models of large extra dimensions that solve the electroweak hierarchy problem. These models are also interesting because they can predict a 4D curvature that is suppressed relative to the mass scale of the brane physics, thereby making progress on the cosmological constant problem by separating the 4D particle physics scale from the scale of the observed 4D vacuum energy. This suppression is technically natural because the curvature vanishes in the

limit that the branes are scale invariant, though this is also the limit in which the runaway potential for the zero mode reappears.

Nontrivial brane physics is an essential ingredient in these models, however there are a number of technical issues associated with branes of codimension-2 or higher, such as short-distance divergences that appear at the classical level and arise from taking the branes to be vanishingly thin. In all but the simplest cases, the back-reaction of higher codimension branes on bulk fields is also poorly understood. Any model that claims to make progress on the cosmological constant problem with brane physics must be able to address such issues, and this thesis presents a UV completion of branes in terms of Nielsen-Olesen vortices. The vortex construction allows these technical issues to be confronted precisely, thereby putting these models on a more solid footing and resolving ambiguous claims in the literature. With issues resolved, this thesis also constructs the correct 4D effective theory that describes the system when length scales of interest are much larger than the size of the extra dimensions.

An effective field theory approach is also adopted in this thesis to study the phenomenology of these models at higher energies. There are only three relevant operators between the brane containing the Standard Model and the stabilizing scalar of the bulk. One of these couplings is a Higgs portal that mixes the Higgs with the bulk scalar, and astrophysical bounds place strong constraints on its strength. Higgs-bulk couplings also generically improve the vacuum stability of the Standard Model, and give rise to an invisible Higgs decay width and missing energy signals that could be detected at the LHC or future colliders. Such a signal could be among the first hints that there are large extra dimensions, which are shown in this thesis to help solve the outstanding naturalness problems of modern particle physics and cosmology.

Acknowledgements

I would like to first thank my supervisor Cliff Burgess for his remarkable guidance and patience over the years. His insightful approach to physics and his supportive, advisory style have enriched my graduate studies. He has been an exceptional role model, and I credit him with whatever progress I made in growing from a calculating machine into a thinking physicist. Cliff, you have certainly lived up to your title: one helluva guy.

Thanks to my collaborators, from whom I also learned a great deal of physics. It was a pleasure to work with Leo van Nierop and Steve Godfrey during the course of my graduate studies, and special thanks goes to Matt Williams for his collaboration on the research that is presented in this thesis.

There is also another handful of physicists that deserve my thanks. To all of my friends at Perimeter Institute, thanks for keeping me company and sharing in the graduate experience. I am fortunate that so many students of physics are interesting and kind individuals. There are too many of you to thank individually. What a burden!

I must thank my family, who were endlessly supportive of my strange choice to study physics. Despite my best efforts to miss incoming calls, you made sure I was doing well and it is thanks to your assistance that I could pursue my interests freely.

Finally, Emily, you're last to be thanked but first in my heart! You are so special to me that you get a page to yourself.

Authorship

Chapters 3 through 6 of this thesis are original papers written by me, Ross Diener, and published in the Journal of High Energy Physics. The references are as follows:

- Chapter 3 - JHEP 1511 (2015) 049
- Chapter 4 - JHEP 1511 (2015) 054
- Chapter 5 - JHEP 1510 (2015) 177
- Chapter 6 - JHEP 1305 (2013) 078

All of these works were collaborative. My supervisor Cliff Burgess was a co-author on each of these articles, and Matthew Williams was a co-author on all but the last of these publications.

All previously published material has been reformatted to conform to the required thesis style. I grant an irrevocable, non-exclusive license to McMaster University and the National Library of Canada to reproduce this material as part of this thesis.

Contents

Abstract	iii
Acknowledgements	v
Authorship	vii
1 Introduction and Problem Statement	1
1.1 Effective field theory	2
1.2 Naturalness	7
1.3 Large extra dimensions	11
1.4 Cosmological constant problem	13
1.5 Curvature and extra dimensions	15
2 Preliminaries	20
2.1 Bulk action	20
2.2 Brane sources	22
2.3 Bulk field equations and Einstein equations	23
2.4 Scale invariance and curvature	26
2.5 Brane sources and boundary conditions	29

2.5.1	Simple example	29
2.5.2	Gravitational inconsistency	34
2.5.3	Localized flux and boundary conditions	37
2.6	Chapter summary	40
3	Dark vortices	42
3.1	Introduction	44
3.2	The system of interest	51
3.2.1	The action and field equations	52
3.2.2	Scales and hierarchies	56
3.3	Isolated vortices	57
3.3.1	Vortex solutions	58
3.3.2	Integral relations	64
3.3.3	Near-vortex asymptotics	68
3.3.4	Effective description of a small vortex	72
3.4	Discussion	85
4	EFT for vortices with dilaton-dependent flux	95
4.1	Introduction	97
4.2	The Bulk	101
4.2.1	Action and field equations	102
4.2.2	Symmetry ansätze	104
4.2.3	Bulk solutions	106
4.3	Sources - the UV picture	116
4.3.1	Action and field equations	117

4.3.2	Dual formulation	128
4.3.3	Vortex solutions	132
4.3.4	Integral relations	138
4.4	Sources - effective IR description	145
4.4.1	The EFT with point sources	145
4.4.2	Parameter matching	148
4.4.3	Near-source boundary conditions	152
4.4.4	Brane and vortex constraints	157
4.5	The scale of the response	160
4.5.1	Generic case	161
4.5.2	Scale invariance	163
4.5.3	Decoupling case: $p = -q = 2r + 1$	165
4.6	Discussion	168
5	Effective description of dilaton capture	175
5.1	Introduction	176
5.2	The higher-dimensional system	182
5.2.1	The Bulk	182
5.2.2	The Branes	184
5.2.3	Brane stress energies	184
5.2.4	Flux quantization	186
5.2.5	Boundary conditions	187
5.2.6	Control of approximations	188
5.2.7	Integral relations	189
5.2.8	Orders of magnitude	191

5.3	EFT below the KK scale	193
5.3.1	Lower-dimensional action	195
5.3.2	Field equations	197
5.3.3	Matching	199
5.3.4	Sources of φ -dependence within U	204
5.4	Self-tuning under scrutiny	208
5.4.1	Implications of ϕ -independent tension	209
5.4.2	Perturbative solutions	213
5.4.3	Scenarios of scale	226
5.4.4	Robustness	231
5.5	Discussion	235
6	The Extra-Dimensional Higgs Portal	243
6.1	Introduction	244
6.1.1	Higher-dimensional stabilization	247
6.1.2	Relevance to the Higgs	249
6.2	Higgs-Bulk Dynamics	254
6.2.1	Field equations and back-reaction	254
6.2.2	Vacuum configurations	257
6.2.3	Higgs-Bulk mixing	263
6.3	Phenomenological implications	274
6.3.1	Virtual Higgs Exchange	275
6.3.2	Invisible final states	285
6.3.3	Mass-coupling relations and vacuum stability	306
6.4	Conclusion	311

7	Summary and outlook	326
A	Appendix for Chapter 3	332
A.1	Stress-energy conservation	332
A.2	Approximate near-vortex solutions	333
B	Appendix for Chapter 4	336
B.1	Scaling and the suppression of $\langle \mathcal{X}_{\text{loc}} \rangle$	336
C	Appendix for Chapter 5	339
C.1	Scale invariant solutions	339
C.1.1	Salam-Sezgin solution	339
C.1.2	Supersymmetric rugby ball	341
C.2	Linearized solutions	343
C.3	Examples of stabilization	355
D	Appendix for Chapter 6	361
D.1	Floating Brane Renormalization	361
D.2	Schwinger-Dyson equation	363
D.3	Toy model: unperturbed modes	366
D.4	Beyond Sturm Liouville	368
D.5	Solving for the KK mode functions	372

List of Figures

- 3.1 A comparison of BPS and non-BPS vortex profiles on a flat background for differing values of $\hat{\beta} = \hat{e}^2/(2\lambda)$. The (blue) profile vanishing at the origin is the scalar profile F and the (red) profile that decreases from the origin is the vector profile P . To find the profiles in flat space we set $B = \rho$ and $W = 1$. The left plot uses $\hat{\beta} = 1$ and the right plot uses $\hat{\beta} = 0.1$, with this being the only parameter that controls vortex profiles in flat space. 62
- 3.2 A comparison of the profiles F and P for the vortex in flat space (dashed curves) and the full gravitating vortex solution (solid lines). For each case the (blue) profile that vanishes at the origin is the scalar profile F and the (red) profile that decreases from the origin is the vector profile P . The parameters used in the plot are $d = 4$, $\varepsilon = 0.3$, $\beta = 3$, $Q = 0.01 ev^2$, $\Lambda = Q^2/2$, $\kappa v = 0.6$ and $\check{R} = 0$ with the same values of β and ε chosen for the non-gravitating solution. 63

3.3 These plots illustrate the bulk geometry for BPS vortices ($\beta = 1$) with parameters $d = 4$, $\varepsilon = 0$, $\beta = \hat{\beta} = 1$, $Q = 0.05 ev^2$, $\Lambda = Q^2/2$ and $\kappa v = 0.3$ (which also imply $\check{R} = 0$). In the top left plot, the solution for B is plotted (in blue) below the (red) metric function B_{sphere} of a sphere with radius $r_B = (200/3)r_v$. The presence of a vortex does not change the size of the bulk (since the full solution for B still vanishes at $\rho = \pi r_B$) and the metric function B is still approximately spherical with $B \approx 0.95 \times B_{\text{sphere}}$ for these parameters. The top right plot shows that when $\beta = 1$ and $\Lambda = Q^2/2$, a constant warp factor solves the field equations. The bottom left plot shows that the derivative of the metric function $B' \approx 0.95$ outside of the vortex core, at $\rho \gtrsim 4r_v$. The bottom right plot shows that $B' \approx -0.95$ at the pole which lies opposite to the vortex core, indicating the presence of a conical singularity at that pole. 65

3.4 An illustration of the matching done at $\rho = \rho_v$. The light grey surface is a cartoon of the bulk geometry. The bump on top of the surface represents the localized modifications to the approximately spherical bulk geometry that arise due to the vortex. The dark ring represents the circle at $\rho = \rho_v$ that lies sufficiently far outside the vortex that its fields are exponentially suppressed, but close enough to the vortex so that that its proper distance from the pole is still $\mathcal{O}(r_v)$ 66

- 3.5 A cartoon illustration of the definition of ρ_* . The (blue) metric function B increases linearly away from the origin with unit slope $B(\rho) \approx \rho$. Outside of the vortex $\rho \gtrsim \rho_v$ the solution is also linear in ρ but with $B(\rho) \approx \alpha\rho$. The straight (red) line extrapolates this exterior behaviour to the point, $\rho = \rho_*$, where the external B would have vanished if the vortex had not intervened first. 69
- 3.6 Log-log plots of the the near vortex geometry for parameters $d = 4$, $\beta = 3$, $\varepsilon = 0.3$, $Q = 0.01 ev^2$, $\Lambda = Q^2/2$, $\kappa v = 0.6$ and $\check{R} = 0$. The bulk in this case has a radius of $r_B = (500/3)r_v$. Outside of the vortex $\rho \gtrsim r_v$ the geometry exhibits Kasner-like behaviour $B' \approx \alpha \neq 1$ and $W' \approx 0$ 71
- 3.7 A plot of defect angle matching in the region exterior but near to the vortex core. The solid (blue) lines represent the metric function $W^4 B'$ and the dotted (red) lines represent $1 - \kappa^2 \check{T}/2\pi$ computed independently for different values of $\varepsilon = \{-0.2, 0.2, 0.4, 0.6\}$ with the other parameters fixed at $d = 4$, $\beta = 3$, $Q = 1.25 \times 10^{-4} ev^2$, $\Lambda = Q^2/2$, $\kappa v = 0.5$ and $\check{R} = 0$. This size of the defect angle $B'_v \approx \alpha$ matches very well with $1 - \kappa^2 \check{T}/2\pi$ at $\rho = \rho_v \approx 4r_v$. The solutions for $W^4 B'$ overlap perfectly when $\varepsilon = \pm 0.2$, as indicated by the dashes in the line. This illustrates that the defect angle is controlled by \check{T} , and the linear dependence of the the defect angle on ε is cancelled. 83

- 4.1 A cartoon illustration of the definition of ρ_* . The (blue) metric function B increases linearly away from the origin with unit slope $B(\rho) \simeq \rho$. Outside of the source $\rho \gtrsim \rho_v$, the solution is a power law in ρ with $B(\rho) \sim \rho^b$. The straight (red) line extrapolates this exterior behaviour to the point, $\rho = \rho_*$, where the external B would have vanished if the vortex had not intervened first. 110
- 4.2 This plot illustrates the near-source Kasner region for bulk fields that are sourced by a generic vortex with tension $v^2 = 0.25/\kappa^2$. In the top left plot, the vortex profiles are shown on a logarithmic axis, with the (blue) scalar profile F increasing towards its asymptotic vacuum value $F \rightarrow 1$ and the (grey) gauge profile P decreasing towards its asymptotic value $P \rightarrow 0$. (See below for more detailed definitions.) These profiles approach their vacuum values exponentially, and they can be neglected in the region $\tau = \ln(\rho/r_v) \gtrsim 2$, which is where the Kasner region $\rho \gtrsim \rho_v$ begins. In the next plot, $\ln(B')$ is seen to be linear in τ in the darkened (blue) near-vortex region, before the bulk sources dominate the behaviour of B' at larger τ . This blue region is the Kasner region, where the bulk fields obey power laws, and this behaviour is also apparent in the plots of $\ln(e^\phi) = \phi$ and $\ln(W^d) = d \ln W$. The Kasner powers can be extracted in this region, and for this particular source we find numerically $dw = 0.0034$, $1 - b = 0.0034$ and $z = 0.082$ which is in agreement with the perturbative solution of (4.28). Finally, we note that these numerical results are also consistent with the estimates $z \sim \delta \sim \kappa^2 v^2$ as is argued below. 113

4.3 These plots demonstrate that the dilaton couplings do not ruin the existence of localized vortex solutions. The left plot contains a comparison of the vortex profiles F and P for a non-gravitating vortex in flat space (dashed curves) and a gravitating vortex coupled to the dilaton (solid curves). The right plot shows the dilaton profile in the vortex region for both cases. The gravitating dilaton is slowly varying in the vortex region, with the change of ϕ over the vortex region being controlled by $\Delta e^\phi \sim \kappa^2 v^2$. The parameters used to generate the gravitating profiles are $d = 4$, $\varepsilon = 0.3$, $\beta = 3$, $\kappa v = 0.5$, $\phi(0) = 0$, $Q = 0.01 e v^2$, $V_0 = Q^2/2$ and the vortex sector is coupled to the dilaton through the generic choices $(p, q, r) = (-1, 0, -1)$. The flat space profiles are generated by choosing $\kappa v = 0$ instead. 136

4.4 These plots show the numerical bulk solution for $n = 1$ BPS vortex sources ($\hat{\beta} = 1$) with scale invariant couplings to the dilaton $(p, q, r) = (-1, 1, -1)$ and $\kappa v = 0.4$. For these choices, the field equations are solved by a constant dilaton and warp factor: $W = 1$ and $\phi = 0$. Because $\phi' = W' = 0$, this solution falls into the simple class of rugby ball solutions described in §4.2.3. In the top left plot the metric function B is plotted against the same solution for a sphere of proper radius $\ell = 250\pi r_v$, $B_{\text{sphere}} = \ell \sin(\rho/\ell)$. The vortices (which cannot be resolved in these plots) introduce a defect angle into the bulk metric such that $B = \alpha \ell \sin(\rho/\ell)$ in the bulk. The defect angle, α , can be determined by extrapolating B' to the apparent singular point at $\rho_* \approx 0$. This yields $1 - \alpha \simeq 0.08 = \kappa^2 \check{T}/2\pi = (\kappa v)^2/2$ as expected from (4.113) and (4.150). 139

4.5 A demonstration of the ϕ -independence of \check{T}_v . Two solutions are presented for the decoupling choice $p = -q = 2r + 1 = 2$ that differ only in the value of the dilaton in the vortex $\phi_v \approx \phi(0) = \{0, -2\}$. The light (grey) lines represent the solution for the choice $\phi(0) = -2$ and the blue lines represent the solution for $\phi(0) = 0$. While the physical mass scales that control the size of the profiles, $m_{\check{\Psi}}^2(\phi_v) = 2\check{\lambda}v^2 e^{q\phi_v}$ and $m_Z^2(\phi_v) = e^{-p\phi_v} e^2 v^2 / (1 - \varepsilon^2)$, are demonstrably heavier for $\phi_v \simeq -2$ (since these profiles fall off much faster), the defect angle $[W^d B']_{\rho_v} \simeq 1 - \frac{\kappa^2 \check{T}_v}{2\pi}$ that measures the tension of the vortex is independent of ϕ_v . The other parameters of this solution are $d = 4$, $\varepsilon = 0.6$, $\beta = 0.8$, $\kappa v = 0.4$, $Q = 1.6 \times 10^{-4}$ and $V_0 = Q^2/2$ 152

- 4.6 Two examples of the vortex constraint (4.160). The light (grey) line is calculated from the expression $\kappa^2 \langle \mathcal{X}_{\text{loc}} \rangle_v \simeq -\pi [B(W^d)']_{\rho_v}$ and the dark (blue) line is calculated using the second brane constraint. Once evaluated outside of the vortex $\rho_v \gtrsim \hat{r}_v \approx r_v$, the two independently calculated quantities are in perfect agreement, and their failure to agree inside the region $\rho_v \lesssim \hat{r}_v$ reflects the fact that the vortex constraint does not hold locally in the source. In the first plot the parameters are $d = 4$, $\varepsilon = 0$, $\beta = 3$, $\kappa v = 0.5$, $\phi_v \approx \phi(0) = 0$, $Q = 2 \times 10^{-4}$ and $V_0 = Q^2/2$. The vortex is coupled to the dilaton via the choice $(p, q) = (0, 2)$ and r is not relevant because gauge kinetic mixing has been shut off. In the second plot, the only change in parameters is that $\phi(0) = 1$ 161
- 6.1 A plot summarizing the various constraints and discovery potential of Higgs-bulk mixing in the $G = \bar{g}/\sqrt{\alpha}$ vs $\Lambda_2 = \bar{\lambda}_2/\alpha$ plane (renormalized at $\bar{r} = 1/m_h$), in the large-volume limit ($m_h \gg m_{KK}$). The quantity $\alpha \sim 1$ is a measure of the defect angle near the brane, as defined in detail in §6.2.1. The dark (blue) shaded region is the region disfavoured by LHC global fits. The medium (blue) shaded region is the conservative bound from nucleon-bulk bremsstrahlung in SN1987a, assuming $T_{SN} = 20$ MeV. The lightest (gray) shade denotes regions excluded by demanding no Landau poles below $\mu_* = 1$ TeV, with the vertical dotted lines denoting how this bound changes with the choice of ultra-violet scale μ_* . Also plotted are lines of constant invisible branching ratio B that will be probed with additional data at the LHC or future experiments, all of which constrain this quantity. 252

6.2	<p>Perturbative calculation of the Green's function for the h operator. Dotted lines represent D_k^ϕ and dashed lines represent D_k^h as defined in the text. Circles are used for the $gvh\phi(0)$ vertex, diamonds represent a $\frac{1}{2}\lambda_2\phi^2(0)$ vertex and \tilde{D}_k^ϕ is the λ_2-resummed Green's function for the bulk field, Fourier transformed in the brane directions but not in the extra dimensions.</p>	264
6.3	<p>Scattering via virtual exchange of the Higgs-bulk tower. A factor of \mathcal{B}_s comes from the vertex between φ_s and both the initial and final state. All modes are summed over because any of the φ_s can mediate this interaction.</p>	275
6.4	<p>The lineshape, $\langle hh^* \rangle_k ^2$, for the KK tower exchange with various values of $(\bar{\lambda}, \bar{\lambda}_2, \bar{g}, \alpha)$ evaluated at $\bar{r} = (125 \text{ GeV})^{-1}$. The dotted black line is the comparison lineshape for a Standard Model Higgs with mass, $m_h = 125 \text{ GeV}$ and a Standard Model width of $\Gamma_{SM} = 4 \text{ MeV}$. (In the Standard Model the Higgs coupling for this mass is $\bar{\lambda} = 0.1291$.) The dashed blue line shows a similarly narrow peak (chosen to lie near 124 GeV rather than 125 GeV to avoid clutter in the figure), obtained using $(\bar{\lambda}, \bar{\lambda}_2, \bar{g}, \alpha) = (0.127, 0, 0.0021, 0.8)$. The solid red line shows instead a broad peak at 125 GeV for an exaggerated choice of couplings $(\bar{\lambda}, \bar{\lambda}_2, \bar{g}, \alpha) = (0.16, 2, 0.35, 0.01)$.</p>	276

6.5	The Higgs quartic coupling $\bar{\lambda}$ required to ensure $m_h = 125$ GeV, as a function of the brane bulk mixing parameter $G = \bar{g}/\sqrt{\alpha}$ for various choices of the coupling parameter $\Lambda_2 = \bar{\lambda}_2/\alpha$ (as listed in the legend). The flat line $\bar{\Lambda}_2 = 0$ corresponds to the Standard Model value $\bar{\lambda} = 0.1291$. All couplings are renormalized and evaluated at a scale $\bar{r} = (125 \text{ GeV})^{-1}$	278
6.6	Bounds on $\Lambda_2 = \bar{\lambda}_2/\alpha$ and $G = \bar{g}/\sqrt{\alpha}$ from constraints on the invisible branching ratio of a Standard Model Higgs. The shaded region is excluded, for two sets of assumptions (described in the main text). Couplings are evaluated at a scale $\bar{r} = (125 \text{ GeV})^{-1}$	281
6.7	The Feynman graph corresponding to the one-loop correction to the muon anomalous magnetic moment in the Higgs-bulk mixing scenario.	283
6.8	The tree level contribution to vector boson fusion with an invisible final state.	285
6.9	Constraints from LEP expressed in the Λ_2 - G plane (with $G = \bar{g}/\sqrt{\alpha}$ and $\Lambda = \bar{\lambda}_2/\alpha$) from LEP constraints. The small shaded region is excluded. All couplings are evaluated at a scale $\bar{r} = (125 \text{ GeV})^{-1}$. . .	292
6.10	The four uncrossed graphs for Higgs-nucleon bremsstrahlung.	304
6.11	Constraints on Higgs-bulk mixing from bulk-nucleon bremsstrahlung in SN1987a. The left panel shows the constraints obtained assuming $T_{SN} = 20$ MeV and the right panel shows the analogous constraints assuming $T_{SN} = 60$ MeV. Couplings are evaluated at $1/\bar{r} = m_h = 125$ GeV.	305

Chapter 1

Introduction and Problem Statement

Naturalness problems are among the foremost issues in modern physics. While the predictions of the Standard Model have been successfully tested with great scrutiny, and the model is self-consistent, some of its experimentally measured parameters do not fit *naturally* within the paradigm of effective field theory. In particular, the massive parameters of the theory – the Higgs mass parameter and the cosmological constant – are observed to be much smaller than they would be in a generic field theory. As stated, this might not seem like a serious problem, but it has been a strong motivation for models of new physics, including those investigated in this thesis, and deserves further exposition.

This chapter provides such an exposition by first describing the modern view of effective field theory. It then describes why the Higgs mass parameter and the cosmological constant are not natural within this framework, since their smallness cannot be understood within low-energy and high-energy versions of the Standard

Model. After this are presented some prospects for solving these naturalness problems with extra dimensions, which are explored in greater detail in the remainder of this thesis.

1.1 Effective field theory

The contemporary understanding of quantum field theory is that a description of a system has two ingredients: its dynamics (which are usually encoded in a local Lagrangian \mathcal{L}_μ) and a mass scale below which the theory can be applied, μ . It might not always be obvious how to choose the scale μ by hand, but it is very plausible that such a scale would exist. For example, a Lagrangian might only be applicable up to the scale μ if there is a particle of mass $M_{\text{heavy}} \gtrsim \mu$ in the system that is being neglected in \mathcal{L}_μ . The effective description of the system, \mathcal{L}_μ , would obviously break down once high energy processes were considered where the neglected particle could be produced on-shell. However, in principle, any observable could be calculated to arbitrary precision using the Lagrangian \mathcal{L}_μ , up to energies of order μ .

In general, increased precision at higher energies comes at the cost of an increasingly complicated Lagrangian. This is because the low-energy relevance of an operator is related to its mass dimension; a limited number of operators with low mass dimensions dominate the low-energy dynamics of a theory, and the effects of the abundant higher-dimension operators are suppressed. For example, in 4 dimensions, an operator of mass dimension 5, \mathcal{O}_5 , must appear in the Lagrangian with a coupling constant that has negative mass dimension. We write

$$\mathcal{L} \supset \frac{\mathcal{O}_5}{\omega_5}, \tag{1.1}$$

where ω_5 has dimensions of mass. Similarly, a dimension 3 operator has a coupling constant with mass dimension 1

$$\mathcal{L} \supset \omega_3 \mathcal{O}_3. \quad (1.2)$$

If both of these operators contribute to, say, a decay process, then the contributions to the decay rate can be organized on dimensional grounds. The matrix element for such a process \mathcal{M} is given schematically by

$$\mathcal{M} = A \omega_3 + B \left(\frac{m^2}{\omega_5} \right), \quad (1.3)$$

where m is the mass of the decaying particle, with A and B representing $\mathcal{O}(1)$ dimensionless constants throughout this chapter. So the overall decay rate is (also schematically) given by

$$\Gamma = \frac{1}{2\pi m} \left[A m^2 \left(\frac{\omega_3}{m} \right)^2 + B m^2 \left(\frac{\omega_3}{\omega_5} \right) + C m^2 \left(\frac{m}{\omega_5} \right)^2 \right]. \quad (1.4)$$

The power of organizing an observable in this way comes when there is a clear separation of scales $\omega_5 \gg m, \omega_3$. In this case, the first term in the decay rate dominates the others, and the rate for this process would have been well-approximated by considering only the dimension 3 interaction, \mathcal{O}_3 . Indeed, the operator with higher mass dimension is less relevant at low energies ($m \ll \omega_5$).

This observation can be used to organize the operators of a Lagrangian by relevance, with the lowest dimensional operators being most relevant at low energies

$$\mathcal{L}_M = c_0 + \sum_{i_1} c_1^{i_1} \mathcal{O}_1^{i_1} + \sum_{i_2} c_2^{i_2} \mathcal{O}_2^{i_2} + \sum_{i_3} c_3^{i_3} \mathcal{O}_3^{i_3} + \dots \quad (1.5)$$

Above, $\mathcal{O}_j^{i_j}$ represents an operator of mass dimension j , and $c_j^{i_j}$ is the associated coupling constant of mass dimension $D - j$, where D is the spacetime dimensionality. It follows that operators with mass dimension exceeding D will generically come with mass suppressed couplings, and these are called higher-dimension operators.

In concluding that higher dimension operators are suppressed at low energies, we assumed that the mass scales suppressing their coupling constants were larger than the energies of interest $E \ll \mu \ll \omega$. It turns out that this is a very safe assumption, and true for generic field theories. To see why, we consider how the Lagrangian description of a system changes as μ is adjusted.

Since μ can be chosen by hand, it cannot have any bearing on physical observables. This is ensured in an effective field theory by having the parameters of theory adjust as μ is adjusted. For example, an observable might depend on μ because it involves an integral over all modes with momentum $k < \mu$. However, this dependence can always be cancelled if the couplings depend on μ appropriately, and the correct choice is dictated by the renormalization group equations. A detailed example of such a cancellation is given in chapter 6 of this thesis.

It is especially interesting to see how a theory's couplings change when μ is decreased below the mass of a heavy state in the theory. The particle can no longer be produced on shell, but the low energy theory is still responsible for reproducing any physics that arose from the virtual effects of the heavy particle. A well-known

example of this can be seen in Fermi theory, which captures the physics of fermions scattering via charged currents at energies below $\mu < M_W$, where M_W is the mass of the W^\pm . At energies above this threshold, a scattering process like $\nu d \rightarrow \ell u$ is described as being mediated by the exchange of a virtual W^- . However, there is no dynamical W^\pm in the low-energy theory; it is said to be integrated out. Nonetheless, the scattering cross section can still be reliably calculated up to energies $E < \mu \approx M_W$ in the low energy theory.

This works because the coupling constant c_6 of a four fermion interaction is adjusted in the low energy theory. Concretely, there is an interaction in the low-energy theory that can result in $\nu d \rightarrow \ell u$ scattering,

$$\mathcal{L}_\mu \supset c_6 \mathcal{O}_6 = c_6 \eta_{\alpha\beta} (\bar{\ell} \gamma^\alpha P_L \nu) (\bar{u} \gamma^\beta P_L d) , \quad (1.6)$$

where α, β here are spacetime indices in four flat dimensions, γ^α represents the Dirac matrices, $P_L = \frac{1}{2}(1 - \gamma^5)$ projects fermions onto eigenstates of the γ^5 chirality operator, $\eta_{\alpha\beta}$ is the Minkowski metric, and the remaining undefined symbols represent fermion fields. The size of this operator's coupling in the low-energy theory must be adjusted as μ is decreased below the M_W threshold

$$c_6(\mu) = c_6(\mu_0) + \frac{g^2}{8M_W^2} . \quad (1.7)$$

Above, g is the weak coupling constant and $c_6(\mu_0)$ is the value of the coupling in the high energy version of the theory with $\mu_0 > M_W$ where the W^\pm is dynamical. These constants appear here because the dimension-6 operator in the low-energy theory must capture the virtual effects of the W^\pm boson that has been integrated

out. Heuristically, the factors of g come from the strength of the $W f_i f_j$ coupling in the high-energy Lagrangian, and the factor of M_W^2 comes from the propagator for the W^\pm at low energies. In the low-energy theory, this information resides in the coupling of the dimension-6 operator (1.7), and in this way either theory gives the same prediction for the $\nu d \rightarrow \ell u$ scattering cross section at low energies.

By similar arguments, $c_6(\mu_0)$ is expected to be controlled by the physics at an even higher mass scale. Even without knowing the details of physics at this higher mass scale, we can estimate the size of $c_6(\mu_0)$ on dimensional grounds and we expect

$$c_6(\mu_0) \sim \frac{1}{M_{\text{heavy}}^2}, \quad (1.8)$$

where $M_{\text{heavy}} \gg \mu_0 \gg M_W$. So we see here the decoupling of scales in action. It is not necessary to know the detailed dynamics of the heavy sector to know that it will have very little bearing on the scattering process $\nu d \rightarrow \ell u$ because its relative effects are suppressed

$$\frac{1}{M_{\text{heavy}}^2} \ll \frac{1}{M_W^2} \quad \implies \quad c_6(\mu_0) \ll c_6(\mu). \quad (1.9)$$

This decoupling is a powerful guide, and it is a crucial ingredient of effective field theory. Because of it, a theory like the Standard Model can, in principle, be built from the bottom up, since it is safe to neglect the impact of high-energy states. However, this same discussion applied to lower-dimension operators will reveal a compelling problem within the observed parameters of the Standard Model.

1.2 Naturalness

In the previous section we discussed how the virtual effects of a high-energy particle can be captured in an effective theory where the particle is integrated out. The punchline was that, even without a detailed understanding of the high-energy physics, simple dimensional analysis is sufficient to conclude that the effects of high-energy physics on low-energy observables is relatively weak when there is a hierarchy of scales.

This was certainly true for higher-dimension operators, whose couplings go like an inverse power of mass, in which case the heaviest particles will typically contribute the least to effective couplings. However, by the same reasoning, lower-dimension operators should be increasingly sensitive to high-energy physics. For example, in four dimensions the mass term for a scalar field is a dimension-2 operator

$$\mathcal{L}_\mu \supset c_2 H^\dagger H . \quad (1.10)$$

If we imagine that there are heavy particles with $M_{\text{heavy}} > \mu$ which are neglected in \mathcal{L}_μ , then we can estimate their contribution to the size of c_2 by dimensional analysis

$$c_2(\mu) - c_2(\mu_0) \sim \sum_{\text{heavy}} M_{\text{heavy}}^2 . \quad (1.11)$$

The appearance of these factors is sensible, since they must capture the virtual effects of heavy particles that would contribute to the Higgs self-energy if they were not integrated out. The result in (1.11) suggests that the mass of a scalar field is very sensitive to high-energy physics, which is in itself is not a problem. It simply means

that light scalars are not at all generic. The problem is that the Standard Model is has been shown experimentally to possess a light scalar field, the Higgs, that is not natural – a notion that we are now equipped to explore in more detail.

A hierarchy in physical quantities is called technically natural if there is a hierarchy in the parameters controlling the physical quantity at every scale. An excellent example of a natural hierarchy is the one that exists between the mass of the electron and the electroweak scale

$$m_e/v \sim 10^{-5}, \quad (1.12)$$

where m_e is the electron mass and v is the Higgs vev. In the Standard Model at high energies with $\mu_0 > v$, the Higgs is a dynamical field in the theory, and there is no explicit mass term for the electron because it would not preserve SU(2) gauge invariance. Nonetheless, the electron has a nonvanishing mass after symmetry breaking because it interacts with the Higgs through a Yukawa coupling. The classical prediction for this mass, $m_e = y_e v$, is small relative to the weak scale because the Yukawa coupling is small: $y_e \sim 10^{-5}$. Just as important to this smallness is the chiral symmetry that emerges when $y_e \rightarrow 0$. This symmetry ensures that virtual particles contribute to the electron mass in a way that vanishes as $y_e \rightarrow 0$, and the quantum prediction for the electron mass is given schematically by

$$m_e = y_e v + y_e v \sum_i A_i \log(M_i/\mu_0), \quad (1.13)$$

where the sum runs over the particles that can contribute to the electron self energy. The structure of the quantum corrections is such that the hierarchy between the weak scale and the electron mass isn't spoiled, $m_e = y_e v(1 + \dots) \ll v$, thanks to the

approximate chiral symmetry.

In the theory at lower energies, $\mu < v$, the weak scale particles are integrated out and the SU(2) symmetry is broken, so the electron has an explicit mass term, $c_3 \bar{e}_L e_R$. On dimensional grounds, one might expect that heavy particles contribute to this term in the following way as they are integrated out

$$c_3(\mu) \stackrel{?}{=} y_e v + \sum_{EW} M_{EW} . \quad (1.14)$$

However, the approximate chiral symmetry of the high-energy theory renders this naive dimensional argument incorrect. It follows from (1.13) that, as heavy particles are integrated out, their virtual effects are captured by shifting the electron mass parameter as follows

$$\delta c_3(\mu) = y_e v A \log(M/\mu) , \quad (1.15)$$

and not linearly in M , as guessed in (1.14). So the electron mass parameter $c_3 = y_e v(1 + \dots)$ remains as small as particles are integrated out, and its smallness can be understood at any energy, thanks predominantly to the chiral symmetry of the theory.

Contrast this natural hierarchy with the recently discovered Higgs mass [1, 2], which is observed to be

$$m_h = 125 \text{ GeV} . \quad (1.16)$$

In the Standard Model at the electroweak scale, the parameter $c_2(\mu)$ should be close to this scale, since the Higgs mass is given by

$$m_h^2 = c_2(\mu) + \sum_i A_i M_i^2 = c_2(\mu) + \mathcal{O}(M_{EW}^2) , \quad (1.17)$$

where i runs over the relevant Standard Model fields, all of which are all lighter than the electroweak scale.

If some new heavy state exists at, say, $M_{\text{heavy}} = 1000 \text{ TeV}$, there would be a 10^4 hierarchy between these scales that could be understood at low energies as coming from the parameter hierarchies $c_2(\mu) \ll M_{\text{heavy}}^2$ and $M_{EW} \ll M_{\text{heavy}}$. However, in the theory at high energies where $\mu_0 > M_{\text{heavy}}$, the prediction for the Higgs mass would be

$$m_h^2 = c_2(\mu_0) + AM_{\text{heavy}}^2. \quad (1.18)$$

The smallness of the Higgs mass in this case cannot be understood from a hierarchy in the theory's parameters. Quite the opposite is true; the physical Higgs mass can only be understood if $c_2(\mu_0)$ is extraordinarily close to the value of the heavy state's contribution to the Higgs mass and of opposite sign

$$\left| 1 + \frac{AM_{\text{heavy}}^2}{c_2(\mu_0)} \right| \ll 1, \quad (1.19)$$

since the left-hand side of (1.18) is at the GeV scale and M_{heavy} is at the 1000 TeV scale. So none of the parameters in the theory at high energies is hierarchically small, yet the physical mass of the Higgs boson certainly is, in a way that is not natural.

Avoiding the electroweak hierarchy problem has become a strong guide towards new physics, since it requires new physics that is not generic, and there are a number of models that somehow invalidate estimates like the one in (1.18). Much like the case of an approximate chiral symmetry rendering the electron mass natural, symmetry can be used to alleviate the electroweak hierarchy problem, and supersymmetry remains the flagship for efforts on this front. There is no shortage of theses to read

on that subject, so we do not discuss it here. Instead, we turn to another interesting possibility, that the scale at which gravity becomes strongly interacting is not far from the electroweak scale. If this can be arranged, then there are no states with $M_{\text{heavy}} \gg m_h$ whose hierarchical mass needs a natural explanation, because quantum gravity kicks in before such a heavy scale is reached. It turns out that this is a phenomenologically viable idea, if there are extra spacelike dimensions that are much larger than the inverse TeV scale.

1.3 Large extra dimensions

The previous section hinted that extra dimensions might allay the electroweak hierarchy problem by lowering the scale at which gravity becomes strongly interacting, which lies ostensibly at the Planck scale ($M_{\text{Pl}} = 10^{19}$ GeV). We show here how this works in more detail.

Since spacetime geometry and gravity are synonymous, the metric field must propagate in any extra dimensions we might consider. So we write the higher dimensional Einstein-Hilbert action in $D = 4 + n$ dimensions

$$S_{EH} = M_*^{2+n} \int d^{4+n}x \sqrt{-g} \mathcal{R}, \quad (1.20)$$

where n is the number of extra dimensions, which are compactified, and M_* is the mass scale of gravity in $n + 4$ dimensions. At low energies, this must reproduce the familiar physics of 4D gravity. In particular, the 4D metric must couple with the observed strength $G_N = M_{\text{Pl}}^{-2}$ in the dimensionally reduced theory, which is obtained by integrating the action over the extra dimensions.

A heuristic estimate for this term is given below

$$S_{4D} = M_*^{2+n} V^n \int d^4x \sqrt{-g_4} R_4, \quad (1.21)$$

where V^n is the volume of the extra dimensions. This allows us to read off the effective 4D gravitational coupling and equate it to M_{Pl}

$$M_{\text{Pl}}^2 = M_*^{2+n} V^n. \quad (1.22)$$

If we want gravity to couple strongly at $M_* \sim M_{EW}$, then this equation fixes the volume of the compactified extra dimensions. For example, assuming each of the extra dimensions to be of size ℓ , gives [3]

$$\ell \sim 10^{\frac{30}{n}-17} \text{ cm}. \quad (1.23)$$

Extra dimensions of this size would imply new physics effects at the same length scales. So, phenomenologically, the situation seems dire unless this length scale is below the inverse TeV scale, $\ell < 10^{-17}$ cm. By this estimate, no phenomenologically viable number of extra dimensions would give a gravity scale around a TeV. However, it is possible for models with extra dimensions to modify only gravitational physics if the rest of the Standard Model particles are confined to a 4D surface that propagates in the extra dimensions, a so-called brane. Deviations from 4D gravitation have only been tested down to tens of micrometres [4], and putting this scale into (1.22) as the size of the extra dimensions with $n = 2$ gives

$$M_* \sim 10 \text{ TeV}. \quad (1.24)$$

This is just beyond the scale that is being probed at colliders, where extra dimensions can have signatures including energy loss when gravitons are produced that propagate into the extra dimensions (missing energy), and deviations from the Drell-Yan process [5] from the exchange of virtual gravitons [6, 7]. Although M_* doesn't lie exactly at the electroweak scale, it is still close enough that the hierarchy between this scale and the Higgs mass is a mild one of order 10^2 . So a theory with two micrometre-sized extra dimensions remains a phenomenologically viable, testable and theoretically interesting possibility.

Finally, it is worth pointing out that there still exists a hierarchy in these models, between the size of the extra dimensions and the weak scale (the Planck scale, on the other hand, is a derived quantity). So if models of extra dimensions are to truly succeed in solving the electroweak hierarchy problem, they must naturally explain this hierarchy too. This issue is revisited in this thesis, which in later chapters investigates a dynamical mechanism for generating large extra dimensions from natural parameters, in a class of models where the size of the extra dimensions can be related to the vacuum value of a higher dimensional scalar field.

1.4 Cosmological constant problem

Thus far we have focused on the electroweak hierarchy problem, whose existence is really a blessing in disguise, since it guides model builders towards sensible new physics at energy scales above a TeV. We now turn to another naturalness problem that appears to be more difficult to solve, since it reveals a lack of naturalness at energies below the electroweak scale that were thought to be well understood.

In the catalogue of the Standard Model's lower dimension operators, there remains

only one operator whose sensitivity to high energy physics might lead to naturalness issues, the constant part of the Lagrangian c_0 , i.e. the cosmological constant. Observations of supernovae redshifts [8] and measurements of the cosmic microwave background [9] suggest that the universe is spatially flat and accelerating. This is consistent with there being a constant energy density of the vacuum

$$\varrho_{\text{vac}} = (2 \text{ meV})^4. \quad (1.25)$$

In the Standard Model at present day Hubble scales, when all massive particles are integrated out except possibly neutrinos, the value of the vacuum energy is directly related to the cosmological constant

$$\varrho_{\text{vac}} = c_0(\mu). \quad (1.26)$$

However, in the theory with $\mu_0 > m_e$ where the electron is not integrated out, we expect on dimensional grounds that the vacuum energy is calculated as follows

$$\varrho_{\text{vac}} = c_0(\mu_0) + A m_e^4. \quad (1.27)$$

In this theory there is a large hierarchy between the electron mass and the energy scale associated with the vacuum energy

$$\frac{\varrho_{\text{vac}}}{m_e^4} \approx 10^{-32}. \quad (1.28)$$

Furthermore, there is no hierarchy in the parameters of the Lagrangian at this scale that would provide a natural explanation of this hierarchy; the observed smallness of

ϱ_{vac} can only be understood in this higher energy theory if $c_0(\mu)$ is incredibly close to Am_e^4 and carries the opposite sign.

This smells very much like the electroweak hierarchy problem, but there is one notable difference. In this case, there are no obvious loopholes that might invalidate estimates like (1.27). This is because the physics above and below the mass of the electron is very well-understood. What is more, the fine tuning becomes increasingly severe at higher and higher energies, where loops of even heavier particles contribute to the vacuum energy density. Solving this problem therefore requires new physics at scales as low as the electron mass, which makes it a very difficult problem.

The silver lining is that a modification to low-energy physics is likely to be testable, and any loophole to the arguments presented in this section will require compelling new physics. One such loophole is provided by theories with extra dimensions.

1.5 Curvature and extra dimensions

The energy of the vacuum is not measured directly in cosmological experiments. Rather, it is deduced from measurements of cosmological spacetime and related to energy density via the 4D Einstein equations, which read

$$R_{\mu\nu} - \frac{1}{2}Rg_{\mu\nu} = 8\pi G_N T_{\mu\nu}, \quad (1.29)$$

where μ, ν are indices that run over the four dimensions. It is the assumption of vacuum Lorentz invariance, which fixes $T_{\mu\nu} = -\varrho_{\text{vac}} g_{\mu\nu}$ and $R_{\mu\nu} = \frac{R_4}{4} g_{\mu\nu}$, that forces

a relation between the vacuum energy density and the observed curvature,

$$g^{\mu\nu} R_{\mu\nu} = 32\pi G_N \varrho_{\text{vac}}. \quad (1.30)$$

Because the prediction of large vacuum energy seems so robust, and the observed spacetime curvature is so small, it is interesting to entertain means of breaking this relation.

Extra dimensions can radically change this expectation. Consider the Einstein equations in six dimensions

$$\mathcal{R}_{MN} - \frac{1}{2}\mathcal{R}g_{MN} = \kappa^2 T_{MN}, \quad (1.31)$$

where $\kappa^2 = 1/2M_\star^4$ is the higher-dimensional gravitational coupling, and capital indices run over all dimensions. Tracing this equation over the extra dimensions shows that the 4D curvature depends on the transverse stress energy, and not the energy along four dimensions,

$$g^{mn}\mathcal{R}_{mn} - \mathcal{R} = -g^{\mu\nu}\mathcal{R}_{\mu\nu} = \kappa^2 g^{mn}T_{mn}, \quad (1.32)$$

where μ, ν run over the 4D coordinates while m, n run over the coordinates of the extra dimension, and the metric was assumed to be diagonal. In a brane model, the vacuum energy associated with the Standard Model would be localized at a point in the extra dimensions, and uniform in the macroscopic dimensions,

$$T_{MN} = \delta_M^\mu \delta_N^\nu g_{\mu\nu} \varrho_{\text{vac}} \delta_2(y - y_b), \quad (1.33)$$

and it is plausible that the 4D curvature in (1.32) could remain small for any value of ρ_{vac} , because it depends on the transverse stress energy that is not *a priori* related to the vacuum energy. Then it would not be a problem that $c_0(\mu)$ is vastly different in different rewritings of the theory, since the observed curvature would be independent of this quantity. This intriguing possibility is explored in the next chapter, and investigated throughout this thesis in great detail.

Bibliography

- [1] G. Aad *et al.* [ATLAS Collaboration], “Observation of a new particle in the search for the Standard Model Higgs boson with the ATLAS detector at the LHC,” Phys. Lett. B **716**, 1 (2012) [arXiv:1207.7214 [hep-ex]].
- [2] S. Chatrchyan *et al.* [CMS Collaboration], “Observation of a new boson at a mass of 125 GeV with the CMS experiment at the LHC,” Phys. Lett. B **716**, 30 (2012) [arXiv:1207.7235 [hep-ex]].
- [3] N. Arkani-Hamed, S. Dimopoulos and G. R. Dvali, “The Hierarchy problem and new dimensions at a millimeter,” Phys. Lett. B **429**, 263 (1998) [hep-ph/9803315].
- [4] D. J. Kapner, T. S. Cook, E. G. Adelberger, J. H. Gundlach, B. R. Heckel, C. D. Hoyle and H. E. Swanson, “Tests of the gravitational inverse-square law below the dark-energy length scale,” Phys. Rev. Lett. **98**, 021101 (2007) [hep-ph/0611184].
- [5] S. D. Drell and T. M. Yan, “Massive Lepton Pair Production in Hadron-Hadron Collisions at High-Energies,” Phys. Rev. Lett. **25**, 316 (1970) [Phys. Rev. Lett. **25**, 902 (1970)].
- [6] G. F. Giudice, R. Rattazzi and J. D. Wells, “Quantum gravity and extra dimensions at high-energy colliders,” Nucl. Phys. B **544**, 3 (1999) [hep-ph/9811291].
- [7] T. Han, J. D. Lykken and R. J. Zhang, “On Kaluza-Klein states from large extra dimensions,” Phys. Rev. D **59** (1999) 105006 [hep-ph/9811350].
- [8] S. Perlmutter *et al.* [Supernova Cosmology Project Collaboration], “Measurements of the cosmological parameters Omega and Lambda from the first 7 supernovae at $z_i=0.35$,” Astrophys. J. **483**, 565 (1997) [astro-ph/9608192].

- [9] P. A. R. Ade *et al.* [Planck Collaboration], “Planck 2013 results. XVI. Cosmological parameters,” *Astron. Astrophys.* **571**, A16 (2014) [arXiv:1303.5076 [astro-ph.CO]].

Chapter 2

Preliminaries

This section provides some preliminary results that will prove useful throughout this thesis. In it are the field equations of a very general Einstein-Maxwell-scalar system in six dimensions that is general enough to encompass all the models investigated in this thesis. This section also introduces the branes that are present in these models, while setting up various conventions. Some important features of these models are explained along the way, and this section introduces the technical issues that are confronted in the later parts of this thesis.

2.1 Bulk action

All of the 6D systems studied in this thesis can be described by various limits of the following very general bulk action

$$S_{\text{bulk}} = - \sum_{c,d} \int d^6x \sqrt{-g} \left[\frac{\mathcal{R}}{2\kappa^2} + \frac{\mathcal{H}^c_d}{2} (\mathcal{D}_M \Phi^d)^\dagger (\mathcal{D}^M \Phi_c) + \frac{\mathcal{F}^c_d}{4} \mathcal{A}_{MN}^d \mathcal{A}^{MN}_c + V(\Phi) \right], \quad (2.1)$$

where g_{MN} is the 6D Einstein frame metric with which spacetime indices are raised and lowered. There is also a target space metric \mathcal{H}^c_d for the N real scalar fields Φ_c with $c = 1, 2, \dots, N$. In general, the target space metric is a function of the scalar fields Φ_c , but is actually constant (and diagonal) in all cases of interest, so this will be assumed, and we will write $\mathcal{H}^1_1 = \mathcal{H}_1$ and so on. There are also N abelian gauge fields \mathcal{A}^c_M with fields strengths defined as follows

$$\mathcal{A}^c_{MN} = \partial_M \mathcal{A}^c_N - \partial_N \mathcal{A}^c_M. \quad (2.2)$$

The corresponding gauge covariant derivatives are given by

$$\mathcal{D}_M \Phi^c = \partial_M \Phi^c - ie_c \Phi^c \mathcal{A}^c_M, \quad (2.3)$$

where e_c is the charge of the scalar field c under the gauge field c . This notation is sufficiently general because each scalar field is charged under at most one unique gauge field, the one labelled by c . Finally, $\mathcal{F}^c_d = \mathcal{F}^c_d(\Phi)$ is the gauge kinetic function that often will depend on the bulk scalar fields, and this can have off-diagonal terms that encode kinetic mixing between different gauge fields. This mixing does not break gauge invariance because the gauge fields are assumed to be Abelian [1].

It is useful and instructive to group the terms in the Lagrangian as follows. The gauge kinetic terms can be grouped together

$$L_{\text{gge}} = \frac{1}{4} \sum_{c,d} \mathcal{F}^c_d \mathcal{A}^d_{MN} \mathcal{A}^{MN}_c \quad (2.4)$$

as can the scalar kinetic terms

$$L_{\text{kin}} = \frac{1}{2} \sum_c \mathcal{H}_c \partial_M \Phi_c \partial^M \Phi_c. \quad (2.5)$$

It is also convenient to group the gauge mass terms

$$L_{\text{gm}} = \frac{1}{2} \sum_c \mathcal{H}_c e_c^2 \mathcal{A}_M^c \mathcal{A}_c^M \Phi_c^2 \quad (2.6)$$

and the total Lagrangian can be rewritten as the sum of these groups of terms

$$L_{\text{bulk}} = L_{EH} + L_{\text{kin}} + L_{\text{gge}} + L_{\text{gm}} + V, \quad (2.7)$$

where $L_{EH} = \mathcal{R}/2\kappa^2$ is the Einstein-Hilbert term.

2.2 Brane sources

The bulk physics described above will often times be supplemented by an action describing sources that are localized in the bulk, so-called branes:

$$S_{\text{brane}} = - \sum_b \int d^4x \sqrt{-\gamma_b} \left[T_0^b(\Phi) + \frac{1}{2} \zeta_j^b(\Phi) \epsilon^{mn} \mathcal{A}_{mn}^j + L_{SM}^b(\Phi, \mathcal{A}_{MN}) \right]_{y=Y_b}. \quad (2.8)$$

In the above action, $\gamma_{\mu\nu}^b = \partial_\mu Y_b^M \partial_\nu Y_b^N g_{MN}(Y_b)$ is the induced metric on the brane labelled by b , and $Y_b^M(x)$ represents the dynamical position of the brane. However, the branes are always assumed to be stationary, $Y_b^M(x) = y_b^M$, and coordinates on the brane are chosen so that $\gamma_{\mu\nu}^b = g_{\mu\nu}(y_b)$. The first term in the brane action is its tension $T_0^b(\Phi)$, its energy per unit volume. In the second term, ϵ^{mn} is the totally

antisymmetric tensor in the extra dimensions. As we will see, this term endows the brane labelled by b with localized \mathcal{A}_M^j flux proportional to $\zeta_j^b(\Phi)$, and we call this the brane localized flux (BLF). Finally, L_{SM}^b represents any matter that is localized to the brane, such as the Standard Model particles, which can couple to the bulk fields in nontrivial ways.

The most obvious reason for including a brane is that the Standard Model needs a 4D arena in which to interact and propagate. There is no experimental evidence that the Standard Model particles live in any more than four dimensions, and the simplest way to accommodate this fact is to assume the Standard Model is localized on a brane. However, the effects of branes on the surrounding geometry, or their back-reaction, is poorly understood in all but the simplest cases. There are a number of technical issues associated with higher codimension branes. This includes the unambiguous determination of their back-reaction effects on the bulk fields, and the need to regularize and renormalize divergences that arise because the bulk fields formally diverge at the position of the branes. This is illustrated in the later sections with a simple examples, and much of this thesis is devoted to resolving such issues.

2.3 Bulk field equations and Einstein equations

Away from the localized sources, the field equations for the bulk scalars read as follows

$$\frac{1}{\sqrt{-g}} \partial_M (\sqrt{-g} \mathcal{H}_c \partial^M \Phi_c) = \mathcal{H}_c e_c^2 A_c^M A_M^c \Phi_c + \sum_{d,f} \frac{1}{4} \left(\frac{\partial \mathcal{F}_f^d}{\partial \Phi_c} \right) \mathcal{A}_d^{MN} \mathcal{A}_{MN}^f + \frac{\partial V}{\partial \Phi_c}. \quad (2.9)$$

Similarly, the bulk gauge field equations read

$$\sum_c \frac{1}{\sqrt{-g}} \partial_M (\sqrt{-g} \mathcal{F}_d^c \mathcal{A}_c^{MN}) = \mathcal{H}_d e_d^2 A_d^N \Phi_d^2. \quad (2.10)$$

For six dimensional models to be phenomenologically viable, the two extra dimensions are usually assumed to be compactified, while four dimensions are infinite in extent. In what follows, we will seek solutions to the field equations that are maximally symmetric in the 4 macroscopic dimensions spanned by x^μ , and axially symmetric in the 2 transverse (extra) dimensions spanned by y^m . We consider geometries surrounding codimension-2 sources whose location defines the points of axial symmetry, and the fields are assumed to depend only on the proper distance, ρ , from these points. For the scalars, this means $\Phi^c = \Phi^c(\rho)$, and the only nonzero components of the gauge field strengths are assumed to lie in the transverse two directions: $\mathcal{A}_{MN}^c = \delta_M^m \delta_N^n \mathcal{A}_{mn}^c(\rho)$. The most general metric ansatz consistent with this symmetry can be written as follows

$$ds^2 = W^2(\rho) \check{g}_{\mu\nu}(x) dx^\mu dx^\nu + B^2(\rho) d\theta^2 + d\rho^2, \quad (2.11)$$

where $\check{g}_{\mu\nu}$ is the maximally symmetric metric on 4D spacetime.

There are a number of curvatures that can be built from this metric. Because the metric is block diagonal, the full Ricci tensor can be expanded as follows

$$\mathcal{R}_{MN} dx^M dx^N = \mathcal{R}_{\mu\nu} dx^\mu dx^\nu + \mathcal{R}_{mn} dy^m dy^n, \quad (2.12)$$

and the 4D components of the full Ricci tensor are related to the Ricci tensor $\check{R}_{\mu\nu}$ of

the metric $\check{g}_{\mu\nu}$ by

$$\mathcal{R}_{\mu\nu} = \check{R}_{\mu\nu} + g^{mn} \left[(d-1) \partial_m W \partial_n W + W \nabla_m \nabla_n W \right] \check{g}_{\mu\nu}, \quad (2.13)$$

where ∇ is the 2D covariant derivative built from g_{mn} .

As noted in §1.5, an attractive feature of higher dimensional models is that the 4D curvature depends on the transverse stress energy, and not the energy along four dimensions. This can be seen directly from the Einstein equations, and for the system and ansatz of interest, eq. (1.32) rewrites as an expression for the 4D curvature

$$\frac{\check{R}}{W^2} + \frac{4}{BW^4} \left(BW^3 W' \right)' = \kappa^2 \left[2L_{\text{gge}} - 2V + (T_{(b)})^\rho{}_\rho + (T_{(b)})^\theta{}_\theta \right], \quad (2.14)$$

where $T_{(b)}$ represents the stress-energy coming from the branes. Integrating this field equation over $\int d^2 y W^4 B$ gives a simple expression for the 4D curvature

$$\frac{\check{R}}{\kappa_4^2} = \int d^2 y W^4 B \left[2L_{\text{gge}} - 2V + (T_{(b)})^\rho{}_\rho + (T_{(b)})^\theta{}_\theta \right], \quad (2.15)$$

where the boundary contributions coming from the integral of the total derivative are assumed (for now) to vanish. In this expression we define

$$\frac{1}{\kappa_4^2} = \frac{1}{\kappa^2} \int d^2 y W^2 B, \quad (2.16)$$

and we will see that this quantity controls the strength of the gravitational coupling in the 4D effective theory describing these systems. As noted in the previous chapter, consistency with well-understood 4D gravitational physics requires $\kappa_4^2 = 8\pi G_N$ where G_N is Newton's constant.

The right hand side of (2.15) allows us to identify each of the contributions to the 4D curvature. The curvature is generically receives a contribution from the integrated bulk energy densities, which are of size m_B^4 where m_B is the characteristic mass scale of the bulk physics. The simplest and most natural assumption is that the bulk scale is near the higher dimensional gravity scale $m_B^2 \sim \kappa^{-1}$ which could lie in the phenomenologically favoured region $\kappa^{-1} \sim (10 \text{ TeV})^2$.

The other contributions to the curvature come from the transverse stress-energy of the branes. A democratic (though perhaps naive) assumption is that the size of these contributions is set by the characteristic brane mass scale, which is given by its tension T_0 . As the constant part of the 4D Standard Model lagrangian, the tension is synonymous with the c_0 term that was described in the previous chapter. As such, it would be sensitive to higher energy physics and it is reasonable to expect the tension to lie near the higher dimensional gravity scale $T_0 \sim \kappa^{-2}$.

This is the generic situation, and a reiteration of the cosmological constant problem: the generic contributions to the 4D curvature are at least as large as the electroweak scale, and very likely as large as some much heavier mass scale, modulo extraordinary fine tuning. These contributions must be suppressed if these models are to make progress on this problem. We now describe the prospects for achieving such a suppression, and the obstacles.

2.4 Scale invariance and curvature

The bulk contributions to \check{R} in (2.15) can be made to vanish by symmetry. To see how, we assume there are no branes, and we suppose that there exists a field

transformation that scales the bulk Lagrangian by some power of a constant:

$$L_{\text{bulk}} \rightarrow s^p L_{\text{bulk}} . \quad (2.17)$$

The action and Lagrangian are not invariant under this transformation, but it does leave the classical field equations unchanged, so we call this property of the bulk scale invariance. Such a scaling symmetry is strong enough to ensure that the 4D curvature vanishes classically, as will be shown here explicitly.

For simplicity, we assume that the symmetry transformation in (2.17) involves a rescaling of the metric

$$g_{MN} \rightarrow s g_{MN} . \quad (2.18)$$

This implies that the Einstein-Hilbert term in (2.1) transforms as follows under the symmetry transformation

$$L_{EH} \rightarrow s^{-1} L_{EH} , \quad (2.19)$$

which gives $p = -1$. In this case, the other fields must transform under the symmetry in a way that ensures the following identities hold:

$$V \rightarrow s^{-1} V \quad \mathcal{F}^c_d \mathcal{A}^c_{MN} \mathcal{A}^d_{PQ} \rightarrow s \mathcal{F}^c_d \mathcal{A}^c_{MN} \mathcal{A}^d_{PQ} \quad \mathcal{D}_M \Phi^c \rightarrow \mathcal{D}_M \Phi^c . \quad (2.20)$$

This guarantees $L_{\text{bulk}} \rightarrow s^{-1} L_{\text{bulk}}$, once the metric factors are taken into account.

To relate this symmetry to the 4D curvature, we now suppose that the matter fields are varied within the action such that (2.20) holds, while the metric is held fixed

$$S' = - \int d^6 x \sqrt{-g} [L_{EH} + s L_{\text{gge}} + L_{\text{kin}} + L_{\text{gm}} + s^{-1} V] . \quad (2.21)$$

The stationarity of the action with respect to this particular field variation gives

$$\left(\frac{dS'}{ds}\right)_{s=1} = \int d^2y W^4 B [L_{\text{gge}} - V] = 0, \quad (2.22)$$

and this result can be read as an identity that will be satisfied by solutions to the classical field equations. Vanishing 4D curvature, $\check{R} = 0$, follows immediately when this result is combined with (2.15) in the absence of branes.

The addition of branes complicates this story in many ways. The most obvious complication is that branes also contribute to the 4D curvature as in (2.14) and it is unclear whether a brane scale symmetry can be used to ensure these contributions vanish. The next-to-leading complication is how the addition of branes might spoil the cancellation between bulk terms in (2.22). It is possible that back reaction changes the solutions to the field equations in a way that no longer accommodates the cancellation between the bulk potential and gauge kinetic terms. Similarly, in going from (2.14) to (2.15), it was necessary to assume that boundary derivatives of bulk metric fields vanished. However, branes generically modify the boundary conditions of bulk fields near the brane position, and their presence might invalidate the argument. Understanding how the branes effect 4D curvature of these models hinges on understanding how they back-react on the bulk fields, and their transverse stress energy. However, neither of these issues is straightforward, and we now turn to the issues associated with branes.

2.5 Brane sources and boundary conditions

In general, localized sources modify the near-source derivative (i.e. the boundary conditions) of bulk fields in a way that is controlled by the source action. This is well-understood for sources of codimension-1, where tools like the Israel junction conditions [2] are well-developed, and even a straightforward treatment of the source with a delta function is sufficient. To cut our teeth on brane back-reaction, generalizations of the junction condition and delta function procedures are presented below for a simple codimension-2 brane coupled to a scalar field. More complicated setups are then investigated, where inconsistencies arise. These highlight the need for a better model of localized sources that is precise enough to resolve these issues.

2.5.1 Simple example

For the purposes of illustrating how branes effect bulk fields, we can study a simple example where gravity is trivial by choosing $\kappa = 0$. In this case, the Einstein equations are solved by the flat metric

$$\mathcal{G}_{MN} = 0 \quad \implies \quad g_{MN} = \eta_{MN} . \quad (2.23)$$

It follows that the metric fields in (2.11) are given by $B(\rho) = \rho$ and $W = 1$ while the 4D metric is flat $\check{g}_{\mu\nu} = \eta_{\mu\nu}$.

To consider a single free scalar field coupled to a bulk gauge field ($N = 1$) through the gauge kinetic function, we set $V = e = 0$ and $\mathcal{H}_1 = 1$ with $\mathcal{F}_1 = e^{a\Phi}$ where a is

some dimensionful parameter. The bulk action simplifies

$$S_{\text{bulk}} = - \int d^6x \sqrt{-g} \left[\frac{1}{2} \partial_M \Phi \partial^M \Phi + \frac{e^{a\Phi}}{4} \mathcal{A}_{MN} \mathcal{A}^{MN} \right]. \quad (2.24)$$

As a simple example, we source the scalar field by a single brane with Φ -dependent tension

$$S_{\text{brane}} = - \int d^4x T_0(\Phi_b) = - \int d^4x \sqrt{-\gamma} \left[\tau_0 + \mu_\Phi^2 \Phi(y_b) + \frac{\lambda_2}{2} \Phi^2(y_b) \right], \quad (2.25)$$

where the second equality rewrites the tension as the most general, renormalizable function of Φ . For now, we assume there is no localized flux but we will revisit this issue shortly.

Codimension-1 branes

There are two popular ways to derive the effects of the codimension-2 brane action of (2.25) on the scalar field equations. The first approach [3] is to promote the codimension-2 brane action to a codimension-1 action on the small cylinder $|y - y_b| = \epsilon$ as follows

$$\hat{S}_{\text{brane}} = -\epsilon \int d^4x d\theta \left[\tau_0^\epsilon + (\mu_\Phi^\epsilon)^2 \Phi_\epsilon + \frac{\lambda_2^\epsilon}{2} \Phi_\epsilon^2 \right], \quad (2.26)$$

where coordinates have been chosen so that the brane is located at $y_b = 0$. In this expression, the factor ϵ comes from the determinant of the induced metric and the bulk scalar is evaluated at the position of the cylinder $\Phi_\epsilon = \Phi(x, \epsilon, \theta)$. Couplings with an ϵ script are new couplings defined on the codimension-1 brane, in analogy with the quantities in (2.25).

This action is chosen because it dimensionally reduces to the original codimension-2 action. The Kaluza-Klein modes of Φ_ϵ in the θ direction acquire a mass n/ϵ so all but the $n = 0$ modes decouple for arbitrarily small ϵ . The surviving $n = 0$ modes have constant profiles in the coordinate θ that we normalize to unity, giving

$$\hat{S}_{\text{brane}} = -2\pi\epsilon \int d^4x \left[\tau_0^\epsilon + (\mu_\Phi^\epsilon)^2 \Phi(y_b) + \frac{\lambda_2^\epsilon}{2} \Phi^2(y_b) \right], \quad (2.27)$$

where we have identified the value of the bulk scalar field at the position of the codimension-2 brane $\Phi(y_b)$ with the angular zero modes of the Φ_ϵ . Matching to the action in (2.25) therefore requires

$$2\pi\epsilon\tau_0^\epsilon = \tau_0 \quad 2\pi\epsilon(\mu_\Phi^\epsilon)^2 = \mu_\Phi^2 \quad 2\pi\epsilon\lambda_2^\epsilon = \lambda_2. \quad (2.28)$$

Having matched the codimension-1 action to the original theory, it can be used to derive a boundary condition for Φ . The variation of (2.24) gives a contribution on the cylinder at $\rho = \epsilon$,

$$\delta S_{\text{bulk}} \supset \int d^4x d\theta \delta\Phi_\epsilon (\rho\partial_\rho\Phi)_{\rho=\epsilon}, \quad (2.29)$$

and this must vanish when combined with the variation of the codimension-1 action in (2.26), giving the boundary condition

$$-(\rho\partial_\rho\Phi)_{\rho=\epsilon} + \epsilon(\mu_\Phi^\epsilon)^2 + \epsilon\lambda_2^\epsilon\Phi_\epsilon = 0. \quad (2.30)$$

This can be rewritten in terms of the couplings in the codimension-2 action

$$-2\pi(\rho\partial_\rho\Phi)_{y=y_b} + \mu_\Phi^2 + \lambda_2\Phi(y_b) = 0, \quad (2.31)$$

where the $\epsilon \rightarrow 0$ limit was taken. This shows more precisely how the near-source derivative of the bulk scalar field is controlled by the parameters of the Lagrangian (and the value of the field itself for $\lambda_2 \neq 0$). The approach generalizes for more complicated branes and the *matching condition* approach to brane back-reaction posits that the near source derivative of a bulk field is given by the derivative of the brane action

$$2\pi(\rho\partial_\rho\Phi)_{y=y_b} = \frac{\delta S_{\text{brane}}}{\delta\Phi(y_b)}. \quad (2.32)$$

This looks very plausible as a general result, but it does not address subtle questions like which fields should be fixed when taking the derivative of the brane action.

Localizing functions

A less formal approach to understanding codimension-2 brane sources is to simply promote the brane action to a 6D action through the use of a localizing function δ_2 as follows

$$\hat{S}_{\text{brane}} = - \int d^6x \sqrt{-g} T_0(\Phi) \left[\frac{\delta_2(y - y_b)}{\sqrt{g_2}} \right], \quad (2.33)$$

where $g_2 = \det(g_{mn})$ is the determinant of the extra dimensional components of the metric, and the subscript on δ_2 reminds us that it is localized around a point in the two extra dimensions and has mass dimension of two. For convenience, we also define

$$\Delta_2(y - z) = \frac{\delta_2(y - z)}{\sqrt{g_2}}. \quad (2.34)$$

In order for (2.33) to reproduce the original brane action, the localizing function must satisfy

$$\int d^2y \delta_2(y - z) F(x, y) = F(x, z), \quad (2.35)$$

and the most obvious choice for such a function is a delta function. The promoted brane action is treated like any other term in the 6D action, and appears in the scalar field equation as follows

$$\square\Phi = \frac{ae^{a\Phi}}{4} \mathcal{A}_{MN} \mathcal{A}^{MN} + T'_0(\Phi) \Delta_2(y - y_b), \quad (2.36)$$

where the localizing function is assumed to be independent of the scalar field.

Similar to the matching conditions approach, the effects of the brane tension can be phrased as a condition on the derivative of the scalar field near the source. Such a relation can be found by integrating the scalar field equation over a small region $|y - y_b| < \epsilon$ that surrounds the brane in the limit $\epsilon \rightarrow 0$. This gives

$$\lim_{\epsilon \rightarrow 0} \int_{|y - y_b| < \epsilon} d^2y \sqrt{g_2} \square\Phi = \lim_{\epsilon \rightarrow 0} 2\pi [\rho \partial_\rho \Phi]_{\rho_b}^{\rho_b + \epsilon} = 2\pi (\rho \partial_\rho \Phi)_{y=y_b} = \mu_\Phi^2 + \lambda_2 \Phi(y_b), \quad (2.37)$$

where the contribution that includes the gauge field is assumed to be smooth and not survive the $\epsilon \rightarrow 0$ limit.

This is the same result as was obtained using the matching condition approach to brane back-reaction, and in most simple cases the two approaches coincide. The codimension-1 brane action (2.26) and localized action (2.33) are really two different UV completions of the original codimension-2 brane, so it is not surprising that they reproduce the same physics at large distances $\rho \gg \epsilon$. However, we now turn to cases

where the correct treatment of a codimension-2 brane is unclear in both of these approaches.

2.5.2 Gravitational inconsistency

The known approaches to codimension-2 brane back reaction are less conclusive in the presence of gravity. A subtlety arises when deciding how δ_2 depends on the fields. In the previous section it proved useful to assume δ_2 was independent of the bulk scalar field, and it is tempting to assume that δ_2 does not depend on the bulk fields at all. However, this assumption is suspicious for the extra-dimensional metric given that $\delta_2(y - z)$ is supposed to discriminate between points based on their proper distance from $y = z$. We now show that this assumption gives rise to contradictory predictions for the near source derivative of the bulk scalar field.

Adopting the metric ansatz of (2.11) gives the following scalar field equation, generalized from (2.36) to account for a dynamical metric

$$\square\Phi = \frac{1}{BW^4} (BW^4\Phi')' = \frac{ae^{a\Phi}}{4} \mathcal{A}_{MN} \mathcal{A}^{MN} + T_0'(\Phi) \Delta_2(y - y_b). \quad (2.38)$$

The associated boundary condition, obtained by integrating over the $\epsilon \rightarrow 0$ region, reads as follows

$$2\pi (BW^4\Phi')_{y=y_b} = (W^4T_0')_{y=y_b}. \quad (2.39)$$

The only assumptions built into this result are that δ_2 is independent of the bulk scalar field, and that the gauge kinetic is not singular enough to contribute to the

boundary condition:

$$\lim_{\epsilon \rightarrow 0} \int_{|y-y_b| < \epsilon} d^2y BW^4 e^{a\Phi} \mathcal{A}_{MN} \mathcal{A}^{MN} = 0. \quad (2.40)$$

Stronger assumptions about the metric dependence of the localizing function are required to derive the Einstein equations, and assuming $\partial\delta_2/\partial g_{MN} = 0$ gives two useful field equations. The first of these follows from the 4D trace of Einstein equations and can be written as follows

$$\frac{\check{R}}{W^2} + \frac{[B(W^4)]'}{BW^4} = \frac{1}{2} \kappa^2 e^{a\Phi} \mathcal{A}_{MN} \mathcal{A}^{MN}. \quad (2.41)$$

The other useful Einstein equation is the $(\rho\rho)$ component because it contains only fields and their first derivatives, and thus furnishes a constraint on their evolution

$$8 \left(\frac{B'W'}{BW} \right) + \frac{\check{R}}{W^2} + 12 \left(\frac{W'}{W} \right)^2 = \kappa^2 (\Phi')^2 + \frac{1}{2} \kappa^2 e^{a\Phi} \mathcal{A}_{MN} \mathcal{A}^{MN}. \quad (2.42)$$

To the extent that one trusts (2.41), then integrating it over the $|y - y_b| < \epsilon$ region gives a trivial boundary condition¹ for the warp factor

$$2\pi [B(W^4)]'_{y=y_b} = 0, \quad (2.43)$$

where it is additionally assumed that the on-brane curvature term is not sufficiently

¹This boundary condition could have alternatively been obtained from the matching conditions approach to back-reaction, if the brane action was assumed to be independent of the transverse metric $\frac{\delta S_{\text{brane}}}{\delta g_{mn}} = 0$.

singular to contribute to the boundary condition:

$$\lim_{\epsilon \rightarrow 0} \int_{|y-y_b| < \epsilon} d^2y BW^4 \left(\frac{\check{R}}{W^2} \right) = 0. \quad (2.44)$$

A problem arises when the boundary condition in (2.43) is combined with the constraint equation in (2.42). Multiplying through by $(W^4B)^2$ and evaluating the constraint in the limit $y \rightarrow y_b$ gives

$$2 \lim_{y \rightarrow y_b} [W^4 B'] [B(W^4)'] + \frac{3}{4} \lim_{y \rightarrow y_b} [B(W^4)']^2 = \kappa^2 \lim_{y \rightarrow y_b} [W^4 B\Phi']^2. \quad (2.45)$$

So this relation, when combined with (2.43), appears to imply

$$2\pi (W^4 B\Phi')_{y=y_b} \stackrel{?}{=} 0. \quad (2.46)$$

This strong result is generally inconsistent with the dilaton boundary condition (2.39) and the most likely origin of the inconsistency is the brane's assumed trivial dependence on the bulk metric. This simple assumption must be discarded,

$$\frac{\delta S_{\text{brane}}}{\delta g_{mn}} \neq 0, \quad (2.47)$$

and a better handle on the brane's metric-dependence, i.e. its transverse stress-energy, is an important step in understanding brane back-reaction, especially since this quantity is one of the leading contributions to the 4D curvature when the bulk is scale invariant.

2.5.3 Localized flux and boundary conditions

The previous section outlined one aspect of brane back-reaction that was rife with ambiguity. We now show that even in flat space ($\kappa = 0$), there are obstacles to understanding codimension-2 brane back-reaction when a brane carries localized flux, as follows

$$S_{\text{brane}} = - \int d^4x \left[\tau_0 + \frac{1}{2} \zeta \epsilon^{mn} \mathcal{A}_{mn} \right]. \quad (2.48)$$

Here, $\epsilon^{mn} \mathcal{A}_{mn} = 2\rho^{-1} \partial_\rho \mathcal{A}_\theta$ in a flat bulk parameterized with cylindrical coordinates. So, in the presence of flux, the brane couples to the transverse components of the bulk gauge field, but deriving the associated boundary condition for bulk gauge field is not as obvious as it is for a scalar.

Because the variation of the bulk action contains the following boundary term

$$\delta S_{\text{bulk}} \supset \int d^4x \, d\theta \delta \mathcal{A}_\theta \left(\frac{e^{a\Phi}}{\rho} \mathcal{A}_\theta \right)_{y=y_b}, \quad (2.49)$$

a straightforward application of the matching conditions would suggest that the near-brane derivative of the bulk gauge field reads as follows

$$\left(\frac{e^{a\Phi}}{\rho} \partial_\rho \mathcal{A}_\theta \right)_{y=y_b} = \frac{\delta S_{\text{brane}}}{\delta \mathcal{A}_\theta(y_b)}. \quad (2.50)$$

However, it is unclear from this prescription how the variation of the brane action with respect to \mathcal{A}_θ is computed, because its normal derivative, $\partial_\rho \mathcal{A}_\theta$, appears in the action. What is more, it is unclear how to correctly UV complete the localized flux term using a codimension-1 brane. It was deceptively simple to construct the codimension-1 UV completion of the brane action in (2.25) because each term in the

action was constructed from Lorentz scalars. However, there is no obvious Lorentz invariant codimension-1 quantity that gives rise to a localized flux term $\propto \epsilon^{mn} \mathcal{A}_{mn}$.

The localizing function approach to UV completing the brane action suggests that it should be replaced with the following 6D action

$$\hat{S}_{\text{brane}} = - \int d^6x \sqrt{-g} \left[\tau_0 + \frac{1}{2} \zeta \epsilon^{mn} \mathcal{A}_{mn} \right] \Delta_2(y - y_b). \quad (2.51)$$

In this approach, the transverse components of the bulk gauge field satisfy the following field equation

$$\partial_\rho \left[\frac{e^{a\Phi} \mathcal{A}_{\rho\theta}}{\rho} + \zeta \Delta_2(y - y_b) \right] = 0. \quad (2.52)$$

This can be integrated to give

$$e^{a\Phi} \mathcal{A}_{\rho\theta} + \zeta \delta_2(y - y_b) = Q\rho, \quad (2.53)$$

where Q is an integration constant. Finally, a boundary condition for the bulk gauge field can be found by integrating this solution over a region $|y - y_b| < \epsilon$ in the $\epsilon \rightarrow 0$ limit, which gives

$$2\pi (e^{a\Phi} \mathcal{A}_\theta)_{y=y_b} + \zeta = 0. \quad (2.54)$$

This is not the usual relation between a bulk field's derivative near the brane and the brane properties. It is also not gauge invariant. Indeed, a more instructive way to understand the effects of the localized flux on the gauge field is to note that

$$\int_{|y-y_b|<\epsilon} d^2y \mathcal{A}_{\rho\theta} = -e^{-a\Phi} \zeta, \quad (2.55)$$

from which we conclude that the flux in the localized region around the brane is nonvanishing, and controlled by ζ .

An issue arises because the bulk gauge field strength is singular near the brane, and this feeds into the scalar field equation, which can be written as follows

$$\square\Phi = \frac{ae^{a\Phi}}{4}\mathcal{A}_{MN}\mathcal{A}^{MN} = \frac{1}{2}Q^2ae^{-a\Phi} - Qae^{-a\Phi}\zeta\Delta_2 + \frac{1}{2}\zeta^2ae^{-a\Phi}\Delta_2^2. \quad (2.56)$$

Integrating over the usual $\epsilon \rightarrow 0$ region then gives the following boundary condition for the scalar field

$$2\pi(e^{a\Phi}\rho\partial_\rho\Phi)_{y_b} + Qa\zeta - \frac{1}{2}\zeta^2a\Delta_2(0) = 0. \quad (2.57)$$

This boundary condition is problematic for a number of reasons. First, it appears to be sensitive to the value of the localizing function at the origin $\Delta_2(0)$, which is supposed to be an arbitrary, unphysical quantity. Furthermore, for the most straightforward localizing function – a delta function – this quantity is highly divergent

$$\Delta_2(0) = \lim_{\rho \rightarrow 0} \frac{\delta_2(\rho)}{\rho}. \quad (2.58)$$

Finally, the boundary condition for the bulk scalar field coming from the localizing function approach (2.57) is very different from the same quantity calculated using the matching conditions approach. Since the brane has no explicit couplings to the bulk scalar, a straightforward application of the the matching conditions predicts

$$2\pi(\rho\partial_\rho\Phi)_{y=y_b} = \frac{\delta S_{\text{brane}}}{\delta\Phi(y_b)} = 0. \quad (2.59)$$

Similar to the gravitational inconsistency of the previous section, the scalar's near-source derivative appears to take two different values, depending on how it is calculated. As we will see, the size of this derivative is closely tied to the size of the 4D curvature in concrete models of interest. So once again, any conclusive statement about the viability of these models as a solution to the cosmological constant problem hinges on resolving this issue.

2.6 Chapter summary

To summarize, there is a large class of 6D models that can be equipped with a scale symmetry which ensures a cancellation between the contributions to the 4D curvature, at least in the absence of branes. The addition of branes may change this story drastically, by modifying the solutions to the bulk fields equations, and by acting as new sources of curvature. However, the branes' back-reaction on bulk fields is poorly-understood in many cases, and entangled with the issue of their dependence on the bulk metric, i.e. their transverse stress energy. The known approaches to brane back-reaction each fail in certain cases, and better technology is necessary to tackle these issues. Progress on these issues is presented in the upcoming chapters.

Bibliography

- [1] B. Holdom, “Two U(1)’s and Epsilon Charge Shifts,” *Phys. Lett. B* **166**, 196 (1986).
- [2] W. Israel, “Singular hypersurfaces and thin shells in general relativity,” *Nuovo Cim. B* **44S10**, 1 (1966) [*Nuovo Cim. B* **48**, 463 (1967)] [*Nuovo Cim. B* **44**, 1 (1966)].
- [3] C. P. Burgess, D. Hoover, C. de Rham and G. Tasinato, “Effective Field Theories and Matching for Codimension-2 Branes,” *JHEP* **0903**, 124 (2009) [arXiv:0812.3820 [hep-th]].

Chapter 3

Dark vortices

This chapter is a condensed version of the following paper

C. P. Burgess, R. Diener and M. Williams, “The Gravity of Dark Vortices: Effective Field Theory for Branes and Strings Carrying Localized Flux,” JHEP 1511 049 (2015), arXiv:1506.08095

Most of this chapter’s content is taken verbatim from this reference. However, some notation was modified, and the wording was revised to better fit within this thesis. Part of the paper’s content was also omitted for clarity, brevity and to avoid redundancies within this thesis.

In the context of this thesis, the primary result of this chapter is that a Nielsen-Olesen vortex can act as a UV completion of a brane that carries flux. These vortices arise as solutions to the field equations of the symmetry breaking Abelian-Higgs model, where the $U(1)$ gauge symmetry is restored in a localized region, and this field configuration is topologically stable with quantized internal flux. Although vortices usually expel external flux, we show that it is possible to endow an external gauge

field with some flux that is localized in the vortex region by kinetically mixing the internal gauge field of the vortex with the external field. The low-energy description of this phenomenon is brane-localized flux.

The gravitational properties of such a vortex are studied analytically and numerically in this chapter, and the results lay the foundation for understanding how branes with localized flux back-react on the bulk fields to which they couple, because branes must capture the physics of the vortices at low energies. So the explicit and unambiguous UV completion of branes with vortices provides a laboratory in which to study the back-reaction of localized codimension-2 objects. One of the more surprising results is that localized flux does not gravitate. More precisely, the gravitational field equations are always insensitive to the amount of external flux that is localized on the vortex (or brane). The only effect of localizing external flux to the source is that the tension of the vortex (or brane) is renormalized in a simple manner.

This result is easy to understand in the vortex picture, where the gauge kinetic mixing (which was required to endow the vortex with localized flux) can be diagonalized so that one gauge field carries all of the localized flux, and the other carries all of the external flux. This diagonalization can be absorbed into the vortex gauge couplings, which in turn renormalizes the vortex tension. Within the IR picture, the renormalization of the tension can be associated with the appearance of the divergent quantity $\Delta_2(0)$ and the vortex construction teaches us how to simply regularize and renormalize this divergence. This chapter also describes how to calculate the transverse components of the localized stress energy without making any assumptions about the nature of the localization (i.e. the metric dependence of Δ_2) which is an important step in understanding how branes affect the 4D curvature of

these models.

Beyond this thesis, kinetically mixed ‘dark’ vortices are of phenomenological interest in models with a hidden gauge sector, which are very popular in the dark matter literature.

3.1 Introduction

In this chapter we study the gravitational response of vortices that carry localized amounts of external magnetic flux, called *dark strings* or *dark vortices* in the literature [1, 2]. The goal is to understand how their back-reaction influences the transverse geometry through which they move, and the geometry that is induced on their own world-sheet. We find the initially surprising result that the gravitational response of such an object is locally independent of the amount of flux it contains, and show how this can be simply understood.

Motivation

Vortices are among the simplest stable solitons and arise in many theories with spontaneously broken $U(1)$ gauge symmetries [3]. They can arise cosmologically as relics of epochs when the universe passes through symmetry-breaking phase transitions. Such cosmic strings are widely studied [4] because, unlike other types of cosmic defects, they need not be poisonous for later cosmology since the resulting cosmic tangle tends not to come to dominate the energy density in a problematic way.

In the simplest models a vortex defines a region outside of which the $U(1)$ symmetry breaks while inside it remains (relatively) unbroken, and as a result all magnetic $U(1)$ flux is confined to lie completely within the vortex interior. However in theories

with more than one $U(1)$ factor more complicated patterns can also exist, for which magnetic fields outside the vortex can also acquire a localized intra-vortex component. Such vortices naturally arise in ‘dark photon’ models [5], for which the ordinary photon mixes kinetically [6] with a second, spontaneously broken, $U(1)$ gauge field (as have been widely studied as dark matter candidates [7]). Cosmic strings of this type could carry localized ordinary magnetic flux, even though the $U(1)_{EM}$ gauge group remains unbroken [1, 2].

Of most interest are parameters where the transverse thickness of the vortex is much smaller than the characteristic size of the geometry transverse to the source. In such situations only a few vortex properties are important, including the tension (energy per unit length) and the amount of flux localized on the vortex (or more generally brane-localized flux, or BLF for short). Indeed these two quantities, call them T_0 and ζ , provide the coefficients of the leading terms in any derivative expansion of an effective string (or brane) action describing a vortex. More explicitly,

$$S_{\text{brane}} = -T_0 \int \omega + \zeta \int \star A + \dots, \quad (3.1)$$

where ω is the volume form of the codimension-two surface and $\star A$ is the Hodge dual of the $U(1)$ field strength, $A_{MN} = \partial_M A_N - \partial_N A_M$, which has some of its flux localized to the brane. These are the leading terms inasmuch as all terms represented by the ellipses involve two or more derivatives.¹ In four dimensions both ω and $\star A$ are 2-forms and so can be covariantly integrated over the 2-dimensional world-sheet of a cosmic string, while in $D = d + 2$ dimensions they are d forms that

¹A single-derivative term involving the world-sheet extrinsic curvature is also possible, but our focus here is on straight motionless vortices.

can be integrated over the d -dimensional world volume of a codimension-2 surface.² Previous workers have studied gravitational response in the absence of brane-localized flux [8], but our particular interest is on how ζ competes with T_0 to influence the surrounding geometry. Our analysis extends recent numerical studies [2] of gravitating dark strings, and includes in particular an effective field theory analysis of the BLF term and its gravitational properties.

Besides being of practical interest for dark photon models, part of our motivation for this study also comes from brane-world models within which the familiar particles of the Standard Model reside on a 3+1 dimensional brane within a higher-dimensional space.³ Comparatively little is known about how higher-codimension branes situated within compact extra dimensions back-react gravitationally to influence their surrounding geometries,⁴ and codimension-2 objects provide a simple nontrivial starting point for doing so. In particular, a key question in any such model is what stabilizes the size and shape of the transverse compact dimensions, and this is a question whose understanding can hinge on understanding how the geometry responds to the presence of the branes. Since long-range inter-brane forces vary only logarithmically in two transverse dimensions, they do not fall off with distance and so brane back-reaction and inter-brane forces are comparatively more important for codimension-2 objects than they are with more codimensions.

Furthermore, several mechanisms are known for stabilizing extra dimensions, and the main ones involve balancing inter-brane gravitational forces against the cost of distorting extra-dimensional cycles wrapped by branes or threaded by topological

²That is, a brane with precisely two transverse off-brane dimensions.

³Our restriction to codimension-2 branes makes $d = 4$ and $D = 6$ the most interesting case of this type [9].

⁴By contrast, back-reaction is fairly well-explored for codimension-1 objects due to the extensive study of Randall-Sundrum models [10].

fluxes [11, 12, 13, 14, 15]. Since brane-localized flux is the leading way fluxes and uncharged branes directly couple to one another, BLF is crucial for understanding how flux-carrying vortices interact with one another and their transverse environment. Localized flux has recently also been recognized to play a role in the stability of compact geometries [16].

Finally, the fact that cosmic strings can have flat world-sheets for any value of their string tension [8] has been used to suggest [17, 18] they may contain the seeds of a mechanism for understanding the cosmological constant problem [19]. But a solution to the cosmological constant problem involves also understanding how the curvature of the world-sheet varies as its tension and other properties vary. This requires a critical study of how codimension-2 objects back-react onto their own induced geometry, such as we give here. Although extra-dimensional branes are not in themselves expected to be sufficient to provide a solution (for instance, one must also deal with the higher-dimensional cosmological constant), the techniques developed here can also be applied to their supersymmetric alternatives [20], for which higher-derivative cosmological constants are forbidden by symmetry and whose ultimate prospects remain open at this point. This appears in subsequent chapters.

Results

Our study leads to the following result about brane back-reaction: *brane-localized flux does not gravitate*. It is most intuitively understood when it is the dual field $F = \star A$ that is held fixed when varying the metric, since in this case the BLF term $S_{BLF} = \zeta_b \int F$ is metric-independent. We show how the same result can also be seen

when A is fixed; and more precisely show that the BLF term of (3.1) induces a universal renormalization of the brane's tension and the brane gravitational response is governed only by the total tension including this renormalization. This renormalization is universal in the sense that it does not depend on the size of any macroscopic magnetic field in which the brane may sit.

Of course the BLF term *does* contribute to the external Maxwell equations, generating a flux localized at the brane position with size proportional to ζ . Among other things this ensures that a test charge that moves around the brane acquires the Aharonov-Bohm phase implied by the localized flux. But the gravitational influence of BLF is precisely cancelled by the back-reaction of the Maxwell field. That is, the brane endows the bulk Maxwell field strength with a localized component, and the stress-energy associated with this localized component exactly cancels against the stress-energy associated with the BLF term of the brane. Since an external macroscopic observer cannot resolve the energy of the brane-localized BLF term from the energy of the localized magnetic field to which it gives rise, macroscopic external gravitational measurements only see their sum, which is zero.

This failure of the BLF term to gravitate has important implications for the curvature that is induced on the vortex world-sheet. To see why, consider the trace-reversed Einstein equations in $D = d + 2$ dimensions, which state

$$\mathcal{R}_{MN} + \kappa^2 \left(T_{MN} + \frac{1}{d} g_{MN} T^P{}_P \right) = 0. \quad (3.2)$$

What is special about this equation is that the factor of $1/d$ ensures that the on-brane stress-energy often drops out of the expression for the on-brane curvature, which is

instead governed purely by the *off*-brane stress energy

$$-g^{\mu\nu}\mathcal{R}_{\mu\nu} = \kappa^2 g^{mn}T_{mn}. \quad (3.3)$$

Consequently it is of particular interest to know when T_{mn} vanishes for some reasonable choice of brane lagrangian.

The off-brane stress-energy would vanish in particular when the brane action is dominated by its tension

$$T_{\mu\nu} = T_0 g_{\mu\nu} \frac{\delta_2(y - y_b)}{\sqrt{g_2}}, \quad (3.4)$$

where $\delta_2(y - y_b)$ is some sort of regularized delta-like function with support only at the brane position. But the derivation of (3.4) from (3.1) is complicated by two issues: is there a dependence on the transverse metric hidden in the regularized $\delta_2(y)$ (which is designed, after all, to discriminate based on proper distance from the vortex); and (for flux-containing branes) what of the metrics appearing in the Hodge dual, $\star A$, of the BLF term?

The results found here imply these two issues are not obstructions to deriving (3.4) from (3.1), as long as tension in question is appropriately renormalized. They do this in two ways. First they show how T_{mn} can be derived without ad-hoc assumptions about the metric-dependence of $\delta_2(y)$. Second, they show that the apparent dependence of the BLF terms on the transverse metric components, g_{mn} , is an illusion, because it is completely cancelled by a similar dependence in the gauge-field back-reaction.

The remainder of this paper shows how this works in detail. We use three different techniques to do so.

- The first works within a UV completion of the BLF brane by a dark vortex, for which we explicitly solve all field equations for a system that allows Nielsen-Olesen type vortex solutions. In this construction the localized flux arises if there is a kinetic mixing, $\varepsilon Z_{MN} A^{MN}$, between the $U(1)$ gauge field, Z_M , of the Nielsen-Olesen vortex, and the external gauge field, A_M , whose flux is to be localized. In this case the mixing of the two gauge fields can be diagonalized explicitly, leading to the advertised cancellation of the BLF coupling as well as a renormalization of the Z_M gauge coupling, $e^2 \rightarrow \hat{e}^2 = e^2/(1 - \varepsilon^2)$.
- Second, we compute the couplings T_0 and ζ of the effective codimension-2 action for the vortex in the limit where the length scales of the transverse geometry are much larger than the vortex size. This has the form of (3.1), with $\zeta \propto \varepsilon/e$. We verify that it reproduces the physics of the full UV theory, including in particular the cancellation of BLF gravitational interaction and the renormalization of the brane tension quadratically in ζ .
- Finally we compare both of these approaches to explicit numerical calculations of the metric-vortex profiles as functions of the various external parameters, to test the robustness of our results.

A road map

The remainder of the chapter is organized as follows.

First, §3.2 describes the action and field equations for the microscopic (or UV) system of interest. This consists of a ‘bulk’ sector (the metric plus a gauge field, A_M) coupled to a ‘vortex’ sector (a charged scalar, Ψ , and a second gauge field, Z_M). The vortex sector is designed to support Nielsen-Olesen vortices and these provide the

microscopic picture of how the codimension-2 objects arise.

Solutions to the field equations describing a single isolated vortex are then described in detail in §3.3, including both analytic and numerical results for the field profiles. The logic of this section is to integrate the field equations in the radial direction, starting from initial conditions at the centre of the vortex and working our way out. The goal is to compute the values of the fields and their first derivatives just outside the vortex. The resulting formulae provide the initial data for further integration into the bulk, and are efficiently captured through their implications for the asymptotic near-vortex form of the bulk solutions, described in §3.3.3. In §3.3.4 these expressions for the near-vortex fields and derivatives are also used to match with the effective description of (3.1) to infer expressions for T_0 and ζ in terms of microscopic parameters. Finally, §3.4 summarizes our results and describes several open directions.

3.2 The system of interest

We start by outlining the action and field equations for the system of interest. Our system consists of an Einstein-Maxwell system (the ‘bulk’) coupled to a ‘vortex’ — or ‘brane’ — sector, consisting of a complex scalar coupled to a second $U(1)$ gauge field. For generality we imagine both of these systems live in $D = d + 2$ spacetime dimensions, though the most interesting cases of practical interest are the cosmic string [with $(D, d) = (4, 2)$] and the brane-world picture [with $(D, d) = (6, 4)$].

3.2.1 The action and field equations

The action of interest is $S = S_B + S_v$ with bulk action given by

$$\begin{aligned} S_B &= - \int d^{d+2}x \sqrt{-g} \left[\frac{1}{2\kappa^2} g^{MN} \mathcal{R}_{MN} + \frac{1}{4} A_{MN}^2 + \Lambda \right] \\ &=: - \int d^{d+2}x \sqrt{-g} \left(L_{EH} + L_A + \Lambda \right) \end{aligned} \quad (3.5)$$

where $A_{MN} = \partial_M A_N - \partial_N A_M$ is a D -dimensional gauge field strength, \mathcal{R}_{MN} denotes the D -dimensional Ricci tensor and the last line defines the L_i in terms of the corresponding item in the previous line. The vortex part of the action is similarly given by

$$\begin{aligned} S_v &= - \int d^{d+2}x \sqrt{-g} \left[\frac{1}{4} Z_{MN}^2 + \frac{\varepsilon}{2} Z_{MN} A^{MN} + D_M \Psi^* D^M \Psi + \lambda \left(\Psi^* \Psi - \frac{v^2}{2} \right)^2 \right] \\ &=: - \int d^{d+2}x \sqrt{-g} \left(L_Z + L_{\text{mix}} + L_\Psi + V_\Psi \right), \end{aligned} \quad (3.6)$$

where $D_M \Psi := \partial_M \Psi - ieZ_M \Psi$, and the second line again defines the various L_i .

For later purposes it is useful to write $\sqrt{2} \Psi = \psi e^{i\Omega}$ and adopt a unitary gauge for which the phase, Ω , is set to zero, though this gauge will prove to be singular at the origin of the vortex solutions we examine later. In this gauge the term L_Ψ in S_v can be written

$$L_\Psi = D_M \Psi^* D^M \Psi = \frac{1}{2} \left(\partial_M \psi \partial^M \psi + e^2 \psi^2 Z_M Z^M \right), \quad (3.7)$$

and the potential becomes

$$V_\psi = \frac{\lambda}{4} \left(\psi^2 - v^2 \right)^2. \quad (3.8)$$

Field equations

We now adopt the symmetry ansatz of (2.11) and specialize the results of that section to the Lagrangians of (3.5) and (3.6). This gives the following gauge field equation

$$\left(\frac{W^d \check{A}'_\theta}{B}\right)' = 0, \quad (3.9)$$

and

$$\frac{1 - \varepsilon^2}{BW^d} \left(\frac{W^d Z'_\theta}{B}\right)' = \frac{e^2 \psi^2 Z_\theta}{B^2}, \quad (3.10)$$

where primes denote differentiation with respect to proper distance, ρ , and we define the mixed gauge field,

$$\check{A}_M := A_M + \varepsilon Z_M. \quad (3.11)$$

Notice that the off-diagonal contribution to L_{gge} vanishes when this is expressed in terms of \check{A}_M rather than A_M , since

$$L_{\text{gge}} = L_A + L_Z + L_{\text{mix}} = \check{L}_A + \check{L}_Z, \quad (3.12)$$

where

$$\check{L}_A := \frac{1}{4} \check{A}_{mn} \check{A}^{mn} \quad \text{and} \quad \check{L}_Z := \frac{1}{4} (1 - \varepsilon^2) Z_{mn} Z^{mn}. \quad (3.13)$$

Notice also that (3.10) has the same form as it would have had in the absence of the $A - Z$ mixing, (3.11), provided we make the replacement $e^2 \rightarrow \hat{e}^2$, with

$$\hat{e}^2 := \frac{e^2}{1 - \varepsilon^2}. \quad (3.14)$$

Clearly stability requires the gauge mixing parameter must satisfy $\varepsilon^2 < 1$ and semi-classical methods require us to stay away from the upper limit. The field equation for $\psi(\rho)$ similarly simplifies to

$$\frac{1}{BW^d} \left(BW^d \psi' \right)' = e^2 \psi \left(\frac{Z_\theta}{B} \right)^2 + \lambda \psi \left(\psi^2 - v^2 \right). \quad (3.15)$$

Einstein equations

The nontrivial components of the matter stress-energy become

$$T_{\mu\nu} = -g_{\mu\nu} \varrho_{\text{tot}}, \quad T^\rho{}_\rho = \mathcal{Z} - \mathcal{X} \quad T^\theta{}_\theta = -(\mathcal{Z} + \mathcal{X}), \quad (3.16)$$

where

$$\varrho := L_{\text{kin}} + L_{\text{gm}} + L_{\text{pot}} + L_{\text{gge}}, \quad (3.17)$$

and

$$\mathcal{X} := L_{\text{pot}} - L_{\text{gge}} \quad \mathcal{Z} := L_{\text{kin}} - L_{\text{gm}}. \quad (3.18)$$

In later sections it is useful to split $\varrho = \varrho_{\text{loc}} + \check{\varrho}_B$, $\mathcal{X} = \mathcal{X}_{\text{loc}} + \check{\mathcal{X}}_B$ and $\mathcal{Z} = \mathcal{Z}_{\text{loc}} + \mathcal{Z}_B$ into vortex and bulk parts. We define the following bulk stress-energies

$$\begin{aligned} \check{\varrho}_B &:= \Lambda + \check{L}_A \\ \check{\mathcal{X}}_B &:= \Lambda - \check{L}_A \\ \mathcal{Z}_B &:= 0 \end{aligned} \quad (3.19)$$

And the localized stress energies are defined as follows

$$\begin{aligned}
\varrho_{\text{loc}} &:= L_{\text{kin}} + L_{\text{gm}} + V_{\psi} + \check{L}_Z \\
\mathcal{X}_{\text{loc}} &:= V_{\psi} - \check{L}_Z \\
\mathcal{Z}_{\text{loc}} &:= L_{\text{kin}} - L_{\text{gm}} = \mathcal{Z}.
\end{aligned} \tag{3.20}$$

The components of the trace-reversed Einstein equations governing the d -dimensional on-vortex geometry therefore become

$$\mathcal{R}_{\mu\nu} = -\kappa^2 X_{\mu\nu} = -\frac{2}{d} \kappa^2 \mathcal{X} g_{\mu\nu}, \tag{3.21}$$

of which maximal symmetry implies the only nontrivial combination is the trace

$$\mathcal{R}_{(d)} := g^{\mu\nu} \mathcal{R}_{\mu\nu} = \frac{\check{R}}{W^2} + \frac{d}{BW^d} (BW'W^{d-1})' = -2\kappa^2 \mathcal{X}, \tag{3.22}$$

and we use the explicit expression for $\mathcal{R}_{(d)}$ in terms of \check{R} and W . There are two independent Einstein equations dictating the 2-dimensional transverse geometry. One can be taken to be the difference between the transverse Einstein equations

$$\mathcal{G}^{\rho}_{\rho} - \mathcal{G}^{\theta}_{\theta} = \mathcal{R}^{\rho}_{\rho} - \mathcal{R}^{\theta}_{\theta} = -\kappa^2 (T^{\rho}_{\rho} - T^{\theta}_{\theta}). \tag{3.23}$$

Writing out the curvature and stress energy shows this last equation becomes

$$\frac{B}{W} \left(\frac{W'}{B} \right)' = -\frac{2}{d} \kappa^2 \mathcal{Z}. \tag{3.24}$$

Another useful, independent Einstein equation is the $(\theta\theta)$ component of the trace-reversed Einstein equation which reads

$$\frac{(B'W^d)'}{BW^d} = -\kappa^2 \left[\varrho - \mathcal{Z} - \left(1 - \frac{2}{d}\right) \mathcal{X} \right] = -2\kappa^2 \left(L_{\text{gm}} + L_{\text{gge}} + \frac{\mathcal{X}}{d} \right). \quad (3.25)$$

Finally, a linear combination of the above Einstein equations that is not independent, but very useful, is the $(\rho\rho)$ Einstein equation, $\mathcal{G}^\rho{}_\rho = -\kappa^2 T^\rho{}_\rho$, which is special in that all second derivatives with respect to ρ drop out. This leaves the following ‘constraint’ on the initial conditions for the integration in the ρ direction:

$$d \left(\frac{B'W'}{BW} \right) + \frac{\check{R}}{2W^2} + \frac{d(d-1)}{2} \left(\frac{W'}{W} \right)^2 = \kappa^2 (\mathcal{Z} - \mathcal{X}). \quad (3.26)$$

3.2.2 Scales and hierarchies

Before solving these field equations, we first briefly digress to summarize the relevant scales that appear in their solutions. The fundamental parameters of the problem are the gravitational constant, κ ; the gauge couplings, e (for Z_M) and g_A (for A_M); the scalar self-coupling, λ , and the scalar vev v . These have the following engineering dimensions in powers of mass:

$$[\kappa] = 1 - D/2, \quad [e] = [g_A] = 2 - D/2, \quad [\lambda] = 4 - D, \quad \text{and} \quad [v] = D/2 - 1. \quad (3.27)$$

To these must be added the dimensionless parameter, ε , that measures the mixing strength for the two gauge fields.

In terms of these we shall find that the energy density of the vortex is of order

$e^2 v^4$ and this is localized within a region of order

$$r_v = \frac{1}{e v}. \quad (3.28)$$

The effective energy-per-unit-area of the vortex is therefore of order $e^2 v^4 r_v^2 = v^2$. These energies give rise to D -dimensional curvatures within the vortex of order $1/L_v^2 = \kappa^2 e^2 v^4$ and integrated dimensional gravitational effects (like conical defect angles) of order $\kappa^2 v^2$. We work in a regime where $\kappa v \ll 1$ to ensure that the gravitational response to the energy density of the vortex is weak, and so, for example, defect angles are small and $L_v \gg r_v$.

By contrast, far from the vortex the curvature scale in the bulk turns out to be of order $1/r_B^2$ where

$$r_B \sim \frac{\kappa}{g_A}. \quad (3.29)$$

Since our interest is in the regime where the vortex is much smaller than the transverse dimensions we throughout assume $r_v \ll r_B$ and so

$$\frac{g_A}{e} \ll \kappa v \ll 1. \quad (3.30)$$

3.3 Isolated vortices

We now describe some solutions to the above field equations, starting with the local properties of an isolated vortex within a much larger ambient bulk geometry. Our goal is to relate the properties of the vortex to the asymptotic behaviour of the bulk fields and their derivatives outside of (but near to) the vortex itself, with a view to using these as boundary conditions when replacing the vortex with an effective

codimension-2 localized object.

3.3.1 Vortex solutions

For vortex solutions the vortex scalar vanishes at the vortex core $\rho = 0$, and the vortex fields approach their vacuum values, $\psi \rightarrow v$ and⁵ $Z_M \rightarrow 0$, at large ρ . Because we work in the regime $\kappa v \ll 1$ these solutions closely resemble familiar Nielsen-Olesen solutions [3] in the absence of gravitational fields. Our analysis in this section reduces to that of [8] in the limit of no gauge mixing, $\varepsilon = 0$, and a trivial bulk.

The asymptotic approach to the far-field vacuum values can be understood by linearizing the field equations about their vacuum configurations, writing $\psi = v + \delta\psi$ and $Z_\theta = 0 + \delta Z_\theta$. We find in this way that both $\delta\psi$ and δZ_M describe massive particles, with respective masses given by

$$m_Z^2 = \hat{e}^2 v^2 \quad \text{and} \quad m_\psi^2 = 2\lambda v^2. \quad (3.31)$$

From this we expect the approach to asymptopia to be exponentially fast over scales of order $r_Z = m_Z^{-1}$ and $r_\psi = m_\psi^{-1}$. Indeed this expectation is borne out by explicit numerical evaluation.

Notice the two vortex scales are identical, $r_v := r_Z = r_\psi$, in the special BPS case, defined by $\hat{\beta} = 1$ where

$$\hat{\beta} := \hat{e}^2 / 2\lambda, \quad (3.32)$$

and so the BPS case satisfies $\hat{e}^2 = 2\lambda$. For convenience we also define $\beta = e^2 / 2\lambda = (1 - \varepsilon^2)\hat{\beta}$.

⁵In unitary gauge.

Boundary conditions near the origin

We start with a statement of the boundary conditions to be imposed at $\rho = 0$, which express that the transverse metric, g_{mn} , is locally flat and that all vectors (and so in particular the gradients of all scalars) must vanish there. For the metric functions we therefore impose the conditions

$$W(0) = W_0, \quad W'(0) = 0 \quad \text{and} \quad B(0) = 0 \quad \text{and} \quad B'(0) = 1. \quad (3.33)$$

We can choose $W_0 = 1$ by rescaling the d -dimensional coordinates, but this can only be done once so the *change*, ΔW , between the inside and the outside of the vortex (or between the centres of different vortices) is a physical thing to be determined by the field equations. Similarly, for the vortex scalar we demand

$$\psi(0) = \psi'(0) = 0, \quad (3.34)$$

or we could also trade one of these for the demand that $\psi \rightarrow v$ far from the vortex core.

Since \check{A}_{mn} is nonsingular it is regular at $\rho = 0$ and so, since $B(\rho) \simeq \rho$ near $\rho = 0$, we must have $\check{A}_{\rho\theta} \propto \rho$ near the origin. Consequently, in a gauge where $\check{A}_M dx^M = \check{A}_\theta(\rho) d\theta$ we should expect $\check{A}_\theta = \mathcal{O}(\rho^2)$ near the origin. Naively, the same should be true for the other gauge fields A_M and Z_M , however the gauge transformation required to remove the phase everywhere from the order parameter $\Psi = \psi e^{i\Omega}$ (*i.e.* to reach unitary gauge) is singular at the origin, where Ψ vanishes and so Ω becomes ambiguous. Consequently in this gauge Z_θ (and so also A_M) does not vanish near the origin like ρ^2 . Instead, because in this gauge $Z_M \rightarrow 0$ far from the vortex, we see that

flux quantization demands that

$$-\frac{2\pi n}{e} = \Phi_z(\rho < \rho_v) := \oint_{\rho=\rho_v} Z = 2\pi \int_0^{\rho_v} d\rho \partial_\rho Z_\theta = 2\pi [Z_\theta(\rho_v) - Z_\theta(0)] = -2\pi Z_\theta(0), \quad (3.35)$$

where n is an integer, and we choose $\rho = \rho_v$ to be far enough from the vortex that $Z_M \rightarrow 0$ there. We therefore ask Z_θ to satisfy the boundary condition:

$$Z_\theta(0) = \frac{n}{e} \quad \text{and so therefore} \quad A_\theta(0) = -\frac{n\varepsilon}{e}, \quad (3.36)$$

where the second equality follows from $\check{A}_\theta(0) = 0$.

Vortex solutions

It is convenient to normalize the vortex fields

$$Z_\theta = \frac{n}{e} P(\rho) \quad \text{and} \quad \psi = v F(\rho) \quad (3.37)$$

so that $F = 1$ corresponds to the vacuum value $\psi = v$, while the boundary conditions at $\rho = 0$ become

$$F(0) = 0, \quad P(0) = 1; \quad (3.38)$$

the vacuum configuration in the far-field limit is

$$F(\infty) = 1, \quad P(\infty) = 0. \quad (3.39)$$

In terms of P and F the Z_M field equations boil down to

$$\frac{1}{BW^d} \left(\frac{W^d P'}{B} \right)' = \frac{\hat{e}^2 v^2 F^2 P}{B^2}, \quad (3.40)$$

while the ψ equation reduces to

$$\frac{1}{BW^d} (BW^d F')' = \frac{P^2 F}{B^2} + \lambda v^2 F (F^2 - 1). \quad (3.41)$$

Although closed form solutions to these are not known, they are easily integrated numerically for given B and W , and the results agree with standard flat-space results when $B = \rho$ and $W = 1$. See, for example, Figure 3.1.

BPS special case

In the special case where $W = 1$ and $\hat{e}^2 = e^2/(1 - \varepsilon^2) = 2\lambda$ (and so $\hat{\beta} = 1$), eqs. (3.40) and (3.41) are equivalent to the first-order equations,⁶

$$BF' = nFP \quad \text{and} \quad \frac{nP'}{\hat{e}B} = \sqrt{\frac{\lambda}{2}} v^2 (F^2 - 1). \quad (3.42)$$

We show later that $W = 1$ also solves the Einstein equations when $\hat{e}^2 = 2\lambda$ and so this choice provides a consistent solution to all the field equations in this case.

When eqs. (3.42) and $W = 1$ hold, they also imply

$$L_{\text{kin}} = \frac{1}{2} (\partial\psi)^2 = \frac{e^2}{2} \psi^2 Z_M Z^M = L_{\text{gm}}, \quad (3.43)$$

⁶The simplicity of these equations is understood in supersymmetric extensions of these models, since supersymmetry can require $e^2 = 2\lambda$ and the vortices in this case break only half of the theory's supersymmetries.

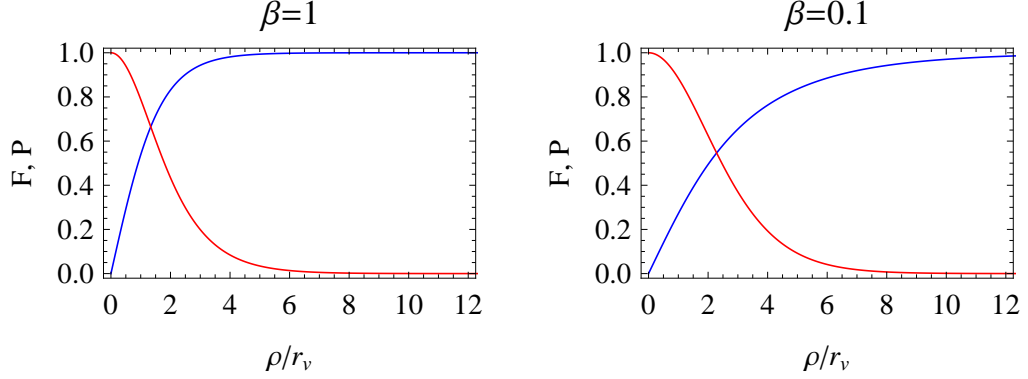


Figure 3.1: A comparison of BPS and non-BPS vortex profiles on a flat background for differing values of $\hat{\beta} = \hat{e}^2/(2\lambda)$. The (blue) profile vanishing at the origin is the scalar profile F and the (red) profile that decreases from the origin is the vector profile P . To find the profiles in flat space we set $B = \rho$ and $W = 1$. The left plot uses $\hat{\beta} = 1$ and the right plot uses $\hat{\beta} = 0.1$, with this being the only parameter that controls vortex profiles in flat space.

and

$$\check{L}_Z := \frac{1}{4}(1 - \varepsilon^2)Z_{mn}Z^{mn} = \frac{\lambda}{4}(\psi^2 - v^2)^2 = V_b, \quad (3.44)$$

which further imply that the vortex contributions to \mathcal{Z} and \mathcal{X} cancel out,

$$\mathcal{Z} = L_{\text{kin}} - L_{\text{gm}} = 0 \quad \text{and} \quad \mathcal{X}_{\text{loc}} = V_b - \check{L}_Z = 0, \quad (3.45)$$

leaving only the bulk contribution to \mathcal{X} :

$$\mathcal{X} = \check{\mathcal{X}}_B = \Lambda - \check{L}_A. \quad (3.46)$$

As can be seen from eq. (3.24), it is the vanishing of \mathcal{Z} that allows $W = 1$ to solve the Einstein equations. Finally, the vortex part of the action evaluates in this case to

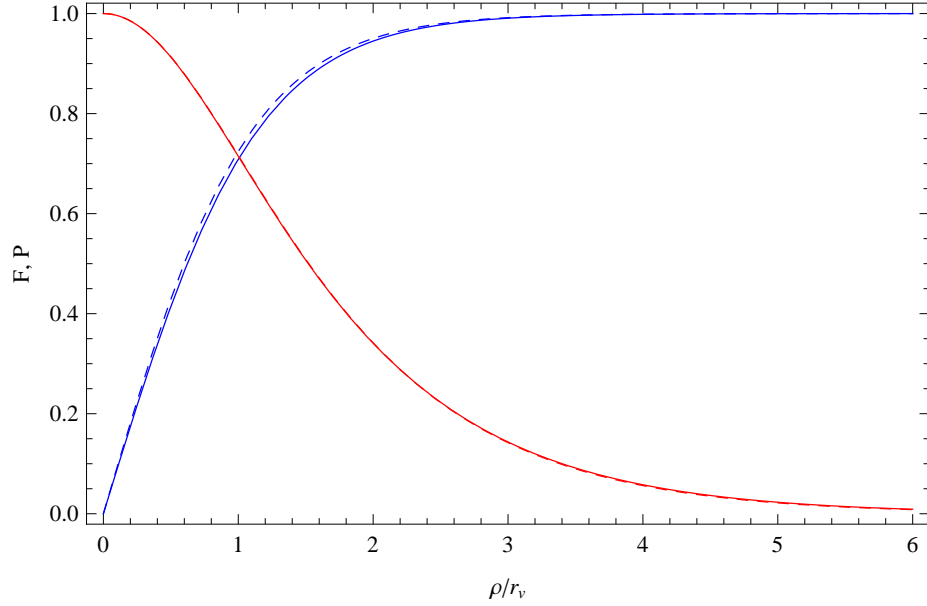


Figure 3.2: A comparison of the profiles F and P for the vortex in flat space (dashed curves) and the full gravitating vortex solution (solid lines). For each case the (blue) profile that vanishes at the origin is the scalar profile F and the (red) profile that decreases from the origin is the vector profile P . The parameters used in the plot are $d = 4$, $\varepsilon = 0.3$, $\beta = 3$, $Q = 0.01 ev^2$, $\Lambda = Q^2/2$, $\kappa v = 0.6$ and $\check{R} = 0$ with the same values of β and ε chosen for the non-gravitating solution.

the simple result

$$\mathcal{T}_v := \frac{1}{\sqrt{-\check{g}}} \int d^2y \sqrt{-g} [L_\Psi + V_b + \check{L}_Z] = 2\pi \int d\rho B [L_\Psi + V_b + \check{L}_Z] = \pi n v^2, \quad (3.47)$$

which confirms the vortex energy density estimate of the previous section.

Bulk equations

To obtain a full solution for a vortex coupled to gravity we must also solve the bulk field equations for W , B and $\check{A}_{\rho\theta}$. The simplest of these to solve is the Maxwell

equation, (3.9), whose solution is

$$\check{A}_{\rho\theta} = \frac{QB}{W^d}, \quad (3.48)$$

where Q is an integration constant. This enters into the Einstein equations like (3.22) and (3.24), through the combination $\check{L}_A = \frac{1}{2}(Q/W^d)^2$.

These can be numerically integrated out from $\rho = 0$, starting with the boundary conditions (3.33) (for which we choose $W_0 = 1$), (3.34) and (3.35), provided that the curvature scalar, \check{R} , for the metric $\check{g}_{\mu\nu}$ is also specified. Once this is done all field values and their derivatives are completely determined by the field equations for $\rho > 0$ and one such solution is shown in Figure 3.3. As we shall see, many useful quantities far from the vortex depend only on certain integrals over the vortex profiles, rather than their detailed form.

3.3.2 Integral relations

Our main interest in later sections is in how the vortices affect the bulk within which they reside, and this is governed by the boundary conditions they imply for the metric — *i.e.* on quantities like W , W' , B , B' — as well as for other bulk fields exterior to, but nearby, the vortex. In particular, simple integral expressions exist for derivatives of bulk fields — *e.g.* W' and B' — in this near-vortex limit, and we pause here to quote explicit expressions for these.

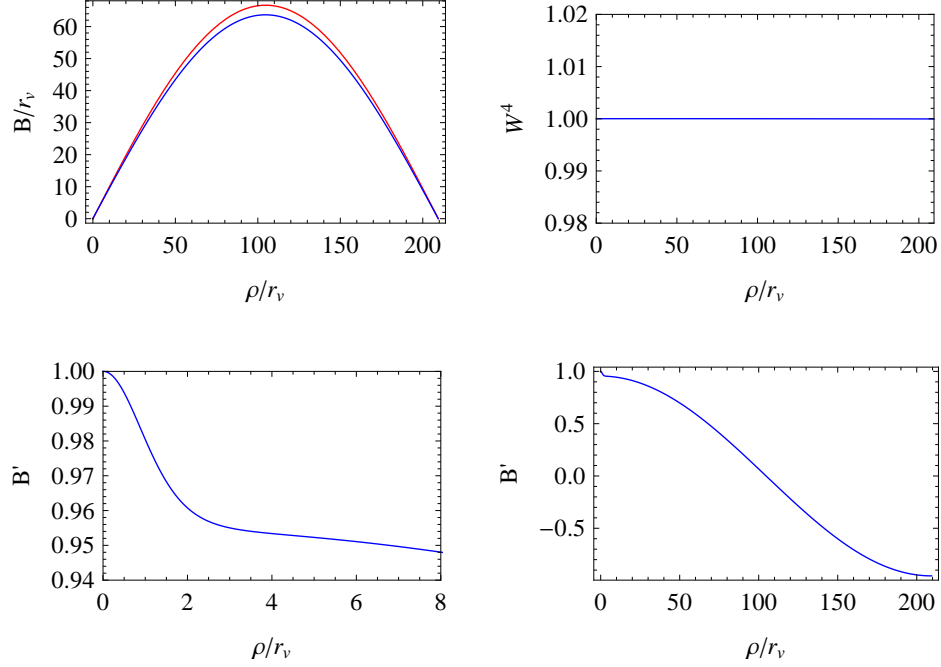


Figure 3.3: These plots illustrate the bulk geometry for BPS vortices ($\beta = 1$) with parameters $d = 4$, $\varepsilon = 0$, $\beta = \hat{\beta} = 1$, $Q = 0.05 ev^2$, $\Lambda = Q^2/2$ and $\kappa v = 0.3$ (which also imply $\check{R} = 0$). In the top left plot, the solution for B is plotted (in blue) below the (red) metric function B_{sphere} of a sphere with radius $r_B = (200/3)r_v$. The presence of a vortex does not change the size of the bulk (since the full solution for B still vanishes at $\rho = \pi r_B$) and the metric function B is still approximately spherical with $B \approx 0.95 \times B_{\text{sphere}}$ for these parameters. The top right plot shows that when $\beta = 1$ and $\Lambda = Q^2/2$, a constant warp factor solves the field equations. The bottom left plot shows that the derivative of the metric function $B' \approx 0.95$ outside of the vortex core, at $\rho \gtrsim 4r_v$. The bottom right plot shows that $B' \approx -0.95$ at the pole which lies opposite to the vortex core, indicating the presence of a conical singularity at that pole.

For instance, consider integrating the Einstein equation, (3.22), over the transverse dimensions out to a proper distance $\rho = \rho_v \simeq \mathcal{O}(r_v)$ outside of (but not too far from) the vortex (see Figure 3.4). This gives

$$d B W^d \partial_\rho \ln W \Big|_{\rho=\rho_v} = \left[B (W^d)' \right]_{\rho=\rho_v} = -\frac{1}{2\pi} \left\langle 2\kappa^2 \mathcal{X} + W^{-2} \check{R} \right\rangle_v, \quad (3.49)$$

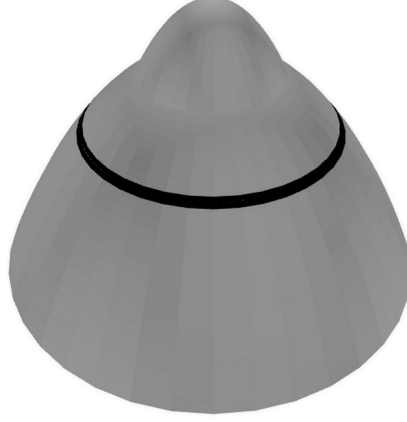


Figure 3.4: An illustration of the matching done at $\rho = \rho_v$. The light grey surface is a cartoon of the bulk geometry. The bump on top of the surface represents the localized modifications to the approximately spherical bulk geometry that arise due to the vortex. The dark ring represents the circle at $\rho = \rho_v$ that lies sufficiently far outside the vortex that its fields are exponentially suppressed, but close enough to the vortex so that its proper distance from the pole is still $\mathcal{O}(r_v)$.

where we introduce the notation

$$\langle \mathcal{O} \rangle_v := \frac{1}{\sqrt{-\tilde{g}}} \int_{X_v} d^2x \sqrt{-g} \mathcal{O} = 2\pi \int_0^{\rho_v} d\rho B W^d \mathcal{O}, \quad (3.50)$$

and use the boundary condition $W'(0) = 0$ at the vortex centre. This identifies explicitly the specific combination of vortex quantities relevant for specifying W' just outside the vortex.

A second integral relation of this type starts instead with (3.25), which integrates to give

$$\left(B' W^d \right)_{\rho=\rho_v} = 1 - \frac{\kappa^2}{2\pi} \left\langle \varrho - \left(1 - \frac{2}{d} \right) \mathcal{X} - \mathcal{Z} \right\rangle_v, \quad (3.51)$$

given the boundary condition $B' W^d \rightarrow 1$ as $\rho \rightarrow 0$. This can be used to infer the implications of the vortex source on B' just outside the vortex.

For many purposes our interest is in the order of magnitude of the integrals on the right-hand sides of expressions like (3.49) or (3.51) and these sometimes contain a surprise. In particular, naively one might think the integrals on the right-hand sides would generically be order v^2 and so would contribute at order $\kappa^2 v^2$ to the quantities on the left-hand sides. Although this is true for ϱ , the surprise is that the quantities $\langle \mathcal{X} \rangle_v$ and $\langle \mathcal{Z} \rangle_v$ can be much smaller than this, being suppressed by powers of r_v/r_B when the vortex is much smaller than the transverse space, $r_v \ll r_B$, and this has important implications for how vortices influence their surroundings.

One way to understand this suppression is to evaluate explicitly the suppressed quantities in the flat-space limit, where it can be shown (for instance) that the vortex solutions described above imply $\langle \mathcal{X} \rangle_v^{\text{flat}} = 0$. Appendix A.1 proves this as a general consequence of stress-energy conservation (or hydrostatic equilibrium) within the vortex, with the vortex dynamically adjusting to ensure it is true. (Alternatively, the vanishing of $\langle \mathcal{X} \rangle_v$ on flat space can also be derived as a consequence of making the vortex action stationary with respect to rescalings of the size of the vortex, as in Appendix B.1.) More generally, for curved geometries we find numerically that in the generic situation when $r_v \sim r_B$ all terms in (3.49) are similar in size and not particularly small, but this is no longer true once a hierarchy in scales exists between the size of the vortex and that of the transverse dimensions.

The next sections provide several other ways to understand this suppression, associated with the constraints imposed by the Bianchi identities on the left-hand sides of near-vortex boundary conditions.

3.3.3 Near-vortex asymptotics

Because the vortex fields, $\delta\psi = \psi - v$ and Z_M , fall off exponentially they can be neglected to exponential accuracy ‘outside’ of the vortex; *i.e.* at distances $\rho_v \gtrsim r_v \sim 1/ev$. The form for the metric functions B and W are then governed by the Einstein equations with only bulk-field stress-energy. This section describes the approximate form taken by these bulk solutions outside of the vortex sources, but not far outside (in units of the bulk curvature radius, say).

Asymptotic forms

In general, the presence of a vortex introduces apparent singularities into the bulk geometry whose properties are dictated by those of the vortex. These singularities are only apparent because they are smoothed out once the interior structure of the vortex is included, since the geometry then responds to the stress-energy of the vortex interior. This section characterizes these singularities more precisely with a view to relating them to the properties of the source vortices.

One way to characterize the position of the apparent singularity is to define it to occur at the point where the expression for $B_{\text{bulk}}(\rho)$ obtained using only the bulk field equations would vanish: $B_{\text{bulk}}(\rho_\star) = 0$ (see Figure 3.5). Here ρ_\star is of order the vortex size, and need not occur precisely at $\rho = 0$ (despite the boundary condition $B(0) = 0$ inside the vortex) because B_{bulk} is found by solving only the bulk field equations without the vortex fields.

The nature of the singularity at $\rho = \rho_\star$ is most simply described by expanding the bulk field equations in powers of proper distance, $\hat{\rho} = \rho - \rho_\star$, away from the apparent

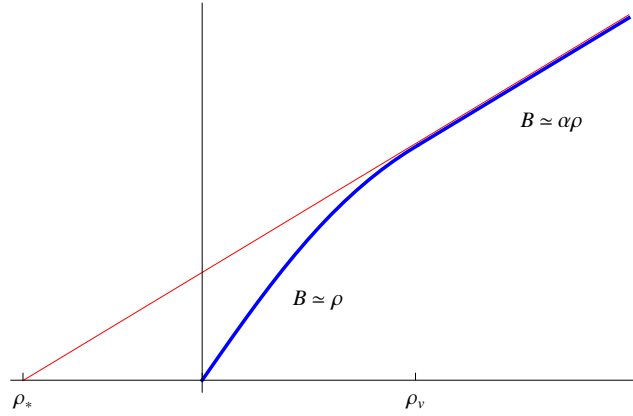


Figure 3.5: A cartoon illustration of the definition of ρ_* . The (blue) metric function B increases linearly away from the origin with unit slope $B(\rho) \approx \rho$. Outside of the vortex $\rho \gtrsim \rho_v$ the solution is also linear in ρ but with $B(\rho) \approx \alpha\rho$. The straight (red) line extrapolates this exterior behaviour to the point, $\rho = \rho_*$, where the external B would have vanished if the vortex had not intervened first.

singularity,

$$\begin{aligned}
 W &= W_0 \left(\frac{\hat{\rho}}{r_B} \right)^w + W_1 \left(\frac{\hat{\rho}}{r_B} \right)^{w+1} + W_2 \left(\frac{\hat{\rho}}{r_B} \right)^{w+2} + \dots, \\
 B &= B_0 \left(\frac{\hat{\rho}}{r_B} \right)^b + B_1 \left(\frac{\hat{\rho}}{r_B} \right)^{b+1} + B_2 \left(\frac{\hat{\rho}}{r_B} \right)^{b+2} + \dots.
 \end{aligned} \tag{3.52}$$

where r_B is again a scale of order the bulk curvature scale. It is the leading powers, b and w , that describe potential singularity, and their form is constrained by the bulk field equations. In particular, as shown in Appendix A.2, in the limit that the size of the source vanishes, $r_v^2/r_B^2 \rightarrow 0$, the leading terms in the expansion of the Einstein equations around $\hat{\rho} = 0$ imply that w and b satisfy the two Kasner conditions⁷ [24]:

$$dw + b = 1 \quad \text{and} \quad dw^2 + b^2 = 1. \tag{3.53}$$

⁷Our treatment here follows closely that of [25], which in turn is based on the classic BKL treatment of near-singularity time-dependence [26].

The last of these in turn implies w and b must reside within the intervals

$$|w| \leq \frac{1}{\sqrt{d}} \quad \text{and} \quad |b| \leq 1. \quad (3.54)$$

The Kasner solutions have precisely two solutions: either $w = 0$ and $b = 1$ (as is true for flat-space solutions) or $w = 2/(1+d)$ and $b = (1-d)/(1+d)$. Since we know that a non-gravitating vortex lives in a geometry with $w = 0$ and $b = 1$, this is also the root we must use in the weak-gravity limit $(\kappa v)^2 \ll 1$. This describes a conical singularity if $B'(\rho = \rho_\star) \neq 1$.

The field equations also dictate all but two of the remaining coefficients, B_i and W_i , of the series solution. For instance eq. (3.24) applied outside the vortex implies $W' = kB$ for constant k . This implies $W_1 = 0$ and $W_2 = \frac{1}{2} k \alpha r_B^2$ and so on.

The Kasner analysis (and the solution $w = 0$ and $b = 1$) is especially powerful when combined with the near-vortex boundary conditions, such as (3.49) or (3.51). For small vortices, the values of the bulk fields at the apparent singularity ρ_\star and the point ρ_v outside of the vortex are indistinguishable up to r_v^2/r_B^2 corrections. So a boundary condition on the bulk fields outside of the vortex rewrites as a condition on the singular behaviour. More explicitly, using the Kasner solution to evaluate W and B at $\rho = \rho_v$ gives

$$W_v = W_0 \left(\frac{\hat{\rho}_v}{r_B} \right)^w [1 + \mathcal{O}(r_v^2/r_B^2) + \dots], \quad B_v = B_0 \left(\frac{\hat{\rho}_v}{r_B} \right)^b [1 + \mathcal{O}(r_v/r_B) + \dots], \quad (3.55)$$

where $\hat{\rho}_v = \rho_v - \rho_\star$. Inserting these into the left-hand side of eqs. (3.49) then gives

$$dw \left(\frac{B_0 W_0^d}{r_B} \right) \left(\frac{\hat{\rho}_v}{r_B} \right)^{dw+b-1} [1 + \mathcal{O}(r_v^2/r_B^2)] = -\frac{1}{2\pi} \left\langle 2\kappa^2 \mathcal{X} + W^{-2} \check{R} \right\rangle_v. \quad (3.56)$$

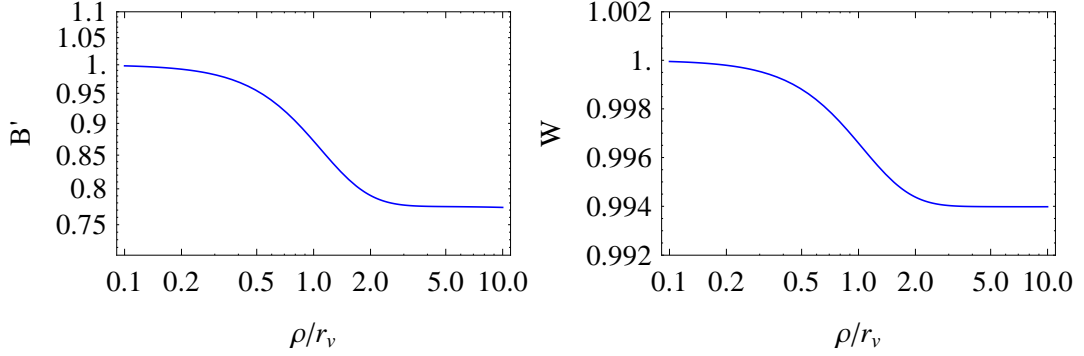


Figure 3.6: Log-log plots of the the near vortex geometry for parameters $d = 4$, $\beta = 3$, $\varepsilon = 0.3$, $Q = 0.01 ev^2$, $\Lambda = Q^2/2$, $\kappa v = 0.6$ and $\check{R} = 0$. The bulk in this case has a radius of $r_B = (500/3)r_v$. Outside of the vortex $\rho \gtrsim r_v$ the geometry exhibits Kasner-like behaviour $B' \approx \alpha \neq 1$ and $W' \approx 0$.

Because of the Kasner condition $dw + b = 1$ and the solution $w = 0$, we have

$$\left\langle 2\kappa^2 \mathcal{X} + W^{-2} \check{R} \right\rangle_v = 0 \quad (3.57)$$

up to $\mathcal{O}(r_v^2/r_B^2)$ corrections. If we further assume that only the localized contributions to the left hand side of (3.57) survive in the pointlike limit for which $r_v^2/r_B^2 \rightarrow 0$, then we have

$$\langle \mathcal{X}_{\text{loc}} \rangle_v = 0. \quad (3.58)$$

This shows how the gravitational dynamics outside of the source can be used to deduce the localized transverse stress energy in the limit that the source is small, without knowing the internal structure of the source.

3.3.4 Effective description of a small vortex

If the vortex is much smaller than the transverse space then most of the details of its structure should not be important when computing how it interacts with its environment. Its dynamics should be well described by an effective d -dimensional action that captures its transverse structure in a multipole expansion.

The lowest-derivative ‘brane’ action of this type that depends on the nontrivial bulk fields outside the vortex is $S_b = \int d^d x \mathcal{L}_b$ with

$$\mathcal{L}_b = -\sqrt{-\gamma} \left[T_0 - \frac{\zeta}{d!} \epsilon^{\mu\nu\lambda\rho} \tilde{A}_{\mu\nu\lambda\rho} + \dots \right]_{\rho=\rho_b} = -\sqrt{-\gamma} \left[T_0 + \frac{\zeta}{2} \epsilon^{mn} A_{mn} + \dots \right]_{\rho=\rho_b}, \quad (3.59)$$

where γ denotes the determinant of the induced metric on the d -dimensional world-volume of the vortex centre of mass (which in the coordinates used here is simply $\gamma_{\mu\nu} = g_{\mu\nu}$ evaluated at the brane position). The tensor $\tilde{A}_{\mu\nu\lambda\rho} := \frac{1}{2} \epsilon_{\mu\nu\lambda\rho mn} A^{mn}$ is proportional to the D -dimensional Hodge dual of the bulk field strength; a quantity that can be invariantly integrated over the d -dimensional world-volume of the codimension-2 vortex. All unwritten terms covered by the ellipses in (3.59) involve two or more derivatives.

The dimensionful effective parameters T_0 and ζ respectively represent the vortex’s tension and localized flux, in a way we now make precise. To fix them in terms of the properties of the underlying vortex we perform a matching calculation; computing their effects on the bulk fields and comparing this to the parallel calculation using the full vortex solution. To do this we must be able to combine the d -dimensional action (3.59) with the D -dimensional action, S_B , for the bulk fields.

To make this connection we promote (3.59) to a D -dimensional action by multiplying it by a ‘localization’ function, $\delta_2(y)$, writing the D -dimensional lagrangian density as

$$\mathcal{L}_{\text{tot}} = \mathcal{L}_B(g_{MN}, A_M) + \mathcal{L}_b(g_{MN}, A_M) \delta_2(y). \quad (3.60)$$

Here \mathcal{L}_B is as given in (3.5) and $\delta_2(y)$ is a delta-function-like regularization function that has support only in a narrow region around the vortex position $\rho = \rho_b$, normalized so that $\int_{X^v} d^2y \delta_2(y) = 1$. Although we can regard $\delta_2(y)$ as being independent of the d -dimensional metric, $g_{\mu\nu}$, and gauge field, A_M , we *cannot* consider it to be independent of the transverse metric, g_{mn} , because $\delta_2(y)$ must depend on the proper distance from the vortex.

Much of the trick when matching with regularized delta-functions is to avoid questions that involve making assumptions about the detailed g_{mn} -dependence of the brane action. This is most awkward when calculating the brane’s gravitational response, but we show below how to infer this response in a model-independent way that does not make ad-hoc assumptions about how $\delta_2(y)$ is regulated.

Gauge-field matching

To determine ζ we compute the contribution of S_b to the gauge field equation, which becomes modified to

$$\partial_m \left(\sqrt{-g} A^{mn} \right) + \frac{\delta S_b}{\delta A_n} = \partial_m \left[\sqrt{-g} \left(A^{mn} + \zeta \epsilon^{mn} \frac{\delta_2(y)}{\sqrt{g_2}} \right) \right] = 0. \quad (3.61)$$

This has solution

$$A_{\rho\theta} = \frac{QB}{W^d} - \zeta \epsilon_{\rho\theta} \frac{\delta_2(y)}{\sqrt{g_2}} = \frac{QB}{W^d} - \zeta \delta_2(y), \quad (3.62)$$

where Q is an integration constant, and so — when integrated over a transverse volume, X_v , completely containing the vortex — gives the flux

$$\Phi_A(X_v) = \int_{X_v} dA = Q \int_{X_v} d^2y \left(\frac{B}{W^d} \right) - \zeta. \quad (3.63)$$

Comparing this to the vortex result in the full UV theory

$$\Phi_A(X_v) = \check{\Phi}_A(V) - \varepsilon \Phi_Z(V) = Q \int_{X_v} d^2y \left(\frac{B}{W^d} \right) + \frac{2\pi n\varepsilon}{e}, \quad (3.64)$$

shows that ζ is given at the classical level by

$$\zeta = -\frac{2\pi n\varepsilon}{e}. \quad (3.65)$$

Notice that this argument does not make use of any detailed properties of $\delta_2(y)$ beyond its normalization and independence of A_m .

Gauge-field back-reaction

Before repeating this argument to match the tension, T_0 , and determine the gravitational response, we first pause to draw attention to an important subtlety. The subtlety arises because the presence of localized flux causes the gauge field to back-react in a way that contributes to the localized energy density, in a manner similar

to the way the classical Coulomb field back-reacts to renormalize the mass of a point charged particle.

To set up this discussion, notice that the effective lagrangian, (3.59) is meant to capture the macroscopic contribution of the vortex part of the lagrangian regarded as a function of applied fields A_m and $g_{\mu\nu}$. Consequently we expect the transverse average of (3.60) to give the same answer as the transverse average of the full lagrangian of the UV theory. Comparing the A_m -dependent and -independent terms of this average then suggests the identifications

$$\begin{aligned} T_0 W_b^d &= \left\langle L_{\text{kin}} + V_b + L_{\text{gm}} + L_z \right\rangle_v \\ \text{and } \frac{\zeta}{2} W_b^d \epsilon^{mn} A_{mn} &= \left\langle L_{\text{mix}} \right\rangle_v = \frac{\varepsilon}{2} \left\langle Z^{mn} A_{mn} \right\rangle_v, \end{aligned} \quad (3.66)$$

where $W_b = W(\rho_b)$ is the warp factor evaluated at the brane position, and the factors W_b^d come from the ratio of $\sqrt{-\gamma}/\sqrt{-\tilde{g}}$.

Now comes the main point. The existence of the localized piece in the solution, (3.62), for A_m has two related consequences in such a transverse average.

- First, evaluating the localized-flux term at the solution to the A_{mn} field equation, (3.62), shows that the localized component of A_m renormalizes the tension,

$$W_b^d \left(T_0 + \frac{\zeta}{2} \epsilon^{mn} A_{mn} \right)_{\rho=\rho_b} = W_b^d \left[T_0 + \frac{\zeta Q}{W_b^d} - \zeta^2 \left(\frac{\delta_2(y)}{B} \right)_{\rho=\rho_b} \right], \quad (3.67)$$

where this follows from taking $\delta_2(y)$ to be sufficiently peaked so that its integral can be treated like that of a Dirac delta-function. Notice that the last term in the last equality is singular as the vortex size goes to zero, requiring a regularization in order to be unambiguous. Such divergences are common for

back-reacting objects with codimension-2 or higher, and are ultimately dealt with by renormalizing the action (3.59) even at the classical level [29].

The ζ -dependent part of this is to be compared with

$$\langle L_{\text{mix}} \rangle_v = -\frac{2\pi\varepsilon Q n}{e} - 2\varepsilon^2 \langle L_z \rangle_v, \quad (3.68)$$

which uses (3.11) and (3.48) to evaluate the integration over L_{mix} , and shows that the result agrees with (3.67), both on the value of the term linear in Q (once the matching value, (4.132), for ζ is used) and by providing an explicit regularization of the singular $\mathcal{O}(\varepsilon^2)$ term.

- The second way the localized term in (3.62) contributes is by introducing a localized contribution to the Maxwell action, L_A , which was naively not part of the vortex

$$\begin{aligned} \langle L_A \rangle_v &= \frac{Q^2}{2} \int_{X_v} d^2y \left(\frac{B}{W^d} \right) - W_b^d \left[\frac{\zeta Q}{W_b^d} - \frac{\zeta^2}{2} \left(\frac{\delta_2(y)}{B} \right)_{\rho=\rho_b} \right] \\ &= \langle \check{L}_A \rangle_v - W_b^d \left[\frac{\zeta Q}{W_b^d} - \frac{\zeta^2}{2} \left(\frac{\delta_2(y)}{B} \right)_{\rho=\rho_b} \right]. \end{aligned} \quad (3.69)$$

This exactly cancels the linear dependence on Q in (3.67), and partially cancels the localized renormalization of the tension.

We see from this that the localized part of the gauge response to the brane action contributes a localized contribution to the bulk action (and energy density) that combines with the direct brane action in precisely the same way as happens microscopically from the mixing from A_m to \check{A}_m (see, for example, (3.12)). This suggests

another useful notion of brane lagrangian, defined as the total localized contribution when Q is fixed (rather than A_m), leading to

$$\check{L}_b := \check{T} W_b^d := \left\langle L_{\text{kin}} + V_b + L_{\text{gm}} + \check{L}_Z \right\rangle_v = W_b^d \left[T_0 - \frac{\zeta^2}{2} \left(\frac{\delta_2(y)}{B} \right)_{\rho=\rho_b} \right]. \quad (3.70)$$

We see that the tension renormalizations described above — associated with the $[\delta_2(y)/B]_{\rho_b}$ terms — are the macroscopic analogs of the renormalization $e^2 \rightarrow \hat{e}^2 = e^2/(1 - \varepsilon^2)$ that occurs with the transition from L_Z to \check{L}_Z in the microscopic vortex picture.

Whether L_b or \check{L}_b is of interest depends on the physical question being asked. Using L_b is best in deriving the brane contribution to the A_m field equations, as above. But because it is \check{L}_b that contains all of the brane-localized contributions to the energy, it plays a more important role in the brane's gravitational response (as we now explore in more detail).

On-brane stress energy

With the above definitions of L_b and \check{L}_b in hand we now turn to the determination of the brane's local gravitational response. To determine the tension, T_0 (or \check{T}), we compute the $(\mu\nu)$ component of the Einstein equations (which we can do unambiguously because we know $\delta_2(y)$ does not depend on $g_{\mu\nu}$). We can do so using either L_b or \check{L}_b to define the brane action.

Using L_b leads to the following stress energy

$$T_{(b)}^{\mu\nu} = \frac{2}{\sqrt{-g}} \left(\frac{\delta S_b}{\delta g_{\mu\nu}} \right) = -W_b^d \left(T_0 + \frac{\zeta}{2} \epsilon^{mn} A_{mn} \right) \frac{\delta_2(y)}{\sqrt{g_2}} g^{\mu\nu}, \quad (3.71)$$

and so ϱ becomes $\varrho = \Lambda + L_A + \varrho_b$ with

$$\varrho_b = W_b^d \left(T_0 + \frac{\zeta}{2} \epsilon^{mn} A_{mn} \right) \frac{\delta_2(y)}{\sqrt{g_2}}. \quad (3.72)$$

Alternatively, using \check{L}_b leads to the stress energy

$$\check{T}_{(b)}^{\mu\nu} = \frac{2}{\sqrt{-g}} \left(\frac{\delta \check{S}_b}{\delta g_{\mu\nu}} \right) = -\check{T} W_b^d \frac{\delta_2(y)}{\sqrt{g_2}} g^{\mu\nu}, \quad (3.73)$$

and so ϱ becomes $\varrho = \Lambda + \check{L}_A + \varrho_{\text{loc}}$ with

$$\varrho_{\text{loc}} = \check{T} W_b^d \frac{\delta_2(y)}{\sqrt{g_2}} = W_b^d \left[T - \frac{\zeta^2}{2} \left(\frac{\delta_2(y)}{B} \right)_{\rho=\rho_b} \right] \frac{\delta_2(y)}{\sqrt{g_2}}. \quad (3.74)$$

In either case the *total* energy density is the same,

$$\langle \varrho \rangle_v = \left\langle \Lambda + L_A \right\rangle_v + W_b^d \left(T + \frac{\zeta}{2} \epsilon^{mn} A_{mn} \right)_{\rho=\rho_b} = \left\langle \Lambda + \check{L}_A \right\rangle_v + W_b^d \check{T}, \quad (3.75)$$

which is the analog of the microscopic statement (3.19)

$$\langle \varrho \rangle_v = \left\langle \Lambda + L_A + L_{\text{kin}} + L_{\text{gm}} + V_b + L_Z + L_{\text{mix}} \right\rangle_v = \left\langle \Lambda + \check{L}_A + L_{\text{kin}} + L_{\text{gm}} + V_b + \check{L}_Z \right\rangle_v. \quad (3.76)$$

The advantage of using (3.74) rather than (3.72) is that ϱ_{loc} contains *all* of the brane-localized stress energy, unlike ϱ_b which misses the localized energy hidden in L_A .

IR metric boundary conditions

A second important step in understanding the effective theory is to learn how the effective action modifies the field equations. So we restate here the general way of

relating brane properties to near-brane derivatives of bulk fields [28]. The idea is to integrate the bulk field equations (including the brane sources) over a small region not much larger than (but totally including) the brane. For instance for a bulk scalar field, Φ , coupled to a brane one might have the field equation

$$\square\Phi + J_B + j_b \delta_2(y) = 0, \quad (3.77)$$

where J_B is the contribution of bulk fields that remains smooth near the brane position and j_b is the localized brane source. Integrating this over a tiny volume surrounding the brane and taking its size to zero — *i.e.* $\rho_v/r_B \rightarrow 0$ — then gives

$$\lim_{\rho_v \rightarrow 0} \langle \square\Phi \rangle_v = 2\pi \lim_{\rho_v \rightarrow 0} B_v W_v^d \Phi'_v = - \lim_{\rho_v \rightarrow 0} \langle J_B + j_b \delta_2(y) \rangle_v = -j_b(\rho = \rho_b), \quad (3.78)$$

where the assumed smoothness of J_B at the brane position ensures $\langle J_B \rangle_v \rightarrow 0$ in the limit $\rho_v \rightarrow 0$. The equality of the second and last terms of this expression gives the desired relation between the near-brane derivative of Φ and the properties j_b of the brane action.

Applying this logic to the Einstein equations, integrating over a tiny volume, X_v , completely enclosing a vortex gives

$$0 = \left\langle \frac{1}{\sqrt{-g}} \frac{\delta S}{\delta g_{MN}} \right\rangle_v = \left\langle \frac{1}{\sqrt{-g}} \frac{\delta S_{EH}}{\delta g_{MN}} \right\rangle_v + \left\langle \frac{1}{\sqrt{-g}} \frac{\delta S_M}{\delta g_{MN}} \right\rangle_v, \quad (3.79)$$

where we have split the action into an Einstein-Hilbert part S_{EH} and a matter part S_M . This matter part can be further divided into a piece that is smooth at the brane

position

$$\check{S}_B = - \int d^D x \sqrt{-g} (\check{L}_A + \Lambda) , \quad (3.80)$$

and one that contains *all* of the localized sources of stress energy,

$$\check{S}_b = - \int d^D x \sqrt{-g} \left(\frac{\delta_2(y)}{\sqrt{g_2}} \right) \check{T} = - \int d^d x \sqrt{-\gamma} \check{T} . \quad (3.81)$$

As above, for a sufficiently small volume, X_v , we need keep only the highest-derivative part of the Einstein-Hilbert term⁸, since the remainder vanishes on integration in the limit $\rho_v \rightarrow 0$. The S_M^B term also vanishes in this limit, by construction, so the result becomes

$$0 = \frac{1}{2\kappa^2} \int d\theta \left[\sqrt{-g} (K^{ij} - K g^{ij}) \right]_0^{\rho_v} + \sqrt{-\check{g}} \left\langle \frac{1}{\sqrt{-g}} \frac{\delta \check{S}_b}{\delta g_{ij}} \right\rangle_v \quad \text{as } \rho_v \rightarrow 0, \quad (3.82)$$

where i and j run over all coordinates except the radial direction, ρ , and K^{ij} is the extrinsic curvature tensor for the surfaces of constant ρ . To proceed, we assume that the derivative of the brane action is also localized such that its integral can be replaced with a quantity evaluated at the brane position

$$\left\langle \frac{1}{\sqrt{-g}} \frac{\delta \check{S}_b}{\delta g_{MN}} \right\rangle_v = \int_{X_v} d^2 y \left(\frac{1}{\sqrt{-\check{g}}} \frac{\delta \check{S}_b}{\delta g_{MN}} \right) = \frac{1}{\sqrt{-\gamma}} \left(\frac{\delta \check{S}_b}{\delta g_{MN}(y_b)} \right) . \quad (3.83)$$

The metric being evaluated at y_b informs us that the derivative is taken at the fixed

⁸Being careful to include the Gibbons-Hawking-York action [29] on the boundary.

point where $\delta_2(y)$ is localized, and so it contains no dependence on the bulk coordinates, and in particular no factors of $\delta_2(y)$. For example its $\mu\nu$ components read

$$\frac{\delta\check{S}_b}{\delta g_{\mu\nu}(y-b)} = -\frac{1}{2}\sqrt{-\gamma}\check{T}\gamma^{\mu\nu}. \quad (3.84)$$

However, at this point we remain agnostic about how to calculate the off-brane component $\delta\check{S}_b/\delta g_{\theta\theta}(y_b)$. Returning to the matching condition (3.82) we have the final result

$$\lim_{\rho_v \rightarrow 0} \int d\theta \left[\sqrt{-g} \left(K^{ij} - K g^{ij} \right) \right]_0^{\rho_v} = -2\kappa^2 \left(\frac{\delta\check{S}_b}{\delta g_{ij}(y_b)} \right), \quad (3.85)$$

which can be explicitly evaluated for the geometries of interest.

Brane stress-energies

We now turn to the determination of the off-brane components of the brane stress-energy. We can learn these directly by computing the left hand side of (3.85) in the UV theory, before taking the limit $\rho_v \rightarrow 0$. We will first do this very explicitly for the $(\mu\nu)$ components of the brane stress-energy, and then proceed to deduce the off-brane components of the brane stress-energy.

The $(\mu\nu)$ stress-energy

For the metric ansatz $ds^2 = W^2(\rho) \check{g}_{\mu\nu} dx^\mu dx^\nu + d\rho^2 + B^2(\rho) d\theta^2$, the extrinsic curvature evaluates to $K_{ij} = \frac{1}{2} g'_{ij}$. This gives

$$K^{\mu\nu} = \frac{W'}{W} g^{\mu\nu} \quad \text{and} \quad K^{\theta\theta} = \frac{B'}{B} g^{\theta\theta}. \quad (3.86)$$

The trace of the $(\mu\nu)$ components of the condition (3.85) therefore evaluates to

$$\lim_{\rho_v \rightarrow 0} \left\{ W_v^d B_v \left[(1-d) \left(\frac{W'_v}{W_v} \right) - \frac{B'_v}{B_v} \right] + 1 \right\} = -\frac{\kappa^2/\pi d}{\sqrt{-\check{g}}} \gamma_{\mu\nu} \left(\frac{\delta \check{S}_b}{\delta g_{\mu\nu}(y_b)} \right) = \frac{\kappa^2 W_b^d \check{T}}{2\pi}, \quad (3.87)$$

for which the limit on the left-hand side can be evaluated using the limit $B_v \rightarrow 0$ as $\rho_v \rightarrow 0$. The result shows that it is the renormalized tension, \check{T} , that determines the defect angle just outside the vortex,

$$1 - \alpha = \frac{\kappa^2 W_b^d \check{T}}{2\pi}. \quad (3.88)$$

This is the macroscopic analog of (3.51) which also relates the defect angle to the localized energy density.

The $(\theta\theta)$ stress-energy

The $(\theta\theta)$ component of the metric matching condition, (3.85), evaluates to

$$\lim_{\rho_v \rightarrow 0} W_v^d B_v \left(\frac{W'_v}{W_v} \right) = \frac{\kappa^2/\pi d}{\sqrt{-\check{g}}} g_{\theta\theta}(y_b) \left(\frac{\delta \check{S}_b}{\delta g_{\theta\theta}(y_b)} \right). \quad (3.89)$$

but at first sight this is less useful because the unknown g_{mn} dependence of $\delta_2(y)$ precludes evaluating its right-hand side. This problem can be side-stepped by using the constraint, eq. (3.26), evaluated at $\rho = \rho_v$ (just outside the brane or vortex) to evaluate $W'_v/W_v = \mathcal{O}(\rho_v/r_B^2)$, and so also the left-hand side of (3.89), in terms of the quantities $B'_v/B_v = 1/\rho_v + \dots$, \check{R}/W_v^2 and \mathcal{X}_B . Once this is done we instead use the $(\theta\theta)$ matching condition to infer the $(\theta\theta)$ component of the vortex stress energy.

Solving the constraint, (3.26), for W'/W at ρ_v (just outside the vortex, where

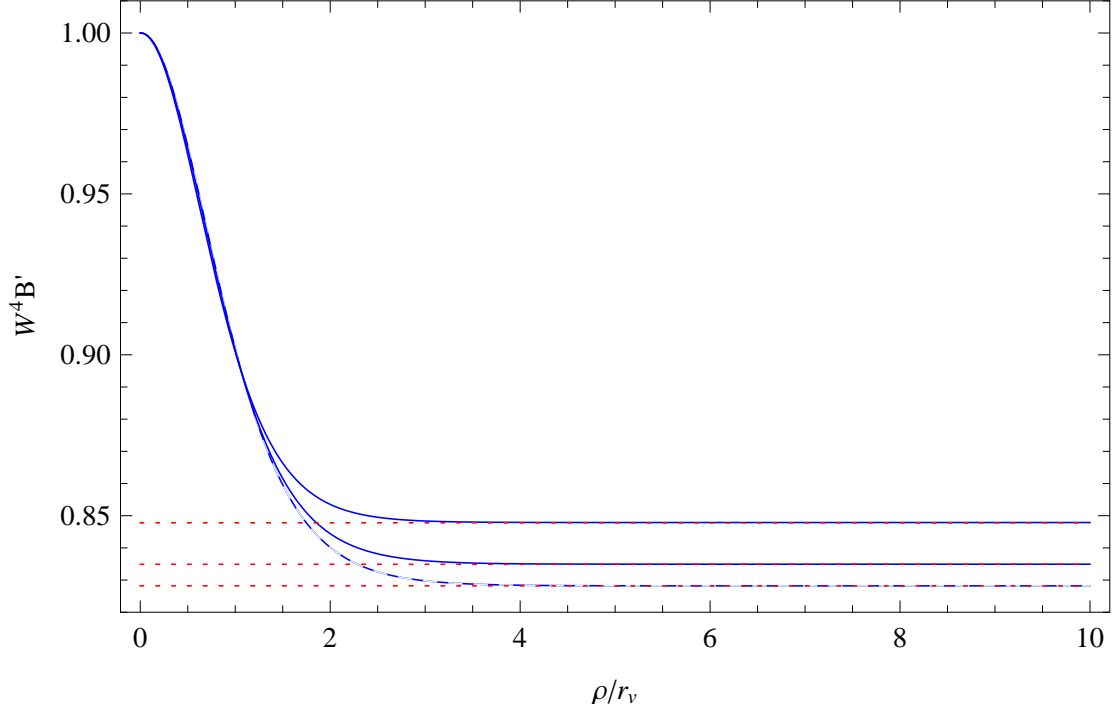


Figure 3.7: A plot of defect angle matching in the region exterior but near to the vortex core. The solid (blue) lines represent the metric function $W^4 B'$ and the dotted (red) lines represent $1 - \kappa^2 \check{T}/2\pi$ computed independently for different values of $\varepsilon = \{-0.2, 0.2, 0.4, 0.6\}$ with the other parameters fixed at $d = 4$, $\beta = 3$, $Q = 1.25 \times 10^{-4} e v^2$, $\Lambda = Q^2/2$, $\kappa v = 0.5$ and $\check{R} = 0$. This size of the defect angle $B'_v \approx \alpha$ matches very well with $1 - \kappa^2 \check{T}/2\pi$ at $\rho = \rho_v \approx 4r_v$. The solutions for $W^4 B'$ overlap perfectly when $\varepsilon = \pm 0.2$, as indicated by the dashes in the line. This illustrates that the defect angle is controlled by \check{T} , and the linear dependence of the the defect angle on ε is cancelled.

$\mathcal{Z} = 0$ and $\mathcal{X} = \mathcal{X}_B = \check{\mathcal{X}}_B$) gives

$$\begin{aligned}
 (d-1) \left(\frac{W'_v}{W_v} \right) &= -\frac{B'_v}{B_v} + \sqrt{\left(\frac{B'_v}{B_v} \right)^2 - \left(1 - \frac{1}{d} \right) \left(2\kappa^2 \mathcal{X}_B(\rho_v) + \frac{\check{R}}{W_v^2} \right)} \\
 &\simeq -\frac{1}{2} \left(1 - \frac{1}{d} \right) \rho_v \left(2\kappa^2 \mathcal{X}_B(\rho_v) + \frac{\check{R}}{W_v^2} \right) + \dots, \quad (3.90)
 \end{aligned}$$

where the root is chosen such that W'_v/W_v vanishes if both \check{R} and $\mathcal{X}_B(\rho_v)$ vanish.

With this expression we see that $B_v W_v^d (W'_v/W_v) \rightarrow 0$ as $\rho_v \rightarrow 0$, and so (3.89) then

shows that

$$\mathcal{T}^{\theta\theta} = \frac{\delta\check{S}_b}{\delta g_{\theta\theta}(y_b)} = 0, \quad (3.91)$$

for any value of T_0 (or \check{T}) and ζ .

Notice that eq. (3.91) is precisely what is needed to ensure $W'_b \rightarrow 0$ at the brane, as required by the Kasner equations (3.53) that govern the near-vortex limit of the bulk. Also notice that (3.91) would be counter-intuitive if instead one were to evaluate directly $\delta S_b/\delta g_{\theta\theta}$ by assuming $\delta_2(y)$ was metric independent and using the explicit metrics that appear within $\epsilon^{mn}A_{mn}$. What is missed by this type of naive calculation is the existence of the localized energy coming from the Maxwell action, L_A , and its cancellation of the terms linear in ζ when converting S_b to \check{S}_b .

The $(\rho\rho)$ stress-energy

Although the $(\rho\rho)$ component of the extrinsic curvature tensor is not strictly well-defined, we can still consider the $(\rho\rho)$ components of the boundary condition in the following form

$$0 = \lim_{\rho_v \rightarrow 0} \left\langle \frac{1}{\sqrt{-g}} \frac{\delta S_{EH}}{\delta g_{\rho\rho}} \right\rangle_v + \left(\frac{1}{\sqrt{-\check{g}}} \frac{\delta \check{S}_b}{\delta g_{\rho\rho}^b} \right)_{\rho=\rho_b}. \quad (3.92)$$

By definition, we have

$$\frac{1}{\sqrt{-g}} \frac{\delta S_{EH}}{\delta g_{\rho\rho}} = -\frac{1}{2\kappa^2} \mathcal{G}^{\rho\rho}. \quad (3.93)$$

As noted in (3.26), this component of the Einstein tensor contains only first derivatives of the metric field. It follows that

$$\lim_{\rho_v \rightarrow 0} \left\langle \frac{1}{\sqrt{-g}} \frac{\delta S_{EH}}{\delta g_{\rho\rho}} \right\rangle_v = -\frac{1}{2\kappa^2} \langle \mathcal{G}^{\rho\rho} \rangle_v = 0 \quad (3.94)$$

since metric functions and their first derivatives are assumed to be smooth. In this

simple way, we once again use the Hamiltonian constraint to conclude that the off-brane component of the brane stress energy is vanishing

$$\mathcal{T}^{\rho\rho} = \frac{\delta\check{S}_b}{\delta g_{\rho\rho}(y_b)} = 0. \quad (3.95)$$

So both off-brane components of brane stress-energy vanish in the limit $\rho_v \rightarrow 0$, and from this we also infer that their sums and differences also vanish in the effective theory

$$\lim_{r_v \rightarrow 0} \langle \mathcal{X}_{\text{loc}} \rangle_v = \mathcal{T}^\rho_\rho + \mathcal{T}^\theta_\theta = 0 \quad (3.96)$$

$$\lim_{r_v \rightarrow 0} \langle \mathcal{Z}_{\text{loc}} \rangle_v = \mathcal{T}^\rho_\rho - \mathcal{T}^\theta_\theta = 0. \quad (3.97)$$

These results are the analog for the effective theory of the KK-suppression of $\langle \mathcal{X} \rangle_v$ in the UV theory once $r_v \ll r_B$. As a consequence, in the effective theory there are only bulk contributions to the transverse stress energies

$$\mathcal{Z} = 0 \quad \text{and} \quad \mathcal{X} = \check{\mathcal{X}}_B = \Lambda - \check{L}_A. \quad (3.98)$$

3.4 Discussion

In this paper we investigated the gravitational properties of branes that carry localized flux of a bulk field, or BLF branes. As noted in the introduction, the treatment of a gravitating BLF branes is not straightforward because the delta-like function used to represent their localization must depend on the proper distance away from the brane. Because of their particularly simple structure, this is not a problem for branes

described only by their tension $\propto T$. However, the presence of metric factors in the BLF term $\propto \epsilon^{mn} A_{mn}$ complicates any calculation of transverse components of the brane's stress energy.

We resolved this ambiguity by constructing an explicit UV completion of BLF branes using Nielsen-Olesen vortices whose gauge sector mixes kinetically with a bulk gauge field. The gauge kinetic mixing, which is controlled by a dimensionless parameter ϵ , endows the bulk field with a non-zero flux in the localized region, even in the limit that this region is taken to be vanishingly small. This allows the UV theory to capture the effects of brane-localized flux.

The main result is that, in the UV picture, the gauge kinetic mixing can be diagonalized resulting in variables that clearly separate the localized sources from the bulk sources. In the diagonal basis, the energy associated with localized flux is always cancelled, and the canonical vortex gauge coupling is renormalized: $\hat{e}^2 = e^2/(1 - \epsilon^2)$. This allows us to identify the renormalized vortex tension as the quantity that controls the size of the defect angle in the geometry exterior to the vortex. We also find that the vortex relaxes to ensure that the average of the localized contributions to the transverse stress energy are controlled by the ratio between the size of the vortex and the characteristic bulk length scale r_v/r_B .

This informs our treatment of the IR theory with branes. We find that the delta-function treatment of the brane is particularly useful for calculating the flux of the bulk field, including its localized contributions, and a delta-function shift in the bulk gauge field strength can diagonalize the brane-localized flux term. This change of variables endows the action with a divergent term that we can interpret as a renormalization of the brane tension, in analogy with the $e \rightarrow \hat{e}$ renormalization of the

gauge coupling. We also show that the transverse components of the brane stress energy must vanish without explicitly calculating them. Rather, we use the Hamiltonian constraint and energy conservation to relate these stress energies to quantities which vanish as $r_v/r_B \rightarrow 0$, thereby circumventing any ambiguity in the metric dependence of the corresponding brane interactions.

The techniques we employ here should be relevant to other brane couplings that contain metric factors. For example, there is a codimension- k analogue of the BLF term that involves the Hodge dual of an k -form. Of particular interest is the case $k = 1$ where the brane can couple to the derivative of a bulk scalar field ϕ as follows $S_b \propto \int \star d\phi$, or a bulk gauge field A as follows $S_b \propto \int \star A$. We have also provided an explicit regularization of a $\delta_2(0)$ divergence. These are commonplace in treatments of brane physics, and usually deemed problematic. However, there is likely a similar renormalization story in these other cases.

Lastly, in the next chapter we apply these techniques to supersymmetric brane-world models that aim to tackle the cosmological constant problem [20]. The back-reaction of branes is a crucial ingredient of such models, and understanding the system in greater detail with an explicit UV completion will put these models on firmer ground and hopefully shed light on new angles from which to attack the CC problem.

Acknowledgements

We thank Ana Acucharro, Asimina Arvanitaki, Savas Dimopoulos, Gregory Gabadadze, Ruth Gregory, Mark Hindmarsh, Stefan Hoffmann, Florian Niedermann, Leo van Nierop, Massimo Porrati, Fernando Quevedo, Robert Schneider and Itay Yavin for useful discussions about self-tuning and UV issues associated with brane-localized

flux.

Bibliography

- [1] T. Vachaspati, “Dark Strings,” *Phys. Rev. D* **80**, 063502 (2009) [arXiv:0902.1764 [hep-ph]];
- J. M. Hyde, A. J. Long and T. Vachaspati, “Dark Strings and their Couplings to the Standard Model,” *Phys. Rev. D* **89**, no. 6, 065031 (2014) [arXiv:1312.4573 [hep-ph]];
- “Cosmic Strings in Hidden Sectors: 1. Radiation of Standard Model Particles,” *JCAP* **1409** (2014) 09, 030 [arXiv:1405.7679 [hep-ph]];
- P. Arias and F. A. Schaposnik, “Vortex solutions of an Abelian Higgs model with visible and hidden sectors,” *JHEP* **1412**, 011 (2014) [arXiv:1407.2634 [hep-th]];
- H. F. Santana Mota and M. Hindmarsh, “Big-Bang Nucleosynthesis and Gamma-Ray Constraints on Cosmic Strings with a large Higgs condensate,” *Phys. Rev. D* **91** (2015) 4, 043001 [arXiv:1407.3599 [hep-ph]].
- [2] B. Hartmann and F. Arbabzadah, “Cosmic strings interacting with dark strings,” *JHEP* **0907**, 068 (2009) [arXiv:0904.4591 [hep-th]];
- [3] H. B. Nielsen and P. Olesen, “Vortex Line Models for Dual Strings,” *Nucl. Phys. B* **61**, 45 (1973).
- [4] A. Vilenkin and E. P. S. Shellard, “Cosmic Strings and other Topological Defects,” Cambridge University Press, 1994;
- M. B. Hindmarsh and T. W. B. Kibble, “Cosmic strings,” *Rept. Prog. Phys.* **58**, 477 (1995) [hep-ph/9411342].

- [5] N. Arkani-Hamed, D. P. Finkbeiner, T. R. Slatyer and N. Weiner, “A Theory of Dark Matter,” *Phys. Rev. D* **79**, 015014 (2009) [arXiv:0810.0713 [hep-ph]];
- R. Essig, J. A. Jaros, W. Wester, P. H. Adrian, S. Andreas, T. Averett, O. Baker and B. Batell *et al.*, “Working Group Report: New Light Weakly Coupled Particles,” arXiv:1311.0029 [hep-ph].
- [6] B. Holdom, “Two U(1)’s and Epsilon Charge Shifts,” *Phys. Lett. B* **166**, 196 (1986).
- [7] M. Pospelov, A. Ritz and M. B. Voloshin, “Bosonic super-WIMPs as keV-scale dark matter,” *Phys. Rev. D* **78**, 115012 (2008) [arXiv:0807.3279 [hep-ph]];
- A. E. Nelson and J. Scholtz, “Dark Light, Dark Matter and the Misalignment Mechanism,” *Phys. Rev. D* **84**, 103501 (2011) [arXiv:1105.2812 [hep-ph]];
- P. Arias, D. Cadamuro, M. Goodsell, J. Jaeckel, J. Redondo and A. Ringwald, “WISPy Cold Dark Matter,” *JCAP* **1206**, 013 (2012) [arXiv:1201.5902 [hep-ph]].
- [8] A. Vilenkin, “Gravitational Field of Vacuum Domain Walls and Strings,” *Phys. Rev. D* **23**, 852 (1981);
- D. Garfinkle, “General Relativistic Strings,” *Phys. Rev. D* **32**, 1323 (1985);
- P. Laguna-Castillo and R. A. Matzner, “Coupled Field Solutions for U(1) Gauge Cosmic Strings,” *Phys. Rev. D* **36**, 3663 (1987);
- R. Gregory, “Gravitational Stability of Local Strings,” *Phys. Rev. Lett.* **59** (1987) 740;
- “Effective Action for a Cosmic String,” *Phys. Lett. B* **206** (1988) 199;
- R. Gregory, D. Haws and D. Garfinkle, “The Dynamics of Domain Walls and Strings,” *Phys. Rev. D* **42** (1990) 343.
- [9] T. Gherghetta, E. Roessl and M. E. Shaposhnikov, “Living inside a hedgehog: Higher dimensional solutions that localize gravity,” *Phys. Lett. B* **491** (2000) 353 [hep-th/0006251];
- T. Gherghetta and M. E. Shaposhnikov, “Localizing gravity on a string - like defect in six-dimensions,” *Phys. Rev. Lett.* **85** (2000) 240 [hep-th/0004014].

- [10] L. Randall and R. Sundrum, “An Alternative to compactification,” *Phys. Rev. Lett.* **83** (1999) 4690 [hep-th/9906064];
- “A Large mass hierarchy from a small extra dimension,” *Phys. Rev. Lett.* **83** (1999) 3370 [hep-ph/9905221].
- [11] A. Salam and E. Sezgin, “Chiral Compactification On Minkowski X S^{*2} Of $N=2$ Einstein-Maxwell Supergravity In Six-Dimensions,” *Phys. Lett. B* **147** (1984) 47.
- [12] For stabilization mechanisms for Type IIB 10D theories see:
- S. B. Giddings, S. Kachru and J. Polchinski, “Hierarchies from fluxes in string compactifications,” *Phys. Rev. D* **66**, 106006 (2002) [hep-th/0105097];
- M. R. Douglas and S. Kachru, “Flux compactification,” *Rev. Mod. Phys.* **79** (2007) 733 [hep-th/0610102].
- [13] For a stabilization mechanism using the competition between brane couplings of a bulk field see
- W. D. Goldberger and M. B. Wise, “Modulus stabilization with bulk fields,” *Phys. Rev. Lett.* **83** (1999) 4922 [hep-ph/9907447].
- [14] For flux-based stabilization mechanisms applied to 6D theories without branes see [11] and
- P. G. O. Freund and M. A. Rubin, “Dynamics of Dimensional Reduction,” *Phys. Lett. B* **97** (1980) 233;
- Y. Aghababaie, C. P. Burgess, S. L. Parameswaran and F. Quevedo, “SUSY breaking and moduli stabilization from fluxes in gauged 6-D supergravity,” *JHEP* **0303** (2003) 032 [hep-th/0212091].
- [15] For stabilization mechanisms applied to 6D theories using brane-bulk interactions see [18, 31] and
- C. P. Burgess and L. van Nierop, “Bulk Axions, Brane Back-reaction and Fluxes,” *JHEP* **1102** (2011) 094 [arXiv:1012.2638 [hep-th]];
- “Large Dimensions and Small Curvatures from Supersymmetric Brane Back-reaction,” *JHEP* **1104**, 078 (2011) [arXiv:1101.0152 [hep-th]].

- [16] A. Dahlen and C. Zukowski, “Flux Compactifications Grow Lumps,” *Phys. Rev. D* **90**, no. 12, 125013 (2014) [arXiv:1404.5979 [hep-th]].
- [17] J. W. Chen, M. A. Luty and E. Ponton, “A Critical cosmological constant from millimeter extra dimensions,” *JHEP* **0009** (2000) 012 [hep-th/0003067];
- [18] S. M. Carroll and M. M. Guica, “Sidestepping the cosmological constant with football shaped extra dimensions,” [hep-th/0302067].
- [19] For reviews of the cosmological constant problem see:
S. Weinberg, “The Cosmological Constant Problem,” *Rev. Mod. Phys.* **61** (1989) 1-23;
J. Polchinski, “The Cosmological Constant and the String Landscape,” [hep-th/0603249];
C.P. Burgess, “The Cosmological Constant Problem: Why it is Hard to Get Dark Energy from Micro-Physics,” in the proceedings of the Les Houches School *Cosmology After Planck*, [arXiv:1309.4133];
T. Banks, “Supersymmetry Breaking and the Cosmological Constant,” *Int. J. Mod. Phys. A* **29** (2014) 1430010 [arXiv:1402.0828 [hep-th]];
A. Padilla, “Lectures on the Cosmological Constant Problem,” [arXiv:1502.05296 [hep-th]].
- [20] Y. Aghababaie, C. P. Burgess, S. L. Parameswaran and F. Quevedo, “Towards a naturally small cosmological constant from branes in 6-D supergravity,” *Nucl. Phys. B* **680** (2004) 389 [hep-th/0304256];
- For reviews see: C. P. Burgess, “Towards a natural theory of dark energy: Supersymmetric large extra dimensions,” *AIP Conf. Proc.* **743** (2005) 417 [hep-th/0411140];
“Supersymmetric large extra dimensions and the cosmological constant: An Update,” *Annals Phys.* **313** (2004) 283 [hep-th/0402200].
- [21] C. P. Burgess, R. Diener and M. Williams, “EFT for Vortices with Dilaton-dependent Localized Flux,” arXiv:1508.00856 [hep-th];
“Self-Tuning at Large (Distances): 4D Description of Runaway Dilaton Capture,” arXiv:1509.04209 [hep-th].

- [22] S. Weinberg, *Gravitation and Cosmology*, Wiley 1973.
- [23] C. W. Misner, J. A. Wheeler and K. S. Thorne, *Gravitation*, W. H. Freeman & Company 1973.
- [24] E. Kasner, Trans. Am. Math. Soc., **27**, 155-162 (1925).
- [25] A. J. Tolley, C. P. Burgess, D. Hoover and Y. Aghababaie, “Bulk singularities and the effective cosmological constant for higher co-dimension branes,” JHEP **0603** (2006) 091 [hep-th/0512218].
- [26] E. M. Lifshitz and I. M. Khalatnikov, Adv. Phys. **12**, 185 (1963);
V. A. Belinsky, I. M. Khalatnikov and E. M. Lifshitz, Adv. Phys. **19**, 525 (1970);
V. A. Belinsky, I. M. Khalatnikov, Sov. Phys. JETP **36**, 591 (1973).
- [29] W. D. Goldberger and M. B. Wise, “Renormalization group flows for brane couplings,” Phys. Rev. D **65**, 025011 (2002) [hep-th/0104170].
C. de Rham, “The Effective field theory of codimension-two branes,” JHEP **0801**, 060 (2008) [arXiv:0707.0884 [hep-th]].
- [28] C. P. Burgess, D. Hoover, C. de Rham and G. Tasinato, “Effective Field Theories and Matching for Codimension-2 Branes,” JHEP **0903**, 124 (2009) [arXiv:0812.3820 [hep-th]].
A. Bayntun, C. P. Burgess and L. van Nierop, “Codimension-2 Brane-Bulk Matching: Examples from Six and Ten Dimensions,” New J. Phys. **12**, 075015 (2010) [arXiv:0912.3039 [hep-th]].
- [29] J.W. York, “Role of conformal three-geometry in the dynamics of gravitation,” Phys. Rev. Lett. **28** (1972) 1082;
G.W. Gibbons, S.W. Hawking, “Action integrals and partition functions in quantum gravity,” Phys. Rev. **D15** (1977) 2752.
- [30] C. P. Burgess, F. Quevedo, S. J. Rey, G. Tasinato and I. Zavala, “Cosmological space-times from negative tension brane backgrounds,” JHEP **0210** (2002) 028 [hep-th/0207104];
Y. Aghababaie, C. P. Burgess, J. M. Cline, H. Firouzjahi, S. L. Parameswaran,

- F. Quevedo, G. Tasinato and I. Zavala, “Warped brane worlds in six-dimensional supergravity,” JHEP **0309** (2003) 037 [arXiv:hep-th/0308064].
- [31] S. Mukohyama, Y. Sendouda, H. Yoshiguchi and S. Kinoshita, “Warped flux compactification and brane gravity,” JCAP **0507**, 013 (2005) [hep-th/0506050].

Chapter 4

EFT for vortices with dilaton-dependent flux

This chapter is a condensed version of the following paper

**C. P. Burgess, R. Diener and M. Williams, “EFT for vortices with
dilaton-dependent localized flux,” JHEP 1511 054 (2015),
arXiv:1508.00856**

Most of this chapter’s content is taken verbatim from this reference. However, some notation was modified, and the wording was revised to better fit within this thesis. Part of the paper’s discussion was also omitted for clarity, brevity and to avoid redundancies within this thesis.

This paper generalizes the discussion of the previous chapter to the case where there is a bulk scalar field, the dilaton, with nontrivial couplings to the vortex sector. In the effective theory, the physics of vortex-dilaton couplings is captured by branes that have dilaton-dependent localized flux and tension. These quantities’ nontrivial

dependence on the dilaton is derived from a matching procedure.

The back reaction of dilaton-dependent branes on bulk the bulk scalar is determined through the requirement that the branes in the IR theory endow the scalar with the same boundary conditions as the vortices. The derived boundary conditions are consistent with the matching conditions statement that the near-brane derivative of a bulk field is controlled by the variation of the brane action with respect to that field. The transverse stress energy of dilaton-dependent branes is also determined in a way that does not make any assumptions about their dependence on the bulk metric. The procedure used is a simple generalization of the arguments from the previous chapter. However, unlike the previous chapter, the brane can have nonvanishing transverse stress energy, when its dilaton-dependence breaks scale invariance.

With a correct picture of brane physics in tow, the curvature of the macroscopic dimensions is determined as a function of the brane properties, and three characteristic sizes are identified. For generic branes with dilaton-dependent tension $T'(\phi) \neq 0$, the curvature is controlled by the same scale as the tension. In this case, the prediction of a large curvature is as much a problem as it is in the unmodified Standard Model. For scale invariant branes, which turn out to be independent of the dilaton, the curvature vanishes. This case is also problematic, since the predicted curvature is too small, and there is a runaway zero mode associated with scale invariance which is not stabilized. However, one promising type of brane is identified, a *decoupled* brane that has dilaton-independent tension but dilaton-dependent localized flux. This case is promising because the curvature is suppressed by the size of the extra dimensions (even if the brane tension is large) and scale invariance is broken. Exactly how this scale breaking stabilizes the zero mode, and the related issue of the extra dimensional

size, are addressed in the next chapter.

Beyond this thesis, the results in this chapter can be easily generalized to determine the effective description of almost any localized object of any codimension, and the associated back reaction.

4.1 Introduction

A ‘vanilla’ Nielsen-Olesen vortex [1, 2] carries $U(1)$ flux but this flux is normally expelled from the region outside of the vortex. In this paper we study the gravitational response of vortices (or ‘fat’ branes) that carry localized amounts of an external magnetic flux that is *not* expelled from its surrounding environment (so-called ‘dark vortices’ or ‘dark strings’ [3]). Our description of these systems closely parallels our companion paper [4] (which was presented in the previous chapter), extending it to the case where effective couplings are functions of the bulk dilaton that tends to appear in supersymmetric theories.

Vortices which partially localize bulk flux can arise within supersymmetric theories in various dimensions, and whether their presence breaks supersymmetry depends on the relative size of their tension and the amount localized bulk flux they carry [5]. Because of this their tension and localized flux compete with one another in the amount of curvature produced by their back-reaction on their surrounding geometry. Our main goal is to explore this competition in detail and to identify precisely how it depends on the various parameters that describe the vortex physics.

We have several purposes in mind when doing so. First and foremost we wish to understand how brane back-reaction influences the transverse geometry through which localized sources move, and in particular how they source the dilaton to set

the size of the transverse dimensions and the curvature of the geometry induced on their world-sheet. Much is known about the systems in the limit when the sources are pointlike [6], and in particular it is known that the world-sheet geometries are exactly flat (at the classical level) if the dilaton should have a vanishing derivative at all source positions [7] (a result which we also re-derive here).¹ What this leaves open is whether there exists any kind of source for which a vanishing near-source dilaton derivative is possible and, even if so, whether the resulting curvature is then nonzero but dominated by finite-size vortex effects that could be suppressed for small vortices but not vanishing.

We find three main results.

- *Vortex-dilaton coupling:* In general the behaviour of a bulk field very near a point source is controlled by the derivative of the source action with respect to the field of interest [6, 11, 12] (much like the quantity $\lim_{r \rightarrow 0} r^2 \partial V / \partial r$ is dictated by a point-source's charge, $Q \propto \delta S / \delta V$ in electrostatics). So naively a vanishing dilaton derivative at the position of a source brane is arranged by not coupling the dilaton to the brane at all. While we confirm the truth of this assertion, we also find it is harder to completely avoid such a brane coupling to the dilaton than one might think. More specifically, we find that although it *is* possible to arrange a dilaton-free tension, it is much more difficult to arrange dilaton-free localized flux. It is more difficult because in a supersymmetric bulk the value of the dilaton sets the local size of the gauge coupling for the flux.
- *Modulus stabilization:* By computing how vortex-bulk energetics depend on the value of the dilaton we verify earlier claims [6, 11, 13] that (with two transverse

¹Indeed this underlies the study of these system as potential approaches [8, 9] to the cosmological constant problem [9, 10].

dimensions) brane couplings generically stabilize the size of the transverse dimensions in supersymmetric models, in a manner similar to Goldberger-Wise stabilization [14] in 5D. They do so because they break the classical scale invariance of the bulk supergravity that prevents the bulk from stabilizing on its own (through *eg* flux stabilization). The tools we provide allow an explicit calculation of the energetics as a function of the dilaton field (and so in principle allow a calculation of the stabilizing dilaton potential).

- *Low-energy on-brane curvature:* We find that the same stabilizing dynamics usually also curves the dimensions along the vortex world-sheets, and generically does so by an amount commensurate with their tension, $R \sim G_N \tilde{T}$, where \tilde{T} is the vortex tension (defined more precisely below) and G_N is Newton's constant for observers living on the brane. For specific parameter regimes the on-vortex curvature can be less than this however, being suppressed by the deviation of the vortex from scale invariance (when this is small) and the ratio of the vortex size to the bulk.
- *Matching and effective descriptions:* We describe our analysis throughout in two complementary ways. On one hand we do so using the full (UV) description within which the vortices are explicit classical solutions. We then do so again using the lower-energy (IR) extra-dimensional effective theory within which the vortices are regarded as point sources because their sizes are not resolved. By comparing these calculations we provide explicit matching formulae that relate dilaton-dependent effective parameters (like tension and localized flux) to underlying properties of the UV completion.

- *Efficient description of point-source back-reaction:* We provide explicit formula that relate the near-source boundary conditions of bulk fields in terms of the source tension and localized flux. Because these boundary conditions determine the integration constants of the external bulk solutions they efficiently solve the back-reaction problem in a way that does not depend on providing a detailed construction of the internal microstructure of the sources. As such they provide the most efficient way to describe how such sources gravitate, and the framework within which to renormalize the divergences associated with the singularity of bulk fields at the source positions [13, 15]. We show in passing why a commonly used δ -function way of trying to infer brane-bulk interactions can give incorrect results.

Our conclusions also include several more technical observations about the gravitational physics of small localized brane sources. In particular, we identify how stress-energy conservation strongly constrains the components of the source stress energy tensor, allowing in particular the extra-dimensional off-brane stress-energy components to be dictated in terms of the effective action governing the on-brane degrees of freedom. We do so by using the vortex system to explicitly construct the effective theory of point sources describing the extra-dimensional response to the vortices on scales too long to resolve the vortex size. In particular we show how the radial Einstein ‘constraint’ determines the two nontrivial off-brane components of stress energy (for rotationally invariant – monopole – sources) on scales much longer than the size of the vortices themselves.

A road map

We organize our discussion as follows. The following section, §4.2, describes the bulk system in the absence of any localized sources. The purposes of doing so is to show how properties of the bulk physics (such as extra-dimensional size and on-brane curvature) are constrained by the field equations, which controls the extent to which they depend on the properties of any source branes.

Then come sources. First, §4.3 describes the source physics in terms of a UV theory within which the branes can be found as explicit classical vortex solutions. This is followed, in §4.4 by a discussion of the higher-dimensional effective theory that applies on length scales too large to resolve the vortices, but small enough to describe the extra-dimensional geometry. In this regime the vortices are described by effective point sources, and we find their properties as functions of the choices made in the full UV theory. Finally, §4.5 summarizes how the main physical quantities scale as functions of the couplings assumed between the vortex and the dilaton. Our conclusions are summarized in a final discussion section, §4.6.

4.2 The Bulk

We start by outlining the action and field equations of the bulk, which we take to be an Einstein-Maxwell-scalar system. Our goal is to understand how bulk properties (such as curvatures) are related to the asymptotic behaviour of the fields near any localized sources. We return in later sections describing the local sources in terms of vortices, with the goal of understanding what features of the source control the near-source asymptotics. We imagine the bulk to span $D = d + 2$ spacetime dimensions

with the d -dimensional sources localized in two transverse dimensions. The most interesting cases of practical interest are the cosmic string [with $(D, d) = (4, 2)$] and the brane-world picture [with $(D, d) = (6, 4)$].

4.2.1 Action and field equations

The bulk action of interest is given by

$$\begin{aligned} S_B &= - \int d^{d+2}x \sqrt{-g} \left[\frac{1}{2\kappa^2} g^{MN} \left(\mathcal{R}_{MN} + \partial_M \phi \partial_N \phi \right) + V_B(\phi) + \frac{1}{4} e^{-\phi} A_{MN} A^{MN} \right] \\ &=: - \int d^{d+2}x \sqrt{-g} \left(L_{EH} + L_\phi + L_A \right) =: - \int d^{d+2}x \sqrt{-g} L_B \end{aligned} \quad (4.1)$$

where² $A_{MN} = \partial_M A_N - \partial_N A_M$ is a D -dimensional gauge field strength and \mathcal{R}_{MN} denotes the D -dimensional Ricci tensor. The second line defines the Einstein-Hilbert, scalar and gauge contributions — *i.e.* L_{EH} , L_ϕ and L_A — in terms of the items in the line above, with L_B denoting their sum. When needed explicitly we take the scalar potential to be

$$V_B(\phi) = V_0 e^\phi, \quad (4.2)$$

and in the special case $V_0 = 2g_R^2/\kappa^4$ this corresponds to a subset of the action for Nishino-Sezgin supergravity [18] when $d = 4$ (so $D = 6$). In this case g_R is the gauge coupling constant for a specific gauged $U(1)_R$ symmetry that does not commute with 6D supersymmetry. In what follows we denote by g_A the gauge coupling for the gauge field A_M , although $g_A = g_R$ in the most interesting³ situation where this gauge field

²We use Weinberg's curvature conventions [16], which differ from those of MTW [17] only by an overall sign in the definition of the Riemann tensor.

³Enhanced interest comes from the unbroken 4D supersymmetry that these configurations can enjoy.

is the $U(1)_R$ gauge field.

Scaling properties

For later purposes notice that L_B scales homogeneously, $L_B \rightarrow s^{-1}L_B$ under the rigid rescalings $g_{MN} \rightarrow s g_{MN}$ and $e^\phi \rightarrow s^{-1}e^\phi$, which as a consequence is a symmetry of the classical equations of motion. The corresponding transformation for the action is $S_B \rightarrow s^{d/2}S_B$, as is most easily seen by transforming to a scale-invariant metric $\hat{g}_{MN} = e^\phi g_{MN}$, in which case all terms of the bulk lagrangian are proportional to $e^{-d\phi/2}$ with ϕ otherwise only appearing through its derivative, $\partial_M \phi$. Besides ensuring classical scale invariance this also shows that it is the quantity $e^{d\phi/2}$ that plays the role of \hbar in counting loops within the bulk part of the theory.

The bulk system enjoys a second useful scaling property. If we rescale the gauge field so $\mathcal{A}_M := g_A A_M$ then arbitrary constant shifts $\phi \rightarrow \phi + \phi_\star$ leave the action unchanged provided we also rescale the couplings by $g_A \rightarrow g_{A\star} := g_A e^{\phi_\star/2}$ and $V_0 \rightarrow V_\star := V_0 e^{\phi_\star}$ (or, if $V_0 = 2g_R^2/\kappa^4$, equivalently $g_R \rightarrow g_{R\star} := g_R e^{\phi_\star/2}$). This is convenient inasmuch as $\phi = 0$ can always be chosen to be the present-day vacuum provided the values of constants like g_A and V_0 are chosen appropriately.

Bulk field equations

The field equations for the Maxwell field arising from the bulk action are

$$\frac{1}{\sqrt{-g}} \partial_M \left(\sqrt{-g} e^{-\phi} A^{MN} \right) = 0, \quad (4.3)$$

which is supplemented (as usual) by the Bianchi identity $dA_{(2)} = 0$, for the 2-form A_{MN} . The bulk dilaton equation is similarly

$$\square\phi = \frac{1}{\sqrt{-g}} \partial_M \left(\sqrt{-g} g^{MN} \partial_N \phi \right) = \kappa^2 (V_B - L_A), \quad (4.4)$$

while the Einstein equations can be written in their trace-reversed form

$$\mathcal{R}_{MN} = -\kappa^2 X_{MN}, \quad (4.5)$$

where $X_{MN} := T_{MN} - (1/d) g_{MN} T^P{}_P$ and the bulk stress-energy tensor is

$$(T_B)_{MN} = \frac{1}{\kappa^2} \partial_M \phi \partial_N \phi + e^{-\phi} A_{MP} A_N{}^P - g_{MN} \left[\frac{(\partial\phi)^2}{2\kappa^2} + V_B + L_A \right]. \quad (4.6)$$

Notice that it is a special feature of the split into $D = d + 2$ dimensions that any maximally symmetric contribution to the d -dimensional part of the stress-energy, $T_{\mu\nu} \propto g_{\mu\nu}$, drops out of $X_{\mu\nu}$ and so naively does not contribute directly to the 4D Ricci curvature, $\mathcal{R}_{\mu\nu}$.

4.2.2 Symmetry ansätze

We adopt the usual axisymmetric symmetry ansatz for the metric and bulk fields

$$ds^2 = W^2(\rho) \tilde{g}_{\mu\nu}(x) dx^\mu dx^\nu + d\rho^2 + B^2(\rho) d\theta^2. \quad (4.7)$$

With these choices the field equations simplify to coupled nonlinear ordinary differential equations. Denoting differentiation with respect to proper distance, ρ , by primes,

the bulk gauge field equation becomes

$$\left(\frac{e^{-\phi}W^d A_{\rho\theta}}{B}\right)' = 0, \quad (4.8)$$

while the field equation for the dilaton becomes

$$\frac{1}{BW^d} \left(BW^d \phi'\right)' = \kappa^2 (V_B - L_A) =: \kappa^2 \mathcal{X}_B, \quad (4.9)$$

where the last equality defines $\mathcal{X}_B := V_B - L_A$. With the assumed symmetries the nontrivial components of the matter stress-energy *in the bulk* are

$$(T_B)_{\mu\nu} = -g_{\mu\nu} \varrho_B, \quad (T_B)^\rho{}_\rho = \mathcal{Z}_B - \mathcal{X}_B \quad \text{and} \quad (T_B)^\theta{}_\theta = -(\mathcal{Z}_B + \mathcal{X}_B), \quad (4.10)$$

where the bulk contribution to \mathcal{X} is \mathcal{X}_B as defined above and we also define the following bulk quantities

$$\varrho_B := \frac{(\phi')^2}{2\kappa^2} + V_B + L_A \quad \text{and} \quad \mathcal{Z}_B := \frac{(\phi')^2}{2\kappa^2}. \quad (4.11)$$

The three independent components of the trace-reversed bulk Einstein equations then consist of those in the directions of the d -dimensional on-brane geometry,

$$\mathcal{R}_{\mu\nu} = -\kappa^2 X_{\mu\nu} \quad (4.12)$$

of which maximal symmetry implies the only nontrivial combination is the trace,

which reads as follows in the bulk

$$\mathcal{R}_{(d)} := g^{\mu\nu} \mathcal{R}_{\mu\nu} = \frac{\check{R}}{W^2} + \frac{d}{BW^d} \left(BW' W^{d-1} \right)' = -2\kappa^2 \mathcal{X}_B. \quad (4.13)$$

The components dictating the 2-dimensional transverse geometry similarly are $\mathcal{R}_{mn} = -\kappa^2 X_{mn}$, which for the bulk has two independent components. We choose one to be the difference between its two diagonal elements

$$\mathcal{G}^\rho_\rho - \mathcal{G}^\theta_\theta = \mathcal{R}^\rho_\rho - \mathcal{R}^\theta_\theta = -\kappa^2 (T^\rho_\rho - T^\theta_\theta), \quad (4.14)$$

which for the assumed geometry becomes (in the bulk)

$$\frac{B}{W} \left(\frac{W'}{B} \right)' = -\frac{2}{d} \kappa^2 \mathcal{Z}_B = -\frac{(\phi')^2}{d} \leq 0. \quad (4.15)$$

This shows that W'/B is a monotonically decreasing function of ρ .

Another useful Einstein equation corresponds to the $(\theta\theta)$ component of the trace-reversed equation, which for the bulk reads

$$\frac{(B'W^d)'}{BW^d} = -\kappa^2 \left[\varrho_B - \mathcal{Z}_B - \left(1 - \frac{2}{d} \right) \mathcal{X}_B \right] = -2\kappa^2 \left(L_A + \frac{\mathcal{X}_B}{d} \right). \quad (4.16)$$

4.2.3 Bulk solutions

We next describe some of the properties of the solutions to these field equations. In order to accommodate our later inclusion of the equations governing any localized sources, we examine solutions of the bulk equations only within a domain, the ‘bulk’: B_{ext} , which consists of the full 2D geometry transverse to the sources from which small

volumes ('Gaussian pillboxes', X_v) are excised. These pillboxes completely enclose any sources that might be present. In practice we define B_{ext} such that the radial proper distance coordinate satisfies $\rho_- \leq \rho \leq \rho_+$, with the sources lying just outside of this range. When not specifying which source is of interest, we generically use $\rho_v = \{\rho_+, \rho_-\}$ to denote the boundary between the source and the bulk.

Integral relations

Before writing some exact and approximate solutions we first record several exact integral expressions that can be derived by directly integrating the field equations over the volume B_{ext} , being careful to keep track of its boundaries at $\rho = \rho_-$ and $\rho = \rho_+$.

Integrating the bulk Maxwell equation, (4.8), with respect to ρ in radial gauge gives

$$A_{\rho\theta} = A'_\theta = \frac{QB e^\phi}{W^d}, \quad (4.17)$$

for integration constant Q , and this in turn integrates locally to give (up to a gauge transformation)

$$A_\theta(\rho_+) - A_\theta(\rho_-) = \frac{Q}{2\pi} \left\langle \frac{e^\phi}{W^{2d}} \right\rangle_{\text{ext}}, \quad (4.18)$$

where we define the notation

$$\left\langle \dots \right\rangle_{\text{ext}} := \frac{1}{\sqrt{-\tilde{g}}} \int_{B_{\text{ext}}} d^2y \sqrt{-g} \left(\dots \right) = 2\pi \int_{\rho_-}^{\rho_+} d\rho B W^d \left(\dots \right). \quad (4.19)$$

These expressions also contain the seeds of flux quantization when applied to spherical transverse dimensions. To see this we take ρ_\pm to lie infinitesimally close to the north and south poles and excise these two points, leaving the topology of

a sphere with two points removed (or an annulus). Integrating (4.18) around the axial direction and using the quantization of any gauge transformation, $g^{-1}\partial_\theta g$, then implies

$$\frac{2\pi N}{g_A} = \oint_{\rho_-} A_\theta d\theta - \oint_{\rho_+} A_\theta d\theta + Q \left\langle \frac{e^\phi}{W^{2d}} \right\rangle_{\text{ext}} = \Phi_{A^-} + \Phi_{A^+} + Q \left\langle \frac{e^\phi}{W^{2d}} \right\rangle_{\text{ext}}, \quad (4.20)$$

where N is an integer and g_A is the gauge coupling for the field A_M and Φ_{A^\pm} denotes the total A flux through the caps over the relevant poles. In the absence of sources at the poles we can contract the circles at $\rho = \rho_\pm$ to a point and learn $\oint_\pm A_\theta d\theta \rightarrow 0$, in which case (4.20) becomes the usual condition on Q required by flux quantization. But when sources are present $\oint_\pm A_\theta d\theta$ need not vanish if there is flux localized within the source. When this is so their presence on the right-hand side of (4.20) modifies the implications for Q of flux-quantization [6].

Similarly integrating the field equation (4.9) for the dilaton gives

$$\left[BW^d \phi' \right]_{\rho_+} - \left[BW^d \phi' \right]_{\rho_-} = \frac{\kappa^2}{2\pi} \langle V_B - L_A \rangle_{\text{ext}} =: \frac{\kappa^2}{2\pi} \langle \mathcal{X}_B \rangle_{\text{ext}}. \quad (4.21)$$

Two of the Einstein equations also provide direct first integrals. Integrating (4.16) leads to

$$\left[B'W^d \right]_{\rho_+} - \left[B'W^d \right]_{\rho_-} = -\frac{\kappa^2}{2\pi} \left\langle \varrho_B - \mathcal{Z}_B - \left(1 - \frac{2}{d}\right) \mathcal{X}_B \right\rangle_{\text{ext}} = -\frac{\kappa^2}{\pi} \left\langle L_A + \frac{\mathcal{X}_B}{d} \right\rangle_{\text{ext}}, \quad (4.22)$$

while the integral of (4.13) implies

$$\left[B (W^d)' \right]_{\rho_+} - \left[B (W^d)' \right]_{\rho_-} = -\frac{1}{2\pi} \left[\check{R} \langle W^{-2} \rangle_{\text{ext}} + 2\kappa^2 \langle \mathcal{X}_B \rangle_{\text{ext}} \right]. \quad (4.23)$$

Of particular interest for present purposes is the simple relationship between the on-brane curvature, \check{R} , and the near-source boundary values of bulk fields obtained by combining (4.21) with (4.23):

$$\left[BW^d \left(\frac{dW'}{W} + 2\phi' \right) \right]_{\rho_+} - \left[BW^d \left(\frac{dW'}{W} + 2\phi' \right) \right]_{\rho_-} = -\frac{\check{R}}{2\pi} \langle W^{-2} \rangle_{\text{ext}} . \quad (4.24)$$

This states that the quantity $BW^d (\phi + \frac{d}{2} \ln W)'$ is monotonic in ρ everywhere outside of the sources, growing or shrinking according to the sign of \check{R} or remaining constant when $\check{g}_{\mu\nu}$ is flat. Should $BW^d (\phi + \frac{d}{2} \ln W)'$ take the same value for two different values of ρ in the bulk, then we can conclude that $\check{R} = 0$. In particular, if there exist sources for which $2\phi' + dW'/W = 0$ at both source positions, then any interpolating geometry between the sources must satisfy $\check{R} = 0$; that is, the vanishing of $(e^\phi W^{d/2})'$ in the near-source limit for both sources is a sufficient condition for $\check{R} = 0$ (as first argued some time ago [7]). A special case of the $\check{R} = 0$ solutions are those for which $BW^d (\phi + \frac{d}{2} \ln W)'$ vanishes everywhere, which have $e^\phi W^{d/2}$ constant.

Asymptotic forms

Given the intimate relationship between \check{R} and near-source derivatives implied by eq. (4.24), we next examine what the field equations imply about the form of the bulk solutions very close to, but outside of, a source much smaller than the transverse dimensional size (*eg* outside a source for which $\rho_v \rightarrow 0$).⁴

As noted in the previous chapter, the presence of such a small source induces an apparent singularity into the external geometry, at the position $\rho = \rho_\star$ defined as

⁴Our treatment here follows closely that of [4] and [19], which are themselves based on the classic BKL treatment of near-singularity time-dependence [20].

the place where $B(\rho)$ vanishes when extrapolated using only the bulk field equations. That is, it implies there would be a singularity in the external geometry if this geometry were extrapolated right down to zero size (rather than being smoothed out by the physics of the source interior, as illustrated in Figure 4.1). If the centre of the source is chosen to be $\rho = 0$ then in order of magnitude ρ_* is of order the source's size: $\rho_* \sim \rho_v$.

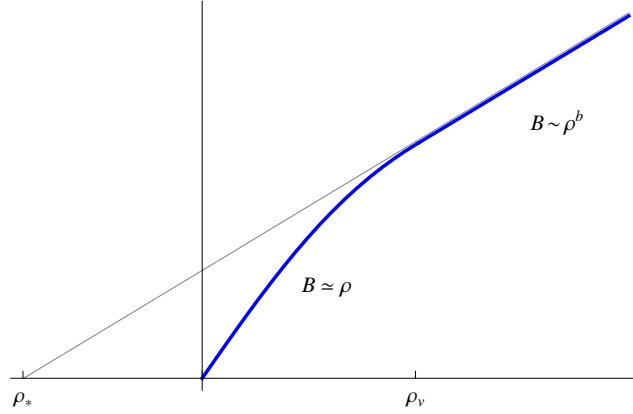


Figure 4.1: A cartoon illustration of the definition of ρ_* . The (blue) metric function B increases linearly away from the origin with unit slope $B(\rho) \simeq \rho$. Outside of the source $\rho \gtrsim \rho_v$, the solution is a power law in ρ with $B(\rho) \sim \rho^b$. The straight (red) line extrapolates this exterior behaviour to the point, $\rho = \rho_*$, where the external B would have vanished if the vortex had not intervened first.

When constructing a near-source solution it is most informative to do so as a series solution expanding in powers of the distance, $\hat{\rho} := \rho - \rho_*$, from the singular source point. That is,

$$\begin{aligned}
 W &= W_0 \left(\frac{\hat{\rho}}{\ell} \right)^w + W_1 \left(\frac{\hat{\rho}}{\ell} \right)^{w+1} + \dots \\
 B &= B_0 \left(\frac{\hat{\rho}}{\ell} \right)^b + B_1 \left(\frac{\hat{\rho}}{\ell} \right)^{b+1} + \dots \\
 \text{and } e^\phi &= e^{\phi_0} \left(\frac{\hat{\rho}}{\ell} \right)^z + \dots,
 \end{aligned} \tag{4.25}$$

where ℓ is a measure of the proper size of the transverse geometry, which we assume to be much larger than the source's size, so $\ell \gg \hat{\rho}$. The powers w , b and z describe the nature of the singularity at $\rho = \rho_*$, and all but three combinations of these parameters and the W_i , B_i and ϕ_i coefficients turn out to be related to one another by the bulk field equations. The three 'free' parameters are instead determined by boundary conditions that the bulk solutions satisfy in the near-source regime.

In particular, for small sources these field equations allow all of the W_i , B_i and ϕ_i to be computed in terms of (say) ϕ_0 , W_0 and B_0 , and further imply the following two 'Kasner' relations [19, 21] amongst the powers b , w and z :

$$dw + b = dw^2 + b^2 + z^2 = 1. \quad (4.26)$$

The second of these in turn implies w , b and z must reside within the intervals

$$|w| \leq \frac{1}{\sqrt{d}} \quad \text{and} \quad |b|, |z| \leq 1. \quad (4.27)$$

It turns out that the rest of the field equations do not give additional constraints on the three parameters b , w and z , and so one combination of these is one of the quantities determined by the physical properties of the source.

Expansion about a regular point — *ie* not the location of a singularity — should correspond to the specific solution $z = w = 0$ and $b = 1$ to eqs. (4.26). In the presence of weakly gravitating sources we expect to find small deviations from these values, whose size can be inferred by solving (4.26) perturbatively. To this end we write $b = 1 + b_1\delta + b_2\delta^2 + \dots$, $w = w_1\delta + \dots$ and $z = z_1\delta + \dots$ and expand. Working to

order δ^2 we find the one-parameter family of solutions

$$z = z_1 \delta + \mathcal{O}(\delta^2), \quad b = 1 - \frac{z^2}{2} + \mathcal{O}(\delta^3) \quad \text{and} \quad dw = \frac{z^2}{2} + \mathcal{O}(\delta^3). \quad (4.28)$$

Quite generally only z can deviate from its background value at linear order, and the leading quadratic contributions to w and $b - 1$ are not independent of this linear deviation in z . In later sections we find z is determined by the coupling of ϕ to the source lagrangian, and so we generically expect δ to be of order $\kappa^2 v^2$, where v^2 is a measure of the energy density (or tension) carried by the source (more about which below). Fig. 4.2 provides numerical evidence for the validity of the Kasner equations and their perturbative solution, (4.28), nearby but outside of an explicit vortex solution.

In terms of these Kasner exponents, the combination appearing on the left-hand side of eq. (4.24) in the near-source limit is

$$\lim_{\rho \rightarrow \rho_*} BW^d \left(\frac{dW'}{W} + 2\phi' \right) = (2z + dw) \left(\frac{B_0 W_0^d}{\ell} \right) \left(\frac{\hat{\rho}}{\ell} \right)^{dw+b-1} = (2z + dw) \left(\frac{B_0 W_0^d}{\ell} \right), \quad (4.29)$$

where the second equality uses the linear Kasner condition (4.26). When eq. (4.29) is order $\kappa^2 v^2$ then eq. (4.24) implies that the curvature \check{R} is of order $\check{R} \sim \kappa_d^2 v^2$ corresponding to a d -dimensional energy density of order v^2 . Here κ_d is the dimensionally reduced gravitational coupling of the low-energy d -dimensional theory, and we use a result, derived below, that $\kappa_d^{-2} \simeq \kappa^{-2} \langle W^{-2} \rangle_{\text{ext}}$.

Of particular interest are situations where the near-source solutions satisfy $z = 0$ since the Kasner conditions imply these also satisfy $w = 0$ and so $2z + dw = 0$. Consequently for any such source the leading contribution, eq. (4.29), to \check{R} vanishes.

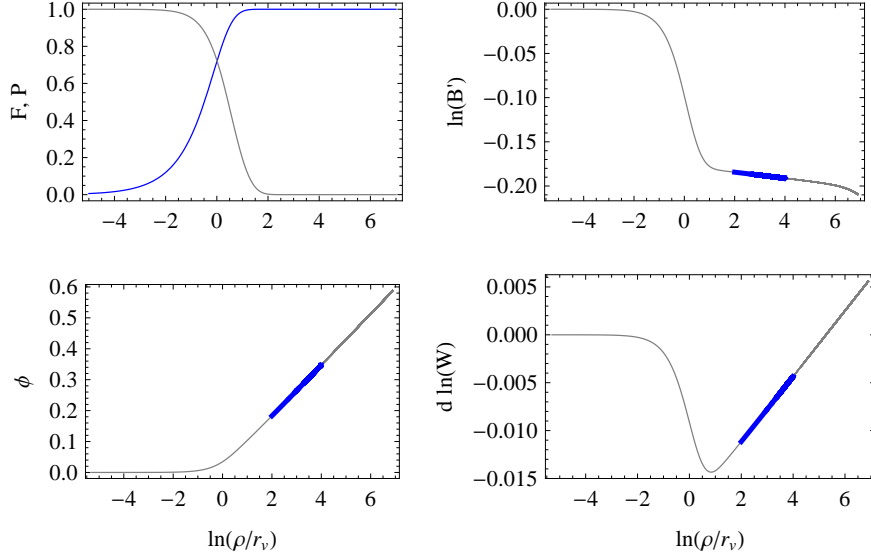


Figure 4.2: This plot illustrates the near-source Kasner region for bulk fields that are sourced by a generic vortex with tension $v^2 = 0.25/\kappa^2$. In the top left plot, the vortex profiles are shown on a logarithmic axis, with the (blue) scalar profile F increasing towards its asymptotic vacuum value $F \rightarrow 1$ and the (grey) gauge profile P decreasing towards its asymptotic value $P \rightarrow 0$. (See below for more detailed definitions.) These profiles approach their vacuum values exponentially, and they can be neglected in the region $\tau = \ln(\rho/r_v) \gtrsim 2$, which is where the Kasner region $\rho \gtrsim \rho_v$ begins. In the next plot, $\ln(B')$ is seen to be linear in τ in the darkened (blue) near-vortex region, before the bulk sources dominate the behaviour of B' at larger τ . This blue region is the Kasner region, where the bulk fields obey power laws, and this behaviour is also apparent in the plots of $\ln(e^\phi) = \phi$ and $\ln(W^d) = d \ln W$. The Kasner powers can be extracted in this region, and for this particular source we find numerically $dw = 0.0034$, $1 - b = 0.0034$ and $z = 0.082$ which is in agreement with the perturbative solution of (4.28). Finally, we note that these numerical results are also consistent with the estimates $z \sim \delta \sim \kappa^2 v^2$ as is argued below.

In this case it is a subleading term that first contributes on the left-hand side of (4.24), implying that \tilde{R} is suppressed relative to $\kappa_d^2 v^2$ by a power of the ratio of source and extra-dimensional sizes: ρ_\pm/ℓ . This asymptotic reasoning is borne out by the explicit numerical and analytic solutions described in the next sections.

Explicit bulk solutions

It is useful to see how the above general arguments go through for explicit solutions to the bulk field equations, which are known in great detail [22, 23] when $\phi' \rightarrow 0$ in the near-source limit in the special case where $d = 4$ and $D = 6$ and $V_0 = 2g_R^2/\kappa^4$. The solutions are most simply written using the symmetry ansatz

$$ds^2 = W^2(\xi) ds_4^2 + r^2(\xi) \left(d\xi^2 + \alpha^2(\xi) \sin^2 \xi d\theta^2 \right), \quad (4.30)$$

where ds_4^2 denotes the maximally symmetric on-vortex geometry, $ds_4^2 = \check{g}_{\mu\nu} dx^\mu dx^\nu$. With this ansatz, as seen above, the field equations ensure $\check{R} = 0$ provided we assume $\phi' \rightarrow 0$ in the near-source limit, which we now do (and so also take $\check{g}_{\mu\nu} = \eta_{\mu\nu}$). The dilaton and metric function then turn out to be

$$e^{\phi(\xi)} = \frac{e^\varphi}{W^2(\xi)}, \quad \alpha(\xi) = \frac{\Upsilon}{W^4(\xi)} \quad \text{and} \quad r(\xi) = r_B W(\xi) e^{-\varphi/2}, \quad (4.31)$$

with

$$W^4(\xi) = e^v \sin^2 \frac{\xi}{2} + e^{-v} \cos^2 \frac{\xi}{2} = \cosh v - \sinh v \cos \xi, \quad (4.32)$$

where v , Υ and φ are integration constants. Notice that $r^2 e^\phi = r_B^2$ for all ξ , with the length-scale r_B set by

$$r_B := \frac{\kappa}{2g_R}. \quad (4.33)$$

The two sources for this geometry are located at the two singular points, $\xi_- = 0$ and $\xi_+ = \pi$, where the transverse space pinches off. In the near-brane limit, $\xi \rightarrow 0$,

we have $W \rightarrow W_- + \mathcal{O}(\xi^2)$, and so the proper radial distance, given by

$$\rho(\xi) = \int d\xi r(\xi) = r_B e^{-\varphi/2} \int d\xi W(\xi), \quad (4.34)$$

in this limit becomes $\rho = r_B e^{-\varphi/2} [W_0 \xi + \mathcal{O}(\xi^3)]$, and so $\alpha \rightarrow \alpha_- = \Upsilon/W_-^4 + \mathcal{O}(\rho^2)$, $B \rightarrow \alpha_- \rho + \mathcal{O}(\rho^3)$ and $e^\phi \rightarrow e^\varphi/W_-^2 + \mathcal{O}(\rho^2)$ in the near-brane limit (corresponding to the Kasner exponents $z = w = 0$ and $b = 1$). Similar properties also hold for $\xi \rightarrow \pi$.

Two of the integration constants — v and Υ — can be traded for the conical defect angles, $2\pi(1 - \alpha_\pm)$, in the two near-brane limits, with

$$\Upsilon = \sqrt{\alpha_+ \alpha_-} \quad \text{and} \quad e^v = \sqrt{\frac{\alpha_-}{\alpha_+}} = W_+^4 = \frac{1}{W_-^4}. \quad (4.35)$$

In terms of these $\alpha(\xi)$ and $W(\xi)$ are given simply by

$$\frac{1}{\alpha(\xi)} = \frac{1}{\alpha_-} \cos^2 \frac{\xi}{2} + \frac{1}{\alpha_+} \sin^2 \frac{\xi}{2} \quad \text{and} \quad W^4(\xi) = W_-^4 \cos^2 \frac{\xi}{2} + W_+^4 \sin^2 \frac{\xi}{2}. \quad (4.36)$$

In particular, in the special case $W_+ = W_-$ the function $W(\xi)$ — and so also $\phi(\xi)$, $r(\xi)$ and $\alpha(\xi)$ — becomes constant, and the geometry reduces to the simple rugby-ball solution [8]. This has proper distance $\rho = \xi r_B e^{-\varphi/2}$ and

$$B(\rho) = \alpha r_B e^{-\varphi/2} \sin \left(\frac{\rho}{r_B e^{-\varphi/2}} \right) =: \alpha \ell \sin \left(\frac{\rho}{\ell} \right), \quad (4.37)$$

and so $\ell = r_B e^{-\varphi/2} = \frac{1}{2} \kappa / g_R(\varphi)$ — where $g_R(\varphi) = g_R e^{\varphi/2}$ — represents the proper ‘radius’ of the transverse dimensions, whose physical volume is $\Omega = 4\pi \ell^2$.

The gauge field for the general solution with different brane properties is given by

$$A_{\xi\theta} = \frac{\mathcal{Q} \Upsilon \sin \xi}{2g_A W^8(\xi)}, \quad (4.38)$$

where g_A is the corresponding gauge coupling constant. Comparing with (4.17) shows \mathcal{Q} is related to Q by $Q = \mathcal{Q}/(2g_A r_B^2)$ and so is not an independent constant. The total amount of flux present in the bulk (region B_{ext}) then is

$$\int A_{(2)} = \int_{-}^{+} d\xi d\theta A_{\xi\theta} = \frac{2\pi \mathcal{Q} \Upsilon}{g_A}, \quad (4.39)$$

so flux quantization, (4.20), relates any source flux to the defect angles by

$$N = \frac{g_A \Phi_{A-}}{2\pi} + \frac{g_A \Phi_{A+}}{2\pi} + \mathcal{Q} \Upsilon. \quad (4.40)$$

This shows why brane-localized flux is generically necessary to satisfy flux quantization for two branes with generic tensions if \mathcal{Q} is otherwise fixed. When there is no localized flux, we can estimate

$$Q \sim \frac{1}{g_A r_B^2} \sim \frac{g_R^2}{g_A \kappa^2} \sim \frac{g_R}{\kappa^2}. \quad (4.41)$$

4.3 Sources - the UV picture

The previous section describes several exact consequences of the bulk field equations that relate bulk properties to the asymptotic near-source behaviour of various combinations of bulk fields. In particular it shows how the on-source curvature, \check{R} , is determined in this way purely by the near-source combination $BW^d (\phi + \frac{d}{2} \ln W)'$,

and so vanishes in particular when ϕ' and W' approach zero in this limit.

This section now turns to the question of how these derivatives are related to source properties, extending the results of the previous chapter to include dilaton couplings and extending those of [24] to include nonzero brane-localized flux (more about which below). In this section this is done by making an explicit construction of the sources within a UV completion, as a generalization of Nielsen-Olesen vortices [1, 2]. We do so by adding new scalar and gauge fields that admit such vortex solutions, with a view to understanding in more detail how near-source behaviour is controlled by the source properties. Because our focus here is mostly on classical issues we do not explicitly embed the new sector into a supersymmetric framework, but we return to this issue when considering quantum corrections in upcoming chapters.

A key assumption in our discussion is that the typical transverse vortex size, \hat{r}_v , is much smaller than the size, ℓ , of the transverse external space: $\hat{r}_v \ll \ell$. Subsequent sections then re-interpret the results found here in terms of the D -dimensional IR effective theory applying over length scales $\hat{r}_v \ll \rho \lesssim \ell$. We follow closely the discussion of the previous chapter, highlighting the differences that arise as we proceed (the main one of which is the presence of the dilaton zero mode).

4.3.1 Action and field equations

We start with the action and field equations for the UV completed system describing the sources. With Nielsen-Olesen solutions in mind, we take this ‘vortex’ — or ‘brane’ — sector to consist of an additional complex scalar coupled to a second $U(1)$ gauge field. Again we work in $D = d+2$ spacetime dimensions, with the cases $(D, d) = (4, 2)$ and $(D, d) = (6, 4)$ being of most later interest.

The full action now is $S = S_B + S_V$ with S_B as given in (4.1) and the vortex part of the action given explicitly by

$$\begin{aligned} S_V &= - \int d^{d+2}x \sqrt{-g} \left[\frac{e^{p\phi}}{4} Z_{MN}^2 + |D_M \Psi|^2 + \lambda e^{q\phi} \left(|\Psi|^2 - \frac{v^2}{2} \right)^2 + L_{\text{mix}} \right] \\ &=: - \int d^{d+2}x \sqrt{-g} \left(L_Z + L_\Psi + V_b + L_{\text{mix}} \right), \end{aligned} \quad (4.42)$$

where $D_M \Psi := \partial_M \Psi - ieZ_M \Psi$, and the second line defines the various L_i . The terms L_Z , L_Ψ and V_b describe scalar electrodynamics and are chosen to allow vortex solutions for which the Z_{MN} gauge flux is localized. We also kinetically mix the bulk and vortex gauge fields

$$L_{\text{mix}} = \frac{\varepsilon}{2} e^{r\phi} Z_{MN} A^{MN} \quad (4.43)$$

This term is chosen – as in the previous chapter – to kinetically mix Z with the bulk gauge field [26] and thereby generate a vortex-localized component to the exterior A_{MN} gauge flux.

As before, we write $\sqrt{2} \Psi = \psi e^{i\Omega}$ and adopt a unitary gauge for which the phase, Ω , is set to zero, though this gauge will prove to be singular at the origin of the vortex solutions we examine later. In this gauge the term L_Ψ in S_V can be written

$$L_\Psi = D_M \Psi^* D^M \Psi = \frac{1}{2} \left(\partial_M \psi \partial^M \psi + e^2 \psi^2 Z_M Z^M \right) \quad (4.44)$$

and the vortex potential becomes

$$V_b(\phi, \psi) = \frac{\lambda}{4} e^{q\phi} \left(\psi^2 - v^2 \right)^2. \quad (4.45)$$

Our interest in what follows is largely in how the dependence on ϕ in these interactions

back-reacts onto the properties of the bulk, and affects the interactions of the various low-energy effective descriptions. We notice in passing that S_V shares the classical scale invariance of S_B only in the special case: $p = r = -1$ and $q = 1$.

It is also useful to group the terms in the vortex and bulk lagrangians together according to how many metric factors and derivatives appear, with

$$\begin{aligned}
L_{\text{kin}} &:= \frac{1}{2} g^{MN} \left(\frac{1}{\kappa^2} \partial_M \phi \partial_N \phi + \partial_M \psi \partial_N \psi \right) \\
L_{\text{gge}} &:= L_A + L_Z + L_{\text{mix}} \\
L_{\text{pot}} &:= V_B(\phi) + V_b(\phi, \psi) \\
L_{\text{gm}} &:= \frac{1}{2} e^2 \psi^2 g^{MN} Z_M Z_N,
\end{aligned} \tag{4.46}$$

so $L_\phi + L_\Psi + V_b = L_{\text{kin}} + L_{\text{pot}} + L_{\text{gm}}$. Notice that for the configurations of later interest we have $L_Z \geq 0$, $L_\Psi \geq 0$ and $V_b \geq 0$ while L_{mix} can have either sign.

Gauge field equations

With these choices the field equations for the two Maxwell fields are

$$\frac{1}{\sqrt{-g}} \partial_M \left[\sqrt{-g} \left(e^{-\phi} A^{MN} + \varepsilon e^{r\phi} Z^{MN} \right) \right] = 0, \tag{4.47}$$

and

$$\frac{1}{\sqrt{-g}} \partial_M \left[\sqrt{-g} \left(e^{p\phi} Z^{MN} + \varepsilon e^{r\phi} A^{MN} \right) \right] = e^2 \psi^2 Z^N, \tag{4.48}$$

and (as usual) these are supplemented by the Bianchi identities $dA = dZ = 0$, for the 2-forms A_{MN} and Z_{MN} . For later purposes it is useful to write (4.47) as

$\partial_M \left(\sqrt{-g} e^{-\phi} \check{A}^{MN} \right) = 0$ with \check{A}_{MN} defined by

$$\check{A}_{MN} := A_{MN} + \varepsilon e^{(r+1)\phi} Z_{MN}, \quad (4.49)$$

in which case (4.48) becomes

$$\frac{1}{\sqrt{-g}} \partial_M \left[\sqrt{-g} \Lambda(\phi) Z^{MN} \right] + \varepsilon(r+1) e^{r\phi} \partial_M \phi \check{A}^{MN} = e^2 \psi^2 Z^N, \quad (4.50)$$

with

$$\Lambda(\phi) := e^{p\phi} - \varepsilon^2 e^{(2r+1)\phi}. \quad (4.51)$$

We see below that the energy density of the system is given by a particular sum of the L_i 's, and when assessing the sign of the energy it is useful to notice that the off-diagonal contribution to L_{gge} vanishes when this is expressed in terms of \check{A}_{MN} rather than A_{MN} , since

$$L_{\text{gge}} = L_A + L_Z + L_{\text{mix}} = \check{L}_A + \check{L}_Z, \quad (4.52)$$

where

$$\check{L}_A := \frac{1}{4} e^{-\phi} \check{A}_{MN} \check{A}^{MN} \quad \text{and} \quad \check{L}_Z := \frac{1}{4} \Lambda(\phi) Z_{MN} Z^{MN}. \quad (4.53)$$

This shows that the kinetic energy of the Z_M gauge field is renormalized⁵ by the mixing of the two gauge fields, with the result only bounded below for all⁶ real ϕ if

⁵This provides a UV perspective to what becomes a divergent renormalization [11, 12, 15] in the limit of zero-size sources.

⁶For some applications requiring boundedness for all ϕ may be too strong a criterion, since the semiclassical approximation relies on the assumption $e^\phi \ll 1$. Since our inference about the boundedness of the energy is itself performed semiclassically, it is also suspect if the unboundedness occurs only when $e^\phi \gtrsim 1$. If this weaker criterion is our guide then we only require $2r+1 \geq p$ rather than strict equality.

$p = 2r + 1$ and $\varepsilon^2 < 1$. It also suggests a better split between the bulk and the vortices is to write $L_B + L_V = \check{L}_B + L_{\text{loc}}$, where $\check{L}_B = L_{EH} + L_\phi + \check{L}_A$ and $L_{\text{loc}} = \check{L}_Z + L_\Psi + V_b$. Split this way all of the localized energy falls within L_{loc} , because of the absence of mixing terms, as we saw in the previous chapter.

Although the quantities \check{L}_A and \check{L}_Z are useful when describing the energy density, unlike in the previous chapter their use directly in the lagrangian can lead to errors. It is important in this regard to keep in mind that there are two important ways in which the transition from A_{MN} to \check{A}_{MN} differs in the present case from the discussion in chapter 3. First, if \check{A}_{MN} is used instead of A_{MN} in the field equations then one must remember that the Bianchi identity for A and Z implies \check{A} also satisfies

$$d\check{A} = \varepsilon(r + 1) e^{(r+1)\phi} d\phi \wedge Z, \quad (4.54)$$

which need not vanish because of the presence in (4.49) of the field ϕ . The second difference is related to the first: one must *never* use eq. (4.49) to trade A_{MN} for \check{A}_{MN} in the action and *then* compute the field equations. This is because (4.49) is not a change of variables in the path integral since it is not a redefinition of the gauge potentials. In practice this kind of substitution is most dangerous in the ϕ field equation, as may be seen from the functional chain rule,

$$\begin{aligned} \left(\frac{\delta S}{\delta \phi(x)} \right)_{A \text{ fixed}} &= \left(\frac{\delta S}{\delta \phi(x)} \right)_{\check{A} \text{ fixed}} + \int d^D y \left(\frac{\delta S}{\delta \check{A}_{MN}(y)} \right)_{\phi \text{ fixed}} \left(\frac{\delta \check{A}_{MN}(y)}{\delta \phi(x)} \right)_{A \text{ fixed}} \\ &= \left(\frac{\delta S}{\delta \phi(x)} \right)_{\check{A} \text{ fixed}} + \varepsilon(r + 1) e^{(r+1)\phi} Z_{MN} \left(\frac{\delta S}{\delta \check{A}_{MN}(x)} \right)_{\phi \text{ fixed}}. \end{aligned} \quad (4.55)$$

The second term on the right-hand side of this relation need *not* vanish when the field equations are satisfied.

For configurations with the symmetries of interest the gauge field equations reduce to

$$\left(\frac{e^{-\phi}W^d\check{A}_{\rho\theta}}{B}\right)' = 0, \quad (4.56)$$

and

$$\frac{1}{BW^d} \left[\Lambda(\phi) \left(\frac{W^d Z'_\theta}{B} \right) \right]' + \varepsilon(r+1) e^{r\phi} \left(\frac{\phi' \check{A}_{\rho\theta}}{B^2} \right) = \frac{e^2 \psi^2 Z_\theta}{B^2}, \quad (4.57)$$

where (as before) primes denote differentiation with respect to proper distance, ρ , and $\Lambda(\phi)$ and \check{A}_{MN} are as defined in eqs. (4.51) and (4.49), respectively.

Flux quantization

The solution to eq. (4.56) is

$$\check{A}_{\rho\theta} = \frac{Q B e^\phi}{W^d}, \quad (4.58)$$

which shows that $\check{A}_{(2)}$ describes the part of the gauge fields that does not see the vortex sources. Ultimately the integration constant Q is fixed by the flux quantization conditions for $A_{(2)}$ and $Z_{(2)}$, which state

$$\Phi_A := \int A_{(2)} = \int d^2y A_{\rho\theta} = \frac{2\pi N}{g_A}, \quad (4.59)$$

and

$$\Phi_Z := \int Z_{(2)} = \int d^2y Z_{\rho\theta} = - \sum_v \frac{2\pi n_v}{e} = - \frac{2\pi n_{\text{tot}}}{e}, \quad (4.60)$$

where N and $n_{\text{tot}} = \sum_v n_v = n_+ + n_-$ are integers while e and g_A are the relevant gauge couplings. Strictly speaking flux quantization only ensures the sum over all vortices, $n_{\text{tot}} = n_+ + n_-$, is an integer. However we imagine here that the two vortices are situated at opposite ends of the (relatively) very large extra dimensions and so

are very well-separated. Consequently in practice each of n_+ and n_- are separately integers, up to exponential accuracy.⁷

On one hand, for $\phi \approx \phi_v$ approximately constant across the narrow width of each vortex, this implies

$$\check{\Phi}_A := \int \check{A}_{(2)} \approx 2\pi \left(\frac{N}{g_A} - \frac{\varepsilon}{e} \sum_v n_v e^{(r+1)\phi_v} \right), \quad (4.61)$$

while on the other hand the left-hand side is related to Q by

$$\check{\Phi}_A = Q \int d^2y \left(\frac{B e^\phi}{W^4} \right) = Q \widehat{\Omega}_{-4}, \quad (4.62)$$

where we define the useful notation

$$\widehat{\Omega}_k := \int d^2y \sqrt{g_2} W^k e^\phi = \int d^2y \sqrt{\widehat{g}_2} W^k, \quad (4.63)$$

to represent the 2D integrals that arise here and in later calculations. Here $\widehat{\Omega}_k$ is the integral of W^k over the transverse dimensions using the scale-invariant metric, $\widehat{g}_{mn} := e^\phi g_{mn}$, and the particular case $k = 0$ represents the extra-dimensional volume, $\widehat{\Omega} := \widehat{\Omega}_0$, as measured by this metric.

We see Q is given by

$$Q = \frac{\check{\Phi}_A}{\widehat{\Omega}_{-4}} \approx \frac{2\pi}{\widehat{\Omega}_{-4}} \left(\frac{N}{g_A} - \frac{\varepsilon}{e} \sum_v n_v e^{(r+1)\phi_v} \right), \quad (4.64)$$

In the special case where $\phi = \varphi$ takes the same value at all of the vortex positions

⁷This could also be alternatively arranged by having two copies of the vortex sector, with each vortex carrying flux from a different $U(1)$ (which would therefore be separately quantized) but with both mixing with the bulk $U(1)$.

this becomes

$$Q \approx \frac{2\pi}{\widehat{\Omega}_{-4}} \left[\frac{N}{g_A} - \left(\frac{\varepsilon n_{\text{tot}}}{e} \right) e^{(r+1)\varphi} \right]. \quad (4.65)$$

Scalar field equations

The vortex scalar field equation in unitary gauge becomes

$$\frac{1}{\sqrt{-g}} \partial_M \left(\sqrt{-g} g^{MN} \partial_N \psi \right) = e^2 \psi Z_M Z^M + \lambda e^{q\phi} \psi \left(\psi^2 - v^2 \right), \quad (4.66)$$

while the dilaton equation is

$$\begin{aligned} \square \phi &= \frac{1}{\sqrt{-g}} \partial_M \left(\sqrt{-g} g^{MN} \partial_N \phi \right) = \kappa^2 \left(V_B - L_A + qV_b + pL_Z + rL_{\text{mix}} \right) \\ &= \kappa^2 \left(\mathcal{X} + \mathcal{Y} \right). \end{aligned} \quad (4.67)$$

Here

$$\mathcal{X} := L_{\text{pot}} - L_{\text{gge}} = V_B + V_b - L_A - L_Z - L_{\text{mix}}, \quad (4.68)$$

is the combination appearing in the stress tensor, $T^m_m = -2\mathcal{X}$, and we define the useful quantity

$$\mathcal{Y} := (q-1)V_b + (1+p)L_Z + (1+r)L_{\text{mix}}. \quad (4.69)$$

Notice that \mathcal{Y} involves only terms from the vortex lagrangian and vanishes identically in the scale-invariant case, for which $p = r = -1$ and $q = 1$, while \mathcal{X} is most usefully split between bulk and localized contributions through $\mathcal{X} = \check{\mathcal{X}}_B + \mathcal{X}_{\text{loc}}$ where $\check{\mathcal{X}}_B = V_B - \check{L}_A$ while $\mathcal{X}_{\text{loc}} := V_b - \check{L}_Z$. It is similarly useful to write $\mathcal{Z} = \mathcal{Z}_B + \mathcal{Z}_{\text{loc}}$ with \mathcal{Z}_B defined as above and $\mathcal{Z}_{\text{loc}} = \frac{1}{2}(\psi')^2 - L_{\text{gm}}$.

Once restricted to the symmetric configurations of interest the scalar equations

simplify to

$$\frac{1}{BW^d} \left(BW^d \psi' \right)' = e^2 \psi \left(\frac{Z_\theta}{B} \right)^2 + \lambda e^{q\phi} \psi (\psi^2 - v^2), \quad (4.70)$$

and

$$\frac{1}{BW^d} \left(BW^d \phi' \right)' = \kappa^2 (\mathcal{X} + \mathcal{Y}). \quad (4.71)$$

Einstein equations

The stress-energy tensor of the entire system including vortices is

$$\begin{aligned} T_{MN} = & \frac{1}{\kappa^2} \partial_M \phi \partial_N \phi + \partial_M \psi \partial_N \psi + e^2 \psi^2 Z_M Z_N + e^{-\phi} A_{MP} A_N{}^P + e^{p\phi} Z_{MP} Z_N{}^P \\ & + \frac{\varepsilon}{2} e^{r\phi} \left(A_{MP} Z_N{}^P + Z_{MP} A_N{}^P \right) - g_{MN} \left(L_{\text{kin}} + L_{\text{gm}} + L_{\text{pot}} + L_{\text{gge}} \right), \end{aligned}$$

and so the nontrivial components of the matter stress-energy are given by (4.10), with $\mathcal{X} = L_{\text{pot}} - L_{\text{gge}}$, as in eq. (4.68), while

$$\varrho := L_{\text{kin}} + L_{\text{gm}} + L_{\text{pot}} + L_{\text{gge}} \quad \text{and} \quad \mathcal{Z} := L_{\text{kin}} - L_{\text{gm}}. \quad (4.72)$$

The lone nontrivial component of the trace-reversed Einstein equations governing the d -dimensional on-brane geometry therefore becomes

$$\mathcal{R}_{(d)} := g^{\mu\nu} \mathcal{R}_{\mu\nu} = \frac{\check{R}}{W^2} + \frac{d}{BW^d} \left(BW' W^{d-1} \right)' = -2\kappa^2 \mathcal{X}. \quad (4.73)$$

The two useful Einstein equations dictating the 2-dimensional transverse geometry similarly can be taken to be

$$\frac{B}{W} \left(\frac{W'}{B} \right)' = -\frac{2}{d} \kappa^2 \mathcal{Z}. \quad (4.74)$$

and

$$\frac{(B'W^d)'}{BW^d} = -\kappa^2 \left[\varrho - \mathcal{Z} - \left(1 - \frac{2}{d}\right) \mathcal{X} \right]. \quad (4.75)$$

For later purposes a useful combination of these equations gives the D -dimensional Ricci scalar, $\mathcal{R}_{(D)} = \mathcal{R}_{(d)} + \mathcal{R}_{(2)}$. Given that the total lagrangian is given by $L = L_B + L_V = (2\kappa^2)^{-1} \mathcal{R}_{(D)} + \varrho$, where ϱ is the total energy density, it turns out this can be written

$$L = L_B + L_V = -\frac{2\mathcal{X}}{d} \quad (4.76)$$

Yet another useful combination of the above equations is the $(\rho\rho)$ component of the Einstein equations $\mathcal{G}^\rho_\rho = -\kappa^2 T^\rho_\rho$ which reads

$$2d \left(\frac{B'W'}{BW} \right) + \frac{\check{R}}{W^2} + d(d-1) \left(\frac{W'}{W} \right)^2 = 2\kappa^2 (\mathcal{Z} - \mathcal{X}). \quad (4.77)$$

This expression contains only first derivatives of metric and matter fields, and acts as a constraint on the solution as it is integrated along the proper distance ρ .

Finally, we see from the above that the gauge fields only enter the Einstein equations through the combination $L_{\text{gge}} = L_A + L_Z + L_{\text{mix}} = \check{L}_A + \check{L}_Z$, and so the Einstein equations are indifferent (unlike the dilaton field equation) to whether they are expressed using A_{MN} or \check{A}_{MN} .

Control of approximations

Since solutions to the classical field equations take up much of what follows, we first briefly digress to summarize the domain of validity of these solutions. The fundamental parameters of the problem are the gravitational constant, κ ; the coefficient of the bulk scalar potential, V_0 (or $V_0 = 2g_R^2/\kappa^4$ for 6D supergravity); the gauge couplings,

$\hat{e}^2(\varphi) = e^2/\Lambda(\varphi)$ and $\hat{g}_A(\varphi) = g_A e^{\varphi/2}$; the scalar self-coupling, $\hat{\lambda}(\varphi) = \lambda e^{q\varphi}$, and the scalar vev v . To these must be added the dimensionless parameter, ε , that measures the mixing strength for the two gauge fields. When discussing 6D supergravity we typically assume $g_A = g_R$ and so can use g_A and g_R interchangeably. We also largely keep to the vortex parameter range $\hat{\lambda} \sim \hat{e}^2$.

The energy density of the vortex turns out below to be of order $\hat{e}^2 v^4$ and when $\hat{\lambda} \sim \hat{e}^2$ the transverse vortex proper radius is of order \hat{r}_v with

$$\hat{r}_v = \frac{1}{\hat{e}v}. \quad (4.78)$$

The effective energy-per-unit-area of the vortex is therefore of order $\hat{e}^2 v^4 \hat{r}_v^2 = v^2$. These energies give rise to D -dimensional curvatures within the vortex of order $1/l_v^2 = \kappa^2 \hat{e}^2 v^4$ and integrated dimensional gravitational effects (like conical defect angles) of order $\kappa^2 v^2$. We work in a regime where $\kappa v \ll 1$ to ensure that the gravitational response to the energy density of the vortex is weak, and so defect angles are small and $l_v \gg \hat{r}_v$. We also define the ϕ -independent quantity $r_v = 1/ev$.

By contrast, we have seen that far from the vortex the curvature scale in the bulk turns out to be proportional to $1/\ell^2$ where

$$\ell = r_B e^{-\varphi/2} = \frac{\kappa}{2\hat{g}_R(\varphi)}. \quad (4.79)$$

Since our interest is in the regime where the vortex is much smaller than the transverse dimensions we throughout assume $\hat{r}_v/\ell \ll 1$ and so the parameter range of interest is

$$\frac{\hat{g}_A(\varphi)}{\hat{e}(\varphi)} \ll \kappa v \ll 1. \quad (4.80)$$

As seen earlier, semiclassical reasoning also depends on the ambient value of the dilaton, φ , because it is $e^{d\varphi/2}$ that counts loops in the bulk theory. Consequently we require

$$e^\varphi \ll 1 \quad (4.81)$$

in order to work semiclassically within the bulk theory. But φ also governs the size of vortex couplings through $\hat{\lambda}(\varphi) = \lambda e^{q\varphi}$ and $\hat{e}^2(\varphi) = e^2/\Lambda(\varphi)$ and we must check these remain small to trust semiclassical reasoning on the vortex.

4.3.2 Dual formulation

Because the gauge coupling to the vortex is magnetic, it can be useful to work with the Hodge dual of the Maxwell field A_{MN} . In this section we restrict to the case of later interest, $(D, d) = (6, 4)$, though the same steps can be easily generalized to other numbers of dimensions.

The terms involving A_M in the 6D action can be written

$$L_A + L_{\text{mix}} + L_{\text{lm}} = \frac{1}{4} e^{-\phi} A_{MN} A^{MN} + \frac{\varepsilon}{2} e^{r\phi} Z^{MN} A_{MN} + \frac{1}{3!} \epsilon^{MNPQRT} V_{MNP} \partial_Q A_{RT}, \quad (4.82)$$

where the functional integration over the newly added 3-form lagrange multiplier, V_{MNP} , ensures A_{MN} satisfies the Bianchi identity and so allows us to directly integrate A_{MN} rather than the gauge potential, A_M in the path integral. Notice that because we wish the constraint $dA_{(2)} = 0$ also to hold on any boundaries we do not include a surface term to restrict the variation of V_{MNP} there.

The integration over A_{MN} is gaussian and so can be performed directly, leaving V_{MNP} as the dual field. Performing the gaussian integration requires an integration

by parts, and so leaves a surface term

$$L_{\text{st}} = +\frac{1}{3!} \nabla_Q \left(\epsilon^{MNPQRT} V_{MNP} A_{RT} \right), \quad (4.83)$$

to which we return later. The saddle point relates the 4-form field strength, $F_{(4)} = dV_{(3)}$, to the 2-form $A_{(2)}$ as follows

$$\check{A}^{MN} = A^{MN} + \varepsilon e^{(r+1)\phi} Z^{MN} = -\frac{1}{2 \cdot 3!} e^\phi \epsilon^{MNPQRT} F_{PQRT}, \quad (4.84)$$

which inverts to

$$F_{MNPQ} = +\frac{1}{2} e^{-\phi} \epsilon_{MNPQRT} \check{A}^{RT}. \quad (4.85)$$

The dual action (obtained after evaluating at this saddle point) for gauge sector, $L_{\text{dual}} = L_{\text{gge}} + L_{\text{lm}}$, then is

$$\begin{aligned} L_{\text{dual}} &= \frac{1}{4} \Lambda(\phi) Z_{MN}^2 - \frac{\varepsilon}{2 \cdot 4!} e^{(r+1)\phi} \tilde{Z}^{PQRT} F_{PQRT} + \frac{1}{2 \cdot 4!} e^\phi F_{PQRT}^2 + L_{\text{st}} \\ &=: \check{L}_Z + L_{BLF} + L_F + L_{\text{st}}, \end{aligned}$$

where $\tilde{Z}^{PQRT} = \epsilon^{PQRTMN} Z_{MN}$ and the last line defines L_{BLF} and L_F , the latter of which also evaluates on shell to

$$L_F := \frac{1}{2 \cdot 4!} F_{MNPQ} F^{MNPQ} = -\check{L}_A = -\frac{1}{2} \left(\frac{Q}{W^4} \right)^2 e^\phi. \quad (4.86)$$

So this term in the Lagrangian is negative and equal in magnitude to \check{L}_A when evaluated on shell. This is exactly what is needed for the dual variables to be consistent with the original ones, as we now show.

For example, keeping in mind that $\mathcal{L}_{\text{st}} = \sqrt{-g} L_{\text{st}}$ does *not* change the bulk equations of motion, in these variables the contribution of the Maxwell field to the RHS of the dilaton equation, (4.67), becomes

$$\kappa^2 \frac{\partial L_{\text{dual}}}{\partial \phi} = \kappa^2 \left[\frac{\Lambda'}{\Lambda} \check{L}_Z + (r+1) L_{BLF} + L_F \right] \quad (4.87)$$

instead of $\kappa^2 (-L_A + pL_Z + rL_{\text{mix}})$ in the original variables. Similarly, since $\mathcal{L}_{BLF} = \sqrt{-g} L_{BLF}$ is proportional to $Z_{(2)} \wedge F_{(4)}$ it does not couple to the metric at all, so the stress energy coming from L_{dual} is

$$T_{\text{dual}}^{MN} = \frac{1}{3!} F^{MABC} F^N{}_{ABC} + \Lambda(\phi) Z^{MA} Z^N{}_A - (L_F + \check{L}_Z) g^{MN}, \quad (4.88)$$

and so contributes to \mathcal{X} as $\mathcal{X}_{\text{dual}} = L_F - \check{L}_Z$. On shell, this gives the same value as \mathcal{X} in the original variables.

If we define \mathcal{Y} so that $\square\phi = \kappa^2 (\mathcal{X} + \mathcal{Y})$ remains true, then we are led to replace (4.69) with

$$\mathcal{Y} = (q-1)V_b + \left(1 + \frac{\Lambda'}{\Lambda}\right) \check{L}_Z + (r+1) L_{BLF}. \quad (4.89)$$

As expected, L_F drops out of this since the bulk Maxwell action does not break the scale symmetry, and \mathcal{Y} should vanish in the limit of scale invariance.

Trading $A_{(2)}$ for $F_{(4)}$ in the surface term, L_{st} , of (4.83) allows it to be written

$$L_{\text{st}} = +\frac{2}{4!} \nabla_Q \left(\epsilon^{MNPQRT} V_{MNP} A_{RT} \right) = +\frac{1}{3!} \nabla_Q \left(V_{MNP} e^\phi \check{F}^{MNPQ} \right), \quad (4.90)$$

where the second equality defines

$$\check{F}_{MNPQ} := F_{MNPQ} - \frac{\varepsilon}{2} e^{r\phi} \epsilon_{MNPQRT} Z^{RT}. \quad (4.91)$$

Because the 4-form field equations imply $\nabla_M (e^\phi \check{F}^{MNPQ}) = 0$, evaluating L_{st} at a 4-form solution gives

$$\left(L_{\text{st}} \right)_{\text{on-shell}} = -\frac{1}{4!} e^\phi \check{F}^{MNPQ} F_{MNPQ} = -2L_F - L_{BLF}, \quad (4.92)$$

and so on-shell the gauge action evaluates to

$$\left(L_{\text{dual}} \right)_{\text{on-shell}} = \check{L}_Z + L_{BLF} + L_F + L_{\text{st}} = \check{L}_Z - L_F, \quad (4.93)$$

in agreement with the expected value, $L_{\text{gge}} = \check{L}_Z + \check{L}_A$, in the original variables.

Although this dual formulation is equivalent to the original one, it makes several features usefully manifest. First, because $F_{(4)}$ turns out to be proportional to $\star\check{A}_{(2)}$ rather than $\star A_{(2)}$, it provides a natural way to express the change of variables from A to \check{A} directly in the action rather than the field equations, even for nontrivial dilaton profiles. In so doing it generates the same renormalization of the Z kinetic term obtained earlier. Second, because the $V - Z$ coupling term has the form of $F_{(4)} \wedge Z_{(2)}$ it is immediate that this term is independent of the metric and so does not directly gravitate. This can also be understood in the original variables, in terms of a cancellation of localized contributions between L_{mix} and L_A , as in the previous chapter.

For the maximally symmetric configurations described above, evaluating $F_{(4)}$ using

the solution to the $\check{A}_{(2)}$ field equation gives

$$F_{\mu\nu\lambda\kappa} = e^{-\phi} \epsilon_{\mu\nu\lambda\kappa\rho\theta} \check{A}^{\rho\theta} = Q \check{\epsilon}_{\mu\nu\lambda\kappa}, \quad (4.94)$$

where $\check{\epsilon}_{\mu\nu\lambda\rho} = \pm\sqrt{-\check{g}}$ is the 4D volume form built from the metric $\check{g}_{\mu\nu}$. Notice that in the scale-invariant case (where $r = -1$) these definitions imply $F_{\mu\nu\lambda\kappa} \rightarrow s^2 F_{\mu\nu\lambda\kappa}$ under the scaling symmetry.

4.3.3 Vortex solutions

This section describes an isolated vortex within a much larger ambient bulk geometry. Our goal is to establish that the presence of the dilaton couplings need not destroy the localized vortex solutions — with exponentially falling solutions beyond the vortex radius, \hat{r}_v — familiar from the dilaton-free case. We also wish to relate the properties of the vortex to the asymptotic behaviour of the bulk fields and their derivatives outside of (but near to) the vortex itself, with a view to using these in the discussion of bulk solutions given earlier.

Nielsen-Olesen vortices

The isolated Abelian-Higgs system contains vortex solutions where the local gauge symmetry is relatively unbroken in a core region [1, 2], and the fields approach their vacuum solutions outside of this region. Although we consider a more complicated gravitating vortex sector that is coupled to a bulk scalar, as in S_V , explicit numerical construction shows this only weakly perturbs the form of the localized vortex solutions in the parameter range of interest (as expected).

We work in a unitary gauge for which $\Psi = \psi$ is real (and for which the gauge

fields Z_M and A_M are singular at the origin). We demand (as usual) the vortex fields approach their vacuum values away from the vortex, corresponding to $\psi \rightarrow v$ and $Z_M \rightarrow 0$ far from the vortex core. Inside the vortex we have scalar boundary conditions $\psi(0) = 0$ and $\psi'(0) = 0$ in addition to gauge boundary condition $Z_\theta(0) = n_v/e$. This second boundary condition is chosen so that Z -flux quantization is satisfied within the vortex,

$$\oint_{\rho=\rho_v} dZ = 2\pi \int_0^{\rho_v} d\rho \partial_\rho Z_\theta = 2\pi [Z_\theta(\rho_v) - Z_\theta(0)] = -\frac{2\pi n_v}{e}, \quad (4.95)$$

where ρ_v is a point chosen sufficiently far from the vortex core that we can assume the gauge field takes on the vacuum value $Z_\theta = 0$, and the integer n_v is the flux quantum of the vortex source in the region X_v defined by $0 \leq \rho \leq \rho_v$.

It is convenient when solving the vortex field equations to scale out the field dimensions by defining

$$Z_\theta = \frac{n_v P(\rho)}{e} \quad \text{and} \quad \psi = vF(\rho). \quad (4.96)$$

In terms of these the boundary conditions become $F(0) = 0$ and $F \rightarrow 1$ far from the vortex, while $P(\rho)$ decreases from $P(0) = 1$ at the vortex core to its asymptotic value $P \rightarrow 0$. In these variables, the vortex field equations read as follows

$$\frac{1}{BW^d} (BW^d F')' = \frac{n_v^2 P^2 F}{B^2} + \lambda v^2 e^{q\phi} F(F^2 - 1), \quad (4.97)$$

and

$$\frac{1}{BW^d} \left[\Lambda(\phi) \left(\frac{W^d P'}{B} \right) \right]' + (r+1)e^{(r+1)\phi} \left(\frac{e\varepsilon Q}{n_v} \right) \left(\frac{\phi'}{BW^d} \right) = \frac{e^2 v^2 F^2 P}{B^2}. \quad (4.98)$$

Examples of numerical solutions for the gravitating vortex profiles with dilaton interactions are shown in Fig. 4.3 and strongly resemble the nongravitating vortex solutions found in [21] with constant dilaton in the vortex region $\phi = \phi_v$. In particular, they approach their asymptotic values exponentially over scales controlled by the ϕ_v -dependent masses $m_Z^2 = \hat{e}^2(\phi_v)v^2$ and $m_{\Psi}^2 = 2\hat{\lambda}(\phi_v)v^2$ with

$$\hat{e}^2(\phi) := \frac{e^2}{\Lambda(\phi)} \quad \text{and} \quad \hat{\lambda}(\phi) := \lambda e^{q\phi}. \quad (4.99)$$

We wish to trace how the vortex solutions depend on ϕ , and to do so it is useful to rescale factors of $\Lambda(\phi)$ into the coordinate ρ (or, equivalently, the transverse metric), by writing

$$g_{mn}dy^m dy^n = \Lambda(\phi)r_v^2 (d\bar{\rho}^2 + \bar{B}^2 d\theta^2) = \hat{r}_v^2(\phi) (d\bar{\rho}^2 + \bar{B}^2 d\theta^2). \quad (4.100)$$

With this choice the $\check{A}_{\bar{\rho}\theta}$ equation becomes

$$\partial_{\bar{\rho}} \left[\frac{W^d e^{-\phi} \check{A}_{\bar{\rho}\theta}}{\bar{B}\Lambda(\phi)} \right] = 0, \quad (4.101)$$

which has solution

$$\check{A}_{\bar{\rho}\theta} = \frac{\bar{Q}\bar{B}\Lambda(\phi)e^\phi}{W^d}, \quad (4.102)$$

with integration constant $\bar{Q} = Q r_v^2$. The vortex field equations rewrite as

$$\frac{1}{\bar{B}W^d} \partial_{\bar{\rho}} [\bar{B}W^d \partial_{\bar{\rho}} F] = \frac{n_v^2 P^2 F}{\bar{B}^2} + e^{q\phi} \Lambda(\phi) \left(\frac{\lambda}{e^2} \right) F(F^2 - 1), \quad (4.103)$$

and

$$\frac{1}{\bar{B}W^d} \partial_{\bar{\rho}} \left(\frac{W^d \partial_{\bar{\rho}} P}{\bar{B}} \right) + (r+1) e^{(r+1)\phi} \left(\frac{e\varepsilon \bar{Q}}{n_v} \right) \left(\frac{\partial_{\bar{\rho}} \phi}{\bar{B}W^d} \right) = \frac{F^2 P}{\bar{B}^2}. \quad (4.104)$$

Now comes the main point. To the extent that the gauge fields do not mix (*ie* $\varepsilon = 0$) or the dilaton is approximately constant in the vortex region ($\partial_{\bar{\rho}} \phi \simeq 0$) these equations show that the vortex system depends on ϕ only through the one single, ϕ -dependent parameter

$$\hat{\beta}(\phi) := e^{q\phi} \Lambda(\phi) \left(\frac{2\lambda}{e^2} \right) = \frac{2\hat{\lambda}(\phi)}{\hat{e}^2(\phi)} = \frac{m_{\Psi}^2}{m_Z^2} = e^{q\phi} \Lambda(\phi) \beta. \quad (4.105)$$

Furthermore, if $p = 2r + 1$ (as required if the Z_M kinetic energy is bounded below for all ϕ) then the ϕ -dependence of $\Lambda(\phi) = e^{p\phi}(1 - \varepsilon^2)$ is simple and it is possible to make $\hat{\beta}$ independent of ϕ by choosing $p + q = 0$.

How important for these statements is the assumption that ϕ not vary across the vortex? Dependence on ϕ can enter if ε is nonzero and ϕ actually does vary across the vortex, as can be seen from eq. (4.98) or (4.104). But because $\phi' \sim \kappa^2 v^2$ generically and $e\bar{Q} = er_v^2 Q \sim (e/g_A)(r_v/r_B)^2$ the vortex system is only weakly sensitive to the value of ϕ for the one-parameter family $p = -q = 2r + 1$, since the ϕ -dependence

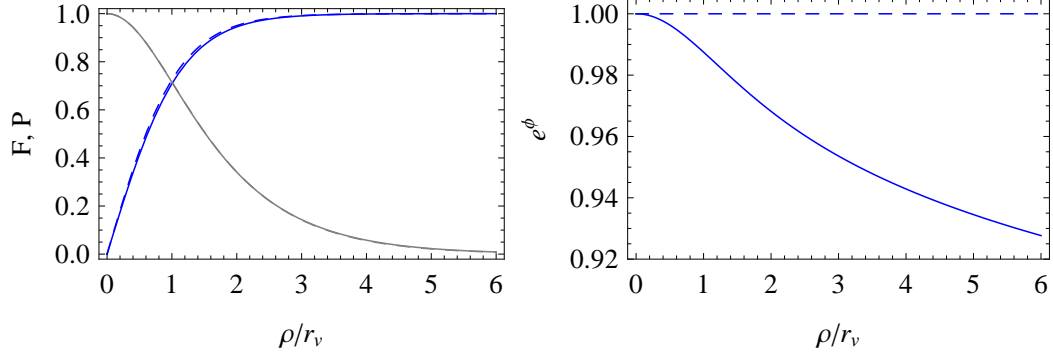


Figure 4.3: These plots demonstrate that the dilaton couplings do not ruin the existence of localized vortex solutions. The left plot contains a comparison of the vortex profiles F and P for a non-gravitating vortex in flat space (dashed curves) and a gravitating vortex coupled to the dilaton (solid curves). The right plot shows the dilaton profile in the vortex region for both cases. The gravitating dilaton is slowly varying in the vortex region, with the change of ϕ over the vortex region being controlled by $\Delta e^\phi \sim \kappa^2 v^2$. The parameters used to generate the gravitating profiles are $d = 4$, $\varepsilon = 0.3$, $\beta = 3$, $\kappa v = 0.5$, $\phi(0) = 0$, $Q = 0.01 ev^2$, $V_0 = Q^2/2$ and the vortex sector is coupled to the dilaton through the generic choices $(p, q, r) = (-1, 0, -1)$. The flat space profiles are generated by choosing $\kappa v = 0$ instead.

arising from the ϕ' term of (4.98) is of relative size

$$\partial_{\bar{\rho}}\phi(r+1)\varepsilon e r_v^2 Q e^{(r+1)\phi} \sim \kappa^2 v^2 (r+1) \left(\frac{\varepsilon e r_v^2}{g_A r_B^2} \right) e^{(r+1)\phi} \sim (r+1) \left(\frac{\varepsilon g_R^2}{e g_A} \right) e^{(r+1)\phi}, \quad (4.106)$$

where the second estimate follows from the definition $r_v = 1/ev$ and $r_B \sim \kappa/g_R$. Because we are assuming $2r+1 = p$, the ϕ -dependence can be absorbed by the hatted couplings to give

$$\partial_{\bar{\rho}}\phi(r+1)\varepsilon e r_v^2 Q e^{(r+1)\phi} \sim (r+1) \left(\frac{\varepsilon \hat{g}_R^2}{\hat{e} \hat{g}_A} \right), \quad (4.107)$$

which is suppressed in the parameter range $\hat{g}_A/\hat{e} \approx \hat{g}_R/\hat{e} \ll \kappa^2 v^2 \ll 1$ required to control the semiclassical approximation and to ensure $\ell \gg \hat{r}_v$.

BPS special case

In the special case where $W = W_v$ and $\phi = \phi_v$ are constant in the vortex (for which a coordinate rescaling allows the choice $W_v = 1$), then the vortex field equations are the same as apply in the absence of the dilaton once we make the replacement $e \rightarrow \hat{e}$ and $\lambda \rightarrow \hat{\lambda}$ with $\hat{e}^2 := e^2/\Lambda(\phi_v)$ and $\hat{\lambda} := \lambda e^{q\phi_v}$. The vortex field equations in this case boil down to

$$\frac{1}{B} \left(\frac{P'}{B} \right)' = \frac{\hat{e}^2 v^2 F^2 P}{B^2}, \quad (4.108)$$

while the ψ equation becomes

$$\frac{1}{B} (B F')' = \frac{n_v^2 P^2 F}{B^2} + \hat{\lambda} v^2 F (F^2 - 1). \quad (4.109)$$

The solutions to these equations are particularly simple when $\hat{e}^2 = 2\hat{\lambda}$, since then eqs. (4.108) and (4.109) are equivalent to the first-order equations,

$$BF' = n_v F P \quad \text{and} \quad \frac{n_v P'}{\hat{e} B} = \sqrt{\frac{\hat{\lambda}}{2}} v^2 (F^2 - 1). \quad (4.110)$$

We show later that $W = 1$ and $\phi = \phi_v$ also solve the bulk field equations when $\hat{e}^2 = 2\hat{\lambda}$, and so this choice provides a consistent solution to all the field equations. Such solutions naturally arise when the vortex sector is itself also supersymmetric, since supersymmetry can require $\hat{e}^2 = 2\hat{\lambda}$ and the vortices leave some supersymmetry unbroken.

When eqs. (4.110) as well as $\phi = \phi_v$ and $W = 1$ hold, they also imply

$$L_{\text{kin}} = \frac{1}{2} (\partial\psi)^2 = \frac{e^2}{2} \psi^2 Z_M Z^M = L_{\text{gm}}, \quad (4.111)$$

and

$$\check{L}_Z := \frac{1}{4} \Lambda(\phi_b) Z_{mn} Z^{mn} = \frac{\lambda}{4} (\psi^2 - v^2)^2 = V_b, \quad (4.112)$$

which further imply that the vortex-localized contributions to \mathcal{Z} and \mathcal{X} cancel out: $\mathcal{Z}_{\text{loc}} = 0$ and $\mathcal{X}_{\text{loc}} = 0$. But the bulk contribution to \mathcal{Z} also vanishes if $\phi' = 0$ and — as can be seen from eq. (4.74) — it is the vanishing of \mathcal{Z} that allows constant W to solve the Einstein equations. Finally, the dilaton field equation with constant ϕ requires $\check{\mathcal{X}}_B + \mathcal{Y} = 0$ everywhere, and so separately evaluating in the bulk and vortex implies $\check{\mathcal{X}}_B = \mathcal{Y} = 0$ separately. Although $\mathcal{Y} = 0$ can be ensured using the scale-invariant choices $p = r = -1$ and $q = 1$, vanishing $\check{\mathcal{X}}_B$ in general either requires a condition on the bulk gauge field, Q (which need not agree with what is required by flux quantization) or a runaway to $e^\phi \rightarrow 0$.

Finally, the vortex part of the action evaluates in this case to the simple result

$$S_v := \frac{1}{\sqrt{-\check{g}}} \int_{X_v} d^2y \sqrt{-g} \varrho_{\text{loc}} = 2\pi \int_0^{\rho_v} d\rho B \left[L_\Psi + V_b + \check{L}_Z \right] = \pi n_v v^2, \quad (4.113)$$

where the second equality also defines the localized energy density $\varrho_{\text{loc}} = L_{\text{loc}}$.

4.3.4 Integral relations

In this section we generalize the integral relations described earlier for the bulk system to include the vortex sources. Instead of integrating only over the exterior region, B_{ext} , we now instead integrate over the small regions, X_\pm , containing each vortex source, and thereby learn how the vortex determines the boundary conditions on the interface with B_{ext} . Using these boundary conditions for the integrated bulk solution is equivalent to integrating the bulk-vortex field equations over the entire

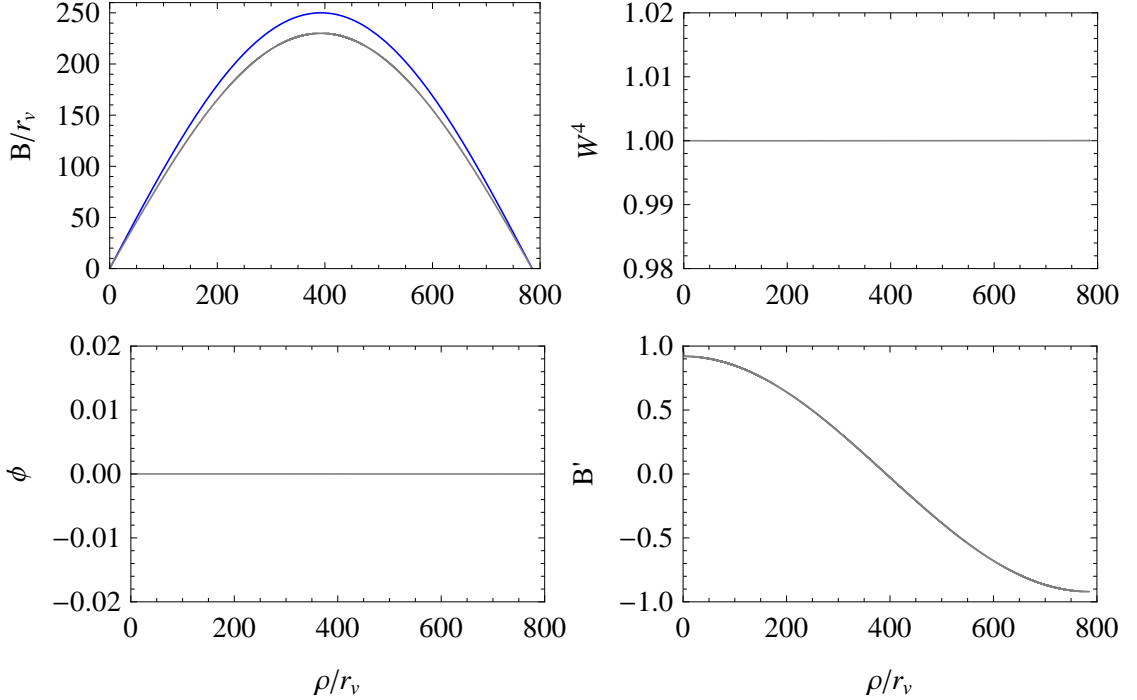


Figure 4.4: These plots show the numerical bulk solution for $n = 1$ BPS vortex sources ($\hat{\beta} = 1$) with scale invariant couplings to the dilaton $(p, q, r) = (-1, 1, -1)$ and $\kappa v = 0.4$. For these choices, the field equations are solved by a constant dilaton and warp factor: $W = 1$ and $\phi = 0$. Because $\phi' = W' = 0$, this solution falls into the simple class of rugby ball solutions described in §4.2.3. In the top left plot the metric function B is plotted against the same solution for a sphere of proper radius $\ell = 250\pi r_v$, $B_{\text{sphere}} = \ell \sin(\rho/\ell)$. The vortices (which cannot be resolved in these plots) introduce a defect angle into the bulk metric such that $B = \alpha \ell \sin(\rho/\ell)$ in the bulk. The defect angle, α , can be determined by extrapolating B' to the apparent singular point at $\rho_* \approx 0$. This yields $1 - \alpha \simeq 0.08 = \kappa^2 \tilde{T}/2\pi = (\kappa v)^2/2$ as expected from (4.113) and (4.150).

space, $X_{\text{tot}} := B_{\text{ext}} \cup X_+ \cup X_-$, which is smooth and compact and without boundary.

In what follows we generically represent by $X_v = \{X_+, X_-\}$ when we do not need to specify which source is of interest.

Integration over near-source pillboxes

We first integrate just over X_v to find the UV theory's perspective on the general boundary conditions [11, 12] that relate near-source derivatives to properties of the

source. These are useful in developing the effective theory of the next section that treats the vortices as point-like sources, or branes.

Maxwell fields

We start with the gauge-field equations. The simplest of these to solve is the Maxwell equation, (4.56), since this does not depend directly on the fields Z_M or ψ . The solution is as before

$$\check{A}_{\rho\theta} = \frac{QB e^\phi}{W^d}, \quad (4.114)$$

where Q is an integration constant. This enters into the Einstein equations (4.73) and (4.74) through the combination $\check{L}_A = \frac{1}{2}(Q/W^d)^2 e^\phi$.

Suppose now we take a test charge that couples only to A_M and ask how much flux it measures when taken around the vortex. We do so by moving around the edge of X_v , remaining everywhere outside the vortex. The edge of the pillbox is at a distance $\rho_v \gtrsim \hat{r}_v$ from the vortex so vortex fields are exponentially small, but we also choose $\rho_v \ll \ell$ so it contains a negligible fraction of the external bulk. The flux seen by this charge is

$$\begin{aligned} \Phi_A(X_v) &:= \int_{X_v} A_{(2)} = \int_{X_v} \left(\check{A}_{(2)} - \varepsilon e^{(r+1)\phi} Z_{(2)} \right) \\ &= 2\pi \left[Q \int_0^{\rho_v} d\rho \frac{B e^\phi}{W^d} - \varepsilon \int_0^{\rho_v} d\rho e^{(r+1)\phi} Z_{\rho\theta} \right]. \end{aligned} \quad (4.115)$$

The first term in the last equality gives the amount of bulk flux lying within $\rho < \rho_v$ in the absence of the vortex source, and so is negligibly small in the limit $\hat{r}_v \rightarrow 0$. The second term does survive this limit, however, because even though bulk fields vary slowly over the small vortex volume, the profile for $Z_{\rho\theta}$ is strongly peaked in such a

way as to give the total quantized Z -flux,

$$\Phi_Z = \int_{X_v} Z_{(2)} \approx -\frac{2\pi n_v}{e}. \quad (4.116)$$

So eq. (4.115) shows that the mixing of A and Z gauge fields through L_{mix} implies the test charge sees a vortex-localized component of flux despite it not coupling directly to the Z field

$$\Phi_A(X_v) \simeq -\varepsilon \Phi_Z(X_v) e^{(r+1)\phi_v} \simeq \frac{2\pi n_v \varepsilon}{e} e^{(r+1)\phi_v}, \quad (4.117)$$

where the approximation is true to the extent that $\hat{r}_v \ll \ell$. This localizes part of the external A flux onto the vortex.

Dilaton

Integrating the dilaton field equation, (4.71), over a vortex-containing pillbox gives

$$\left(BW^d \phi' \right)_{\rho=\rho_v} = \frac{\kappa^2}{2\pi} \int_{X_v} d^2 y \sqrt{g_2} W^d (\mathcal{X} + \mathcal{Y}) = \frac{\kappa^2}{2\pi} \left\langle \mathcal{X} + \mathcal{Y} \right\rangle_v, \quad (4.118)$$

where we use that $BW^d \phi'$ vanishes at the vortex centre $\rho = 0$. This exact result expresses how the near-source limit of ϕ' just outside the vortex is determined by the detailed vortex profiles (keeping in mind that for both regions X_{\pm} , ϕ' in this expression is evaluated for a proper-distance coordinate for which ρ *increases* as one moves away from the vortex).

If ρ_v lies within the Kasner regime — for which (4.25) applies — the the left-hand

side of (4.118) becomes

$$\left(BW^d \phi' \right)_{\rho=\rho_v} = \left(\frac{zB_0W_0^d}{\ell} \right) \left(\frac{\hat{\rho}_v}{\ell} \right)^{dw+b-1} \left[1 + \mathcal{O} \left(\frac{\hat{\rho}_v}{\ell} \right) \right] = z\Gamma \left[1 + \mathcal{O} \left(\frac{\hat{\rho}_v}{\ell} \right) \right], \quad (4.119)$$

where $\hat{\rho}_v := \rho_v - \rho_\star$ and the second equality defines the quantity $\Gamma := B_0W_0^d/\ell$ and uses the linear Kasner relation $dw + b = 1$. When combined with (4.118) this shows how vortex properties constrain combinations of bulk parameters (such as the Kasner power z) not already fixed by the bulk field equations.

Metric

Similar conditions are obtained by integrating the Einstein equations over X_v . The trace-reversed Einstein equation, (4.73), governing the curvature $\mathcal{R}_{(d)}$ integrates to give

$$dw\Gamma \left[1 + \mathcal{O} \left(\frac{\hat{\rho}_v}{\ell} \right) \right] = \left[B(W^d)' \right]_{\rho_v} = -\frac{1}{2\pi} \left[\check{R} \langle W^{-2} \rangle_v + 2\kappa^2 \langle \mathcal{X} \rangle_v \right], \quad (4.120)$$

which uses the boundary condition $B(W^d)' = 0$ at $\rho = 0$ and rewrites $[B(W^d)']_{\rho_v}$ using (4.25). This relates a different combination of bulk parameters to vortex properties. Integrating the $(\theta\theta)$ trace-reversed equation instead implies

$$b\Gamma \left[1 + \mathcal{O} \left(\frac{\hat{\rho}_v}{\ell} \right) \right] = (B'W^d)_{\rho_v} = 1 - \frac{\kappa^2}{2\pi} \left\langle \varrho - \mathcal{Z} - \left(1 - \frac{2}{d} \right) \mathcal{X} \right\rangle_v, \quad (4.121)$$

because of the boundary condition $B'W^d = 1$ at $\rho = 0$.

Notice that the powers z , w and b are not independent since the bulk field equations imply they must satisfy the Kasner conditions (4.26), and so the right-hand sides of the above expressions also cannot be completely independent in the limit

$\hat{\rho}_v \ll \ell$. The resulting relations among the vortex integrals are developed in more detail in §4.4 and play an important role in determining the off-brane components of the bulk stress energy in the effective theory applying at scales where the vortex size cannot be resolved. Because these relations follow from the bulk Einstein equations they can be regarded as general consequences of stress-energy conservation for the vortex integrals.

Integration over the entire transverse space

We see that the integral relations of §4.2 give bulk properties in terms of near-vortex derivatives of bulk fields, and the integral relations just described then relate these near-vortex derivatives to explicit vortex integrals. The resulting relation between bulk properties and vortex integrals is more directly obtained by integrating over *all* of the transverse dimensions, $X_{\text{tot}} = B_{\text{ext}} \cup X_+ \cup X_-$, at once. In such an integral all boundary terms cancel, as they must for any smooth compact transverse space. In the case of the Maxwell field integrating over the entire transverse space gives the flux-quantization condition, as discussed earlier.

Dilaton

Integrating the dilaton field equation, (4.71), over the entire compact transverse dimension gives

$$\langle \mathcal{X} + \mathcal{Y} \rangle_{\text{tot}} = 0 \approx \langle \check{\mathcal{X}}_B \rangle_{\text{tot}} + \sum_v \langle \mathcal{X}_{\text{loc}} + \mathcal{Y} \rangle_v, \quad (4.122)$$

where the approximate equality drops exponentially suppressed vortex terms when replacing a localized integral over the entire space with a localized integral over the source regions. Integration over the transverse space can be regarded as projecting the field equations onto the zero mode in these directions, and so (4.122) can be

interpreted as the equation that determines the value of the dilaton zero-mode. (This conclusion is also shown more explicitly from the point of view of the effective d -dimensional theory in the next chapter.) In the absence of the sources this zero mode is an exact flat direction of the classical equations associated with the scale invariance of the bulk field equations (for instance $\mathcal{X}_B = 0$ for the source-free Salam-Sezgin solution [25]) and the vortex contribution to (4.122) expresses how this flat direction becomes fixed when the sources are not scale-invariant.

Metric

Integrating the trace-reversed Einstein equation over the entire transverse space leads to

$$\left\langle \varrho - \mathcal{Z} - \left(1 - \frac{2}{d}\right) \mathcal{X} \right\rangle_{\text{tot}} = 0, \quad (4.123)$$

and

$$\check{R} \langle W^{-2} \rangle_{\text{tot}} = -2\kappa^2 \langle \mathcal{X} \rangle_{\text{tot}} = d\kappa^2 \langle L \rangle_{\text{tot}}, \quad (4.124)$$

which shows how it is the stress-energy transverse to the source, $\langle \mathcal{X} \rangle_{\text{tot}} = -\frac{d}{2} \langle L \rangle_{\text{tot}}$, that ultimately controls the size of the on-source curvature [7]. Using (4.122) to eliminate \mathcal{X} from the right-hand-side similarly gives

$$\check{R} \langle W^{-2} \rangle_{\text{tot}} = 2\kappa^2 \langle \mathcal{Y} \rangle_{\text{tot}} \approx \sum_{\nu} 2\kappa^2 \langle \mathcal{Y} \rangle_{\nu}, \quad (4.125)$$

whose approximation drops exponentially suppressed terms.

A final useful rewriting of these expressions uses the formula relating the D - and d -dimensional gravitational couplings, κ^2 and κ_d^2 respectively. Dimensionally reducing

the Einstein-Hilbert action shows that this states

$$\frac{1}{\kappa_d^2} = \frac{1}{\kappa^2} \langle W^{-2} \rangle_{\text{tot}}, \quad (4.126)$$

when the would-be zero-mode for ϕ is evaluated at the solution to its field equations, and so eqs. (4.123) and (4.125) at this point become

$$\check{R} = 2\kappa_d^2 \langle \mathcal{Y} \rangle_{\text{tot}} = -2\kappa_d^2 \langle \mathcal{X} \rangle_{\text{tot}} = - \left(\frac{2d}{d-2} \right) \kappa_d^2 \langle \varrho - \mathcal{Z} \rangle_{\text{tot}}. \quad (4.127)$$

4.4 Sources - effective IR description

This section takes the point of view of a low-energy observer, and recasts the expressions for the UV theory found above into the language of the effective field theory appropriate in D dimensions at scales much larger than the transverse vortex size, \hat{r}_v , but smaller than or of order the KK scale, ℓ . We specialize for concreteness' sake to the case $(D, d) = (6, 4)$, though our conclusions also hold more for general $D = d + 2$.

4.4.1 The EFT with point sources

If the relevant length scale of an observable r_{obs} exceeds the length scale of the vortex, $r_{\text{obs}} \gg \hat{r}_v$, then effects of the vortex can be organized as a series in the small quantity \hat{r}_v/r_{obs} . For sufficiently large r_{obs} , the internal structure of the vortex becomes irrelevant and it can be replaced with an idealized point-like object. This observation underlies the well-known description of vanilla Abelian-Higgs vortices using the Nambu-Goto string action [1, 2].

We here generalize this to include brane-localized flux, extending the previous

chapter to include dilaton dependence. It is most convenient to do so using the dual formulation of the bulk action,

$$S_B = - \int d^6x \sqrt{-g} \left[\frac{1}{2\kappa^2} g^{MN} (\mathcal{R}_{MN} + \partial_M \phi \partial_N \phi) + \frac{e^\phi}{2 \cdot 4!} (F_{MNPQ})^2 + \frac{2g_R^2}{\kappa^4} e^\phi \right], \quad (4.128)$$

and to include localized flux in the brane action we include the first subdominant term in a derivative expansion⁸

$$\check{S}_{\text{eff}} = - \sum_v \int_{x=z_v(\sigma)} d^4\sigma \sqrt{-\gamma} \left[\check{T}_v(\phi) - \frac{1}{4!} \zeta_v(\phi) \varepsilon^{\mu\nu\lambda\rho} F_{\mu\nu\lambda\rho} \right] =: \sum_v \int_{z_v} d^4x \check{\mathcal{L}}_v, \quad (4.129)$$

where $\gamma_{\mu\nu}(\sigma) = g_{MN} \partial_\mu z_v^M \partial_\nu z_v^N$ is the induced metric at the position of the brane (with $z_v^M(\sigma)$ denoting the brane position fields) and $\varepsilon^{\mu\nu\lambda\rho}$ is the totally antisymmetric 4-tensor associated with this metric. Since in what follows our interest is not in the dynamics of the brane position modes we assume a static vortex and choose coordinates so that it is located at fixed $y^m = y_v^m$ and identify $\sigma^\mu = x^\mu$ so $\gamma_{\mu\nu}(x) = g_{\mu\nu}(x, y_v) = W^2(y_v) \check{g}_{\mu\nu}(x)$. It is clear in both the UV and IR theories that the term linear in $F_{(4)}$ does not gravitate because it is metric independent, though this can also be inferred using the original A_M variables as in the dilaton-free case.

Because the effective theory cannot resolve the vortex structure it also cannot distinguish between the quantities ρ_v and associated ρ_\star used in previous sections. For each vortex we define the brane position in the effective theory to be the corresponding place where the external metric is singular when extrapolated using only bulk field equations. In practice this situates them at $y = y_v$ where $B(y_v) = B(\rho_\star) = 0$,

⁸The check here conforms with the notation of [4] and is to remind that the use of the 4-form field automatically unmixes the gauge kinetic terms.

and it is also true that $W(y_v) = W(\rho_v) = W_v$ and so on. So we use the notations $\phi_\star = \phi(\rho_\star) = \phi(\rho_v) = \phi_v = \phi(y_v)$ interchangeably for the various bulk fields.

We show in this section that \check{S}_{eff} captures all of the physics of the full vortex action, up to linear order in the hierarchy \hat{r}_v/ℓ , provided that the parameters $\check{T}_v(\phi)$ and $\check{\zeta}_v(\phi)$ are chosen appropriately. In general, these can be ϕ -dependent quantities and we identify this dependence by demanding agreement between the predictions of \check{S}_{eff} and \check{S}_v to this order. Working to quadratic or higher order in \hat{r}_v/ℓ would require also including higher-derivative terms in \check{S}_{eff} . To connect the point-brane action to the bulk fields we promote it to higher dimensions using a ‘localization’ delta-function, $\delta_2(y)$. More precisely, we write

$$\check{S}_{\text{eff}} = \sum_v \int d^D x \check{\mathcal{L}}_v \left(\frac{\delta_2(y - y_v)}{\sqrt{g_2}} \right), \quad (4.130)$$

where $\delta_2(y)$ is localized around zero and it is normalized so that integrating over a single source region X_v gives $\int_{X_v} d^2 y \delta_2(y - y_v) = 1$. Performing the integration over the extra dimensions recovers the brane action in (5.5).

As in [4] a key question asks what fields the localizing function depends on since this affects how \check{S}_{eff} enters the bulk field equations. Although we assume in what follows that $\delta_2(y)$ is independent of the fields A_M , ϕ and $g_{\mu\nu}$, we cannot also do so for the metric components g_{mn} because it is designed to discriminate points based on proper distance from the vortex center. But because this metric dependence is only implicit it complicates the calculation of the brane’s stress-energy components $T_{(b)}^{mn}$. One of the purposes of this section is to show how to determine these components without making ad-hoc assumptions about how $\delta_2(y)$ depends on g_{mn} , instead deducing them using properties of the bulk Einstein equations. Our conclusion ultimately is

that the naive treatment of ignoring metric dependence in $\delta_2(y)$ need not be justified in the presence brane-dilaton couplings, and a cleaner way of inferring how a brane interfaces with the bulk is to demand consistency with the constraint in the Einstein equations (along the lines of [11, 12]).

4.4.2 Parameter matching

We start by matching the coefficients \check{T}_v and ζ_v by comparing with the UV theory. A direct way to do so is by dimensionally reducing the UV action, and we verify that this also is what is required for \check{S}_{eff} to agree with \check{S}_v for observables like the components of the stress energy. When doing so it is crucial to notice that any such a comparison between the UV and IR theories need only be done up to linear order in \hat{r}_v/ℓ since it is only at this accuracy that the action (5.5) must capture the physics of earlier sections. This allows considerable simplification since integration of any slowly varying bulk quantity over X_v vanishes quadratically with \hat{r}_v for $\hat{r}_v \ll \ell$, allowing any such terms to be dropped to the accuracy with which we work. In what follows we accordingly take the formal limit $\hat{r}_v \rightarrow 0$ when discussing such integrals, by which we mean we drop terms that vanish at least quadratically in \hat{r}_v/ℓ in this limit. We take care *not* to similarly drop terms suppressed only by a single power of \hat{r}_v/ℓ , however.

The term linear in $F_{\mu\nu\lambda\rho}$ in the UV action is given in (4.86) as

$$L_{BLF} = -\frac{\varepsilon}{2 \cdot 4!} e^{(r+1)\phi} \epsilon^{MNPQRT} Z_{MN} F_{PQRT} = -\frac{\varepsilon}{2 \cdot 4!} e^{(r+1)\phi} \epsilon^{mn\mu\nu\lambda\rho} Z_{mn} F_{\mu\nu\lambda\rho}, \quad (4.131)$$

and because the 4-form Bianchi identity, $dF_{(4)} = 0$, ensures the components $F_{\mu\nu\lambda\rho}$ cannot depend on the transverse coordinates, y^m , we know $F_{\mu\nu\lambda\rho}$ cannot be strongly peaked (unlike Z_{mn}) in the off-brane directions. Consequently integrating over the

vortex area and comparing with the corresponding term in the IR theory gives

$$\zeta_v(\phi_v) = \frac{\varepsilon}{2} \lim_{\hat{r}_v \rightarrow 0} \int_{X_v} d^2y B e^{(r+1)\phi} \epsilon^{mn} Z_{mn} \simeq - \left(\frac{2\pi n_v \varepsilon}{e} \right) e^{(r+1)\phi_v}, \quad (4.132)$$

where the approximate equality neglects the small variations of ϕ away from a constant value, ϕ_v , at the vortex position, and uses Z -flux quantization to evaluate $\Phi_Z(X_v) = \frac{1}{2} \int d^2y \epsilon^{mn} Z_{mn} = -2\pi n_v/e$.

To match the tension \check{T} we compute the source contribution to the energy density. In the IR theory we have

$$T_{\mu\nu} = -g_{\mu\nu} \left[V_B + L_\phi - L_F + \sum_v \left(\frac{\delta_2(y - y_v)}{\sqrt{g_2}} \right) \check{T}_v \right], \quad (4.133)$$

and this is to be compared with the localized contribution to the stress energy of the UV theory integrated across the vortex,

$$\begin{aligned} T_{\mu\nu} &= \frac{1}{3!} F^{\mu M \dots N} F^\nu_{M \dots N} - g_{\mu\nu} (V_B + L_\phi + L_F + \check{L}_Z + L_\Psi + V_b) \\ &= -g_{\mu\nu} (V_B + L_\phi - L_F + \check{L}_Z + L_\Psi + V_b) \\ &= -g_{\mu\nu} (\check{\varrho}_B + \varrho_{\text{loc}}). \end{aligned} \quad (4.134)$$

Comparing $\langle T_{\mu\nu} \rangle_v$ from these two results in the limit $\hat{r}_v \rightarrow 0$ reveals the localized contribution to the energy density in the UV theory to be

$$W_v^4 \check{T}_v[\phi_v] = \lim_{\hat{r}_v \rightarrow 0} \int_{X_v} d^2y B W^4 (\check{L}_Z + L_\Psi + V_b) = \lim_{\hat{r}_v \rightarrow 0} \left\langle \check{L}_Z + L_\Psi + V_b \right\rangle_v = \lim_{\hat{r}_v \rightarrow 0} \langle \varrho_{\text{loc}} \rangle_v. \quad (4.135)$$

We pause here to highlight one important feature of this result. The near-brane

behaviour of the warp factor is $W \propto \rho^w$ and for $w > 0$ the quantity $W_\star^4 = W^4(\rho_\star)$ formally vanishes. The power law vanishing of W can be reinterpreted as the logarithmic divergence of the field $\ln(W)$ and such divergences are common in theories with higher codimension brane sources. These divergences can be classically renormalized into the brane couplings [13, 15] and in this case the tension would be renormalized such that the physical combination $W_v^4 \check{T}_v$ remains finite. The UV complete theory provides an explicit regularization of this divergence, since the vortex physics intervenes near the source to ensure $W > 0$ everywhere in the vortex region.

Unlike for ζ , the result in (4.135) gives the ϕ -dependence of \check{T}_v only implicitly, so we next display this dependence more explicitly. We first compute how \check{T}_v depends on ϕ assuming ϕ to be constant over a vortex. We expect the errors we make by doing so to be suppressed by powers of \hat{r}_v/ℓ , and come back to verify this estimate shortly. The ϕ -dependence of the tension is determined by the ϕ -dependence of vortex integrals like

$$\begin{aligned} \langle V_b \rangle_v &= \frac{1}{4} \int_{X_v} d^2y BW^4 \lambda(\phi) (\psi^2 - v^2)^2, & \langle \check{L}_z \rangle_v &= \frac{1}{4} \int_{X_v} d^2y BW^4 \Lambda(\phi) Z_{mn} Z^{mn} \\ \langle L_{\text{gm}} \rangle_v &= \frac{1}{2} \int_{X_v} d^2y BW^4 e^2(\phi) \psi^2 Z_m Z^m, & \langle L_{\psi \text{ kin}} \rangle_v &= \frac{1}{2} \int_{X_v} d^2y BW^4 \partial_m \psi \partial^m \psi, \end{aligned}$$

and earlier sections show that the ϕ -dependence of the vortex profiles appearing in these integrals is fairly simple once expressed in terms of dimensionless variables, F and P . Then the implicit ϕ -dependence within the profiles themselves arises only through the combination $\hat{\beta}(\phi) = 2\hat{\lambda}(\phi)/\hat{e}^2(\phi)$, with $\hat{\lambda}(\phi) := \lambda e^{q\phi}$ and $e^2/\hat{e}^2(\phi) := \Lambda(\phi) = e^{p\phi} - \varepsilon^2 e^{(2r+1)\phi}$. We now ask whether any additional ϕ -dependence arises from the integrations to set the scale of the above integrals.

To this end, it is useful to return to the variables used in (4.100) in which \bar{B} is dimensionless, as is the radial coordinate $\bar{\rho}$. The integration measure $d^2y BW^4 = (1/\hat{e}v)^2 d^2\bar{y} \bar{B}W^4$ and we have, for example,

$$\langle V_b \rangle_v \simeq \frac{\hat{\lambda}(\phi)v^2}{4\hat{e}^2(\phi)} \int_{X_v} d^2\bar{y} \bar{B}W^4 (F^2 - 1)^2 = \hat{\beta}(\phi) \frac{v^2}{8} \int_{X_v} d^2\bar{y} \bar{B}W^4 (F^2 - 1)^2, \quad (4.136)$$

where the approximation assumes the dilaton profile is constant in the integration region. Similarly for the kinetic terms

$$\langle \check{L}_z \rangle_v \simeq \frac{v^2}{2} \int_{X_v} d^2\bar{y} \left(\frac{W^4 [P']^2}{\bar{B}} \right), \quad \langle L_{\psi \text{ kin}} \rangle_v \simeq \frac{v^2}{2} \int_{X_v} d^2\bar{y} \bar{B}W^4 (F')^2, \quad (4.137)$$

and so on. In these expressions the integrands are all proportional to $\hat{e}^2 v^4$, but the \hat{e}^2 dependence cancels the factors of $\hat{r}_v^2 = 1/(\hat{e}^2 v^2)$ coming from the integration measure to leave integrated results that again depend on ϕ only through $\hat{\beta}(\phi) \propto e^{q\phi} \Lambda(\phi)$.

Consequently, we see that the tension depends on ϕ only through its dependence on β

$$\check{T}_v(\phi) = \check{T}_v[\hat{\beta}(\phi)], \quad (4.138)$$

and in particular \check{T}_v is ϕ -independent for the one-parameter family of choices $p = -q = 2r + 1$. Because $\zeta_v(\phi) \propto e^{(r+1)\phi_v}$, having *both* \check{T}_v and ζ_v be ϕ -independent happens only in the special case of scale invariance, for which $p = r = -q = 1$. This inference of the ϕ -independence of the tension is verified numerically, as seen in Fig. 4.5.

What happens once we drop the assumption that ϕ' is negligible within the vortex? In this case our earlier estimate — eq. (4.107) — of the leading ϕ -dependence of

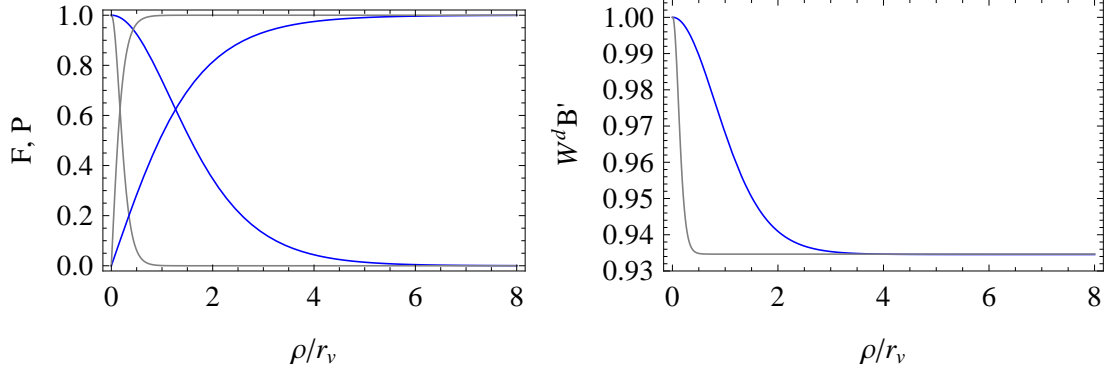


Figure 4.5: A demonstration of the ϕ -independence of \tilde{T}_v . Two solutions are presented for the decoupling choice $p = -q = 2r + 1 = 2$ that differ only in the value of the dilaton in the vortex $\phi_v \approx \phi(0) = \{0, -2\}$. The light (grey) lines represent the solution for the choice $\phi(0) = -2$ and the blue lines represent the solution for $\phi(0) = 0$. While the physical mass scales that control the size of the profiles, $m_\Psi^2(\phi_v) = 2\lambda v^2 e^{q\phi_v}$ and $m_Z^2(\phi_v) = e^{-p\phi_v} e^2 v^2 / (1 - \varepsilon^2)$, are demonstrably heavier for $\phi_v \simeq -2$ (since these profiles fall off much faster), the defect angle $[W^d B']_{\rho_v} \simeq 1 - \frac{\kappa^2 \tilde{T}_v}{2\pi}$ that measures the tension of the vortex is independent of ϕ_v . The other parameters of this solution are $d = 4$, $\varepsilon = 0.6$, $\beta = 0.8$, $\kappa v = 0.4$, $Q = 1.6 \times 10^{-4}$ and $V_0 = Q^2/2$.

vortex profiles implies that the leading ϕ -dependent corrections to quantities like \tilde{T}_v and $\langle \mathcal{X}_{\text{loc}} \rangle_v$ have the KK-suppressed form

$$\frac{\delta \tilde{T}_v}{\tilde{T}_v} \approx \frac{\delta \langle \mathcal{X}_{\text{loc}} \rangle_v}{\langle \mathcal{X}_{\text{loc}} \rangle_v} \approx (r+1) \left(\frac{g_R}{e} \right) e^{(r+1)\phi_v} \approx (r+1) \left(\frac{\hat{g}_R}{\hat{e}} \right) \approx (r+1) \kappa v \left(\frac{\hat{r}_v}{\ell} \right), \quad (4.139)$$

which uses $g_A \sim g_R$ and $p = 2r + 1$ as well as $\hat{r}_v \sim 1/(\hat{e}v)$ and $\ell \sim \kappa/\hat{g}_R$.

4.4.3 Near-source boundary conditions

As noted earlier, the hidden dependence of the localization function $\delta_2(y)$ on g_{mn} complicates the inference of how branes contribute to the bulk field equations. In this section we give a δ -independent way of expressing the bulk-brane interaction wherein knowledge of the brane action, \tilde{S}_{eff} , directly gives the near-brane asymptotic

derivatives of the bulk fields. This connection is the analogue in the IR theory of the expressions in §4.3.4 relating the near-vortex derivatives of bulk fields to integrals over the vortex. The agreement between the UV and IR descriptions of these boundary conditions provides a check on the matching between the two versions of the theory. The discussion found here also parallels the dilaton-free case.

Dilaton

Since the general discussion is simplest for a scalar field we treat the dilaton first. In the effective theory of point-like branes the field equation for the dilaton reads

$$\frac{1}{\kappa^2} \square \phi = V_B - L_A + \sum_v \left(\frac{\delta_2(y - y_v)}{\sqrt{g_2}} \right) \left(\check{T}'_v(\phi) - \frac{1}{4!} \check{C}'_v(\phi) \epsilon^{\mu\nu\lambda\rho} F_{\mu\nu\lambda\rho} \right). \quad (4.140)$$

As before we integrate this equation over a source-containing pillbox to isolate the near-brane derivative of the dilaton, recognizing that this pillbox can be taken to have infinitesimal size in the effective theory (within which the vortex size cannot be resolved). On the left-hand side the result is

$$\lim_{\hat{r}_v \rightarrow 0} \langle \square \phi \rangle_v = 2\pi \lim_{\rho \rightarrow \rho_*} \left(B W^d \phi' \right) = 2\pi z \Gamma, \quad (4.141)$$

where the last equality uses the near-brane asymptotic bulk solution (4.25) and again uses the definition $\Gamma := B_0 W_0^d / \ell$. Performing the same operation on the right hand side gives

$$\lim_{\hat{r}_v \rightarrow 0} \left\langle V_B - L_A + \frac{\partial \check{L}_{\text{eff}}}{\partial \phi} \right\rangle_v = W_v^d \left(T'_v(\phi) - \frac{1}{4!} \check{C}'_v(\phi) \epsilon^{\mu\nu\lambda\rho} F_{\mu\nu\lambda\rho} \right)_{y=y_v}, \quad (4.142)$$

where the smoothness of the bulk sources ensures their integral does not survive the

limit $\hat{r}_v \rightarrow 0$. The localized sources do survive this limit, however, and give the final result

$$z \Gamma = \lim_{y \rightarrow y_v} \left(BW^d \phi' \right) = \frac{\kappa^2 W_v^d}{2\pi} \left(T'_v(\phi) - \frac{1}{4!} \zeta'_v(\phi) \epsilon^{\mu\nu\lambda\rho} F_{\mu\nu\lambda\rho} \right)_{y_v} = -\frac{\kappa^2}{2\pi\sqrt{-\check{g}}} \left(\frac{\delta \check{S}_{\text{eff}}}{\delta \phi(y_v)} \right), \quad (4.143)$$

in agreement with [11, 12]. Eq. (4.143) is useful because it directly extracts the impact of the brane-dilaton coupling on the bulk dilaton without reference to the localization function $\delta_2(y)$.

This argument shows it is useful to divide quantities like ϱ , \mathcal{X} and \mathcal{Z} into a localized piece, whose integral survives the point-like limit, and a smooth bulk piece that does not. For instance: $\mathcal{X} = \check{\mathcal{X}}_B + \mathcal{X}_{\text{loc}}$, where the bulk part, $\check{\mathcal{X}}_B := V_B - \check{L}_A$, depends only on bulk fields and so satisfies $\langle \check{\mathcal{X}}_B \rangle_v \rightarrow 0$ as $\hat{r}_v \rightarrow 0$. The same need not be true for vortex-localized quantities like $\mathcal{X}_{\text{loc}} = V_b - \check{L}_Z$ and \mathcal{Y} .

The analogous relation between the near-vortex derivative of the dilaton and the vortex sources in the UV theory is given by (4.118), which we rewrite for convenience of comparison here

$$\lim_{\rho \rightarrow \rho_v} BW^d \phi' = \frac{\kappa^2}{2\pi} \lim_{\hat{r}_v \rightarrow 0} \left\langle \mathcal{X}_{\text{loc}} + \mathcal{Y} \right\rangle_v = \frac{\kappa^2}{2\pi} \lim_{\hat{r}_v \rightarrow 0} \left\langle qV_b + \frac{\Lambda'}{\Lambda} \check{L}_Z + (r+1)L_{BLF} \right\rangle_v. \quad (4.144)$$

Comparing with this UV version allows a check the consistency of our inference of the ϕ -dependence of \check{L}_{eff} . Comparing terms linear in $F_{(4)}$ gives

$$\zeta'_v(\phi) = (r+1) \lim_{\hat{r}_v \rightarrow 0} \frac{\varepsilon}{2} \int_{X_v} d^2y B e^{(r+1)\phi} \epsilon^{mn} Z_{mn}, \quad (4.145)$$

which is consistent with the earlier result (4.132), assuming the dilaton is approximately constant in the region X_v and provided differentiation with respect to ϕ is performed with fixed vortex fields. Similarly comparing the 4-form-independent terms gives

$$W_v^d \check{T}'_v = \lim_{\hat{r}_v \rightarrow 0} \left\langle qV_b + \frac{\Lambda'}{\Lambda} \check{L}_z \right\rangle_v, \quad (4.146)$$

which is also consistent with the earlier expression (4.135).

Metric

A similar argument relates near-source metric derivatives to properties of the brane action. As above one integrates the Einstein equations over a region X_v enclosing the vortex and finds two kinds of terms that survive the limit $\hat{r}_v \rightarrow 0$ of vanishingly small vortex size. One such class of terms comes from the vortex parts of the stress energy while the other come from terms inside the Einstein tensor involving second derivatives with respect to ρ , with all other contributions not singular enough to survive the small-vortex limit.

The simplest equation to analyze is the $(\rho\rho)$ Einstein equation, (4.77), since this involves no second derivatives at all. Consequently its integral over X_v simply states

$$\mathcal{T}^\rho_\rho = \lim_{\hat{r}_v \rightarrow 0} \langle T^\rho_\rho \rangle_v = \lim_{\hat{r}_v \rightarrow 0} \langle \mathcal{Z}_{\text{loc}} - \mathcal{X}_{\text{loc}} \rangle_v \simeq 0. \quad (4.147)$$

Physically, this is a consequence of dynamical equilibrium for the non-gravitational microphysics of which the vortex is built, since this requires there to be no net radial pressure.

For all of the remaining Einstein equations the Einstein tensor does include second derivatives and so their integration over \mathcal{X}_v leads to the following relation between the

near-source derivatives of the metric and the metric derivative of the source action

$$2\pi \lim_{\hat{r}_v \rightarrow 0} \left[\sqrt{-g} (K^{ij} - K g^{ij}) \right]_0^{\rho_v} = -\kappa^2 \sqrt{-g} \mathcal{T}^{ij} = -2\kappa^2 \frac{\delta \check{S}_{\text{eff}}}{\delta g_{ij}(y_v)}, \quad (4.148)$$

where the derivative on the right-hand side is with respect to the metric evaluated at the brane position and K_{ij} is the extrinsic curvature for surfaces of constant ρ (with $K = g^{ij} K_{ij}$). The indices i and j run over all coordinates but ρ .

The derivative on the right-hand-side can be taken reliably for on-brane components of the metric $(ij) = (\mu\nu)$ using the action (5.5) and gives

$$\frac{\delta \check{S}_{\text{eff}}}{\delta g_{\mu\nu}(y_v)} = -\frac{1}{2} \sqrt{-\gamma} \check{T}^{\gamma\mu\nu}. \quad (4.149)$$

For the metric ansatz of interest the extrinsic curvature components are $K_{\mu\nu} = WW' \check{g}_{\mu\nu}$ and $K_{\theta\theta} = BB'$, so the on-brane components of (4.148) give

$$\lim_{\hat{r}_v \rightarrow 0} \left[1 - BW^4 \left(\frac{3W'}{W} + \frac{B'}{B} \right) \right]_{\rho=\rho_v} = \lim_{y \rightarrow y_v} \left[1 - \frac{3}{4} B (W^4)' - B' W^4 \right] = \frac{\kappa^2 W_v^4 \check{T}_v}{2\pi}. \quad (4.150)$$

This result is to be compared with the appropriate linear combination of (4.121) and (4.120) in the UV theory, keeping only those vortex-localized terms that survive in the limit $\hat{r}_v \rightarrow 0$:

$$\lim_{\hat{r}_v \rightarrow 0} \left[1 - BW^4 \left(\frac{3W'}{W} + \frac{B'}{B} \right) \right]_{\rho=\rho_v} \simeq \frac{\kappa^2}{2\pi} \lim_{\hat{r}_v \rightarrow 0} \langle \varrho_{\text{loc}} + \mathcal{X}_{\text{loc}} - \mathcal{Z}_{\text{loc}} \rangle_v \simeq \frac{\kappa^2}{2\pi} \lim_{\hat{r}_v \rightarrow 0} \langle \varrho_{\text{loc}} \rangle_v. \quad (4.151)$$

The last equality here uses (4.147), leaving a result consistent with our earlier identification in eq. (4.135) that $W_v^d \check{T}_v \simeq \lim_{\hat{r}_v \rightarrow 0} \langle \varrho_{\text{loc}} \rangle_v$.

4.4.4 Brane and vortex constraints

We now turn to the remaining case, where $(ij) = (\theta\theta)$ in (4.148), which gives

$$\lim_{\hat{r}_v \rightarrow 0} \left[B (W^d)' \right]_{\rho_v} = \lim_{y \rightarrow y_v} B (W^d)' = \frac{\kappa^2}{\pi \sqrt{-\check{g}}} g_{\theta\theta}(y_v) \left(\frac{\delta \check{S}_{\text{eff}}}{\delta g_{\theta\theta}(y_v)} \right). \quad (4.152)$$

The trouble with this expression is that the dependence of \check{S}_{eff} on $g_{\theta\theta}$ is only known implicitly, so we cannot perform the differentiation on the right-hand side to learn about the near-brane derivatives on the left-hand side. Fortunately we may instead read this equation in the other direction: it tells us the right-hand side because the radial constraint – eq. (4.77) – already determines the derivatives on the left-hand side in terms of known quantities. It is ultimately this observation that allows us to determine $\langle \mathcal{X}_{\text{loc}} \rangle_v$ and $\langle \mathcal{Z}_{\text{loc}} \rangle_v$ separately in terms of the quantities \check{T} and ζ [11, 12].

To see this we first compare with the corresponding UV expression, using (4.120) to rewrite

$$\lim_{\rho \rightarrow \rho_v} B (W^d)' \simeq -\frac{\kappa^2}{\pi} \lim_{\hat{r}_v \rightarrow 0} \langle \mathcal{X}_{\text{loc}} \rangle_v, \quad (4.153)$$

and so

$$\mathcal{T}^\theta_\theta = \frac{2}{\sqrt{-\check{g}}} g_{\theta\theta}(y_v) \left(\frac{\delta \check{S}_{\text{eff}}}{\delta g_{\theta\theta}(y_v)} \right) = -2 \lim_{\hat{r}_v \rightarrow 0} \langle \mathcal{X}_{\text{loc}} \rangle_v \simeq -\lim_{\hat{r}_v \rightarrow 0} \langle \mathcal{X}_{\text{loc}} + \mathcal{Z}_{\text{loc}} \rangle_v, \quad (4.154)$$

which confirms that the vortex stress-energy component $\mathcal{T}^\theta_\theta$ captures the integral of the vortex-localized part of T^θ_θ in the UV theory.

To fix $\mathcal{T}^\theta_\theta$ we follow [11, 12] and again use the constraint equation (4.77), but rather than integrating it over the vortex we instead evaluate it at $\rho = \rho_v$, just outside

the vortex, and solve it for $B (W^d)'$ to find

$$\left(\frac{d-1}{d}\right) B (W^d)' = - (B'W^d) + (B'W^d) \sqrt{1 + \left(\frac{d-1}{d}\right) E}, \quad (4.155)$$

where we define

$$E := \left(\frac{B}{B'}\right)^2 [2\kappa^2 (\mathcal{Z}_B - \check{\mathcal{X}}_B) - W^{-2}\check{R}]. \quad (4.156)$$

Because this gives $B (W^d)'$ in terms of $B'W^d$ and other known quantities we use it in (4.152) to get an explicit expression for $\mathcal{T}^\theta_\theta$ (and so also for $\langle \mathcal{Z}_{\text{loc}} \rangle_v \simeq \langle \mathcal{X}_{\text{loc}} \rangle_v$).

So far eq. (4.155) assumes only that ρ_v is sufficiently far from the vortex that localized contributions to \mathcal{X} and \mathcal{Z} are exponentially small. However, since $\rho_v \sim \hat{r}_v$ in size we can also drop terms quadratically small in ρ_v when comparing with the point-brane theory. Since both the \check{R} and $\check{\mathcal{X}}_B$ terms in (4.156) are proportional to $B^2(\rho_v) \sim \rho_v^2 \sim \hat{r}_v^2$ they can be dropped in this limit. By contrast, the term containing $2\kappa^2 \mathcal{Z}_B(\rho_v) = [\phi'(\rho_v)]^2$ need not vanish quadratically in this limit, since the asymptotic power-law form (4.25) allowed in this region implies

$$\lim_{\hat{r}_v \rightarrow 0} E \simeq \lim_{\rho \rightarrow \rho_*} 2\kappa^2 \left(\frac{B}{B'}\right)^2 \mathcal{Z}_B \simeq \lim_{\rho \rightarrow \rho_*} \left(\frac{B\phi'}{B'}\right)^2 = \left(\frac{z}{b}\right)^2, \quad (4.157)$$

and the final equality uses (4.119) and (4.121) to rewrite the right-hand side in terms of Kasner powers. Indeed, using this final result in (4.155) and trading the remaining terms for Kasner powers leads to

$$(d-1)w \simeq -b + b \sqrt{1 + \left(\frac{d-1}{d}\right) \left(\frac{z}{b}\right)^2}, \quad (4.158)$$

which reveals it not to be independent in this limit of the two Kasner conditions,

(4.26).

In passing we pause to remark on a point already alluded to in earlier sections: that the constraints imposed by the Einstein equations also imply the existence of relations among vortex integrals — like $\langle \mathcal{X}_{\text{loc}} \rangle_v$ and $\langle \mathcal{Y} \rangle_v$ — for *arbitrary* vortex microphysics in the point-source limit. The constraint is found by eliminating B' and W' in terms of vortex integrals using the near-vortex expressions (4.121) and (4.120), leading for instance to

$$\lim_{\hat{r}_v \rightarrow 0} E \simeq \left(\frac{z}{b} \right)^2 \simeq \left(\frac{\kappa^2 \langle \mathcal{X}_{\text{loc}} + \mathcal{Y} \rangle_v}{1 - \frac{\kappa^2}{2\pi} \langle \varrho_{\text{loc}} - 2\mathcal{X}_{\text{loc}} \left(\frac{d-1}{d} \right) \rangle_v} \right)^2. \quad (4.159)$$

In limit of small $\kappa^2 \langle \mathcal{Y} \rangle_v$ and $\kappa^2 \langle \mathcal{X}_{\text{loc}} \rangle_v$ the resulting constraint simplifies to

$$\kappa^2 \langle \mathcal{X}_{\text{loc}} \rangle_v \approx -\frac{\kappa^4 \langle \mathcal{Y} \rangle_v^2}{4\pi}. \quad (4.160)$$

This brane constraint can be verified using explicit numerical solutions, as is illustrated in Fig. 4.6. The suppression it implies for $\kappa^2 \langle \mathcal{X}_{\text{loc}} \rangle_v$ relative to $\kappa^2 \langle \mathcal{Y} \rangle_v$ is the analog of the suppression found earlier, (4.28), between the various Kasner exponents that imply w and $1 - b$ are order z^2 when $z \ll 1$. This is seen most explicitly by dividing (4.119) by (4.120) and evaluating in the $\hat{r}_v \rightarrow 0$ limit, which gives

$$\frac{2\langle \mathcal{X}_{\text{loc}} \rangle_v}{\langle \mathcal{X}_{\text{loc}} + \mathcal{Y} \rangle_v} \simeq -\frac{dw}{z} \approx -\frac{z}{2} + \mathcal{O}(z^2) \quad (4.161)$$

where the approximation follows from (4.28). The integrated vortex sources $\langle \mathcal{X}_{\text{loc}} \rangle_v$ and $\langle \mathcal{Y} \rangle_v$ cannot adjust independently to leading order in δ and \hat{r}_v/ℓ . This is explored in more detail in the next subsection.

To summarize, it is possible to be very explicit about the transverse localized stress-energies, $\kappa^2 \langle \mathcal{X}_{\text{loc}} \rangle_v$ and $\kappa^2 \langle \mathcal{Z}_{\text{loc}} \rangle_v$ in the limit when these vortex integrals are

small. In this case $\langle \mathcal{Y} \rangle_v$ is given by differentiating \check{S}_{eff} by eqs. (4.143) and (4.144),

$$z \Gamma = \lim_{y \rightarrow y_v} \left(BW^d \phi' \right) = -\frac{\kappa^2}{2\pi\sqrt{-\check{g}}} \left(\frac{\delta \check{S}_{\text{eff}}}{\delta \phi(y_v)} \right) \simeq \frac{\kappa^2}{2\pi} \lim_{\hat{r}_v \rightarrow 0} \langle \mathcal{Y} \rangle_v, \quad (4.162)$$

Then $\langle \mathcal{Z}_{\text{loc}} \rangle_v$ and $\langle \mathcal{X}_{\text{loc}} \rangle_v$ are obtained from (4.147) and (4.160).

This section also shows how errors can arise when treating the localizing function $\delta_2(y)$ as a naive delta-function that is independent of g_{mn} . Such a treatment would mistakenly conclude that the brane action in (5.5) is independent of the bulk metric, and give

$$\lim_{y \rightarrow y_v} B(W^d)' = \frac{\kappa^2}{\pi\sqrt{-\check{g}}} g_{\theta\theta}(y_v) \left(\frac{\delta \check{S}_{\text{eff}}}{\delta g_{\theta\theta}(y_v)} \right) = 0 \quad (\text{naive result}). \quad (4.163)$$

This not consistent with (4.153) unless the vortex source has vanishing $\langle \mathcal{X}_{\text{loc}} \rangle_v$ in the limit $\hat{r}_v \rightarrow 0$, which is not necessarily true, since the vortex must satisfy the simplified vortex constraint (4.160). In the next section we estimate this quantity's (often nonvanishing) size.

4.5 The scale of the response

This section summarizes the implications of the previous sections for the generic size of back-reaction effects on physical quantities. In particular we broadly scope out how the size of the on-vortex curvature, \check{R} , varies with the parameters p , q and r governing the size of the vortex-dilaton couplings.

As (4.127) suggests, the d -dimensional curvature is sensitive to p , q and r through the size of $\kappa_d^2 \langle \mathcal{Y} \rangle_{\text{tot}}$. We now trace how the size of \check{R} can drastically change as these

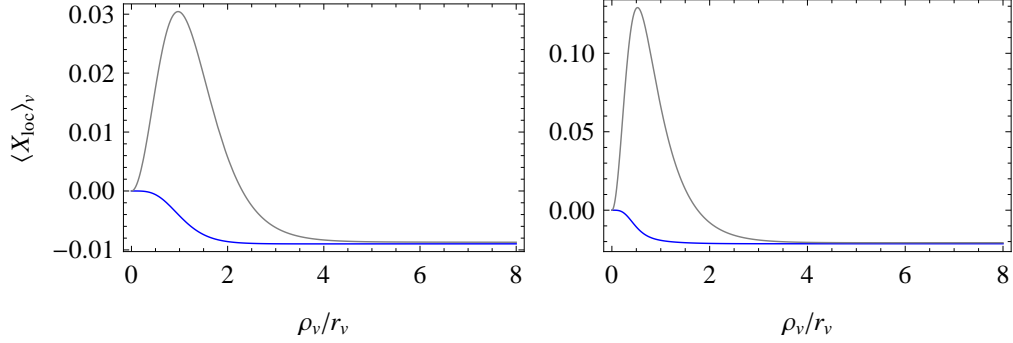


Figure 4.6: Two examples of the vortex constraint (4.160). The light (grey) line is calculated from the expression $\kappa^2 \langle \mathcal{X}_{\text{loc}} \rangle_v \simeq -\pi [B(W^d)]_{\rho_v}$ and the dark (blue) line is calculated using the second brane constraint. Once evaluated outside of the vortex $\rho_v \gtrsim \hat{r}_v \approx r_v$, the two independently calculated quantities are in perfect agreement, and their failure to agree inside the region $\rho_v \lesssim \hat{r}_v$ reflects the fact that the vortex constraint does not hold locally in the source. In the first plot the parameters are $d = 4$, $\varepsilon = 0$, $\beta = 3$, $\kappa v = 0.5$, $\phi_v \approx \phi(0) = 0$, $Q = 2 \times 10^{-4}$ and $V_0 = Q^2/2$. The vortex is coupled to the dilaton via the choice $(p, q) = (0, 2)$ and r is not relevant because gauge kinetic mixing has been shut off. In the second plot, the only change in parameters is that $\phi(0) = 1$.

parameters take various limits. The size of the quantity $\langle \mathcal{X}_{\text{loc}} \rangle_v$ also varies strongly in these limits since it is also related to $\langle \mathcal{Y} \rangle_v$ as in (4.160).

4.5.1 Generic case

Before examining special cases we first establish a baseline by considering the generic case. Recall from the definition of \mathcal{Y} in the dual variables,

$$\mathcal{Y} = (q - 1)V_b + \left(1 + \frac{\Lambda'}{\Lambda}\right) \check{L}_Z + (r + 1)L_{BLF}, \quad (4.164)$$

that each term contains localized vortex fields and for generic choices of parameters these all integrate over a vortex to give

$$\langle \mathcal{Y} \rangle_v \sim \langle \varrho_{\text{loc}} \rangle_v \sim \check{T} \sim v^2, \quad (4.165)$$

much as we saw earlier.

When this is true, it follows from the vortex constraints (4.160) and (4.147) that the vortex integrals of the transverse stress-energy components are suppressed relative to $\langle \mathcal{Y} \rangle$ by an additional factor of $\kappa^2 v^2$,

$$\kappa^2 \langle \mathcal{Z}_{\text{loc}} \rangle_v \simeq \kappa^2 \langle \mathcal{X}_{\text{loc}} \rangle_v \sim \kappa^4 v^4. \quad (4.166)$$

This suppression is perhaps not surprising given that these quantities vanish in the flat space limit, as discussed in Appendix B.1, as a consequence of the equations of motion.

In this generic case eq. (4.144) then implies the following size for the near-source dilaton derivative

$$\lim_{\hat{r}_v \rightarrow 0} [BW^d \phi']_{\rho_v} \simeq \frac{\kappa^2}{2\pi} \langle \mathcal{X}_{\text{loc}} + \mathcal{Y} \rangle_v \sim \frac{\kappa^2}{2\pi} \langle \mathcal{Y} \rangle_v \sim \kappa^2 v^2, \quad (4.167)$$

with a similar size predicted by (4.151) for the near-brane form of B' (and so also the brane defect angle)

$$1 - \lim_{\hat{r}_v \rightarrow 0} (B'W^d)_{\rho_v} \simeq \frac{\kappa^2}{2\pi} \langle \mathcal{Q}_{\text{loc}} \rangle_v \sim \kappa^2 v^2. \quad (4.168)$$

By contrast, (4.153) predicts the near-brane limit of W' is additionally suppressed,

$$\lim_{\hat{r}_v \rightarrow 0} [B(W^d)']_{\rho_v} \simeq -\frac{\kappa^2}{\pi} \langle \mathcal{X}_{\text{loc}} \rangle_v \sim \kappa^4 v^4. \quad (4.169)$$

All of these estimates are confirmed by the numerical results displayed in Fig. 4.2 and Fig. 4.6, and they are consistent with the weakly gravitating solutions to the Kasner

equations (which state that $1 - b$ and dw are order z^2 when $z \ll 1$).

The d -dimensional curvature in this generic case is not particularly small, since it is of order

$$\check{R} = 2\kappa_d^2 \langle \mathcal{Y} \rangle_{\text{tot}} \sim \kappa_d^2 v^2, \quad (4.170)$$

corresponding to a vacuum energy of order v^2 .

4.5.2 Scale invariance

The other extreme is the scale invariant case: $(p, q, r) = (-1, 1, -1)$. As noted previously, in this case the quantity \mathcal{Y} everywhere vanishes,

$$\mathcal{Y} = 0, \quad (4.171)$$

and so the vortex constraints, (4.160) and (4.147), then also imply

$$\langle \mathcal{Z}_{\text{loc}} \rangle_v \simeq \langle \mathcal{X}_{\text{loc}} \rangle_v \simeq 0. \quad (4.172)$$

This in turn leads to the a vanishing near-brane limits for both ϕ' and W' ,

$$\lim_{\hat{r}_v \rightarrow 0} [BW^d \phi']_{\rho_v} \simeq \frac{\kappa^2}{2\pi} \langle \mathcal{X}_{\text{loc}} \rangle_v \simeq 0 \quad \text{and} \quad \lim_{\hat{r}_v \rightarrow 0} [B(W^d)']_{\rho_v} \simeq -\frac{\kappa^2}{\pi} \langle \mathcal{X}_{\text{loc}} \rangle_v \simeq 0, \quad (4.173)$$

although the brane defect angle is again given by (4.168) and so is not particularly suppressed.

This suppression of W' in the near-brane limit resembles the pure Maxwell-Einstein (dilaton-free) case considered in chapter 3, for which the radial Einstein constraint also generically forces $\langle \mathcal{X}_{\text{loc}} \rangle_v$ and the near-brane limit of W' to vanish. It

is also consistent with the observation that, in the scale invariant case, there exists the BPS choice of couplings $\hat{\beta} = 1$ for which $\mathcal{X}_{\text{loc}} = \mathcal{Z}_{\text{loc}} = 0$ locally and to all orders in \hat{r}_v/ℓ . This is particularly obvious in the numerical BPS solution of Fig. 4.4 which has constant warp factor and dilaton.

Lastly, the scale-invariant choice ensures the vanishing of the d -dimensional curvature

$$\check{R} = 2\kappa_d^2 \langle \mathcal{Y} \rangle_{\text{tot}} = 0, \quad (4.174)$$

although this is less interesting than it sounds since this is typically achieved by having the dilaton zero mode φ run away, $e^\varphi \rightarrow 0$, since this is the only generic solution to the zero-mode equation $0 = \langle \mathcal{X} + \mathcal{Y} \rangle_{\text{tot}} = \langle \mathcal{X} \rangle_{\text{tot}} \propto e^\varphi$.

Special case: supersymmetric ‘BPS’ branes

The coefficient of the scale invariant runaway potential vanishes if the flux quantization condition can be satisfied such that $Q = Q_{\text{susy}}$, where

$$Q_{\text{susy}} := \frac{2g_R}{\kappa^2}. \quad (4.175)$$

In other words, $\langle \mathcal{X} \rangle_{\text{tot}}$ can be made to vanish in a ϕ -independent way if this relation holds, because it ensures that $\check{\mathcal{X}}_B = V_B - L_A = 0$ by having the individual contributions cancel against one another locally. The localized contributions to $\langle \mathcal{X} \rangle_{\text{tot}}$ also vanish locally if $\check{\beta} = 1$ and are otherwise suppressed.

In the scale invariant case, for which $\phi' = 0$ at the source, we can insert this desired value of $Q = Q_{\text{susy}}$ into the the flux quantization condition in (4.40), and

derive a local condition relating tension and localized flux. For $N = +1$ it reads

$$\Phi_A(X_v) = \frac{\pi}{g_R}(1 - \alpha) \quad \implies \quad \kappa^2 \check{T}_v = -2g_R \zeta_v \quad (4.176)$$

so long as $\alpha_+ = \alpha_- = \alpha$. Otherwise, the defect angles contribute in a nonlinear way to the flux quantization condition via $\Upsilon := \sqrt{\alpha_+ \alpha_-}$ and no such local condition can be found. Note also that the relation (4.175) can only be made to hold if the gauge symmetry has the coupling strength of the R -symmetry, $g_A = g_R$.

Such a relation between the defect angle and flux is also expected from the supersymmetry conditions, in order to guarantee the continued cancellation of spin and gauge connections within the Killing spinor's covariant derivative, once localized sources are introduced [5?]. However, past works did not properly identify the defect angle with the renormalized brane tension, as in (4.176).

4.5.3 Decoupling case: $p = -q = 2r + 1$

The ‘decoupling’ choice $p = -q = 2r + 1$ is special because it ensures that $\hat{\beta}$ is ϕ -independent. This suppresses the dilaton-dependence of the brane tension, as in (4.107), which also makes it similar in form to the ϕ -dependence of the brane-localized flux, ζ . Notice both become ϕ -independent in the scale-invariant special case where $r = -1$.

We here ask whether this suppression of brane-dilaton couplings also suppresses the brane's gravitational response, and if so by how much. To decide, recall that for the decoupling choice, \mathcal{Y} takes on the special form

$$\mathcal{Y} = (q - 1)(V_b - \check{L}_Z) + (r + 1)L_{BLF} = (q - 1)\mathcal{X}_{\text{loc}} + (r + 1)L_{BLF}, \quad (4.177)$$

and the vortex constraint in (4.160) becomes

$$\kappa^2 \langle \mathcal{Z}_{\text{loc}} \rangle_v \simeq \kappa^2 \langle \mathcal{X}_{\text{loc}} \rangle_v \simeq -\frac{\kappa^2}{4\pi} \langle q\mathcal{X}_{\text{loc}} + (r+1)L_{BLF} \rangle_v^2 \simeq -\frac{1}{4\pi} (r+1)^2 \kappa^4 \langle L_{BLF} \rangle_v^2, \quad (4.178)$$

which uses that (4.160) requires $\langle \mathcal{X}_{\text{loc}} \rangle_v \ll \langle L_{BLF} \rangle_v$.

Conveniently, the quantity $\langle L_{BLF} \rangle_v$ can be estimated using the on-shell value of the 4-form field strength (4.85) and the bulk gauge field strength (4.114). This gives

$$\langle L_{BLF} \rangle_v = \varepsilon Q \int d\rho Z_{\rho\theta} e^{(r+1)\phi} \simeq -Q \left(\frac{2\pi n_v \varepsilon}{e} \right) e^{(r+1)\phi_v}, \quad (4.179)$$

where n_v and ϕ_v are the flux quantum and approximately constant value of the dilaton in the vortex region X_v . To get a handle on its size we use the source free estimate $Q \sim g_R/\kappa^2$ and write the result more transparently in terms of $\hat{r}_v^{-1} = \hat{e}(\phi)v = ev e^{-p\phi/2}$ and $\ell^{-1} = 2\hat{g}_R(\phi)/\kappa = (2g_R/\kappa)e^{-\phi/2}$, to find

$$\kappa^2 \langle L_{BLF} \rangle_v \simeq -2\pi n_v \varepsilon \left(\frac{\kappa^2 Q}{e} \right) e^{(r+1)\phi_v} \approx -4\pi n_v \varepsilon \left(\frac{\hat{g}_R(\phi_v)}{\hat{e}(\phi_v)} \right) = -4\pi n_v \varepsilon \kappa v \left(\frac{\hat{r}_v}{\ell} \right). \quad (4.180)$$

For small vortices, $\hat{r}_v/\ell \ll 1$, this reveals the decoupling case to lie between the generic and scale-invariant cases, with $\kappa^2 \langle \mathcal{Y} \rangle_v$ suppressed by a single power of the vortex size in KK units, as might be expected given that the leading ϕ -dependence of the point brane action arises within the single-derivative localized-flux term of the point-brane action.

These estimates lead to the following expectations for near-brane bulk derivatives.

As always, B' near the sources is dominated by the energy density, with

$$1 - \lim_{\hat{r}_v \rightarrow 0} [B'W^d]_{\rho_v} \simeq \frac{\kappa^2}{2\pi} \langle \varrho_{\text{loc}} \rangle_v, \quad (4.181)$$

while (by contrast) the near-source derivatives ϕ' and W' are KK suppressed

$$\lim_{\hat{r}_v \rightarrow 0} [BW^d \phi']_{\rho_v} \simeq \frac{\kappa^2}{2\pi} \langle \mathcal{Y} \rangle_v \simeq \mp (r+1) 2n_v \varepsilon \kappa v \left(\frac{\hat{r}_v}{\ell} \right), \quad (4.182)$$

and

$$\lim_{\hat{r}_v \rightarrow 0} [B(W^d)']_{\rho_v} \simeq -(r+1)^2 (2n_v \varepsilon \kappa v)^2 \left(\frac{\hat{r}_v}{\ell} \right)^2. \quad (4.183)$$

Because it is suppressed by two powers of \hat{r}_v/ℓ this last expression is of the same size as terms we have neglected, such as second-derivative terms in the brane action, so we should not trust its precise numerical prefactor.

The d -dimensional curvature in this case can be written similarly to give $\check{R} = 2\kappa_d^2 \langle \mathcal{Y} \rangle_{\text{tot}}$, whose size corresponds to an effective vacuum energy, U_{eff} , of order

$$U_{\text{eff}} \approx \langle \mathcal{Y} \rangle_{\text{tot}} \simeq \mp 4\pi n_v \varepsilon \kappa v \left(\frac{\hat{r}_v}{\ell} \right) \frac{1}{\kappa^2}. \quad (4.184)$$

Strictly speaking, this expression is somewhat self-referential because it is a function of the would-be dilaton zero-mode, φ , whose value must be obtained by minimizing a quantity like (4.184). Although this generically leads to runaway behaviour in the scale-invariant case (with $U_{\text{eff}} \propto e^{2\varphi}$ implying the minimum occurs for $\varphi \rightarrow -\infty$), the same need not be true when $r \neq -1$ since the vortex action then breaks scale invariance and so changes the functional form of $U_{\text{eff}}(\phi)$.

What the above expressions leave open is what this precise form is, since this

requires a more detailed evaluation of the ϕ -dependence of all quantities that has been done here, including all of the ϕ -dependence implicit within $\langle \mathcal{X} \rangle_{\text{tot}}$, and not just the near-source part $\langle \mathcal{X}_{\text{loc}} \rangle_v$ estimated here. Although this takes us beyond the scope of this (already long) chapter, we do describe such a more detailed calculation in the next chapter, including a description of the 4D perspective obtained by integrating out the extra dimensions entirely.

4.6 Discussion

This paper's aim has been to carefully determine the way in which codimension-two objects back-react on their environment, for a specific UV completion which captures the physics of brane-localized flux coupled to the bulk dilaton. To this end, we have determined the way in which the microscopic details of the vortex get encoded in IR observables, such as the size of the transverse dimensions and the on-brane curvature.

Quite generally, we find that the breaking of scale invariance in the vortex sector leads to a nonzero on-brane curvature and — for the particular ‘decoupling’ choice of couplings $p = -q = 2r + 1$ — we find a parametric suppression in the value of the on-brane curvature, by a single power of the small ratio \hat{r}_v/ℓ . What remains to be determined is whether reasonable choices for vortex-dilaton couplings can stabilize the extra dimensions with a sufficiently large hierarchy, ℓ/\hat{r}_v , to profit from this suppression. We explore this in more detail in the next chapter, where we find such a stabilization to be possible.

This work leaves many open questions. One such asks what the effective description is for the dilaton dynamics in the theory below the KK scale within which the

extra dimensions are integrated out. In particular how does such a theory learn about flux quantization, which we've seen is central to the dynamics that stabilizes the extra dimensions. We also address this question in the next chapter.

Another open direction asks whether vortex configurations can be contrived that break supersymmetry in a *distributed* way (as proposed in [27], for example, with some supersymmetry unbroken everywhere locally but with all supersymmetries broken once the entire transverse space is taken into account). One might hope to construct a locally half-BPS UV vortex — using, *eg*, a configuration of hyperscalars as in [28] — and embed two (or more) of them in the bulk in such a way that leaves supersymmetry completely broken globally.

We leave these questions for future work.

Acknowledgements

We acknowledge Florian Niedermann and Robert Schneider for collaborations at early stages of this work as well as discussions about this paper and [4] while they were in preparation. We thank Ana Achucarro, Asimina Arvanitaki, Savas Dimopoulos, Gregory Gabadadze, Ruth Gregory, Mark Hindmarsh, Stefan Hoffmann, Leo van Nierop, Massimo Porrati, Fernando Quevedo, and Itay Yavin for useful discussions about self-tuning and UV issues associated with brane-localized flux.

Bibliography

- [1] H. B. Nielsen and P. Olesen, “Vortex Line Models for Dual Strings,” Nucl. Phys. B **61**, 45 (1973).
- [2] For reviews see, for example:
A. Vilenkin and E. P. S. Shellard, “Cosmic Strings and other Topological Defects,” Cambridge University Press, 1994;
M. B. Hindmarsh and T. W. B. Kibble, “Cosmic strings,” Rept. Prog. Phys. **58**, 477 (1995) [hep-ph/9411342].
- [3] T. Vachaspati, “Dark Strings,” Phys. Rev. D **80**, 063502 (2009) [arXiv:0902.1764 [hep-ph]];
- B. Hartmann and F. Arbabzadah, “Cosmic strings interacting with dark strings,” JHEP **0907**, 068 (2009) [arXiv:0904.4591 [hep-th]];
- J. M. Hyde, A. J. Long and T. Vachaspati, “Dark Strings and their Couplings to the Standard Model,” Phys. Rev. D **89**, no. 6, 065031 (2014) [arXiv:1312.4573 [hep-ph]];
- “Cosmic Strings in Hidden Sectors: 1. Radiation of Standard Model Particles,” JCAP **1409** (2014) 09, 030 [arXiv:1405.7679 [hep-ph]].
- P. Arias and F. A. Schaposnik, “Vortex solutions of an Abelian Higgs model with visible and hidden sectors,” JHEP **1412**, 011 (2014) [arXiv:1407.2634 [hep-th]];
- H. F. Santana Mota and M. Hindmarsh, “Big-Bang Nucleosynthesis and

- Gamma-Ray Constraints on Cosmic Strings with a large Higgs condensate,” *Phys. Rev. D* **91** (2015) 4, 043001 [arXiv:1407.3599 [hep-ph]];
- [4] C. P. Burgess, R. Diener and M. Williams, “The Gravity of Dark Vortices: Effective Field Theory for Branes and Strings Carrying Localized Flux,” arXiv:1506.08095 [hep-th].
- [5] H. M. Lee and A. Papazoglou, “Supersymmetric codimension-two branes in six-dimensional gauged supergravity,” *JHEP* **0801**, 008 (2008) [arXiv:0710.4319 [hep-th]];
- C. P. Burgess, L. van Nierop, S. Parameswaran, A. Salvio and M. Williams, “Accidental SUSY: Enhanced Bulk Supersymmetry from Brane Back-reaction,” *JHEP* **1302**, 120 (2013) [arXiv:1210.5405 [hep-th]].
- [6] C. P. Burgess and L. van Nierop, “Bulk Axions, Brane Back-reaction and Fluxes,” *JHEP* **1102** (2011) 094 [arXiv:1012.2638 [hep-th]];
- “Large Dimensions and Small Curvatures from Supersymmetric Brane Back-reaction,” *JHEP* **1104**, 078 (2011) [arXiv:1101.0152 [hep-th]].
- [7] Y. Aghababaie, C. P. Burgess, J. M. Cline, H. Firouzjahi, S. L. Parameswaran, F. Quevedo, G. Tasinato and I. Zavala, “Warped brane worlds in six-dimensional supergravity,” *JHEP* **0309**, 037 (2003) [hep-th/0308064].
- [8] Y. Aghababaie, C. P. Burgess, S. L. Parameswaran and F. Quevedo, “Towards a naturally small cosmological constant from branes in 6-D supergravity,” *Nucl. Phys. B* **680** (2004) 389 [hep-th/0304256];
- For reviews see: C. P. Burgess, “Towards a natural theory of dark energy: Supersymmetric large extra dimensions,” *AIP Conf. Proc.* **743** (2005) 417 [hep-th/0411140];
- “Supersymmetric large extra dimensions and the cosmological constant: An Update,” *Annals Phys.* **313** (2004) 283 [hep-th/0402200].
- [9] C.P. Burgess, “The Cosmological Constant Problem: Why it is Hard to Get Dark Energy from Micro-Physics,” in the proceedings of the Les Houches School *Cosmology After Planck*, [arXiv:1309.4133];
- [10] For reviews of the cosmological constant problem from other points of view see:
- S. Weinberg, “The Cosmological Constant Problem,” *Rev. Mod. Phys.*

- 61**, 1 (1989);
- E. Witten, “The Cosmological constant from the viewpoint of string theory,” [hep-ph/0002297];
- J. Polchinski, “The Cosmological Constant and the String Landscape,” [hep-th/0603249];
- T. Banks, “Supersymmetry Breaking and the Cosmological Constant,” Int. J. Mod. Phys. A **29** (2014) 1430010 [arXiv:1402.0828 [hep-th]];
- A. Padilla, “Lectures on the Cosmological Constant Problem,” [arXiv:1502.05296 [hep-th]].
- [11] C. P. Burgess, D. Hoover and G. Tasinato, “UV Caps and Modulus Stabilization for 6D Gauged Chiral Supergravity,” JHEP **0709** (2007) 124 [arXiv:0705.3212 [hep-th]].
- [12] C. P. Burgess, D. Hoover, C. de Rham and G. Tasinato, “Effective Field Theories and Matching for Codimension-2 Branes,” JHEP **0903** (2009) 124 [arXiv:0812.3820 [hep-th]];
- A. Bayntun, C. P. Burgess and L. van Nierop, “Codimension-2 Brane-Bulk Matching: Examples from Six and Ten Dimensions,” New J. Phys. **12** (2010) 075015 [arXiv:0912.3039 [hep-th]].
- [13] R. Diener and C. P. Burgess, “Bulk Stabilization, the Extra-Dimensional Higgs Portal and Missing Energy in Higgs Events,” JHEP **1305** (2013) 078 [arXiv:1302.6486 [hep-ph]].
- [14] For a stabilization mechanism using the competition between brane couplings of a bulk field see
W. D. Goldberger and M. B. Wise, “Modulus stabilization with bulk fields,” Phys. Rev. Lett. **83** (1999) 4922 [hep-ph/9907447].
- [15] W. D. Goldberger and M. B. Wise, “Renormalization group flows for brane couplings,” Phys. Rev. D **65**, 025011 (2002) [hep-th/0104170].
- C. de Rham, “The Effective field theory of codimension-two branes,” JHEP **0801**, 060 (2008) [arXiv:0707.0884 [hep-th]].
- [16] S. Weinberg, *Gravitation and Cosmology*, Wiley 1973.

- [17] C. W. Misner, J. A. Wheeler and K. S. Thorne, *Gravitation*, W. H. Freeman & Company 1973.
- [18] H. Nishino and E. Sezgin, *Phys. Lett.* **144B** (1984) 187; “The Complete N=2, D = 6 Supergravity With Matter And Yang-Mills Couplings,” *Nucl. Phys.* **B278** (1986) 353;
- S. Randjbar-Daemi, A. Salam, E. Sezgin and J. Strathdee, “An Anomaly Free Model in Six-Dimensions” *Phys. Lett.* **B151** (1985) 351.
- [19] A. J. Tolley, C. P. Burgess, D. Hoover and Y. Aghababaie, “Bulk singularities and the effective cosmological constant for higher co-dimension branes,” *JHEP* **0603** (2006) 091 [arXiv:hep-th/0512218].
- [20] E. M. Lifshitz and I. M. Khalatnikov, *Adv. Phy.* **12**, 185 (1963);
- V. A. Belinsky, I. M. Khalatnikov and E. M. Lifshitz, *Adv. Phys.* **19**, 525 (1970).
- V. A. Belinsky, I. M. Khalatnikov, *Sov. Phys. JETP* **36**, 591 (1973).
- [21] E. Kasner, *Trans. Am. Math. Soc.*, **27**, 155-162 (1925).
- [22] G. W. Gibbons, R. Guven and C. N. Pope, “3-branes and uniqueness of the Salam-Sezgin vacuum,” *Phys. Lett. B* **595** (2004) 498 [hep-th/0307238];
- C. P. Burgess, F. Quevedo, G. Tasinato and I. Zavala, “General axisymmetric solutions and self-tuning in 6D chiral gauged supergravity,” *JHEP* **0411** (2004) 069 [hep-th/0408109];
- [23] C. P. Burgess, L. van Nierop and M. Williams, “Distributed SUSY breaking: dark energy, Newton’s law and the LHC,” *JHEP* **1407**, 034 (2014) [arXiv:1311.3911 [hep-th]].
- [24] A. Vilenkin, “Gravitational Field of Vacuum Domain Walls and Strings,” *Phys. Rev. D* **23**, 852 (1981);
- D. Garfinkle, “General Relativistic Strings,” *Phys. Rev. D* **32**, 1323 (1985);
- P. Laguna-Castillo and R. A. Matzner, “Coupled Field Solutions for U(1) Gauge Cosmic Strings,” *Phys. Rev. D* **36**, 3663 (1987);
- R. Gregory, “Gravitational Stability of Local Strings,” *Phys. Rev. Lett.* **59** (1987) 740;

- “Effective Action for a Cosmic String,” *Phys. Lett. B* **206** (1988) 199;
- R. Gregory, D. Haws and D. Garfinkle, “The Dynamics of Domain Walls and Strings,” *Phys. Rev. D* **42** (1990) 343.
- [25] A. Salam and E. Sezgin, “Chiral Compactification On Minkowski $\times S^2$ Of N=2 Einstein-Maxwell Supergravity In Six-Dimensions,” *Phys. Lett. B* **147** (1984) 47.
- [26] B. Holdom, “Two U(1)’s and Epsilon Charge Shifts,” *Phys. Lett. B* **166**, 196 (1986).
- [27] C. P. Burgess, R. C. Myers and F. Quevedo, “A Naturally small cosmological constant on the brane?,” *Phys. Lett. B* **495**, 384 (2000) [arXiv:hep-th/9911164].
- [28] S. L. Parameswaran, G. Tasinato and I. Zavala, “The 6D SuperSwirl,” *Nucl. Phys. B* **737**, 49 (2006) [hep-th/0509061].

Chapter 5

Effective description of dilaton capture

This chapter is a condensed version of the following paper

C. P. Burgess, R. Diener and M. Williams, “Self-Tuning at Large (Distances): 4D Description of Runaway Dilaton Capture,” JHEP 1510 177 (2015), arXiv:1509.04209

Most of this chapter’s content is taken verbatim from this reference. However, some notation was modified, and the wording was revised to better fit within this thesis. Part of the paper’s discussion was also omitted for clarity, brevity and to avoid redundancies within this thesis.

This chapter completes the study of scale breaking branes in a scale invariant, 6D bulk by constructing the 4D effective theory for such systems at scales below the Kaluza-Klein scale. At low energies, the field content of the theory includes the would-be zero mode associated with bulk scale invariance and the 4D metric field. The

effective potential for the zero mode is calculated as a function of brane properties, and the minimization of the potential determines the 4D curvature and the size of the extra dimensions in a way that is shown to be consistent with the 6D theory.

The effective potential for the zero mode has a special form $U(\varphi) = e^{2\varphi}F(\varphi)$ which is consistent with there being a runaway potential for scale invariant systems, and this allows for a general study. Branes that are perturbatively close to scale invariant are identified as giving naturally suppressed curvatures, with the suppression of the curvature relative to the Standard Model scale being controlled by the branes' deviation from scale invariance. When concerns about small curvatures are discarded, then a number of ways to stabilize the zero mode are identified such that the extra dimensions are exponentially large relative to underlying physics scales. Having both quantities at the phenomenologically preferred values remains a challenge, but the best case scenarios, future prospects and underlying concerns are all discussed.

5.1 Introduction

In this paper we study the very low-energy dynamics of six-dimensional supergravity interacting with two non-supersymmetric, space-filling, codimension-two branes. Our interest is in situations where the back-reaction of the branes breaks a degeneracy of the bulk system and lifts an otherwise flat direction. As in two earlier papers [1, 2] we focus on systems for which the interactions are weak enough to ensure that the energetics lifting this flat direction are amenable to understanding in the effective 4D theory below the Kaluza-Klein (KK) scale. We compute this low-energy potential explicitly within the classical limit, to identify how it depends on the various parameters describing the underlying UV completion.

To this end we study a specific system of branes interacting through the bosonic fields of chiral, gauged six-dimensional supergravity [3]. We use this specific theory for two reasons. First, it is known to admit explicit stabilized extra-dimensional solutions — both without branes [4] and with them [5, 6, 7, 8, 9, 10, 11] — for which gravity competes with flux quantization and brane back-reaction to stabilize the extra dimensions. This makes it a good laboratory for studying in detail how interactions amongst branes and fluxes can compete to shape the extra dimensions while going beyond the restriction to one extra dimension of the well-explored 5D Randall-Sundrum models [12]. In this motivation one wishes to know whether or not it is possible to achieve dynamically stable extra dimensions that are exponentially large functions of the not-too-large parameters of the fundamental theory.

Second, this system was proposed some time ago [5, 13, 14] (and again recently in more detail [15]) as a concrete laboratory in which to explore whether the interplay between supersymmetry and extra dimensions can help resolve the cosmological constant problem [14, 16], essentially by having the quantum zero-point fluctuations of the particles we see curve the extra dimensions instead of the four large dimensions explored by cosmologists. In the simplest picture ordinary particles are localized on the 4D branes and so their quantum fluctuations contribute to the brane tensions, while many of the simplest brane solutions [5, 6] are flat for any value of the tension. In this motivation the issue is to understand how (and whether) the 4D theory captures this special feature of the extra-dimensional picture, and thereby to understand how robustly (and whether) the effective 4D curvature can be suppressed relative to naive expectations.

In the simplest model [4], flux quantization and gravity drive the system to a supersymmetric ground state with a single flat direction corresponding to a breathing mode with origins in an accidental scaling symmetry generic to the classical supergravity field equations. Brane back-reaction then typically lifts this degeneracy (and generically breaks supersymmetry) leading to a vacuum configuration whose properties involve a competition between inter-brane forces and flux quantization. Because the energy cost of this lifting is often smaller than the Kaluza-Klein (KK) scale it can be understood purely within the low-energy 4D theory, and a puzzle for these systems has been how this low-energy theory ‘knows’ about extra-dimensional flux quantization (as it must if it is to properly reproduce the competition with other effects in the 6D UV completion).

An important part of this story is the ability of the branes to carry localized amounts of the stabilizing external magnetic flux [17],

$$S_{BLF} \propto \int \mathcal{A}(\phi) \star F, \quad (5.1)$$

where the integral is over the 4D brane world-sheet $\star F$ is the 6D Hodge dual of the 2-form Maxwell field-strength and \mathcal{A} is a dilaton-dependent coefficient. This is important because the system often responds to perturbations by moving flux onto and off of the branes, since it is energetically inexpensive to change the value of ϕ . We use the effective theory that captures the low-energy dynamics of this flux in the higher-dimensional theory — developed in the previous chapters — to work out the effective 4D description provided here, identifying in particular the precise form of the scalar potential that governs the energetics of vacuum determination.

We find the following main results.

- *4D effective description:* We describe the low-energy 4D effective theory appropriate for physics below the Kaluza-Klein (KK) scale, within which the extra dimensions themselves are too small to be resolved, and show how this reproduces the dynamics of the known cases where the 6D dynamics is explicitly known. We find that the news of flux quantization comes to the low-energy theory by a space-filling 4-form gauge field, $F_{\mu\nu\lambda\rho}$, whose value satisfies general quantization conditions [18, 19] that are ultimately inherited from the higher-dimensional quantization of Maxwell flux.
- *Dynamics of modulus stabilization:* Most trivially we verify in more detail earlier claims [17, 20, 21] that (with two transverse dimensions) brane couplings generically do stabilize the size of the transverse dimensions in supersymmetric models, in a manner similar to Goldberger-Wise stabilization [22] in 5D. They do so because they break the classical scale invariance of the bulk supergravity that prevents the bulk from stabilizing on its own (through *eg* flux stabilization).
- *Exponentially large dimensions:* We show that simple choices for brane-bulk couplings allow the extra dimensions to be stabilized at a size, ℓ , that is large relative to other microscopic scales, r_B , exponentially¹ in the parameters of the underlying theory — *i.e.* $\ell^2/r_B^2 = e^{-\varphi}$, so ℓ/r_B can be enormous if φ is only moderately large, say $\mathcal{O}(10)$, and negative. This presents a natural way to generate a hierarchy between the electroweak scale and the higher dimensional gravity scale.

¹This echoes a similar claim of [17] but fixes an error made there (see next bullet point) and provides a precise 4D formulation of the mechanism.

- *Connection between brane-dilaton couplings and curvature:* As has been known for some time [23] there is a strong connection between the strength of brane-dilaton couplings and on-brane curvatures, with vanishing brane-dilaton couplings implying vanishing on-brane curvatures. More recently [2] — see also [24] — it was found that the absence of dilaton couplings is *not* as straightforward as demanding dilaton-independence of the brane tension and BLF coefficient, $\mathcal{A}(\phi)$, of (5.1), due to the necessity to hold fixed the Maxwell field far from the brane, rather than at the brane position, when deriving the dilaton dependence of the brane. Complete dilaton-independence of the brane action instead turns out to be equivalent to the condition for scale-invariance, despite the presence of the metrics in the Hodge dual of (5.1). Our 4D potential allows us to compute the subdominant size of the curvature as explicit functions of the deviations from scale-invariance, and verify that they reproduce the curvatures found directly within the 6D UV completion.
- *Low-energy on-brane curvature:* We find that the dynamics of modulus stabilization usually also curves the dimensions along the brane world-sheets, and generically does so by an amount commensurate with their tension, $R \sim G_N \tilde{T}$, where \tilde{T} is the brane tension (defined more precisely below) and G_N is Newton's constant for observers living on the brane. For specific parameter regimes the on-brane curvature can be less than this however, being parametrically suppressed relative to the tension.

In some cases the suppression of R in the near-scale-invariant limit can be regarded as a consequence of the generic runaway present for scale-invariant potentials: weak scale-breaking tends to place minima out at large fields for which

the potential is relatively small. In this way it potentially converts Weinberg's no-go theorem [25] from a bug into a feature.

Although our personal motivation for studying this system is because of its potential application [5, 14] to the cosmological constant problem [14, 16, 25], the ability to stabilize two transverse dimensions with exponentially large size given only moderately large input parameters potentially puts large-extra-dimensional models [26] on a similar footing as warped Randall-Sundrum models [12].

A road map

We organize our discussion as follows. The following section, §5.2, describes the 6D system whose 4D physics is of interest, summarizing the main results explained in more detail in the previous chapters. The purposes of doing so is to show how properties of the bulk physics (such as extra-dimensional size and on-brane curvature) are constrained by the field equations, which controls the extent to which they depend on the properties of any source branes. This provides the tools required for matching to the 4D effective theory, relevant to energies below the KK scale. This matching is itself described in §5.3, which determines the 4D effective theory required to reproduce the dynamics of the full higher-dimensional theory.

Next, §5.4 uses this effective description to explore the implications of several choices of parameters within a class that minimize the couplings between the brane and the bulk dilaton while still breaking scale invariance. In particular we compute here the classical predictions for the modulus mass and vev (and so also the size of the extra dimensions) as well as the on-brane curvature at the minimum. We find examples that produce exponentially large dimensions and with parametrically suppressed

curvature in the on-brane directions. Then, §5.4 offers a brief discussion about the robustness of the various examples, and surveys some ways that quantum corrections might be expected to complicate the picture. Our conclusions are summarized in a final discussion section, §5.5.

5.2 The higher-dimensional system

We here briefly outline the action and field equations of the UV theory whose low-energy description we wish to capture: the system studied in the previous chapter, consisting of a bulk Einstein-Maxwell-Dilaton sector that arises as the bosonic part of six-dimensional supergravity, plus two space-filling 3-branes situated within two transverse extra dimensions.

5.2.1 The Bulk

The bulk action is a subset of the action for Nishino-Sezgin supergravity [?] given by

$$\begin{aligned}
 S_B &= - \int d^6x \sqrt{-g} \left[\frac{1}{2\kappa^2} g^{MN} \left(\mathcal{R}_{MN} + \partial_M \phi \partial_N \phi \right) + \frac{2g_R^2}{\kappa^4} e^\phi + \frac{1}{4} e^{-\phi} A_{MN} A^{MN} \right] \\
 &=: - \int d^6x \sqrt{-g} \left(L_{EH} + L_\phi + L_A \right), \tag{5.2}
 \end{aligned}$$

where² κ denotes the 6D gravitational coupling and \mathcal{R}_{MN} denotes the 6D Ricci tensor while $A_{MN} = \partial_M A_N - \partial_N A_M$ is a gauge field strength for a specific $U(1)_R$ symmetry that does not commute with 6D supersymmetry (with gauge coupling g_R). The second

²We (still) use Weinberg's curvature conventions [27], which differ from those of MTW [28] only by an overall sign in the definition of the Riemann tensor.

line sets up notation for the Einstein-Hilbert, scalar and gauge parts of the action in terms of the items in the line above.

Notice S_B scales homogeneously, $S_B \rightarrow s^2 S_B$ under the rigid rescalings $g_{MN} \rightarrow s g_{MN}$ and $e^\phi \rightarrow s^{-1} e^\phi$, making this a symmetry of the classical equations of motion. Besides ensuring classical scale invariance this also shows that it is the quantity $e^{2\phi}$ that plays the role of \hbar in counting loops within the bulk part of the theory.

The bulk system enjoys a second useful scaling property: physical properties depend only on g_R through a field-dependent combination $\hat{g}_R(\phi) = g_R e^{\phi/2}$. The value $\phi = 0$ can always be chosen as the present-day vacuum provided the values of g_R is chosen appropriately.

For many purposes it is useful to work with a 4-form field strength, F_{MNPQ} that is dual to A_{MN} , in terms of which the bulk action can be written

$$\begin{aligned} S_B &= - \int d^6x \sqrt{-g} \left[\frac{1}{2\kappa^2} g^{MN} (\mathcal{R}_{MN} + (\partial\phi)^2) + \frac{2g_R^2}{\kappa^4} e^\phi + \frac{1}{2 \cdot 4!} e^\phi F_{MNPQ}^2 + L_{st} \right] \\ &=: - \int d^6x \sqrt{-g} (L_{EH} + L_\phi + L_F + L_{st}), \end{aligned} \quad (5.3)$$

where L_{st} is a surface term that emerges when performing the duality transformation from $A_{(2)}$ to $F_{(4)} = dV_{(3)}$,

$$\mathcal{L}_{st} := \sqrt{-g} L_{st} = \frac{1}{3!} \partial_M \left(\sqrt{-g} \epsilon^{MNPQRT} V_{NPQ} A_{RT} \right). \quad (5.4)$$

5.2.2 The Branes

We take the brane action to include the first two terms in a derivative expansion³

$$\begin{aligned}
 S_{\text{eff}} &= - \sum_{\nu} \int_{x=z_{\nu}(\sigma)} d^4\sigma \sqrt{-\gamma} \left[T_{\nu}(\phi) - \frac{1}{4!} \zeta_{\nu}(\phi) \varepsilon^{\mu\nu\lambda\rho} F_{\mu\nu\lambda\rho} \right] \\
 &=: \sum_{\nu} \int_{z_{\nu}} d^4\sigma \left(\mathcal{L}_{\nu}^T + \mathcal{L}_{\nu}^{\zeta} \right) = \sum_{\nu} S_{\nu},
 \end{aligned} \tag{5.5}$$

where the tension term, \mathcal{L}_{ν}^T , is built from the induced metric $\gamma_{\mu\nu}(\sigma) = g_{MN} \partial_{\mu} z_{\nu}^M \partial_{\nu} z_{\nu}^N$ at the position of the brane (with $z_{\nu}^M(\sigma)$ denoting the brane position fields). Despite its appearances, the localized-flux term, $\mathcal{L}_{\nu}^{\zeta}$, does not depend on this metric because the explicit dependence cancels with that hidden within the totally antisymmetric 4-tensor, $\varepsilon^{\mu\nu\lambda\rho}$, associated with the metric. Since it turns out the branes repel one another their position modes are massive enough to be integrated out in the 4D effective theory, and so we simply assume static branes and choose coordinates so that they are located at opposite ends of the transverse extra dimensions.

It is also possible to frame the branes using a more UV-complete theory for which they arise as classical vortex-like solutions (as is done explicitly in previous chapters), though we do not need the details of this explicit extension in what follows. Below, we simply reiterate the main results, entirely within the contexts of branes.

5.2.3 Brane stress energies

The integrated localized contributions to the stress energy and to \mathcal{Y} can be written as sums over each brane of known functions of the brane tension, T_{ν} , and localized

³The quantity T here is denoted \tilde{T} in previous chapters.

flux, ζ_v . For instance, the energy density is given by

$$\langle \varrho_{\text{loc}} \rangle = \sum_v \varrho_v = \sum_v W_v^4 T_v, \quad (5.6)$$

where W_v is the metric warp-factor evaluated at the corresponding brane position and we reuse the notation

$$\langle \dots \rangle_{\text{tot}} := \frac{1}{\sqrt{-\bar{g}}} \int d^2y \sqrt{-g} (\dots) = 2\pi \int d\rho B W^4 (\dots). \quad (5.7)$$

It may happen that W_v — or ϕ_v , if $T_v = T_v(\phi_v)$ — vanishes or diverges at the brane positions, but if so eq. (5.6) shows this can be absorbed into a renormalization of T_v [21, 29], such as would be expected physically if the value of T_v were to be inferred from a measurement of (say) a defect angle, whose size is governed by the physical energy ϱ_v . This is addressed in more detail in Appendix C and the following chapter, both of which give explicit examples of brane renormalization.

Similarly the scale-breaking brane contributions to the dilaton equation are given by

$$\langle \mathcal{Y} \rangle_{\text{tot}} = \sum_v \mathcal{Y}_v, \quad (5.8)$$

with

$$\mathcal{Y}_v = \frac{W_v^4}{2\pi} \left(T'_v(\phi) - \frac{1}{4!} \zeta'_v(\phi) \epsilon^{\mu\nu\lambda\rho} F_{\mu\nu\lambda\rho} \right) = - \sum_v \frac{1}{2\pi\sqrt{-\bar{g}}} \left(\frac{\delta S_v}{\delta \phi} \right). \quad (5.9)$$

The brane does not break scale invariance if both the tension and localized flux are independent of ϕ : $T'_v = \zeta'_v = 0$. Again, any singularities associated with the vanishing or diverging of fields near the branes can be renormalized into the bulk-brane effective couplings.

The off-brane components of the brane stress-energy are somewhat more subtle to obtain since the dependence of the brane action on the extra-dimensional metric is often only given implicitly. In general, however, stress-energy conservation and the equilibrium balancing of stress-energy within any localized brane ensures these are given by

$$\langle \mathcal{Z}_{\text{loc}} \rangle_{\text{tot}} = \sum_v \mathcal{Z}_v \quad \text{and} \quad \langle \mathcal{X}_{\text{loc}} \rangle_{\text{tot}} = \sum_v \mathcal{X}_v, \quad (5.10)$$

with

$$\kappa^2 \mathcal{Z}_v \simeq \kappa^2 \mathcal{X}_v \simeq -\frac{\kappa^4 \mathcal{Y}_v^2}{4\pi}, \quad (5.11)$$

where the approximation is valid up to terms that are suppressed by at least two powers of the assumed small ratio between the size of the brane and the size of the bulk.

5.2.4 Flux quantization

The symmetry ansatz requires the 4-form field to satisfy

$$F_{\mu\nu\lambda\rho} = Q \epsilon_{\mu\nu\lambda\rho}, \quad (5.12)$$

with Q independent of the 4 space-filling coordinates. The Bianchi identity, $dF = 0$, then implies Q also cannot depend on the transverse two coordinates and so is a constant. This constant is the integration constant we would have found if we had explicitly solved the Maxwell field equation for A_{mn} .

Recall that the value of Q is fixed by flux quantization as follows

$$Q = \frac{1}{\widehat{\Omega}_{-4}} \left[\frac{2\pi N}{g_R} + \sum_v \zeta_v(\phi_v) \right], \quad (5.13)$$

where N is the integer measuring the total flux of A_{MN} through the transverse two dimensions, and ζ_v is the parameter in (5.5) that measures the amount of this flux that is localized onto the position of the brane. Here, ϕ_v denotes the value of the dilaton at this brane position, and

$$\widehat{\Omega}_k := \int d^2y \sqrt{g_2} W^k e^\phi = \int d^2y \sqrt{\widehat{g}_2} W^k, \quad (5.14)$$

represents the integral of W^k over the transverse dimensions using the scale-invariant metric, $\widehat{g}_{mn} := e^\phi g_{mn}$, so the particular case $k = 0$ gives the extra-dimensional volume, $\widehat{\Omega} := \widehat{\Omega}_0$, as measured by this metric.

5.2.5 Boundary conditions

The near source behaviour of the bulk fields is controlled by the properties of the brane sources, and this manifests in boundary conditions that must be satisfied by the bulk fields as they approach the branes. In practice, these boundary conditions can be derived by integrating the field equations over the localized region containing the brane source, as described earlier in more detail. Performing this operation on the dilaton field equation (4.71) in chapter 4, for example, gives the following boundary conditions for the dilaton at the positions of the branes

$$B_v W_v^4 \phi'_v = \frac{\kappa^2}{2\pi} (\mathcal{X}_v + \mathcal{Y}_v) \simeq \frac{\kappa^2 \mathcal{Y}_v}{2\pi}, \quad (5.15)$$

where the approximation uses (5.11) to identify \mathcal{Y}_v as the leading contribution to this boundary condition. Similarly,

$$1 - W_v^4 B'_v = \frac{\kappa^2}{2\pi} \left(\varrho_v - \mathcal{Z}_v - \frac{1}{2} \mathcal{X}_v \right) \simeq \frac{\kappa^2}{2\pi} \varrho_v = \frac{\kappa^2 W_v^4 T_v}{2\pi}, \quad (5.16)$$

where the suppression of \mathcal{X}_v and \mathcal{Z}_v implies they are subdominant to the energy density $\varrho_v = W_v^4 T_v$. Lastly, the boundary condition for the warping in the metric is given by

$$B_v (W_v^4)' = -\frac{\kappa^2 \mathcal{X}_v}{\pi}. \quad (5.17)$$

Here and above, a v subscript on a bulk field (or its derivative) denotes that this quantity is evaluated at the brane position $y = y_v$.

5.2.6 Control of approximations

Because we explore classical behaviour it is important to specify its domain of validity. The fundamental parameters of the problem are the gravitational constant, κ ; the gauge coupling, $\hat{g}_R(\varphi) = g_R e^{\varphi/2}$; and the size of the brane tensions, T_v , and flux-localization parameters, ζ_v .

In the exact, scale invariant solutions of Appendix C.1, the size of the transverse dimensions, ℓ , can be written in terms of parameters of the lagrangian and the ambient value of dilaton, φ , as follows

$$\ell = (\kappa/2g_R) e^{-\varphi/2} = \kappa/2\hat{g}_R. \quad (5.18)$$

In these solutions, the flux integration constant introduced above is given by $Q =$

$2g_R/\kappa^2$ and we use this as a benchmark value when making various estimates.

Weak gravitational response to the energy density of the brane requires $\kappa^2 T_v \ll 1$, and this ensures physical observables such as defect angles are small. Similarly, the response to localized flux is controlled by $\kappa^2 Q\zeta' \sim g_R \zeta'$ and so requires $g_R \zeta' \ll 1$.

Since our interest is in the regime where the intrinsic brane width is much smaller than the transverse dimensions we assume throughout $\ell \gg \hat{r}_v$ where ℓ (\hat{r}_v) is a measure of the extra-dimensional (brane) size. This is accomplished if

$$\hat{r}_v/\ell \sim (\hat{r}_v g_R/\kappa) e^{\varphi/2} \ll 1, \quad (5.19)$$

which can usually be ensured by requiring

$$e^{\varphi} \ll 1, \quad (5.20)$$

although we discuss below an example where the brane size also depends on the value of the dilaton, thus complicating this argument.

Finally, in supergravity, semiclassical reasoning also depends on φ because it is $e^{2\varphi}$ that counts loops in the bulk theory. Consequently we also require $e^{\varphi} \ll 1$ in order to work semiclassically.

5.2.7 Integral relations

From the point of view of the low-energy theory, it is the field equations integrated over the extra dimensions that carry the most useful information.

Integrating the dilaton field equation, (4.71), over the entire compact transverse

dimension gives

$$\langle \mathcal{X} + \mathcal{Y} \rangle = 0. \quad (5.21)$$

Since integration over the transverse space can be regarded as projecting the field equations onto the zero mode in these directions, (5.21) can be interpreted as the equation that determines the value of the dilaton zero-mode and must agree with what is found by varying the potential of the effective 4D theory obtained in later sections. In the absence of the sources this zero mode is an exact flat direction of the classical equations associated with the scale invariance of the bulk field equations and the localized contribution to (5.21) expresses how this flat direction becomes fixed when the sources are not scale-invariant.

Integrating the trace-reversed Einstein equation over the entire transverse space leads to

$$\left\langle \varrho - \mathcal{Z} - \frac{\mathcal{X}}{2} \right\rangle = 0, \quad (5.22)$$

and

$$\check{R} \langle W^{-2} \rangle = -2\kappa^2 \langle \mathcal{X} \rangle = -4\kappa^2 \langle \varrho - \mathcal{Z} \rangle, \quad (5.23)$$

where the second equality uses (5.22). This again emphasizes that it is the integrated *off-source* stress-energy, $\langle \mathcal{X} \rangle$, that ultimately controls the size of the on-source curvature [23] for generic ϕ , and that this receives contributions coming from both bulk and brane-localized contributions to the integral. By contrast, using (5.21) to evaluate $\langle \mathcal{X} \rangle$ — at the specific value of the would-be zero-mode of ϕ that minimizes its potential — gives a result for the curvature that depends only on brane properties:

$$\check{R} \langle W^{-2} \rangle = 2\kappa^2 \langle \mathcal{Y} \rangle. \quad (5.24)$$

As we see below, the 6D coupling, κ , is related to its 4D counterpart, κ_4 , by

$$\frac{1}{\kappa_4^2} = \frac{\langle W^{-2} \rangle}{\kappa^2}, \quad (5.25)$$

once evaluated at the minimum of the potential for the would-be zero-mode. So (5.24) shows that the curvature \check{R} has a size that is equivalent to what would be obtained by a 4D cosmological constant, U_* , of size

$$U_* = \frac{1}{2} \langle \mathcal{X} \rangle = \langle \varrho - \mathcal{Z} \rangle = -\frac{1}{2} \langle \mathcal{Y} \rangle. \quad (5.26)$$

This explicitly relates the size of the potential at its minimum to the size of scale-breaking on the branes.

5.2.8 Orders of magnitude

The previous chapter's investigation of how the bulk solutions depend on the brane parameters in the UV-complete theories show several kinds of bulk response to branes are possible. We reiterate this analysis here, entirely within the language of branes.

Generic case

In the generic situation

$$\kappa^2 \mathcal{Y}_v \sim \kappa^2 T'_v \sim \kappa^2 T_v, \quad (5.27)$$

is of order the generic size of a gravitational field coming from the brane energy density. When this is true, it follows from the brane constraints in (5.11) that

$$\kappa^2 \mathcal{Z}_v \simeq \kappa^2 \mathcal{X}_v \sim \kappa^4 T_v^2, \quad (5.28)$$

and so are suppressed compared to the naive estimate $\kappa^2 T_v$, as noted in the previous chapter. Eq. (5.26) then shows the resulting 4D curvature corresponds to an effective 4D cosmological constant of order

$$U_\star \sim \sum_v \mathcal{Y}_v \sim \sum T_v, \quad (5.29)$$

and so is generically of order the brane tension.

Scale invariant case

In the scale invariant case we have $T'_v = \zeta'_v = 0$ and so the quantities \mathcal{Y}_v vanish. Eq. (5.11) then implies the off-brane components of the brane stress-energies also satisfy

$$\mathcal{Z}_v \simeq \mathcal{X}_v \simeq 0. \quad (5.30)$$

Lastly, the vanishing of \mathcal{Y}_v ensures the same for the 4D curvature:

$$\check{R} = U_\star = 0. \quad (5.31)$$

As we shall see, in the 4D Einstein frame the scalar potential for the dilaton zero-mode, φ , turns out to be proportional to $\langle \mathcal{X} \rangle \propto e^{2\varphi}$, so this vanishing of $\langle \mathcal{X} \rangle$ and \check{R} is achieved by having the zero-mode run away to $e^\varphi \rightarrow 0$ [25].

Decoupling case $T'_v = 0$

An intermediate situation is given by the decoupling choice, for which T_v is ϕ -independent but $\zeta_v(\phi)$ is not. In this case \mathcal{Y} is not exactly zero, but should be suppressed because \mathcal{Y} arises purely from the ϕ -dependence of a derivatively suppressed

term in the brane action

$$\kappa^2 \mathcal{Y}_v \sim \kappa^2 Q \zeta'_v \sim g_R \zeta'_v \sim \left[\frac{\kappa \zeta'_v(\varphi)}{\ell} \right] e^{-\varphi/2}, \quad (5.32)$$

where the last estimate shows how the derivative suppression can be rewritten as a suppression by the size of the extra dimensions. As a consequence we also have suppressions in the off-brane stress-energy components,

$$\kappa^2 \mathcal{Z}_v \sim \kappa^2 \mathcal{X}_v \sim g_R^2 (\zeta'_v)^2 \sim \left[\frac{\kappa \zeta'_v(\varphi)}{\ell} \right]^2 e^{-\varphi}, \quad (5.33)$$

and the effective cosmological constant corresponding to \check{R} satisfies

$$\kappa^2 U_\star \sim g_R \zeta'_v \sim \left[\frac{\kappa \zeta'_v(\varphi_\star)}{\ell} \right] e^{-\varphi_\star/2}. \quad (5.34)$$

Our goal in the next sections is to reproduce these estimates using a more carefully computed potential for the low-energy 4D effective theory, and to determine the value of the zero mode that ultimately controls the size of these estimates.

5.3 EFT below the KK scale

Consider next the viewpoint of a lower-dimensional observer with access only below the KK scale. In particular we address the following puzzle. We know in the full D -dimensional theory that flux quantization plays a crucial role in determining the d -dimensional curvature that would be seen by any observer below the KK scale [17]. (We know this because it determines Q through (5.13), and this then governs the size of $\check{L}_A = -L_F$ appearing in ϱ and \mathcal{X} .) But how is this flux-dependence seen by a

lower-dimensional observer who cannot resolve the extra dimensions?

The field content naively available in the generic case to the lower-dimensional observer is fairly limited: a massless graviton $g_{\mu\nu}$; massless gauge bosons, one arising from the higher-dimensional gauge field, A_μ , and another, B_μ , arising from the metric due to the unbroken axial rotational invariance of the extra dimensions; and the dilaton zero-mode, φ , arising due to classical scale-invariance. Although our tale can be told purely using these fields, our interest in practice is in a bulk coming from higher-dimensional supergravity for which additional light particles also exist.

The low-energy field content available in 6D within Nishino-Sezgin supergravity [?] also includes the ‘model-independent’ axion, a , that is dual to the components $C_{\mu\nu}$ of the bulk Kalb-Ramond field, as well as the harmonic part of the extra-dimensional components of the same field, C_{mn} . Because the supersymmetry breaking scale in the bulk is also the KK scale these do not appear with superpartners as supermultiplets in the 4D theory. One of these fields, C_{mn} , turns out to Higgs the would-be massless gauge boson, A_μ , which then acquires a mass at the KK scale [30].⁴

To understand how flux quantization trickles down to the low-energy EFT it is useful to supplement these fields with the 4-form field, $F_{(4)}$, that is dual to $A_{(2)}$. Although this field has trivial dynamics in the low-energy theory, its constant value knows about flux quantization and so can bring the news about it to the lower-dimensional world.

⁴The full story is a bit more complicated, with Green-Schwarz cancellation [31] of gravitational anomalies in 6D [32] implying that the massless 4D field is really a mixture of the two gauge fields, B_μ and A_μ .

5.3.1 Lower-dimensional action

With these comments in mind we seek that part of the low-energy 4D EFT describing the dynamics of the 4D metric, the dilaton zero mode, $\varphi(x)$, and the 4-form field strength, $F_{\mu\nu\lambda\rho}$. Because of the appearance of the low-energy scalar we distinguish several important metric frames: the 6D Einstein-frame (EF) metric, $g_{\mu\nu}$, in terms of which the UV theory is formulated; the scale-invariant frame $\hat{g}_{\mu\nu} = e^\varphi g_{\mu\nu}$ which does not transform under the classical scaling symmetry of the UV theory; and the 4D Einstein-frame metric, $\tilde{g}_{\mu\nu}$, which must be given by

$$\tilde{g}_{\mu\nu} \propto e^{-\varphi} g_{\mu\nu} = e^{-2\varphi} \hat{g}_{\mu\nu}, \quad (5.35)$$

since this ensures $\tilde{g}_{\mu\nu} \rightarrow s^2 \tilde{g}_{\mu\nu}$ under the scale transformations, as required for the lower-dimensional Einstein-Hilbert term to scale properly.

For subsequent applications it is important to get right the proportionality constant in (5.35). In particular, we want it to be unity in the present-day vacuum, $\varphi = \varphi_*$, which we determine below by minimizing the φ scalar potential. Having $\tilde{g}_{\mu\nu}$ and $g_{\mu\nu}$ differ in normalization amounts to a change of units, and so needlessly complicates the dimensional estimate of the size of terms in the low-energy potential. Consequently we use below the following, more precise, version of (5.35),

$$\tilde{g}_{\mu\nu} = e^{-(\varphi - \varphi_*)} g_{\mu\nu}. \quad (5.36)$$

The most general lagrangian for these fields at the two-derivative level can be

written

$$\begin{aligned} \mathcal{L}_4 = & -\sqrt{-\tilde{g}} \left[\frac{1}{2k_4^2} \tilde{g}^{\mu\nu} \left(\tilde{R}_{\mu\nu} + Z_\varphi(\varphi) \partial_\mu \varphi \partial_\nu \varphi \right) + V_4(\varphi) \right. \\ & \left. + \frac{1}{2 \cdot 4!} Z_F(\varphi) F_{\mu\nu\lambda\rho} \widetilde{F^{\mu\nu\lambda\rho}} - \frac{1}{4!} \xi(\varphi) \tilde{\epsilon}^{\mu\nu\lambda\rho} F_{\mu\nu\lambda\rho} \right] + \mathcal{L}_{st4}, \end{aligned}$$

where tildes on upper indices indicate that they are raised using the inverse metric $\tilde{g}^{\mu\nu}$, and $\tilde{\epsilon}^{\mu\nu\lambda\rho}$ is the appropriate volume tensor built from $\tilde{g}_{\mu\nu}$ (whose nonzero components are $\pm(-\tilde{g})^{-1/2}$). The surface term, \mathcal{L}_{st4} , is given by

$$\mathcal{L}_{st4} := \frac{1}{3!} \partial_\mu \left(\sqrt{-\tilde{g}} Z_F \check{F}^{\mu\nu\lambda\rho} V_{\nu\lambda\rho} \right), \quad (5.37)$$

and is required to the extent there are boundaries (including asymptotic infinity) whose behaviour we wish to track [18]. This last equation uses the definition

$$\check{F}_{\mu\nu\lambda\rho} := F_{\mu\nu\lambda\rho} - \frac{\xi}{Z_F} \tilde{\epsilon}_{\mu\nu\lambda\rho}. \quad (5.38)$$

Notice that the equations of motion for the 3-form gauge potential, $\partial_\mu (\sqrt{-\tilde{g}} Z_F \check{F}^{\mu\nu\lambda\rho}) = 0$, imply that evaluating \mathcal{L}_{st4} at a solution gives

$$\begin{aligned} \left(\mathcal{L}_{st4} \right)_{\text{on-shell}} &= \frac{Z_F}{4!} \sqrt{-\tilde{g}} \check{F}^{\mu\nu\lambda\rho} F_{\mu\nu\lambda\rho} = \frac{Z_F}{4!} \sqrt{-\tilde{g}} F^{\mu\nu\lambda\rho} F_{\mu\nu\lambda\rho} - \frac{\xi}{4!} \sqrt{-\tilde{g}} \tilde{\epsilon}^{\mu\nu\lambda\rho} F_{\mu\nu\lambda\rho} \\ &= -\sqrt{-\tilde{g}} (-2L_F - L_\xi). \end{aligned} \quad (5.39)$$

Combining this with the above, evaluating the gauge part of the 4D action using the

4-form equations of motion therefore gives

$$\left(L_{4\text{form}}\right)_{\text{on-shell}} := L_F + L_\xi + L_{st4} = -L_F. \quad (5.40)$$

5.3.2 Field equations

The field equations obtained from the EF 4D action, \mathcal{L}_4 , are the field equation for the 3-form gauge potential,

$$\partial_\mu \left[\sqrt{-\tilde{g}} \left(Z_F \widetilde{F^{\mu\nu\lambda\rho}} - \xi \tilde{\epsilon}^{\mu\nu\lambda\rho} \right) \right] = 0. \quad (5.41)$$

Writing $F_{\mu\nu\lambda\rho} = f_4 \tilde{\epsilon}_{\mu\nu\lambda\rho}$ shows that f_4 is algebraically fixed in terms of an integration constant, K_4 and couplings in the lagrangian,

$$f_4 = \frac{K_4 + \xi}{Z_F}, \quad (5.42)$$

and because of this $F_{(4)}$ does not describe propagating degrees of freedom. In terms of f_4 we have $L_F = -\frac{1}{2} Z_F f_4^2$, so evaluating the action using (5.40) shows that the influence of the 4-form field is to shift the scalar potential of the remaining scalar-tensor theory to

$$U(\varphi) := V_4(\varphi) - L_F(\varphi) = V_4(\varphi) + \frac{Z_F}{2} f_4^2(\varphi) = V_4(\varphi) + \frac{1}{2Z_F} (K_4 + \xi)^2. \quad (5.43)$$

The Einstein equations similarly are

$$\tilde{R}_{\mu\nu} + Z_\varphi \partial_\mu \varphi \partial_\nu \varphi = -\kappa_4^2 S_{\mu\nu}, \quad (5.44)$$

where $S_{\mu\nu} = T_{\mu\nu} - \frac{1}{2} \tilde{g}^{\lambda\rho} T_{\lambda\rho} \tilde{g}_{\mu\nu}$ with stress tensor

$$T^{\mu\nu} = \frac{Z_F}{3!} \left[F^{\widetilde{\mu\lambda\rho\kappa}} F^{\widetilde{\nu}}{}_{\lambda\rho\kappa} - \frac{1}{8} \tilde{g}^{\mu\nu} \widetilde{F}^2 \right] - V_4 \tilde{g}^{\mu\nu}, \quad (5.45)$$

so

$$S^{\mu\nu} = \frac{Z_F}{3!} \left[F^{\widetilde{\mu\lambda\rho\kappa}} F^{\widetilde{\nu}}{}_{\lambda\rho\kappa} - \frac{3}{8} \tilde{g}^{\mu\nu} \widetilde{F}^2 \right] + V_4 \tilde{g}^{\mu\nu}. \quad (5.46)$$

The traced Einstein equation therefore is

$$\tilde{R} + Z_\varphi \left(\widetilde{\partial\varphi} \right)^2 = \kappa_4^2 \left[\frac{Z_F}{2 \cdot 3!} F^2 - 4V_4 \right] = -4\kappa_4^2 (V_4 - L_F), \quad (5.47)$$

which again shows the effect of the 4-form field is to shift the potential of the scalar field from V_4 to $U = V_4 - L_F$.

Finally, the dilaton equation becomes

$$\begin{aligned} Z_\varphi \tilde{\square}\varphi &= \kappa_4^2 (V'_4 + L'_F + L'_\xi + L'_{st4}) \\ &= \kappa_4^2 (V'_4 - L'_F), \end{aligned} \quad (5.48)$$

where primes here denote derivatives with respect to φ . This is again consistent with the replacement $V_4 \rightarrow U = V_4 - L_F$. In this argument it may come as a surprise that \mathcal{L}_{st4} can contribute at all to the field equations for φ , given that \mathcal{L}_{st4} is a surface term which therefore should not contribute to equations of motion at all. It is indeed true that because \mathcal{L}_{st4} is a surface term it can only contribute to the variation of the action with respect to field variations that are nonzero at the boundaries of spacetime. But when evaluating the φ potential we first evaluate the lagrangian (and so in particular \mathcal{L}_{st4}) at the solution to the $V_{\mu\nu\lambda}$ equation of motion, and this solution necessarily

contributes to the surface terms whenever its field strength satisfies $F_{\mu\nu\lambda\rho} = f_4 \tilde{\epsilon}_{\mu\nu\lambda\rho}$. It is for this reason that \mathcal{L}_{st4} contributes to the variation of the action with respect to φ if f_4 depends on φ and the variation is made *after* $V_{(3)}$ is eliminated as a function of φ . This is why its presence resolves [18] paradoxes that would otherwise arise [33] when handling 4-form fields.

5.3.3 Matching

Next we try to identify the unknown functions of φ in the 4D theory in a way that captures all of the properties of the 6D theory. Since the main focus is on the 4D theory, we adopt in this section (and in the next section) the notation where $g_{\mu\nu}(x)$ (rather than $\check{g}_{\mu\nu}$) denotes just the x^μ -dependent 4D part of the 6D metric, $g_{MN}(x, y)$, *without* the warp factors, $W^2(y)$, in 6D Einstein frame. So (for instance) $\sqrt{-g_6} = \sqrt{-g_4} \sqrt{g_2} W^4 = \sqrt{-g_4} B W^4$.

Form field

We first match the 4-form field, since this is what passes the flux-quantization conditions down to the low-energy theory. The 6D dual Maxwell field equation, integrated over the extra dimensions, for the geometries of interest is

$$\partial_\mu \left\{ \sqrt{-g_4} \left[\int d^2y \left(\frac{B}{W^4} \right) e^\phi F^{\mu\nu\lambda\kappa} - \sum_v \zeta_v \epsilon^{\mu\nu\lambda\kappa} \right] \right\} = 0, \quad (5.49)$$

where warp factors are written explicitly so that 4D indices are raised (and $\epsilon^{\mu\nu\lambda\kappa}$ is built) with the 4D $g^{\mu\nu}$ rather than the 6D version. This is to be compared with its

4D counterpart, derived above in 4D EF,

$$\partial_\mu \left[\sqrt{-\tilde{g}_4} \left(Z_F \widetilde{F^{\mu\nu\lambda\rho}} - \xi \tilde{\epsilon}^{\mu\nu\lambda\rho} \right) \right] = \partial_\mu \left[\sqrt{-g_4} \left(Z_F e^{2(\varphi-\varphi_*)} F^{\mu\nu\lambda\rho} - \xi \epsilon^{\mu\nu\lambda\rho} \right) \right] = 0, \quad (5.50)$$

where the first equality transforms to 6D EF from 4D EF. Equating coefficients gives

$$\widehat{Z}_F := Z_F e^{2(\varphi-\varphi_*)} = \int d^2y \left(\frac{B}{W^4} \right) e^\phi = \widehat{\Omega}_{-4}, \quad (5.51)$$

and

$$\xi(\varphi) = \sum_v \zeta_v(\phi_v) \simeq \sum_v \zeta_v(\varphi). \quad (5.52)$$

In the first equality the dilaton evaluated at the brane positions, $\phi_v = \phi(y_v) = \varphi u_0(y_v)$, is implicitly expressed in terms of the amplitude, φ , of the would-be bulk zero-mode. The second, approximate, equality assumes the zero mode $u_0(y)$ to be y -independent so that $\phi_v = \varphi$ is the same at the position of all branes.

The solution to the 4-form field equation in 4D is given by

$$\widehat{Z}_F F^{\mu\nu\lambda\rho} - \xi \epsilon^{\mu\nu\lambda\rho} = K_4 \epsilon^{\mu\nu\lambda\rho}, \quad (5.53)$$

where K_4 is an integration constant. But in 6D the Bianchi identity of previous chapters also tells us that

$$F_{\mu\nu\lambda\rho} = Q \epsilon_{\mu\nu\lambda\rho}, \quad (5.54)$$

where 6D flux-quantization requires

$$Q = \frac{1}{\widehat{\Omega}_{-4}} \left[\frac{2\pi N}{g_A} - \varepsilon \sum_v e^{(r+1)\phi_v} \left(\frac{2\pi n_b}{e} \right) \right] =: \frac{\mathcal{N} + \xi}{\widehat{Z}_F}, \quad (5.55)$$

with $\mathcal{N} := 2\pi N/g_R$. This determines $K_4 = (\mathcal{N} + \xi) - \xi = \mathcal{N}$ so that

$$F_{\mu\nu\lambda\rho} = \left(\frac{\mathcal{N} + \xi}{\widehat{Z}_F} \right) \epsilon_{\mu\nu\lambda\rho}, \quad (5.56)$$

and so brings the news about flux quantization to the lower-dimensional world [18, 19].

With this choice L_F evaluates in 4D to

$$L_F(\varphi) = \frac{1}{2 \cdot 4!} \widehat{Z}_F F_{\mu\nu\lambda\rho} F^{\mu\nu\lambda\rho} = -\frac{1}{2\widehat{Z}_F} [\mathcal{N} + \xi(\varphi)]^2 = -\frac{1}{2\widehat{\Omega}_{-4}} [\mathcal{N} + \xi(\varphi)]^2. \quad (5.57)$$

Einstein-Hilbert term

The 4D Einstein-Hilbert terms dimensionally reduce in the usual way to give

$$\begin{aligned} \mathcal{L}_4 &= -\frac{1}{2\kappa^2} \sqrt{-g_4} g^{\mu\nu} R_{\mu\nu} \int_{\text{tot}} d^2y \sqrt{g_2} W^2 \\ &= -\frac{1}{2\kappa^2} \sqrt{-g_4} g^{\mu\nu} R_{\mu\nu} e^{-\varphi} \int_{\text{tot}} d^2y \sqrt{\widehat{g}_2} W^2 e^{-\phi+\varphi} \\ &= -\frac{1}{2\kappa^2} e^{-\varphi_*} \sqrt{-\widetilde{g}_4} \widetilde{g}^{\mu\nu} \widetilde{R}_{\mu\nu} \int_{\text{tot}} d^2y \sqrt{\widehat{g}_2} W^2 e^{-\phi+\varphi}, \end{aligned} \quad (5.58)$$

which uses $\sqrt{g_2} = \sqrt{\widehat{g}_2} e^{-\phi}$ to express things in terms of the scale-invariant 2D measure and we absorb the net zero-mode factor, $e^{-\varphi}$ into the metric when transforming to the 4D EF metric: $\widetilde{g}_{\mu\nu} = e^{-\varphi} g_{\mu\nu}$ (with $\partial\varphi$ terms not written, but handled below). Comparing this with the 4D action gives the following φ -independent expression for the 4D gravitational coupling,

$$\frac{1}{\kappa_4^2} = \frac{1}{\kappa^2} e^{-\varphi_*} \int_{\text{tot}} d^2y \sqrt{\widehat{g}_2} W^2 e^{-\phi+\varphi} = \frac{2\pi}{\kappa^2} e^{\varphi-\varphi_*} \int_{\text{tot}} d\rho B W^2 = \frac{1}{\kappa^2} e^{\varphi-\varphi_*} \langle W^{-2} \rangle_{\text{tot}}. \quad (5.59)$$

Earlier sections remarked on the freedom to shift $\phi \rightarrow \phi - \varphi_*$ in the bulk provided one also rescales coupling constants such as $g_R \rightarrow g_{R*} = g_R e^{\varphi_*/2}$. Eq. (5.59) reflects this freedom in the following way. If $\phi = 0$ is chosen so that $g_R^2 \lesssim \kappa$, then $r_B \sim \kappa/g_R$ is not particularly large so having a large transverse space requires $e^{\varphi_*} \ll 1$ so that $\ell = r_B e^{-\varphi_*/2} \gg r_B$. In this case (5.59) shows that it is the explicit factor of $e^{-\varphi_*}$ that makes the 4D Planck mass large compared with the 6D Planck mass. On the other hand if ϕ is shifted so that $\varphi_* \simeq 0$ then we have $g_{R*}^2 \ll \kappa$ and so $\ell^2 \sim r_{B*}^2 \gg \kappa$. In this case (5.59) gives a large 4D Planck mass because of the large integration volume, which is of order ℓ^2 rather than order κ .

Scalar-tensor properties

To determine the scalar potential and kinetic terms we evaluate the 6D actions at the solution of the 2D metric and 4-form equations of motion, but do *not* use the 4D metric or scalar field equations so that these can be kept free. The starting point in 6D is the 2D integral of the 6D EF lagrangian density, which has the form

$$\int_{\text{tot}} d^2y \mathcal{L}_6 = - \int_{\text{tot}} d^2y \sqrt{-g_6} \left[\frac{1}{2\kappa^2} (\mathcal{R}_{(4)} + \mathcal{R}_{(2)}) + L_\phi + L_F + L_{st} \right] + \sum_v \mathcal{L}_v. \quad (5.60)$$

We first evaluate the 4-form field at the solution to its field equations, using a result proven in previous chapters that all the terms containing the gauge fields evaluate to simplify on-shell

$$\left[- \int d^2y \sqrt{-g} (L_F + L_{st}) + \sum_v \mathcal{L}_v^\zeta \right]_{F \text{ eq}} = \int d^2y \sqrt{-g} L_F.$$

Using this in the full action gives

$$\begin{aligned} \int d^2y \left(\mathcal{L}_6 \right)_{F \text{ eq}} &= - \int_{\text{tot}} d^2y \sqrt{-g_6} \left[\frac{1}{2\kappa^2} (\mathcal{R}_{(4)} + \mathcal{R}_{(2)}) + L_\phi - \check{L}_F \right] + \sum_v \mathcal{L}_v^T \\ &= \int d^2y \sqrt{-g_6} \left\{ \frac{1}{2\kappa^2} \left[g^{\mu\nu} (\mathcal{R}_{\mu\nu} + \partial_\mu \phi \partial_\nu \phi) + \mathcal{R}_{(2)} \right] + \varrho \right\}, \end{aligned}$$

where we also split the ϕ kinetic term into its 4D and 2D parts, and use (5.6) with $\varrho = L_\phi - L_F + \varrho_v$ in the second equality. We then eliminate $\mathcal{R}_{(2)}$ using the result derived from (4.76) that

$$\frac{1}{2\kappa^2} \mathcal{R}_{(2)} + \rho = \frac{\mathcal{X}}{2}, \quad (5.61)$$

which can be used to write the 6D action with F and g_{mn} eliminated

$$\frac{1}{\sqrt{-g_4}} \int d^2y \left(\mathcal{L}_6 \right)_{g_2, F \text{ eq}} = - \int d^2y \sqrt{-g_4} B W^4 \left[\frac{1}{2\kappa^2} g^{\mu\nu} (\mathcal{R}_{\mu\nu} + \partial_\mu \phi \partial_\nu \phi) + \frac{\mathcal{X}}{2} \right], \quad (5.62)$$

where $\mathcal{X} = \check{\mathcal{X}}_B + \mathcal{X}_{\text{loc}}$ with $\check{\mathcal{X}}_B = V_B + L_F$ and $\langle \mathcal{X}_{\text{loc}} \rangle = \sum_v \mathcal{X}_v$ given as before. In these expressions the combination $\langle L_F \rangle$ is to be regarded as the function of φ and flux quanta given by (5.57).

These are to be compared with the 4D action evaluated using only the 4-form field equations,

$$\left(\mathcal{L}_4 \right)_{F \text{ eq}} = -\sqrt{-\tilde{g}} \left[\frac{1}{2\kappa_4^2} \tilde{g}^{\mu\nu} (\tilde{R}_{\mu\nu} + Z_\varphi \partial_\mu \varphi \partial_\nu \varphi) + V_4 - L_F \right], \quad (5.63)$$

in which we are also to regard L_F as the 4D φ -dependent combination

$$L_F(\varphi) = \frac{1}{2 \cdot 4!} Z_F e^{2\varphi} F_{\mu\nu\lambda\rho} F^{\mu\nu\lambda\rho} = -\frac{1}{2Z_F} (\mathcal{N} + \xi)^2 e^{-2\varphi} = -\frac{1}{2\hat{\Omega}_{-4}} [\mathcal{N} + \xi(\varphi)]^2. \quad (5.64)$$

The φ kinetic term comes partly from the dimensional reduction of the kinetic term for ϕ and partly from the kinetic term for the radion, ℓ , in the 6D Einstein-Hilbert action [30]. When the additional factors of $\tilde{g}^{\mu\nu}\partial_\mu\varphi\partial_\nu\varphi$ coming from the radion are taken into account, the 6D theory gives $Z_\varphi = 2$.

The remaining terms determine the scalar potential, which we seek in 4D Einstein frame. Comparing the non-kinetic terms of the 4D and 6D theory gives

$$e^{-2(\varphi-\varphi_*)}(V_4 - L_F) = \frac{1}{2}\langle\mathcal{X}\rangle, \quad (5.65)$$

and this can be rewritten in terms of more relevant quantities

$$e^{-2(\varphi-\varphi_*)}U(\varphi) = \frac{1}{2}\left\{\langle V_B\rangle + \sum_v \mathcal{X}_v - \frac{1}{2\hat{\Omega}_{-4}}[\mathcal{N} + \xi(\varphi)]^2\right\}. \quad (5.66)$$

This is the final result for the zero mode potential $U(\varphi)$.

A check on the normalization comes from the 4D Einstein equation which in Einstein frame states $\tilde{R} = -4\kappa_4^2 U$. This agrees with the above given that it implies $U = \frac{1}{2}\langle\mathcal{X}\rangle e^{2(\varphi-\varphi_*)}$ while on the other hand

$$\frac{1}{\kappa^2}\langle\mathcal{R}_{(4)}\rangle = \frac{1}{\kappa^2}R\langle W^{-2}\rangle = \frac{1}{\kappa^2}\tilde{R}\langle W^{-2}\rangle e^{-(\varphi-\varphi_*)} = \frac{1}{\kappa_4^2}\tilde{R}e^{-2(\varphi-\varphi_*)}, \quad (5.67)$$

and the 6D field equations state $\langle\mathcal{R}_{(4)}\rangle = -2\kappa^2\langle\mathcal{X}\rangle$.

5.3.4 Sources of φ -dependence within U

Eq. (5.66) is one of our main results, since it gives the effective potential whose minimization determines the value of the dilaton zero-mode, $\varphi = \varphi_*$, and thereby

also fixes the size of the extra dimensions, since $\ell^2 = r_B^2 e^{-\varphi_\star}$. The value of the potential at this minimum, $U(\varphi_\star)$ also determines the response of the gravitational field implied when φ seeks its minimum in this way.

To make this φ -dependence more explicit we use $V_B = V_0 e^\phi$ (with $V_0 = 2g_R^2/\kappa^4$) so that

$$U(\varphi) = \frac{1}{2} \left(V_0 \widehat{\Omega}_4 + \sum_v \mathcal{X}_v - \frac{1}{2\widehat{\Omega}_4} [\mathcal{N} + \xi(\varphi)]^2 \right) e^{2(\varphi - \varphi_\star)}. \quad (5.68)$$

There are four main ways that φ enters into this expression.

- The explicit overall factor of $e^{2\varphi}$.
- The φ -dependence of the explicit factors of the flux-localization parameter, $\xi(\varphi) = \sum_v \zeta_v(\varphi)$.
- The explicit φ -dependence of the brane stress-energy parameters, $\sum_v \mathcal{X}_v(\varphi)$.
- Some φ -dependence potentially enters through the integration volumes $\widehat{\Omega}_k$. Because $\widehat{\Omega}_k$ is scale invariant it contains no explicit factors of φ , but there can be a hidden φ -dependence because $\widehat{\Omega}_k$ usually also depends implicitly on T_v and ζ_v (eg through the defect angle, $\alpha_v - 1 \propto \kappa^2 T_v$) and so inherits any φ -dependence carried by the brane parameters.

We next check several special cases the above potential should reproduce.

Scale invariance

When neither T_v nor ζ_v depend on ϕ the branes preserve the bulk scale-invariance. In this case all of $\widehat{\Omega}_k$, T_v , \mathcal{X}_v and ξ are φ -independent, so the only dependence on φ is

the overall factor of $e^{2\varphi}$,

$$U(\varphi) = \frac{1}{2} \left[V_0 \widehat{\Omega}_4 + \sum_v \mathcal{X}_v - \frac{1}{2\widehat{\Omega}_{-4}} (\mathcal{N} + \xi)^2 \right] e^{2(\varphi - \varphi_*)}, \quad (5.69)$$

as would be dictated in general grounds by scale invariance. Although this is always minimized at $U = 0$, unless the square bracket vanishes this is achieved by a runaway to zero coupling, $\varphi \rightarrow -\infty$, as required by Weinberg's no-go theorem [25].

Vanishing $U(\varphi)$

Whenever \mathcal{X}_v vanishes (such as happens for the BPS vortices of previous chapters, for example) or is negligible, and $V_0 = \frac{1}{2}\mathcal{V}_0^2$ is positive, the quantity $e^{-2\varphi}U(\varphi)$ becomes proportional to a difference of squares and it is simple to enumerate sufficient conditions for it to vanish. In particular

$$\begin{aligned} U &= \frac{1}{4} \left\{ \mathcal{V}_0^2 \widehat{\Omega}_4(\varphi) - \frac{1}{\widehat{\Omega}_{-4}(\varphi)} [\xi(\varphi) + \mathcal{N}]^2 \right\} e^{2(\varphi - \varphi_*)} \\ &= -\frac{1}{4\widehat{\Omega}_{-4}(\varphi)} [\xi(\varphi) + \mathcal{N} - \mathcal{V}_0 \widetilde{\Omega}(\varphi)] [\xi(\varphi) + \mathcal{N} + \mathcal{V}_0 \widetilde{\Omega}(\varphi)] e^{2(\varphi - \varphi_*)}, \end{aligned} \quad (5.70)$$

where $\widetilde{\Omega}^2 := \widehat{\Omega}_4 \widehat{\Omega}_{-4}$. This clearly vanishes for all φ whenever the functions $\xi(\varphi)$ and $\widetilde{\Omega}(\varphi)$ are related by

$$\xi(\varphi) = -\mathcal{N} \pm \mathcal{V}_0 \widetilde{\Omega}(\varphi), \quad (5.71)$$

for all φ . When $\widehat{\Omega}_k$ and $\widetilde{\Omega}$ are φ -independent (which at least requires T_v to be independent of φ) then (5.71) can only be satisfied for all φ if ξ is also φ -independent, which implies scale invariance.

Salam-Sezgin solution

The Salam-Sezgin solution [4] described in Appendix C.1.1 has no sources and so $\xi = T_v = \mathcal{X}_v = 0$. It is a supersymmetric solution to 6D supergravity and so $V_0 = 2g_R^2/\kappa^4$ and $\mathcal{N} = \pm 2\pi/g_R$. The solution is unwarped, $W = 1$, so $\widehat{\Omega}_k = \widehat{\Omega}_s := \pi\kappa^2/g_R^2$ for all k . With these choices the scalar potential becomes

$$e^{-2(\varphi-\varphi_*)} U = \frac{1}{2} \left[\left(\frac{2g_R^2}{\kappa^4} \right) \widehat{\Omega}_4 - \frac{\mathcal{N}^2}{2\widehat{\Omega}_{-4}} \right] = \frac{1}{2} \left[\left(\frac{2g_R^2}{\kappa^4} \right) \widehat{\Omega}_s - \frac{\mathcal{N}^2}{2\widehat{\Omega}_s} \right] = \frac{1}{2} \left(\frac{2\pi}{\kappa^2} - \frac{2\pi}{\kappa^2} \right) = 0, \quad (5.72)$$

as it should, revealing φ as the flat direction.

Rugby ball solutions

We can also investigate the shape of the effective potential when scale invariant branes are added to the system. The rugby-ball solutions presented in Appendix C.1.2 are generated by identical, scale-invariant, supersymmetric [34] branes, and the potential is expected to vanish in this special case. Explicit solutions are also known when more general scale-invariant branes source the bulk [6], although these solutions generally have bulk fields with nontrivial profiles.

We side-step the technical issues associated with nontrivial warping and dilaton profile and treat both cases simultaneously, by assuming that branes' tension, T , and localized flux, $\xi = 2\zeta$, are small enough that we can linearize about the Salam-Sezgin solution (and so also choose flux quantum $\mathcal{N} = \pm 2\pi/g_R$). This assumption allows us to use the linearized scalar potential (C.73) calculated in Appendix C.2. When

specialized to the Salam-Sezgin background around which we are perturbing, it reads

$$e^{-2(\varphi-\varphi_\star)}U \simeq \frac{1}{2} \sum_v \mathcal{X}_v + \frac{2}{\kappa^2} (\kappa^2 T + g_R \xi). \quad (5.73)$$

Above, we have tracked the \mathcal{X}_v contribution to the potential, but the branes are scale invariant, so this quantity is also suppressed as in (5.30), and can be neglected. It then follows that the potential vanishes when the branes satisfy

$$\kappa^2 T = -g_R \xi. \quad (5.74)$$

This is identical to the supersymmetry condition on the branes [34], as expected. Incidentally, when the branes are UV completed as supersymmetric vortices as in previous chapters, it is also true that the vortex BPS conditions ensure $\mathcal{X}_v = 0$ identically.

When the branes are not supersymmetric, the right-hand side reduces to $2T$ at linear order when $\xi = 0$, in agreement with the expectations of the non-SUSY theory [1]. In this case, the resulting potential has the standard runaway form expected for scale-invariant couplings [25].

5.4 Self-tuning under scrutiny

Now that the tools for computing the dilaton potential are assembled, we can minimize it to explore the size of e^{φ_\star} and $U_\star = U(\varphi_\star)$ as functions of the microscopic choices (like T_v and ζ_v) that describe the branes.

5.4.1 Implications of ϕ -independent tension

We expect special things to happen if we can ensure a small ϕ derivative near the branes, since we know the curvature vanishes exactly if ϕ' vanishes at both branes [23]. This asks the brane lagrangian to be chosen to depend as weakly as possible on ϕ . The simplest choice is to demand complete ϕ -independence for both T_v and ζ_v for all branes, but although it is true that this leads to solutions with $R = 0$ it also implies scale invariance⁵ and the results of the previous section confirm that flat curvature in this case is found by having φ run away to infinity (thereby not breaking scale invariance) [25]. Consequently in this section we instead choose ϕ -independence just for the leading term, T_v , in the hopes that the resulting curvatures can be suppressed.

In this case only two sources of φ -dependence remain in U : the overall factor of $e^{2\varphi}$ and any dependence arising within $\xi(\phi) = \sum_v \zeta_v(\phi)$. (The latter of these includes both the explicit ξ -dependence and any implicit dependence of $\widehat{\Omega}_k$ on ξ .) Because the branes break scale invariance we expect the flat direction for φ to be lifted and the dynamics to choose an energetically preferred value, φ_* . Furthermore, since the lifting comes from ξ , which arises only from the derivatively once-suppressed localized-flux term, we expect \mathcal{Y}_v and direct brane contributions to the potential like \mathcal{X}_v to be KK-suppressed — as argued in more detail in chapter 4.

This leaves the bulk contribution to U , but because of (5.26) this is also expected to be suppressed once φ adjusts to approach the value φ_* . What we do here that the previous chapters did *not* do is compute the shape of U explicitly and minimize it to determine φ_* and $U_* = U(\varphi_*)$, thereby showing in detail how direct brane

⁵This point is less clear when the brane action is formulated using the original Maxwell field, $A_{(2)}$, rather than $F_{(4)}$, and because of this the equivalence between ϕ -independence and scale-invariance for brane-localized flux terms was misstated in [15, 17].

contributions to U compete with the interference the branes cause in the cancelations among the bulk terms in U .

Because $\ell \propto e^{-\varphi_\star/2}$ in the vacuum this calculation of φ_\star also computes the size of the extra dimensions, and we seek solutions with a large hierarchy between the brane size and the size of the transverse dimensions: $\ell \gg \hat{r}_v$. It is only for such solutions that the above arguments would suggest any suppression in U_\star .

Consequences of $\partial T/\partial\phi = 0$

For these reasons our main interest is in situations where T is φ -independent but $\zeta_v = \zeta_v(\varphi)$. We next argue that this ensures the contribution of \mathcal{X}_v to U becomes negligible.

Ultimately, it is the derivative suppression of ζ within the brane action in (5.9) that suppresses \mathcal{X}_v in the potential. For instance, neglecting any φ -dependence in $\widehat{\Omega}$ gives the first estimate

$$\mathcal{Y} = \sum_v \mathcal{Y}_v \sim Q \sum_v \zeta'_v = Q \xi' \simeq \frac{1}{\widehat{\Omega}_{-4}} (\mathcal{N} + \xi) \xi', \quad (5.75)$$

which uses flux quantization to eliminate the bulk flux Q . This expression for \mathcal{Y} determines $\sum_v \mathcal{X}_v$ through the brane constraint, (5.11), which implies

$$\sum_v \mathcal{X}_v \simeq \frac{\kappa^2 \mathcal{Y}^2}{4\pi} \sim \frac{1}{4\pi} (\kappa Q \xi')^2 \simeq \frac{1}{4\pi} \left(\frac{\kappa}{\widehat{\Omega}_{-4}} \right)^2 [(\mathcal{N} + \xi) \xi']^2. \quad (5.76)$$

Inserting this information into U then shows that the contribution of \mathcal{X}_v may be dropped relative to the $(\mathcal{N} + \xi)^2/\widehat{\Omega}_{-4}$ term whenever $(\kappa\xi')^2 \ll 2\pi\widehat{\Omega}_{-4}$, as is true when the extra dimensions are much larger than the microscopic sizes determining the scale

of κ and ξ' .

As before, for supergravity we have $V_0 = 2g_R^2/\kappa^4$ and as argued above the only φ dependence enters through ξ and the overall factor of $e^{2\varphi}$ dictated by scaling, making the scalar potential in the 4D theory

$$\begin{aligned} U(\varphi) &= \frac{1}{2} \left\{ \left(\frac{2g_R^2}{\kappa^4} \right) \widehat{\Omega}_4(\varphi) - \frac{1}{2\widehat{\Omega}_{-4}(\varphi)} [\mathcal{N} + \xi(\varphi)]^2 \right\} e^{2(\varphi - \varphi_*)} \\ &= \frac{1}{4\widehat{\Omega}_{-4}} \left(\frac{2g_R \tilde{\Omega}}{\kappa^2} + \mathcal{N} + \xi \right) \left(\frac{2g_R \tilde{\Omega}}{\kappa^2} - \mathcal{N} - \xi \right) e^{2(\varphi - \varphi_*)}, \end{aligned} \quad (5.77)$$

where $\tilde{\Omega}^2 := \widehat{\Omega}_4 \widehat{\Omega}_{-4}$ and in the first line we write $\widehat{\Omega}_k(\varphi)$ to emphasize that the volumes can also depend on φ through ξ .

General features

Broadly speaking the potential described above has the form

$$U(\varphi) = F(\varphi) e^{2(\varphi - \varphi_*)}, \quad (5.78)$$

and so its extrema, φ_* , make the derivative

$$U'(\varphi) = (2F + F') e^{2(\varphi - \varphi_*)}, \quad (5.79)$$

vanish. Our interest is in minima, so we demand the second derivative

$$U''(\varphi) = (4F + 4F' + F'') e^{2(\varphi - \varphi_*)}, \quad (5.80)$$

be positive.

There are two classes of solution:

1. The runaway: $\varphi_\star = \varphi_\infty = -\infty$, with $e^{\varphi_\star} = 0$ and so $U_\star = U_\star'' = 0$; and
2. Any nontrivial solutions to $F'(\varphi_\star) + 2F(\varphi_\star) = 0$. Evaluated at any of these latter extrema we have⁶

$$U_\star = -\frac{1}{2} F_\star' \quad \text{and} \quad U_\star'' = 2F_\star' + F_\star'' . \quad (5.81)$$

Control of approximations requires we check that at any such a minimum e^{φ_\star} is small enough to justify our semiclassical analysis.

Our main interest is in the non-runaway minima, and for these notice that using (5.77) to infer F and neglecting the φ -dependence of $\tilde{\Omega}$ when differentiating the result gives an expression for U_\star that agrees with the estimate of (5.75). This shows in a more pedestrian way how the low-energy theory knows of the higher-dimensional connection between U_\star and $\langle \mathcal{Y} \rangle$.

Of particular interest is how specific choices for ζ_v (and so also $\xi = \sum_v \zeta_v$) influence the shape of $F(\varphi)$, and through this the values of φ_\star and U_\star . We seek to arrange two things: (i) that $-\varphi_\star$ be moderately large (to achieve large extra dimensions, given $\ell \propto e^{-\varphi_\star/2}$); and (ii) that U_\star be suppressed below the generic brane scale T_v (as required to make progress on the cosmological constant problem if ordinary particles are localized on the branes and so contribute their vacuum energies as corrections to the corresponding brane tension).

One way to achieve these ends would be to arrange $F(\varphi) = F_0 \mathcal{F}(\epsilon\varphi)$, where ϵ is a

⁶Notice that the factor of $e^{2\varphi}$ does not suppress U_\star because of the compensating factor of $e^{-2\varphi_\star}$. Although $e^{2\varphi} \propto 1/\ell^4$ ensures the potential is generically suppressed by $1/\ell^4$, the $e^{-2\varphi_\star}$ compensates by converting the prefactor from 6D to 4D Planck density.

moderately small dimensionless parameter and F_0 is a very small energy density. In this case the linearity of (5.79) ensures the value of φ_* does not depend on F_0 at all, and if $\mathcal{F}(x)$ contains only order-unity parameters we expect to find $|\varphi_*| \sim \mathcal{O}(1/\epsilon)$. Having $\varphi_* \sim -75$ would ensure $e^{-\varphi_*/2} \sim 10^{16}$; adequate even for models with very large extra dimensions [5, 26]. The question is whether there is enough freedom available in $\xi(\varphi)$ to arrange both of these conditions, and if so whether the choices made can be technically natural.

The next sections explore this question by choosing $\xi = \mu f(\varphi)$ for several simple choices, where μ is a mass scale that can be adjusted independently from the scale in T_v . Although we find no obstruction in principle to being able to obtain both large φ_* and small U_* , the simple examples we explore so far each only appear to accomplish one or the other and not both simultaneously.

5.4.2 Perturbative solutions

As argued in §5.3.4, there are several values of φ for which we know $U(\varphi)$ must vanish. One of these is the limit $\varphi \rightarrow -\infty$, for which $U \rightarrow 0$ because of its exponential prefactor. The second case where we know $U = 0$ is when $\varphi = \varphi_s$ is such that $\xi(\varphi)$ happens by accident to pass through a point where its value agrees with the supersymmetric limit for the given tension. (As shown in Appendix C, at the linearized level this occurs for any φ_s satisfying $g_R \xi(\varphi_s) = \mp \kappa^2 T$, if the two branes share equal tensions.) Whenever this occurs Q also takes its supersymmetric value, which ensures $\check{R} = 0$ (and so $U = 0$).

The significance of such a zero is that it guarantees the existence of at least one maximum or a minimum for U in the range $-\infty < \varphi < \varphi_s$. (A similar conclusion

is also possible for any interval between two distinct solutions to $g_R \xi(\varphi_s) = -\kappa^2 T$, should more than one of these exist.) If this extremum is sufficiently close either to φ_∞ or to φ_s then we can analyze the shape of the potential by perturbing around the situation where U vanishes.

To that end let us write the brane properties as $T_v = T_0 + \delta T_v$ and $\zeta_v = \zeta_0 + \delta \zeta_v$, where T_0 and ζ_0 define a supersymmetric configuration for which $g_R \xi_0 = g_R \xi(\varphi_s) = 2g_R \zeta_0 = \mp \kappa^2 T_0$. Then the unperturbed potential vanishes, $U_0 = 0$, and deviations from this can be computed perturbatively in δT_v and $\delta \zeta_v$. There are two naturally occurring small parameters with which to linearize, $\kappa^2 \delta T \ll 1$ and $g_R \delta \xi(\varphi) \ll 1$, whose relative size is a knob we get to dial. Both of these are small to the extent that the bulk is only weakly perturbed by the source branes.

This leads to a potential of the generic form

$$U = \left(A + By + \dots \right) e^{2(\varphi - \varphi_*)}, \quad (5.82)$$

where $y(\varphi) := g_R \delta \xi / 2\pi \ll 1$, and the linearized calculation of the Appendix — culminating in (C.73) — shows the coefficients A and B are given by

$$A \simeq \sum_v \delta T_v = 2 \delta T_{\text{avg}} \quad \text{and} \quad B \simeq \frac{4\pi}{\kappa^2}, \quad (5.83)$$

where $\delta T_{\text{avg}} = \frac{1}{2} \sum_v \delta T_v$. Consequently $A/B \simeq \kappa^2 \delta T_{\text{avg}} / 2\pi \ll 1$.

For this potential

$$U' = \left[2A + 2By + By' + \dots \right] e^{2(\varphi - \varphi_*)}, \quad (5.84)$$

and at non-runaway solutions, $U'_\star = U'(\varphi_\star) = 0$, we have

$$U_\star = -\frac{1}{2}By'_\star + \dots \quad \text{and} \quad U''_\star = 2By'_\star + By''_\star + \dots \quad (5.85)$$

We now describe several types of extrema that such a potential generically possesses. In each case we do not propose an explicit form for $\delta\xi$ for all φ (and so also do not compute the potential U for all φ), but instead investigate its structure near the extrema of U subject to various assumptions about how $\delta\xi$ varies in this region. As a result we do not in these first examples try to compute the value of φ_\star from first principles, but only its difference from the position, φ_r , of a nearby reference point (such as a zero of U or a minimum of $\xi(\varphi)$ *etc*). We solve for all quantities in terms of the reference point, φ_r , and comment on the size of U_\star , the KK scale, ℓ and the zero-mode mass, m_φ , at the minimum.

Case I: Near a zero of U

Consider first the simplest situation where $\delta\xi$ depends very weakly on φ so we may Taylor expand ξ about the point $\varphi = \varphi_s$ where U vanishes

$$y(\varphi) \simeq \left(\frac{g_R\mu}{2\pi}\right) \left[(\varphi - \varphi_s) + \mathcal{O}[(\varphi - \varphi_s)^2] \right], \quad (5.86)$$

and we assume $|g_R\mu/2\pi| \ll 1$. The potential near $\varphi = \varphi_s$ becomes

$$U = \left[b(\varphi - \varphi_s) + \dots \right] e^{2(\varphi - \varphi_\star)}, \quad (5.87)$$

where $b \simeq 2g_R\mu/\kappa^2$.

Extrema are determined by the vanishing of

$$U' = \left[b + 2b(\varphi - \varphi_s) + \dots \right] e^{2(\varphi - \varphi_*)}, \quad (5.88)$$

and so for finite φ_* this implies

$$\varphi_* \simeq \varphi_s - \frac{1}{2}. \quad (5.89)$$

The condition $g_R \mu / 2\pi \ll 1$ ensures that $|y_*| \ll 1$ at this point, justifying our perturbative analysis of the extremum. The corresponding physical KK scale is

$$\ell = r_B e^{-\varphi_*/2} = \left(\frac{\kappa}{2g_R} \right) e^{1/4} e^{-\varphi_s/2}. \quad (5.90)$$

In agreement with [17, 20], the breaking of scale-invariance by the branes allows their back-reaction to stabilize the size of the extra-dimensions, in a 6D version of the Goldberger-Wise [22] mechanism in 5D. The stabilized size of the extra dimensions is exponentially large compared to microscopic scale r_B to the extent that φ_s is large and negative. The full linearization of the 6D system for this example is also given in Appendix C.3, including a discussion of the warping and dilaton profile generated by the bulk response to the brane perturbations, and of the renormalizations of brane couplings that these require. Later examples also provide concrete cases for which the value of φ_s can be computed in terms of brane properties, and briefly discuss choices that can make φ_s large and negative.

At this extremum we have

$$U_* \simeq b(\varphi_* - \varphi_s) \simeq -\frac{b}{2} \approx -\frac{g_R \mu}{\kappa^2}, \quad (5.91)$$

while

$$U''_{\star} \simeq 4b + 4b(\varphi_{\star} - \varphi_s) \simeq 2b \approx \frac{4g_R\mu}{\kappa^2}. \quad (5.92)$$

We see we have a local minimum (maximum) between $\varphi = \varphi_s$ and $\varphi \rightarrow -\infty$ when $b \propto g_R\mu$ is positive (negative), for which U_{\star} is negative (positive).⁷

Keeping in mind the normalization of the φ kinetic term in the 4D theory we see the classical prediction for its mass at this minimum is

$$m_{\varphi}^2 = \frac{1}{2} \kappa_4^2 U''_{\star} \simeq 2\kappa_4^2 |U_{\star}| \simeq \frac{2g_R\mu}{\langle W^{-2} \rangle}. \quad (5.93)$$

Since generically $\langle W^{-2} \rangle$ is of order the KK volume we see m_{φ} is suppressed below the KK scale by the small factor $g_R\mu/2\pi$, justifying its calculation in the 4D EFT. This same factor provides the suppression of U_{\star} relative to the 6D Planck scale, and as a result $m_{\varphi}^2 \sim |U_{\star}|/M_p^2$. We return below to a discussion of the robustness of such predictions to quantum corrections.

Case II: Near a minimum of ξ

Consider next a situation where $\varphi = \varphi_m$ is a local minimum of $\xi(\varphi)$, and where $\xi_m = \xi(\varphi_m)$ is *not* a point where U vanishes. In this case we expand ξ in powers of $\varphi - \varphi_m$ to write $T_v = T_0 + \delta T_v$ and $\xi = \xi_0 + \mu(\varphi - \varphi_m)^2$. Here T_0 is chosen so that $g_R\xi_0 = -\kappa^2 T_0$ (and we choose $N = +1$) so that it is $\delta T_{\text{avg}} = \frac{1}{2} \sum_v \delta T_v$ that controls the value of U at $\varphi = \varphi_m$. To justify the perturbative analysis we assume the resulting δT satisfies $|\kappa^2 \delta T| \ll 1$ and $|g_R\mu/2\pi| \ll 1$.

⁷We are not too concerned here if U_{\star} turns out negative at the minimum, even for applications to the cosmological constant problem. That is because the goal then is just to have the classical value be *smaller* than the inevitable quantum corrections (such as bulk Casimir energies) whose size is hoped to describe the observed (positive) dark energy in any ultimately successful model.

With these choices we then have

$$y(\varphi) \simeq \left(\frac{g_R \mu}{2\pi}\right) (\varphi - \varphi_m)^2 + \dots, \quad (5.94)$$

and the potential becomes

$$U = \left[a + b(\varphi - \varphi_m)^2 + \dots \right] e^{2(\varphi - \varphi_*)}, \quad (5.95)$$

where $a \simeq \sum_v \delta T_v = 2 \delta T_{\text{avg}}$ and $b \simeq 2g_R \mu / \kappa^2$. Their dimensionless ratio

$$\frac{a}{b} \simeq \frac{\kappa^2 \delta T}{g_R \mu}, \quad (5.96)$$

is a free parameter.

The extrema, φ_* , are determined by the vanishing of

$$U' \simeq 2 \left[a + b(\varphi - \varphi_m) + b(\varphi - \varphi_m)^2 + \dots \right] e^{2(\varphi - \varphi_*)}, \quad (5.97)$$

and so the non-runaway solutions satisfy

$$\varphi_{*\pm} \simeq \varphi_m - \frac{1}{2} \left(1 \pm \sqrt{1 - \frac{4a}{b}} \right). \quad (5.98)$$

Reality of this root requires $4a/b \leq 1$ and so $4\kappa^2 \delta T \leq g_R \mu$.

If $|a/b| \ll 1$ the roots take the approximate forms

$$\varphi_{*+} \approx \varphi_m - 1, \varphi_{*-} \approx \varphi_m - \frac{a}{b}, \quad (5.99)$$

and if a/b is large and negative they become

$$\varphi_{*\pm} \approx \varphi_m \mp \sqrt{\frac{a}{b}}. \quad (5.100)$$

Because φ_{*-} approaches φ_m as $a/b \rightarrow 0$ perturbation theory also justifies the expansion of $\delta\xi$ in powers of $\varphi - \varphi_m$ for this root. It may nonetheless be justified in any case for the other roots if it happens that $\delta\xi$ remains quadratic out to sufficiently large $\varphi - \varphi_m$, and that y remains small for all of this range.

There are two parameter regimes of interest. The first is $|4a/b| \ll 1$ and for this choice $\varphi_* - \varphi_m$ has the same order of magnitude as $a/b \sim \kappa^2 \delta T / g_R \mu$. As before, the corresponding physical KK scale is $\ell = (\kappa/2g_R) e^{-\varphi_*/2}$, and because $\varphi_* - \varphi_m$ is at most order unity, having this be large compared to microscopic scales requires φ_m large and negative.

At the extremum $\varphi_* - \varphi_m \approx -a/b$ we have

$$U_* \simeq a + b(\varphi_* - \varphi_m)^2 \simeq -b(\varphi_* - \varphi_m) \approx a \simeq 2\delta T_{\text{avg}}, \quad (5.101)$$

while

$$U_*'' = 2[2a + b + 4b(\varphi_* - \varphi_m) + 2b(\varphi_* - \varphi_m)^2] \simeq 2b[1 + 2(\varphi_* - \varphi_m)] \approx 2b \simeq \frac{4g_R \mu}{\kappa^2}. \quad (5.102)$$

We see that this is a local minimum when $b \propto g_R \mu$ is positive (*ie* whenever $\varphi = 0$ was a minimum for $\delta\xi$). Furthermore the back-reaction with the bulk drags the value of φ_* to be smaller (larger) than the minimum of $\delta\xi$ depending on whether or not $a \simeq 2\delta T_{\text{avg}}$ is positive (negative). The value of the potential at this point is

$U_\star \approx 2\delta T_{\text{avg}}$ and so is unsuppressed relative to (and shares the same sign as) δT_{avg} . At this minimum the classical prediction for the would-be zero-mode mass is driven by its potential on the brane,

$$m_\varphi^2 = \frac{1}{2} \kappa_4^2 U_\star'' \sim \frac{g_R \mu}{\langle W^{-2} \rangle}, \quad (5.103)$$

and so is below the KK scale because $g_R \mu \ll 1$.

Another interesting parameter range enumerated above takes a/b large and negative. In this case

$$\varphi_\star = \varphi_m - \sqrt{\left| \frac{a}{b} \right|}, \quad (5.104)$$

provided the quadratic form for $\delta\xi$ applies for fields this large. Notice that $y_\star \sim g_R \mu (\varphi_\star - \varphi_m)^2 \sim a \sim \kappa^2 \delta T_{\text{avg}}$ remains small.

Of special interest in this case is where $\sqrt{|a/b|}$ dominates φ_m , since this could explain why φ_\star is also large and negative (and so why $\ell \propto e^{-\varphi_\star/2}$ could be potentially enormous without needing to explain the size of φ_m).

At this extremum the size of the potential is

$$U_\star \simeq a + b(\varphi_\star - \varphi_m)^2 \simeq -b(\varphi_\star - \varphi_m) \approx b \sqrt{\left| \frac{a}{b} \right|} = \sqrt{|ab|} (\text{sign } b), \quad (5.105)$$

which is suppressed relative to the tension scale, $a = 2\delta T_{\text{avg}}$, by the assumed small quantity $\sqrt{|b/a|} \simeq |g_R \mu / \kappa^2 \delta T_{\text{avg}}|^{1/2} \ll 1$. Similarly,

$$\begin{aligned} U_\star'' &= 2[2a + b + 4b(\varphi_\star - \varphi_m) + 2b(\varphi_\star - \varphi_m)^2] \\ &\simeq 2b[1 + 2(\varphi_\star - \varphi_m)] \approx -4b \sqrt{\left| \frac{a}{b} \right|} = -4\sqrt{|ab|} (\text{sign } b) \simeq -4U_\star. \end{aligned} \quad (5.106)$$

and the concavity of the potential is once again controlled by b , with $b < 0$ (and so $a > 0$) giving a minimum at large negative values of φ_* . The classical mass of the would-be zero mode at this minimum is

$$m_\varphi^2 = \frac{1}{2}\kappa_4^2 U_*'' \simeq -2\kappa_4^2 U_* \sim \frac{\sqrt{\kappa^2 \delta T |g_R \mu|}}{\langle W^{-2} \rangle}, \quad (5.107)$$

and this lies below the KK scale because $|g_R \mu| \ll \kappa^2 \delta T \ll 1$ by assumption. Although this gives large dimensions or small U_* , it does not provide a phenomenologically viable value for both simultaneously, inasmuch as a large-volume value like $\varphi_* \sim -75$ only provides a moderate suppression of U_* relative to tension scales.

The extension of this example to a perturbation in the full 6D theory is also given in Appendix C.3, including a discussion of brane renormalization.

Case III: Near a singular point of ξ

The previous examples assume ξ varies smoothly with φ , so we next consider a singularity in ξ at $\varphi = \varphi_c$. Singularities can arise in low-energy actions at places in field space where the low-energy approximation fails, such as places where integrated-out species of particles become massless.

For purposes of illustration we consider a branch point of the form $\xi = \xi_0 + \delta\xi = \mu(\varphi - \varphi_c)^\eta$ with η an arbitrary exponent. The case η near zero is particularly interesting because this profits by being near the scale-invariant case $\eta = 0$. As above, we write $T_v = T_0 + \delta T_v$ and dial T_0 so that it is related to ξ_0 by $g_R \xi_0 = -\kappa^2 T_0$.

The potential becomes

$$U = \left[a + b(\varphi - \varphi_c)^\eta + \dots \right] e^{2(\varphi - \varphi_*)}, \quad (5.108)$$

where the ratio between $a \simeq \sum_v \delta T_v = 2 \delta T_{\text{avg}}$ and $b \simeq 2g_R\mu/\kappa^2$ is again a dial we can exploit. Assuming $0 < \eta < 1$ the extrema are determined by the vanishing of

$$U' \simeq \left[2a + 2b(\varphi - \varphi_c)^\eta + \frac{\eta b}{(\varphi - \varphi_c)^{1-\eta}} + \dots \right] e^{2(\varphi - \varphi_*)}, \quad (5.109)$$

which has solutions in the regime $|\varphi - \varphi_c| \gg 1$ of the form

$$\varphi_* - \varphi_c \simeq \left(-\frac{a}{b} \right)^{1/\eta}, \quad (5.110)$$

which for small η is true even if $a/b = \kappa^2 \delta T_{\text{avg}} / g_R \mu$ is only moderately large and negative. (For instance choosing $\eta = \frac{1}{3}$ and $\kappa^2 \delta T_{\text{avg}} \sim -4g_R\mu$ gives $\varphi_* - \varphi_c \simeq -64$.)

At this point we have

$$U_* = a + b(\varphi_* - \varphi_c)^\eta \simeq -\frac{\eta b}{2(\varphi_* - \varphi_c)^{1-\eta}} \simeq -\frac{\eta b}{2} \left(-\frac{b}{a} \right)^{(1-\eta)/\eta}. \quad (5.111)$$

Small η has the virtue of amplifying both the size of φ_* and the suppression of U_* , although not in a way that seems phenomenologically viable for both at the same time.

Case IV: Exponential ξ

Next consider an example whose solutions are perturbatively close to the asymptotic runaway. This example is similar to the scaling case examined for the UV vortex completion in chapter 4, where $T = T_0 + \delta T$ and $\xi = \xi_0 + \mu e^{s\varphi}$, where $g_R \xi_0 = -\kappa^2 T_0$ and our main interest is in s not far from zero. In this case $y = (g_R \mu / 2\pi) e^{s\varphi}$ so

$y' = sy$, and

$$U = \left(a + b e^{s\varphi} + \dots \right) e^{2(\varphi - \varphi_*)}, \quad (5.112)$$

with $a \simeq 2\delta T$ and $b \simeq 2g_R\mu/\kappa^2$. Then the non-runaway solutions to $U' = 0$ satisfy

$$2a + b(2 + s)e^{s\varphi_*} + \dots = 0. \quad (5.113)$$

If $e^{s\varphi_*}$ is small enough to drop all but the first two terms we have

$$e^{s\varphi_*} \simeq -\frac{2a}{b(2 + s)} \simeq -\frac{2\kappa^2\delta T}{(2 + s)g_R\mu}, \quad (5.114)$$

which requires a and b to have opposite signs. The value of U at the extremum is

$$U_* \simeq -\frac{sb}{4} e^{s\varphi_*} \simeq \frac{sa}{2(2 + s)} \simeq \frac{s\delta T}{2 + s}. \quad (5.115)$$

The factor of s found in U_* can be understood because when $s \rightarrow 0$ the potential becomes scale-invariant and so must then be minimized at $U_* = 0$ with $\varphi_* \rightarrow -\infty$.

If $s > 0$ then having small e^{φ_*} means we must also have $|a| \ll |b|$ (which corresponds to $\kappa^2|\delta T| \ll |g_R\mu| \ll 1$). In this case U asymptotes to zero as $\varphi \rightarrow -\infty$ from below (above) if a is negative (positive), so the extremum is a minimum if $a < 0$ and $b > 0$ (*ie* when $g_R\mu > 0$ and $\delta T < 0$) in which case $U_* < 0$.

Conversely, if $s < 0$ then having small e^{φ_*} means we instead must have $|a| \gg |b|$ (and so $|g_R\mu| \ll \kappa^2|\delta T| \ll 1$), and in this case it is for $b < 0$ and $a > 0$ (*ie* for $g_R\mu < 0$ and $\delta T > 0$) that the above root is a minimum. Writing $s = -\sigma$

$$e^{\sigma\varphi_*} \simeq -\frac{b(2 - \sigma)}{2a} \simeq -\frac{g_R\mu(2 - \sigma)}{2\kappa^2\delta T}, \quad (5.116)$$

which again requires μ and δT to have opposite signs. The value of U at the extremum is

$$U_\star \simeq \frac{\sigma b}{4} e^{-\sigma\varphi_\star} \simeq -\frac{\sigma a}{2(2-\sigma)} \simeq -\frac{\sigma\delta T}{2-\sigma}, \quad (5.117)$$

which is again negative and order $\sigma\delta T$. To be much smaller than δT we would need $\sigma \ll 1$.

The corresponding physical KK scale is

$$\begin{aligned} \ell = r_B e^{-\varphi_\star/2} &\sim \left(\frac{\kappa}{2g_R}\right) \left(-\frac{g_R\mu}{2\kappa^2\delta T}\right)^{1/2s} && \text{(if } s > 0\text{)} \\ &\sim \left(\frac{\kappa}{2g_R}\right) \left(-\frac{2\kappa^2\delta T}{g_R\mu}\right)^{1/2\sigma} && \text{(if } s = -\sigma < 0\text{)}, \end{aligned} \quad (5.118)$$

and the classical prediction for the mass of the would-be zero mode is

$$m_\varphi^2 = \frac{1}{2}\kappa_4^2 U_\star'' \sim -s\kappa_4^2\delta T \simeq -(2+s)\kappa_4^2 U_\star. \quad (5.119)$$

The minimum found above is most interesting when $|s| \ll 1$, for two reasons. First, small s ensures that e^{φ_\star} can be *extremely* small even if both $\kappa^2\delta T$, $g_R\mu$ and their ratio are only moderately small. For example, taking $\kappa^2\delta T \sim 0.3$ and $g_R\mu \sim -0.0003$ gives $\kappa^2\delta T/g_R\mu \sim -10^3$ and so $s = -\sigma \sim -0.1$ gives the enormous hierarchy $e^{\varphi_\star} \simeq r_B/\ell \sim 10^{-15}$ appropriate to a picture with micron-sized extra dimensions [5, 26] when the bulk is controlled by TeV scale physics. Such large radii arise because the choice $0 < |s| \ll 1$ makes the setup close to scale-invariant, and so the potential in this limit is close to its runaway form, $U \sim U_0 e^{2\varphi}$. The small scale-breaking parameters then give a weak φ -dependence to the prefactor U_0 , creating a minimum out at large negative φ . The minimum occurs at large $-\varphi$ precisely because of the potential's

close-to-runaway form.

Small $|s|$ is also interesting because of the suppression implied by (5.115) for the value of U_\star . As mentioned earlier, this suppression arises generically because the system becomes classically scale invariant in the $s \rightarrow 0$ limit, and so U_\star must vanish in this limit. Effectively this converts Weinberg's runaway no-go from a bug to a feature, with weak scale-breaking driving U_\star to be small precisely because the minimum gets driven out to infinity in the scale-invariant limit. As before, however, although both large ℓ and small U_\star are possible, no one choice of parameters gets both right at the same time (without very precise tuning to make $|a/b|$ extremely close to unity.)

When large φ does not imply large dimensions

Equating large negative φ_\star to a large hierarchy between KK size, ℓ , and brane size, \hat{r}_v , (as done in the previous examples) implicitly makes an assumption about the φ -dependence of \hat{r}_v . The issue is whether or not obtaining large $e^{-\varphi_\star}$ — eg (5.118) — is sufficient to imply a large hierarchy between ℓ and the transverse brane size, \hat{r}_v . It need not be, depending on the other microscopic details that determine \hat{r}_v . In particular it depends on how the brane size itself depends on φ_\star .

For instance, the UV completion considered in the previous chapter provides an example where the connection between large φ_\star and large ℓ/\hat{r}_v can fail. In this example the branes are resolved in the UV as Nielsen-Olesen vortices [3] with tension, $T_v \simeq v^2$, set by a scalar vev, v , and brane-localized flux, $\xi \simeq (2\pi n \varepsilon/e)e^{s\varphi}$, set by a dimensionless mixing parameter, ε , an integer, n , and a gauge coupling, e . In this UV completion the physical size of the vortex is $\hat{r}_v^{-1} \simeq v\hat{e}(\varphi) = ev \exp[\frac{1}{2}(1+2s)\varphi]$, which turns out to inherit a dependence on φ from the effective coupling $\hat{e}(\varphi)$. Consequently

\hat{r}_v/ℓ can be related to the tension and localized flux by

$$\frac{\hat{r}_v}{\ell} = \left(\frac{2g_R}{\kappa} e^{\varphi_*/2} \right) \left(\frac{1}{e\nu} e^{-(1+2s)\varphi_*/2} \right) = \left(\frac{2g_R}{e\kappa\nu} \right) e^{s\varphi} = \frac{g_R \xi}{n\pi\epsilon\kappa\nu} = \frac{g_R \xi}{n\pi\epsilon\sqrt{\kappa^2 T}}, \quad (5.120)$$

for any choice of s or φ . What is important here is that \hat{r}_v/ℓ is φ -independent when expressed in terms of the parameters, T and ζ , appearing in the brane effective lagrangian, since these are the combinations that are relevant to the long-distance physics governing the size of ℓ . As a result, in this particular model it doesn't matter how large φ_* is when predicting \hat{r}_v/ℓ .

Notice that this line reasoning relies on *all* of ξ depending on φ in the same way, rather than there being several contributions involving different scales and depending differently on φ . This is why it does not also apply to the previous examples, for which $\xi = \xi_0 + \delta\xi(\varphi)$.

5.4.3 Scenarios of scale

Before turning to the robustness of the above examples it is useful to have some idea in mind for the the mass scales appearing in all sectors of the theory. This is important when estimating quantum corrections in particular, since for naturalness problems the heaviest scales are usually the most dangerous. We also imagine at least one brane lagrangian being modified to include brane-localized particles, including the known Standard Model (SM) particles.

There are several mass scales potentially in play: the inverse brane width, $M \sim 1/\hat{r}_v$; the SM electroweak scale, m ; and the scale set by bulk couplings, $\kappa^{-1/2}$ and g_R^{-1} . Without loss we may shift φ in the bulk so that $\varphi = 0$ corresponds to $g_R^{-1} \sim \kappa^{-1/2} \sim M_g$ defining the same scale. The effective bulk gauge coupling, $g_\star = g_R e^{\varphi_*/2}$ and the

KK scale, $m_{KK} \sim 1/\ell \sim g_*/\kappa = (g_R/\kappa)e^{\varphi_*/2}$, are then computed from these once the dilaton is stabilized at $\varphi = \varphi_*$. We assume the hierarchy

$$M_g \sim \kappa^{-1/2} \sim g_R^{-1} \gg M \gg m, \quad (5.121)$$

and ask how loops might depend on these scales.

It is also useful to imagine the UV completion of the brane eventually becomes supersymmetric at high enough energies, since this is likely necessary to deal with naturalness at the highest scales possible. This could happen at the string scale if the brane UV completes as an object within string theory, or it could happen above or below the scale M if the branes UV complete as vortices in a higher-dimensional field theory. For concreteness we consider the vortex completion, since the extension to string theory of the system used here remains an open question [37]. Since our goal is to explore extra-dimensional approaches to the hierarchy problem, we always take the brane SUSY-breaking scale, M_s , much larger than electroweak scales: $M_s \gg m$.

If we choose $M_s \ll M$ then the vortex sector would be supersymmetric (in that it would preserve at most half of the supersymmetries of the bulk [40]) with the branes likely arising as BPS solutions. Until distorted by supersymmetry-breaking effects (if any) we would then expect the largest contributions to T and ζ to be ϕ -independent, with $T = T_s \sim \mathcal{O}(M^4)$. The breaking of supersymmetry that such branes generically imply for the bulk sector is then minimized if the branes carry the supersymmetric amount of flux [34], so we take $\kappa^2 T_s = \pm \frac{1}{2} g_R \zeta_s$. This implies $\zeta_s \sim \kappa^2 T_s / g_R \sim M^4 / M_g^3 \ll M$ in magnitude. These assumptions ensure a flat potential, $U = 0$, for φ and allows supersymmetry to protect this shape from scales higher than M_s , leaving nontrivial corrections to the low-energy theory (where we

can try to estimate them).

We expect nonzero $\delta T = T(\varphi) - T_s$ and $\delta\zeta = \zeta(\varphi) - \zeta_s$ once effects of the SUSY-breaking brane sector are included. This includes but need not be limited to the SM sector (which is assumed to be localized to one of the branes). On dimensional grounds, if SUSY breaks on the branes with scale M_s such that $m \ll M_s \ll M$ then we expect the dominant deviations from the supersymmetric limit to be of order $\delta T(\varphi) \sim M_s^4$ and $\delta\zeta(\varphi) \sim M_s$. If the supersymmetry breaking physics respects the bulk scale invariance then δT and $\delta\zeta$ remain φ -independent; otherwise not.

Suppose the supersymmetry-breaking sector *does* break scale invariance but only through the localized flux term as examined above, so $T = T_s + \delta T$ with $\delta T \sim M_s^4$ and $\zeta = \zeta_s + \delta\zeta$ with $\delta\zeta(\varphi) \sim M_s f(\varphi)$, for some function $f(\varphi)$, although the precise form for f is not yet crucial. Assuming $M_s \gg M^4/M_g^3$ then there should exist a value, $\varphi = \varphi_s$, for which $U(\varphi_s) = 0$ because $\zeta(\varphi_s)$ accidentally takes the supersymmetric value corresponding to $T = T_s + \delta T$,

$$\pm \frac{1}{2} g_R \zeta(\varphi_s) = \pm \frac{1}{2} g_R [\zeta_s + \delta\zeta(\varphi_s)] \sim \kappa^2 T = \kappa^2 (T_s + \delta T). \quad (5.122)$$

We imagine the value, φ_s , where this occurs to be moderately large (of order -75 or so in the extreme case of very large dimensions).

This scenario fits very cleanly into the class of models for which the perturbative methods explored earlier apply, with $y(\varphi) \sim g_R \delta\zeta(\varphi) \sim g_R M_s \delta f(\varphi) := g_R M_s [f(\varphi) - f(\varphi_s)] = \mathcal{O}(M_s/M_g)$. If δf varies slowly enough to be approximated as linear near φ_s the analysis of earlier sections would predict a minimum with $\varphi_* - \varphi_s \simeq -\frac{1}{2}$ at which point the classical 4D energy density is $U_* \sim -g_R M_s / \kappa^2$. Other forms for $f(\varphi)$ would predict different scalings.

Finally, loops of Standard Model particles should also contribute to T and ζ and further perturb them away from their supersymmetric relationship, by an amount at least $\delta T_{SM} \sim m^4$ and $\delta \zeta_{SM} \sim \epsilon m$ (where $\epsilon \lesssim 1$ is a dimensionless measure of the strength with which the SM sector couples to the bulk gauge field). Even if not supersymmetric, such SM contributions need not contribute any φ -dependence if they preserve scale invariance.

There are two natural ranges of values to think through, depending on whether our interest is in the electroweak hierarchy (quantum corrections to scalar masses) or the cosmological constant problem (quantum corrections to vacuum energies). We consider each of these briefly in turn.

Electroweak Hierarchy

For applications to the electroweak hierarchy we ask the extra dimensions to be large and take the large scales all to be of order the electroweak scale, with the minimal hierarchy required for control of approximations. In this case the premium is on predicting the value of φ_* from first principles to ensure sufficiently large ℓ/r_B using only a relatively modest hierarchy amongst lagrangian parameters, and we are happy to fine-tune away any cosmological constant. This can be done, for example, if the vortex size, \hat{r}_v , is φ -independent and controls the supersymmetric brane physics at scale M , and the supersymmetry-breaking brane physics at scale M_s generates an exponential $\delta\zeta \sim M_s e^{s\varphi}$.

Taking for illustrative purposes $M_g \sim 50$ TeV, $M \sim M_s \sim 5$ TeV and $m \sim 100$ GeV with $s \simeq 0.2$ then gives $M_g \ell \sim 10^{15}$, which is in the ballpark required. Such a dynamical explanation for the exponentially large size of ℓ elevates the large-dimensional models [26] to a footing similar to their warped competitors [12], although

this would be more satisfying with a more explicit picture for the SUSY-breaking brane physics to see more explicitly how it generates the required φ -dependence for ζ and T .

The challenge and opportunity in this scenario is to better construct the SUSY breaking physics, partly to see what signals it could imply at the LHC. There is clearly some freedom to dial scales somewhat, though if M_s and M_g are both taken much larger than the electroweak scale we must again ask what protects the value of the Higgs mass on the brane. Implicit in any such model is that whatever quantum gravity eventually kicks in at M_g does not allow the higher scales to feed into the Higgs mass and thereby ruin the naturalness of the low-energy picture.

Vacuum Energies

Although the ideal situation would be to explain the observed dark energy density, it would already be progress on the cosmological constant problem to suppress U_\star below the electroweak scale. This requires the classical contribution be smaller than the known quantum effects (usually not hard), while choosing parameters so that the quantum effects themselves can be smaller than the electroweak scale (usually much harder). The hope here is that because SM loops generate changes to the brane tension, $\delta T \sim m^4$, we seek choices that keep this from directly contributing to U_\star .

A best case in this type of scenario is to imagine that all physics couples to φ in the scale-invariant way down to as low an energy (say μ) as possible. If $\mu \ll m \ll M_s \ll M$ then this implies the UV physics is to first approximation scale invariant though not supersymmetric, so that T and ζ are constants for which $\kappa^2 T$ and $g_R \zeta$ are not similar in size.

In this case we imagine the scale-invariance breaking at scale μ introduces a φ -dependence only to $\delta\zeta$, in such a way that ζ accidentally passes through the supersymmetric point, $\zeta \sim \pm 2\kappa^2 T/g_R$ at $\varphi_s \sim -75$ or so. This ensures the extra dimensions can be very large (best of all would be in the micron range) as desired. Provided the variation in φ is slow enough to justify Case I above, the classical prediction for U_\star is negative⁸ with magnitude $\sim g_R\mu/\kappa^2$. Choosing M_g as low as possible (in the 10 TeV regime, say) then gives a suppression of U_\star relative the electroweak scale by of order $g_R\mu$.

How much suppression depends on how small μ can be, which requires a better theory of the origins of the φ -dependence. Since $U_\star \sim \mu M_g^3$ we see that having $|U_\star| \lesssim (10^{-2} \text{ eV})^4$ and $M_g \sim 10 \text{ TeV}$ requires fantastically small values like $\mu \lesssim |U_\star|/M_g^3 \sim 10^{-47} \text{ eV}$. To the extent that useful progress on lowering U_\star below the electroweak scale requires scale-invariant couplings of φ to ordinary matter, the obstacle is likely to be solar-system constraints on the existence of light Brans-Dicke scalars with gravitational couplings.

5.4.4 Robustness

As for any approach to naturalness problems the key question concerns robustness of the result. One must check whether conclusions survive the inclusion of subdominant terms in the various approximations being made. Although a full analysis of all of these corrections goes beyond the scope of this article, we make a few preliminary estimates of the size of some of the usual suspects.

⁸Having $U_\star < 0$ need not be a problem if its magnitude is small enough that the vacuum energy is dominated by its quantum parts (which must then be positive).

Potentially fragile choices

Assessments of robustness turn on the generality of the choices for parameters in the classical theory. Because it is the branes that are responsible for breaking supersymmetry we might expect that it is choices made for the brane actions in particular that are the most susceptible to perturbations (such as by receiving quantum corrections once these are included).

The basic choices used in previous sections concern the magnitude and ϕ -dependence of the brane action, parameterized by the small dimensionless quantities $\kappa^2 T(\phi)$ and $g_R \zeta(\phi)$ for each of the branes. In particular the previous sections make two non-generic assumptions about the brane action:

- We choose no ϕ -dependence for T but allow ϕ -dependence for ζ ;
- We dial freely the relative magnitudes of $\kappa^2 T$ and $g_R \zeta$.

It is the sensitivity of these choices to quantum corrections on which we focus.

Some quantum estimates

UV sensitive quantum corrections in this type of model come in two broad classes: quantum corrections to the bulk lagrangian due to loops of bulk fields; and quantum corrections to the brane lagrangians due to loops of fields on the brane and loops involving bulk fields located close to the brane. In both cases it is loops of the most massive particles that are potentially the most dangerous.

Corrections to the Bulk Sector

Loops within the supergravity describing the bulk have been studied in some detail [34, 38, 39], and although loops of individual massive states do renormalize all terms

in the bulk and brane lagrangians their contributions to the bulk lagrangian tend to cancel once summed over 6D supermultiplets [39]. The only bulk renormalizations that survive these cancelations are renormalizations of those interactions allowed by bulk supersymmetry, for which we do not make any special requirements.

This is required physically because UV modes far from the branes effectively do not know that supersymmetry is broken. The UV dangerous renormalizations coming from the supersymmetric sector are those that renormalize the non-supersymmetric brane physics. These should not be dangerous to the extent we do not make special assumptions about the sizes (or the dependence on bulk fields) of couplings like T and ζ in the brane action.

From the point of view of the vacuum energy, the most dangerous renormalizations of the bulk are dimension-four interactions involving curvature squared terms (and their partners under supersymmetry) since these can acquire renormalizations proportional to the squared-mass, \mathcal{M}^2 , of the massive bulk supermultiplet [34, 38, 39]. These can generate contributions to the 4D vacuum energy of order \mathcal{M}^2/ℓ^2 , and so be larger than the $1/\ell^4$ desired to describe Dark Energy in SLED models. But they are generically smaller than the $\mathcal{O}(\mathcal{M}^4)$ contributions described below, and so represent a lesser worry than the brane renormalizations we describe next.

The Brane Sector: Bulk Loops

Loops of bulk fields involving virtual particles physically near the branes also renormalize the brane lagrangian, as computed in [34, 38]. These loops turn out not to be dangerous for our two brane choices, however, for two reasons.

The first statement is that although bulk loops contribute of order \mathcal{M}^4 to the brane tension, they do not introduce nontrivial ϕ -dependence to the tension if this

was not already present because of the underlying scale invariance of the bulk system. Secondly, bulk loops involving massive multiplets that carry gauge charge can also renormalize ζ . But because the correction is of order $\delta\zeta \sim g_R^2 \mathcal{M}^2 \zeta$ [34] it is technically natural (from the point of view of these loops) to choose ζ to be small.

The Brane Sector: Brane Loops

Massive fields localized on the branes are among the most dangerous (and arguably the most difficult to understand) from the point of view of naturalness, because these fields can be heavy and are not constrained by supersymmetry (at least at scales below M_s). In principle these include loops of familiar SM fields that are the origin of the cosmological constant problem in the first place.

Integrating out such particles of mass M generically renormalizes the brane tension by an amount of order M^4 , so we run into naturalness problems as soon as we must demand δT be smaller than this. For applications to the cosmological constant problem this is why all contributions to U_\star of order δT are not regarded as being progress.

In general such loop contributions to T could also play a role by introducing nontrivial ϕ -dependence, although this can be protected against by demanding the couplings of the brane matter to preserve scale invariance. For SM fields this is trouble to the extent that it gives them Brans-Dicke couplings [41] to the light scalar φ of gravitational strength [42], which are ruled out phenomenologically (for sufficiently light φ) by PPN solar-system tests of gravity [43]. Of course, mechanisms exist for weakening the couplings of light scalars [35, 44], usually by making these couplings φ - or environment-dependent or by making the scalar massive enough not to mediate a sufficiently long-range force. Although much model-building could be forgiven if

progress could be made on the cosmological constant problem, we regard this to be a real worry whose resolution goes beyond the scope of this (already very long) study.

The same kinds of problems need not be a worry for brane corrections to ζ , however, because these cannot be generated unless the field in the loop already couples to the bulk gauge field. Brane-generated contributions to $\delta\zeta$ should be easy to suppress simply by not coupling heavy brane particles to this field.

5.5 Discussion

This paper's aim is to carefully determine how codimension-two objects in 6D supergravity back-react on their environment through their interactions with the bulk metric, Maxwell field and dilaton, and how this back-reaction gets encoded into the effective potential of the low-energy 4D world below the KK scale.

To this end, we construct the corresponding four-dimensional effective theory, and show how the flux quantization conditions of the UV theory are brought to 4D by a four-form gauge flux dual to the Maxwell field. The 4D theory generically contains a light scalar dilaton to the extent that the branes do not strongly break the classical bulk scale invariance. We identify the scalar potential for this scalar and show at the linearized level that it agrees with what is obtained by explicitly linearizing the higher-dimensional field equations. This calculation in particular corrects some errors in [17], which misidentified some of the boundary conditions associated with the brane-localized flux term.

We confirm the result of [17] that the breaking of scale invariance by the branes can lead to modulus stabilization and allow explicit computation of the extra-dimensional

size, in a codimension-two version of the Goldberger-Wise mechanism [22]. We confirm that this size can be exponentially large in the brane couplings. A moderate hierarchy of order 75 amongst the brane couplings can be amplified to produce enormous extra dimensions in this way, thereby fixing a long-standing problem with the use of large extra dimensions to solve the electroweak hierarchy problem.

For the particular choice of near scale-invariant couplings we can (but need not) also find some parametric suppression in the value of the on-brane curvature and dilaton mass, although for those examined so far this suppression seems fairly weak. We are unable to find simple examples which both generate exponentially large dimensions and suppress the classical vacuum energy (though we also are unable to prove this to be impossible).

Although we make preliminary estimates about the size of quantum corrections and the robustness of the parametric suppressions of the potential, we leave a more detailed treatment to later work.

Acknowledgements

We acknowledge Florian Niedermann and Robert Schneider for collaborations at early stages of this work as well as discussions about this paper and [1, 2] while they were in preparation. We thank Ana Achucarro, Asimina Arvanitaki, Savas Dimopoulos, Gregory Gabadadze, Ruth Gregory, Mark Hindmarsh, Stefan Hoffmann, Leo van Nierop, Massimo Porrati, Fernando Quevedo and Itay Yavin for useful discussions about self-tuning and UV issues associated with vortices and brane-localized flux.

Bibliography

- [1] C. P. Burgess, R. Diener and M. Williams, “The Gravity of Dark Vortices: Effective Field Theory for Branes and Strings Carrying Localized Flux,” arXiv:1506.08095 [hep-th].
- [2] C. P. Burgess, R. Diener and M. Williams, “EFT for Vortices with Dilaton-dependent Localized Flux,” arXiv:1508.00856 [hep-th].
- [3] H. Nishino and E. Sezgin, *Phys. Lett.* **144B** (1984) 187; “The Complete N=2, D = 6 Supergravity With Matter And Yang-Mills Couplings,” *Nucl. Phys.* **B278** (1986) 353;

S. Randjbar-Daemi, A. Salam, E. Sezgin and J. Strathdee, “An Anomaly Free Model in Six-Dimensions” *Phys. Lett.* **B151** (1985) 351.
- [4] A. Salam and E. Sezgin, “Chiral Compactification On Minkowski X S**2 Of N=2 Einstein-Maxwell Supergravity In Six-Dimensions,” *Phys. Lett. B* **147** (1984) 47.
- [5] Y. Aghababaie, C. P. Burgess, S. L. Parameswaran and F. Quevedo, “Towards a naturally small cosmological constant from branes in 6-D supergravity,” *Nucl. Phys. B* **680** (2004) 389 [hep-th/0304256].
- [6] G. W. Gibbons, R. Guven and C. N. Pope, “3-branes and uniqueness of the Salam-Sezgin vacuum,” *Phys. Lett. B* **595** (2004) 498 [hep-th/0307238];

C. P. Burgess, F. Quevedo, G. Tasinato and I. Zavala, “General axisymmetric solutions and self-tuning in 6D chiral gauged supergravity,” *JHEP* **0411** (2004) 069 [hep-th/0408109].
- [7] S. L. Parameswaran, G. Tasinato and I. Zavala, “The 6D SuperSwirl,” *Nucl. Phys. B* **737** (2006) 49 [arXiv:hep-th/0509061];

- [8] H. M. Lee and C. Ludeling, “The general warped solution with conical branes in six-dimensional supergravity,” *JHEP* **0601** (2006) 062 [arXiv:hep-th/0510026];
- [9] N. Kaloper and D. Kiley, “Exact black holes and gravitational shockwaves on codimension-2 branes,” *JHEP* **0603** (2006) 077 [hep-th/0601110].
- [10] A. J. Tolley, C. P. Burgess, D. Hoover and Y. Aghababaie, “Bulk singularities and the effective cosmological constant for higher co-dimension branes,” *JHEP* **0603** (2006) 091 [arXiv:hep-th/0512218].
- [11] A. J. Tolley, C. P. Burgess, C. de Rham and D. Hoover, “Scaling solutions to 6D gauged chiral supergravity,” *New J. Phys* **8** (2006) 324 [arXiv:0608.083 [hep-th]];
- E. J. Copeland and O. Seto, “Dynamical solutions of warped six dimensional supergravity,” *JHEP* **0708** (2007) 001 [arXiv:0705.4169 [hep-th]];
- A. J. Tolley, C. P. Burgess, C. de Rham and D. Hoover, “Exact Wave Solutions to 6D Gauged Chiral Supergravity,” *JHEP* **0807** (2008) 075 [arXiv:0710.3769 [hep-th]];
- M. Minamitsuji, “Instability of brane cosmological solutions with flux compactifications,” *Class. Quant. Grav.* **25** (2008) 075019 [arXiv:0801.3080 [hep-th]];
- H. M. Lee and A. Papazoglou, “Codimension-2 brane inflation,” *Phys. Rev. D* **80** (2009) 043506 [arXiv:0901.4962 [hep-th]].
- [12] L. Randall and R. Sundrum, “An Alternative to compactification,” *Phys. Rev. Lett.* **83** (1999) 4690 [hep-th/9906064];
- “A Large mass hierarchy from a small extra dimension,” *Phys. Rev. Lett.* **83** (1999) 3370 [hep-ph/9905221].
- [13] For early review of the SLED early reviews of the SLED proposal see: C. P. Burgess, “Towards a natural theory of dark energy: Supersymmetric large extra dimensions,” *AIP Conf. Proc.* **743** (2005) 417 [hep-th/0411140];
- “Supersymmetric large extra dimensions and the cosmological constant: An Update,” *Annals Phys.* **313** (2004) 283 [hep-th/0402200].
- [14] For a review of the cosmological constant problem, including (but not restricted to) a brief summary of the SLED proposal see:

- C.P. Burgess, “The Cosmological Constant Problem: Why it is Hard to Get Dark Energy from Micro-Physics,” in the proceedings of the Les Houches School *Cosmology After Planck*, [arXiv:1309.4133];
- [15] C. P. Burgess and L. van Nierop, “Technically Natural Cosmological Constant From Supersymmetric 6D Brane Backreaction,” *Phys. Dark Univ.* **2** (2013) 1 [arXiv:1108.0345 [hep-th]].
- [16] For a sampling of other reviews of the cosmological constant problem see:
E. Witten, “The Cosmological constant from the viewpoint of string theory,” [hep-ph/0002297];
J. Polchinski, “The Cosmological Constant and the String Landscape,” [hep-th/0603249];
T. Banks, “Supersymmetry Breaking and the Cosmological Constant,” *Int. J. Mod. Phys. A* **29** (2014) 1430010 [arXiv:1402.0828 [hep-th]];
- A. Padilla, “Lectures on the Cosmological Constant Problem,” [arXiv:1502.05296 [hep-th]].
- [17] C. P. Burgess and L. van Nierop, “Bulk Axions, Brane Back-reaction and Fluxes,” *JHEP* **1102** (2011) 094 [arXiv:1012.2638 [hep-th]];
- “Large Dimensions and Small Curvatures from Supersymmetric Brane Back-reaction,” *JHEP* **1104**, 078 (2011) [arXiv:1101.0152 [hep-th]].
- [18] R. Bousso and J. Polchinski, “Quantization of four form fluxes and dynamical neutralization of the cosmological constant,” *JHEP* **0006**, 006 (2000) [hep-th/0004134].
- [19] J. Polchinski and A. Strominger, “New vacua for type II string theory,” *Phys. Lett. B* **388** (1996) 736 [hep-th/9510227].
- [20] C. P. Burgess, D. Hoover and G. Tasinato, “UV Caps and Modulus Stabilization for 6D Gauged Chiral Supergravity,” *JHEP* **0709** (2007) 124 [arXiv:0705.3212 [hep-th]].
- [21] R. Diener and C. P. Burgess, “Bulk Stabilization, the Extra-Dimensional Higgs Portal and Missing Energy in Higgs Events,” *JHEP* **1305** (2013) 078 [arXiv:1302.6486 [hep-ph]].

- [22] For a stabilization mechanism using the competition between brane couplings of a bulk field see
W. D. Goldberger and M. B. Wise, “Modulus stabilization with bulk fields,” *Phys. Rev. Lett.* **83** (1999) 4922 [hep-ph/9907447].
- [23] Y. Aghababaie, C. P. Burgess, J. M. Cline, H. Firouzjahi, S. L. Parameswaran, F. Quevedo, G. Tasinato and I. Zavala, “Warped brane worlds in six-dimensional supergravity,” *JHEP* **0309**, 037 (2003) [hep-th/0308064].
- [24] F. Niedermann and R. Schneider, “Fine-tuning with Brane-Localized Flux in 6D Supergravity,” arXiv:1508.01124 [hep-th];

C.P. Burgess, R. Diener and M. Williams, “Reply to Fine-tuning with Brane-Localized Flux in 6D Supergravity,” arXiv:1508.xxxxx [hep-th].
- [25] S. Weinberg, “The Cosmological Constant Problem,” *Rev. Mod. Phys.* **61**, 1 (1989).
- [26] N. Arkani-Hamed, S. Dimopoulos and G. R. Dvali, “The hierarchy problem and new dimensions at a millimeter,” *Phys. Lett. B* **429** (1998) 263 [arXiv:hep-ph/9803315];
I. Antoniadis, N. Arkani-Hamed, S. Dimopoulos and G. R. Dvali, “New dimensions at a millimeter to a Fermi and superstrings at a TeV,” *Phys. Lett. B* **436** (1998) 257 [arXiv:hep-ph/9804398].
- [27] S. Weinberg, *Gravitation and Cosmology*, Wiley 1973.
- [28] C. W. Misner, J. A. Wheeler and K. S. Thorne, *Gravitation*, W. H. Freeman & Company 1973.
- [29] W. D. Goldberger and M. B. Wise, “Renormalization group flows for brane couplings,” *Phys. Rev. D* **65**, 025011 (2002) [hep-th/0104170].

C. de Rham, “The Effective field theory of codimension-two branes,” *JHEP* **0801**, 060 (2008) [arXiv:0707.0884 [hep-th]].
- [30] Y. Aghababaie, C. P. Burgess, S. L. Parameswaran and F. Quevedo, “SUSY breaking and moduli stabilization from fluxes in gauged 6-D supergravity,” *JHEP* **0303** (2003) 032 [hep-th/0212091].
- [31] M. B. Green and J. H. Schwarz, “Anomaly Cancellation in Supersymmetric D=10 Gauge Theory and Superstring Theory,” *Phys. Lett. B* **149**, 117 (1984).

- [32] M. B. Green, J. H. Schwarz and P. C. West, “Anomaly Free Chiral Theories in Six-Dimensions,” Nucl. Phys. B **254**, 327 (1985);
- J. Erler, “Anomaly cancellation in six-dimensions,” J. Math. Phys. **35** (1994) 1819 [hep-th/9304104].
- [33] M. J. Duff, “The Cosmological Constant Is Possibly Zero, but the Proof Is Probably Wrong,” Phys. Lett. B **226**, 36 (1989) [Conf. Proc. C **8903131**, 403 (1989)].
- [34] C. P. Burgess, L. van Nierop, S. Parameswaran, A. Salvio and M. Williams, “Accidental SUSY: Enhanced Bulk Supersymmetry from Brane Back-reaction,” JHEP **1302**, 120 (2013) [arXiv:1210.5405 [hep-th]].
- [35] A. Albrecht, C. P. Burgess, F. Ravndal and C. Skordis, “Natural quintessence and large extra dimensions,” Phys. Rev. D **65** (2002) 123507 [astro-ph/0107573].
- [36] H. B. Nielsen and P. Olesen, “Vortex Line Models for Dual Strings,” Nucl. Phys. B **61**, 45 (1973).
- [37] M. Cvetič, G. W. Gibbons, C. N. Pope, “A String and M theory origin for the Salam-Sezgin model,” Nucl. Phys. **B677** (2004) 164-180. [hep-th/0308026];
- T. G. Pugh, E. Sezgin, K. S. Stelle, “D=7 / D=6 Heterotic Supergravity with Gauged R-Symmetry,” JHEP **1102** (2011) 115. [arXiv:1008.0726 [hep-th]];
- M. Cicoli, C. P. Burgess, F. Quevedo, “Anisotropic Modulus Stabilisation: Strings at LHC Scales with Micron-sized Extra Dimensions,” [arXiv:1105.2107 [hep-th]];
- B. Crampton, C.N. Pope and K.S. Stelle, “Braneworld localisation in hyperbolic spacetime,” JHEP **1412** (2014) 035 [arXiv:1408.7072 [hep-th]].
- [38] C. P. Burgess, L. van Nierop and M. Williams, “Distributed SUSY breaking: dark energy, Newton’s law and the LHC,” JHEP **1407**, 034 (2014) [arXiv:1311.3911 [hep-th]].
- [39] C. P. Burgess and D. Hoover, “UV sensitivity in supersymmetric large extra dimensions: The Ricci-flat case,” Nucl. Phys. B **772** (2007) 175 [hep-th/0504004];
- D. M. Ghilencea, D. Hoover, C. P. Burgess and F. Quevedo, “Casimir energies for 6D supergravities compactified on T(2)/Z(N) with Wilson lines,” JHEP **0509** (2005) 050 [hep-th/0506164];

- D. Hoover and C. P. Burgess, “Ultraviolet sensitivity in higher dimensions,” JHEP **0601** (2006) 058 [hep-th/0507293];
- [40] J. Hughes, J. Liu and J. Polchinski, “Virasoro-shapiro From Wilson,” Nucl. Phys. B **316** (1989) 15.
- “Supermembranes,” Phys. Lett. B **180** (1986) 370.
- J. Hughes and J. Polchinski, “Partially Broken Global Supersymmetry and the Superstring,” Nucl. Phys. B **278** (1986) 147.
- [41] C. Brans and R. H. Dicke, “Mach’s Principle and a Relativistic Theory of Gravitation,” Phys. Rev. **124** (1961) 925;
- R. H. Dicke, “Mach’s Principle and Invariance under Transformation of Units,” Phys. Rev. **125** (1962) 2163;
- C. Brans, “Mach’s Principle and a Relativistic Theory of Gravitation. II,” Phys. Rev. **125** (1962) 2194.
- [42] C. P. Burgess, L. van Nierop and M. Williams, “Gravitational Forces on a Codimension-2 Brane,” JHEP **1404** (2014) 032 [arXiv:1401.0511 [hep-th]].
- [43] C. M. Will, “The Confrontation between general relativity and experiment,” Living Rev. Rel. **9** (2006) 3 [gr-qc/0510072].
- [44] J. Khoury and A. Weltman, “Chameleon cosmology,” Phys. Rev. D **69** (2004) 044026 [astro-ph/0309411];
- J. Khoury and A. Weltman, “Chameleon fields: Awaiting surprises for tests of gravity in space,” Phys. Rev. Lett. **93** (2004) 171104 [astro-ph/0309300];
- P. Brax, C. van de Bruck, A. C. Davis, J. Khoury and A. Weltman, “Chameleon dark energy,” AIP Conf. Proc. **736** (2005) 105 [astro-ph/0410103];
- K. Hinterbichler, J. Khoury and H. Nastase, “Towards a UV Completion for Chameleon Scalar Theories,” JHEP **1103** (2011) 061 [JHEP **1106** (2011) 072] [arXiv:1012.4462 [hep-th]].

Chapter 6

The Extra-Dimensional Higgs Portal

This chapter is a verbatim presentation of the following paper

R. Diener and C. P. Burgess, “Bulk Stabilization, the Extra-Dimensional Higgs Portal and Missing Energy in Higgs Events,” JHEP 1305 078 (2013), arXiv:1302.6486

This paper presents a detailed phenomenological study of extra-dimensional stabilization. The previous chapters identified a mechanism for stabilizing the size of the extra dimensions at exponentially large values that relied on nontrivial couplings between a brane and bulk scalar field, which is an important part of the solution to the hierarchy problem. This paper adopts the point of view that, at energies much higher than the Kaluza Klein scale, the details of such a coupling are not important and the implications of the stabilization mechanism can be understood in a bottom-up model that considers only relevant interactions between a bulk scalar and the Standard Model

brane.

Among these interactions is the extra-dimensional Higgs portal coupling $g \Phi H^\dagger H$. This interaction, which mixes the Higgs field with the bulk scalar field, is dimension-4 and is not suppressed at low energies, unlike the usual brane-bulk interactions which are gravitational. The resulting phenomena are therefore expected to be observable and subject to phenomenological constraints, and this is shown to be the case. Invisible Higgs decay width and missing energy signals at colliders are identified as signatures of Higgs bulk mixing, while the strongest observational constraints on Higgs-bulk mixing come from considering energy loss in astrophysical objects.

To understand these phenomena, it is necessary to absorb short-distance divergences into a renormalization of brane couplings and the classical renormalization of brane couplings, which was alluded to in other parts of this thesis, is presented here in detail. The classical running of couplings is shown to have positive implications for vacuum stability. Classical running can also give rise to Landau poles at low energies, and avoiding such poles furnishes a theoretical constraint on Higgs-bulk mixing. Nonetheless, even when these are combined with observational constraints, there remains a large region of parameter space that can be probed at the Large Hadron Collider and future colliders. So it is possible that the Higgs-bulk portal could be the first sign of large extra dimensions.

6.1 Introduction

In particle physics it is the best of times, and it is the worst of times. On one hand the recent discovery [1] of a new particle at the LHC moves us into the long-awaited study of the new particle's properties, after several decades spent exploring the physics of

constraints. If the new particle's interpretation as a Higgs — or *the* Higgs, if the Standard Model description continues to work — survives, then we can anticipate an unprecedented new era probing vacuum physics.

On the other hand, the LHC has yet to produce compelling evidence for the kinds of physics widely expected to lie beyond the Standard Model. The hierarchy problem lies at the heart of these expectations, leading broadly to three main options¹ for LHC-observable new electroweak physics over the years: compositeness models [3, 4]; supersymmetry [5, 6] (linearly realized²); and extra-dimensional scenarios (both warped [9] and unwarped [10]). Absent compelling evidence for any of these three categories, it is crucial for theorists to seek new ways to distinguish the mechanisms underlying each.

The purpose of this paper is to identify new ways to use the properties of the Higgs to explore extra-dimensional models. Building on earlier work — in 5D [11] and higher dimensional scenarios [12, 13, 14, 15] — we track how the vacuum energetics of the Higgs potential interacts with the physics that stabilizes the extra dimensions, and show how this can open a new observable portal onto extra-dimensional dynamics.

At present most bounds on extra dimensions come from the kinematics of mixing and energy loss with the bulk gravitational degrees of freedom [16]. Yet a central part of solving the hierarchy problem using extra dimensions is understanding the vacuum physics that stabilizes their size at the required value, both for RS models (where the hierarchy between the electroweak and Planck scales comes from a

¹These need not be mutually exclusive, with some composite models potentially being equivalent to some extra-dimensional models [2].

²See, however, [7] for how supersymmetry could be present (but nonlinearly realized [8]) at electroweak energies and below, without requiring the existence of the superpartners that remain missing from experiments.

size-dependent warp factor) and for ADD-type models (where it is the large extra-dimensional volume itself that provides the hierarchy). All of the known mechanisms for this stabilization involve introducing new bulk degrees of freedom (typically scalar fields), whose couplings to ordinary matter are only slightly less robust than those of the metric. It is these couplings to the Higgs that we aim to constrain. We identify two kinds of observable consequences for these couplings.

- *Modified Higgs mass-coupling relations:* due to the dependence of the Higgs potential on the new bulk fields. The interplay between these two fields changes the relationship between the Higgs mass and its couplings relative to Standard Model expectations;
- *Contributions to the Higgs invisible ‘width’:* due to mixing between the Higgs and bulk states. In particular, we find that the expected LHC bounds on this width are competitive with bounds from lower-energy observables, such as energy loss from astrophysical systems, anomalous magnetic moments and the like.

Two things are crucial about both of these effects. First, because the bulk fields involved are not the graviton, their couplings need not be precisely gravitational in strength. In particular (a point made earlier for ADD models in [15]) depending on the number of extra dimensions present, they can involve dimensionless couplings, and so be less suppressed at low energies than are graviton interactions. (Dimensionless couplings can also arise for Higgs-curvature interactions in 6D, but unlike the Higgs-bulk portal they remain suppressed at low energies because of the derivative nature of the curvature couplings [12].)

Second, the interplay between the (brane-localized) Higgs and extra-dimensional (bulk) stabilization mechanisms depends crucially on understanding how branes back-react on the bulk. Although this is understood relatively well for branes with one transverse dimension (such as arise in RS models) in terms of Israel junction conditions [17], it has only recently been systematically developed [18] for branes with two or more transverse dimensions, such as appear in the ADD picture. The understanding of codimension-2 back-reaction came comparatively late because of technical complications associated with the divergence of bulk fields near brane positions (which happens only with two or more transverse dimensions), and the need to absorb these into renormalizations of the brane couplings [19, 20].

6.1.1 Higher-dimensional stabilization

Until recently a big competitive advantage of RS models over ADD models was the existence of a simple and robust way to stabilize the extra dimensions: the Goldberger-Wise mechanism [21]. In this mechanism a bulk scalar field is introduced that couples to the branes situated at both ends of the RS scenario's one extra dimension, with couplings chosen to frustrate the scalar's ability to reach a constant vacuum configuration. (This can be achieved by having branes disagree with one another about the field value that minimizes the scalar potential.) Because branes are located at specific places in the extra dimension, the resulting frustration sets up gradients in the bulk scalar that make the minimum energy depend on the distance between the branes (and so also on the extra-dimensional size). An attractive feature of the RS model is that the warp factor then naturally exponentiates a modestly large extra-dimensional size into an enormous electroweak hierarchy. (Similar frustration can

also be arranged with bulk scalars in more than one extra dimension, with sometimes intriguing implications for the Higgs vacuum [13, 14].)

A similarly robust mechanism for stabilizing large dimensions has been missing for standard ADD models, but an analogue was recently found [22] for their supersymmetric generalizations [23, 24, 25] by applying to them a 6D cousin [26] of the Goldberger-Wise mechanism. In such theories the extra dimensions are stabilized classically through flux-stabilization, as is often possible for supersymmetric systems (and for which 6D systems provided the first examples [24]). In this mechanism the flux of a bulk magnetic field (which is typically required by anomaly cancellation to exist among the field content of the 6D supergravity [23, 24, 25]) threads the two extra dimensions, that have the topology of a sphere. Dirac quantization of this flux makes it energetically costly to shrink the dimensions, providing a counterbalance against its gravitational collapse.

However complete stabilization purely within the bulk is never quite possible because of a classical scale invariance of the 6D supergravity action, which leaves a flat direction parameterized by a bulk scalar field, χ (the ‘dilaton’, which sits within the ‘extended’ metric supermultiplet). Flux stabilization relates the extra-dimensional radius to this flat direction through the expression

$$r^2 = \ell^2 e^{-\chi}, \quad (6.1)$$

where ℓ is a length of order (but, in controlled calculations, parametrically moderately larger than) the 6D Planck scale, set by the flux stabilization.

Fixing r completely requires breaking the classical scale invariance, and lifting the classical bulk flat direction. As shown in ref. [22], this can be achieved classically

through its couplings to branes, whose interactions need not share the scale invariance of the bulk. In particular it is not difficult to arrange for moderately large negative values. Once this is done flux stabilization — *via* eq. (6.1) — ensures the resulting radius is exponentially large in χ , naturally ensuring an exponentially large hierarchy in these models as well. In the special case of supersymmetric ADD models [25?] $\ell \sim (10 \text{ TeV})^{-1}$, and so micron-sized dimensions can be achieved with $\chi \sim -70$. But the stabilization mechanism itself doesn't rely on using an ADD framework, and could equally well apply if it were the Kaluza-Klein (KK) scale that were of electroweak size.

Of course quantum effects can modify eq. (6.1) because they break the classical bulk scale invariance. But since each loop breaks scale invariance by a specific amount, these turn out to generate corrections as a series in $e^{2\chi}$ [28], and so do not ruin the exponentially large size of r .

6.1.2 Relevance to the Higgs

From the point of view of the Higgs, what is important about the above mechanisms (in both 5 and 6 dimensions) is that they require the presence of a coupling between a bulk scalar field and the brane on which the Higgs sits. For instance, in the 6D case the most general renormalizable interactions between a brane-localized Standard Model and a (canonically normalized) electroweak singlet bulk scalar, Φ , have the form

$$S_{\text{int}} = - \int d^4x \sqrt{-\gamma} U(H^\dagger H, \Phi) , \quad (6.2)$$

with

$$\begin{aligned} U(H^\dagger H, \Phi) &= T_0 + \frac{\lambda_2}{2} (\Phi_b + V^2)^2 + g H^\dagger H \Phi_b + \lambda \left(H^\dagger H - \frac{v^2}{2} \right)^2 \\ &= T + \mu_\Phi^2 \Phi_b + \frac{\lambda_2}{2} \Phi_b^2 - (\mu_H^2 - g \Phi_b) H^\dagger H + \lambda (H^\dagger H)^4, \end{aligned} \quad (6.3)$$

where

$$T := T_0 + \frac{\lambda_2 V^4}{2} + \frac{\lambda v^4}{4}, \quad \mu_\Phi^2 := \lambda_2 V^2 \quad \text{and} \quad \mu_H^2 := \lambda v^2, \quad (6.4)$$

and $\Phi_b = \Phi(x, y = y_b)$, denotes the evaluation of the bulk scalar at the position of the brane. It is the dimensionless coupling g that represents the unique Standard Model portal into extra dimensions within this six-dimensional context.

This means that the vacuum energetics of the Higgs field interacts with the physics that stabilizes the extra dimensions, and both Higgs and bulk fields must be varied to find the proper vacuum configuration. In particular, the bulk scalar couplings can act to help or hinder the propensity for electroweak symmetry breaking. For instance, to the extent that large volume requires $\Phi_b < 0$ we see that this acts to increase³ the effective value $\mu_{H\text{eff}}^2 = \mu_H^2 - g \Phi_b$, and so assists the formation of a nonzero *v.e.v.* for H . In what follows §6.2.2 fleshes this out more explicitly, with care being taken to handle properly the renormalizations required because Φ_b actually diverges at the brane position.

Similarly, using the replacement

$$H = \frac{1}{\sqrt{2}} \begin{pmatrix} 0 \\ v + h \end{pmatrix}, \quad (6.5)$$

³For $g > 0$.

in the term $g H^\dagger H \Phi_b$ contributes to Higgs-bulk mixing, and so to invisible channels where energy leaks into the extra dimensions during Higgs-production processes. As we show below, such leakage looks like a Higgs invisible width, and so is subject to similar constraints. Furthermore, since the coupling g is dimensionless, this loss rate is less suppressed at lower energies than would have been true for gravitational energy loss, and so allows better bounds and opportunities for detection [15]. §6.2.3 computes this more carefully, extending the results of [15] by taking full account of the Higgs-KK mixing brought about by brane-bulk back-reaction.

The calculation in 6D in many ways resembles earlier work which considered Higgs-curvature mixing [12], of the form $H^\dagger H R$, but with three differences. First, because the curvature couplings involve more derivatives than do the Higgs-scalar couplings, the curvature mixing remains suppressed at low energies (like other gravitational interactions). Secondly, unlike these earlier calculations, we are able to compute both the real and imaginary parts of the Higgs production amplitude and so can compute the full line-shape rather than just its effective width. We can do so because our treatment of back-reaction allows us to renormalize the divergences that complicate obtaining the real part, associated with the near-brane divergences of the bulk fields. This technology allows us to extend the study of mixing to invisible final states in astrophysics, and at colliders. Finally, we include *all* possible renormalizable interactions, including in particular the quadratic self-coupling, λ_2 , for the bulk field on the brane. This inclusion has important consequences, since bounds on g weaken with increasing λ_2 , ultimately allowing a detectable invisible width at the LHC be consistent with strong constraints from low-energy astrophysics (see Fig. 6.1).

Although our results apply both to the cases of large dimensions ($m_h \gg m_{KK}$)

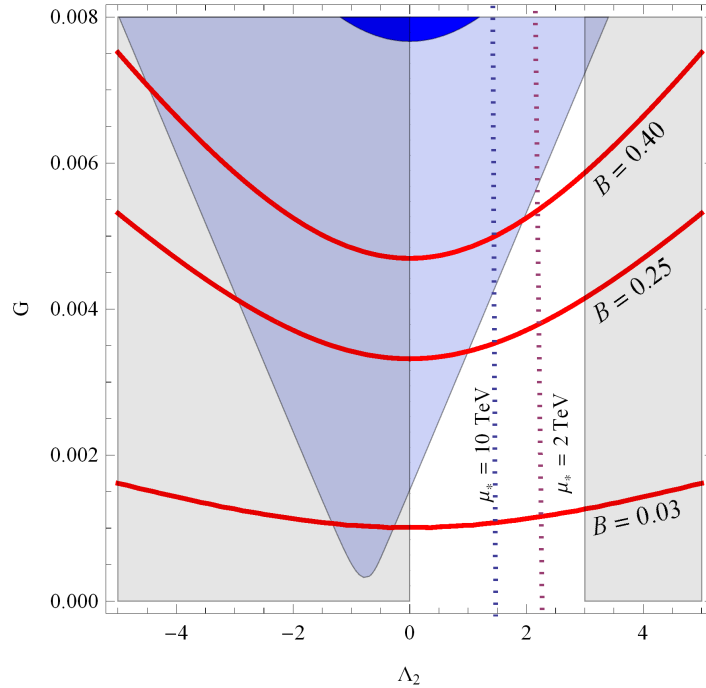


Figure 6.1: A plot summarizing the various constraints and discovery potential of Higgs-bulk mixing in the $G = \bar{g}/\sqrt{\alpha}$ vs $\Lambda_2 = \bar{\lambda}_2/\alpha$ plane (renormalized at $\bar{r} = 1/m_h$), in the large-volume limit ($m_h \gg m_{KK}$). The quantity $\alpha \sim 1$ is a measure of the defect angle near the brane, as defined in detail in §6.2.1. The dark (blue) shaded region is the region disfavoured by LHC global fits. The medium (blue) shaded region is the conservative bound from nucleon-bulk bremsstrahlung in SN1987a, assuming $T_{SN} = 20$ MeV. The lightest (gray) shade denotes regions excluded by demanding no Landau poles below $\mu_* = 1$ TeV, with the vertical dotted lines denoting how this bound changes with the choice of ultraviolet scale μ_* . Also plotted are lines of constant invisible branching ratio B that will be probed with additional data at the LHC or future experiments, all of which constrain this quantity.

and small ones ($m_h \ll m_{KK}$), when discussing the phenomenology we focus on the case when the dimensions are large. We find, as did earlier authors [12, 15], that a Higgs undergoing Higgs-bulk mixing in many ways resembles a Higgs that can decay into invisible channels. Indeed once both real and imaginary parts of the amplitude are computed, we find that the resemblance becomes perfect for processes with the Higgs resonantly produced in the narrow-width limit.

However, because the resonant, narrow-width limit is not always sufficient, there

are also important differences between a bulk-mixed Higgs and one with access to invisible decays. Most important among these is the existence of strong bounds from astrophysical processes like SN1987a. These are not normally relevant for a Higgs with invisible decay channels (or for Higgs-bulk mixing through the $H^\dagger H R$ term), because the rate for producing the Higgs is too small at low energies to give an appreciable energy-loss channel. The same is not true for Higgs-bulk mixing in the scalar potential, however, since this is not suppressed at low energies, and is not dominated by resonant Higgs production. It is instead enhanced by the kinematic availability of a large number of very light states for which the couplings cannot be neglected. The resulting constraint is shown in Fig. 6.1, together with the constraint coming from the successful Standard Model description of the observed Higgs, and contours indicating the size of the effective invisible Higgs width. Although astrophysics furnishes a very strong constraint, it does not exclude the range of interest to future LHC measurements. It does not do so because it is not a resonant process, and so involves a different combination of parameters than are measured at the LHC in the $g - \lambda_2$ plane.

The next sections present the details of this analysis as follows. First, §6.2 derives the main expressions for the propagation eigenstates when the Higgs mixes with bulk. Armed with these calculations we discuss some of the resulting phenomenology in §6.3, including the lineshape for Higgs production at the LHC, and various bounds from lower energy phenomena. Our conclusions are summarized briefly in §6.4.

6.2 Higgs-Bulk Dynamics

In this section we compute in detail the implications of a Higgs-bulk interaction of the form given in eq. (6.3). For concreteness we restrict from here on to the 6D case, for which back-reaction issues are much less well-explored.

We start, in §6.2.1 where the bulk and brane actions and field equations, including the conditions for back-reaction, are described. The next subsection, §6.2.2 then calculates how eq. (6.1) changes the energy minimization for the Higgs and bulk scalar fields and so alters the expression for the Higgs *v.e.v.* in terms of the parameters in its potential. This is followed in §6.2.3 by a calculation of the spectrum of fluctuations, including a treatment of how the on-brane Higgs mixes with the bulk KK states. We consider two limits of interest in this mixing, depending on whether the KK mass is small or of the same order as the on-brane Higgs mass. The former is of most interest for ADD and supersymmetric large-dimension (SLED) scenarios, while the latter would be of interest for dimensions whose KK scale is of order the electroweak scale. We specialize to the case of large dimensions when examining phenomenology more explicitly.

6.2.1 Field equations and back-reaction

We start by describing the 6D bulk and 4D brane systems of interest. For simplicity we focus purely on a single bulk scalar field, coupled to a Standard Model Higgs doublet on a space-filling codimension-2 brane situated at a specific spot in the two extra dimensions.

The Action

Consider a massless, free, 6D bulk scalar, Φ , with action

$$S_B = - \int d^6x \sqrt{-\mathcal{G}} \left(\frac{1}{2} \mathcal{G}^{MN} \partial_M \Phi \partial_N \Phi \right). \quad (6.6)$$

We do not include a scalar potential in the bulk, and for ADD-type models this could be naturally enforced through a shift symmetry. The presence of scalars in the gravity supermultiplet and in the massless hypermultiplet representations of 6D supersymmetry also make it natural to include light bulk scalars when the extra dimensions are supersymmetric. In the simplest case for bulk stabilization the supergravity of interest is gauged, chiral supergravity, and $\Phi = V^2 \chi$ represents the canonically normalized dilaton that transforms in the (extended) gravity multiplet [23, 24]. In this case there is a bulk scalar potential, $U_B(\chi) \propto e^\chi$, which considerably complicates the treatment of fluctuations once the metric is included. However because the gravitational couplings are RG-irrelevant we omit them for simplicity of presentation, and expect our considerations explored here to apply at sufficiently low energies.

Next, consider a space-filling 4D brane that is located at a particular point, $y = y_b$, within the extra dimensions. With eq. (6.3) in mind we take the brane action to be

$$S_b = \int d^4x \sqrt{-\gamma} \left(\mathcal{L}_{SM} - T_0 - \frac{\lambda_2}{2} (\Phi_b + V^2)^2 - g H^\dagger H \Phi_b \right), \quad (6.7)$$

where $\Phi_b := \Phi(x, y = y_b)$ and $\gamma_{\mu\nu} = \mathcal{G}_{MN}(x, y = y_b) \partial_\mu z^M \partial_\nu z^N$ is the induced metric on the brane, whose world-sheet is denoted $z^M = \{x^\mu, y^m = y_b^m(x)\}$. \mathcal{L}_{SM} denotes the Standard Model action, but for the present purposes we need only work with its

Higgs part:

$$-\mathcal{L}_{SM} = \gamma^{\mu\nu} \partial_\mu H^\dagger \partial_\nu H + \lambda \left(H^\dagger H - \frac{\mu_H^2}{2\lambda} \right)^2. \quad (6.8)$$

Thus, the complete, on-brane scalar potential reads

$$U_b = T - \mu_H^2 H^\dagger H + \lambda (H^\dagger H)^2 + \mu_\Phi^2 \Phi_b + \frac{\lambda_2}{2} \Phi_b^2 + g H^\dagger H \Phi_b, \quad (6.9)$$

as anticipated in eq. (6.1). This contains all possible terms involving only H and the Standard Model that are local and involve only relevant or marginal couplings.

Background Geometry

For the purposes of discussing Higgs energetics, consider the following unwarped, axisymmetric background geometry,

$$ds^2 = \mathcal{G}_{MN} dx^M dx^N = \eta_{\mu\nu} dx^\mu dx^\nu + f^2(r) d\theta^2 + dr^2, \quad (6.10)$$

where r denotes proper distance away from the brane on which the Higgs resides. We allow for the possibility of a conical singularity at this brane by allowing a defect angle: $0 < \theta < 2\pi\alpha$, with $0 < \alpha < 1$. Control of approximations usually requires a small defect angle, so $|\alpha - 1| \ll 1$. In real examples of interest the radial coordinate runs through a finite range, $0 < r < \pi R$, with $r = \pi R$ associated with another 4D brane at the opposite end of the extra dimensions.

For the present purposes we ask for simplicity that the singular behaviour of the extra-dimensional geometry be no worse than a conical singularity at the brane position, and so require $f(r) \approx r$ for $r \ll R$. This is not the most general case but is broad enough to include a variety of back-reacted examples, such as locally flat extra

dimensions — corresponding to $f(r) = r$ — and spherical (or rugby-ball, for nonzero deficit angle) extra dimensions — for which $f(r) = R \sin(r/R)$ — as well as other potentially more exotic geometries.

We do not specify $f(r)$ explicitly other than this near-brane limit. This generality is possible because for collider applications to ADD-type models not much depends on $f(r)$. Physically, this is because it is only the enormous phase space associated with the large number of very high energy modes that allows observably large contributions to collider physics at all. But these modes have such short wavelengths that they are insensitive to the large-scale shape of the extra dimensions (see, for example, [29] for explicit calculations that illustrate this point).

6.2.2 Vacuum configurations

We now seek vacuum solutions to the coupled brane-bulk field equations, subject to the assumptions of 4D Lorentz invariance and axisymmetry in the extra dimensions.

Bulk field equations and vacuum solutions

Using $\Phi = \Phi(r)$ in the bulk field scalar equation, $\square\Phi = 0$, then gives

$$\partial_r(f\partial_r\Phi) = 0, \tag{6.11}$$

which integrates to give

$$\partial_r\Phi = \frac{\mathcal{A}}{f(r)}, \tag{6.12}$$

for integration constant \mathcal{A} . A second integration gives

$$\Phi(r) = \mathcal{A} \int_{\hat{r}}^r \frac{du}{f(u)} := \mathcal{A}F(r, \hat{r}), \quad (6.13)$$

where we define a new coordinate, F , using the condition $dF := dr/f$.

In principle we also must satisfy the Einstein equations (and equations for any other bulk fields), but instead we use the fact that we do not require more than the near-brane form for $f(r)$ to side-step the effort of doing so. (See, however, [30] for many explicit solutions to the 6D supergravity equations, including both those where the branes at $r = 0$ and $r = \pi R$ have different properties. Many among these solutions are consistent with the near-brane forms being assumed here.)

Boundary conditions and back-reaction

We seek to eliminate the integration constants – \mathcal{A} , \hat{r} , *etc.* — of the bulk solution in terms of the physical couplings of the brane action, and this is done using the near-brane boundary conditions that express how the branes back-react onto the bulk [18]. Specialized to the bulk scalar field considered here these state

$$-2\pi\alpha f \Phi'_b - \frac{\delta S_b}{\delta \Phi} = -2\pi\alpha \mathcal{A} + gH^\dagger H + \lambda_2 \Phi_b + \mu_\Phi^2 = 0, \quad (6.14)$$

where $\Phi_b := \Phi(0)$, $\Phi'_b := (\partial_r \Phi)_{r=0}$ and the second equality in eq. (6.14) uses the field equation, eq. (6.12), as well as the form, eq. (6.7), of the brane action. [One way of deriving this boundary condition – for completeness, sketched in more detail in Appendix D.1 – is by excising the codimension-2 brane with a small regularizing codimension-1 cylinder (designed to dimensionally reduce to the above codimension-2

action when the cylinder's radius is very small), and using Israel junction conditions for the cylinder.]

There are similar equations governing the near-brane form of the metric and any other bulk fields, but for the present purposes these just dictate how the defect angle depends on the value of U_b when evaluated at the classical solutions for H and Φ . Similar boundary conditions also apply for the brane at $r = \pi R$, and together with eq. (6.14) these generically can be used to remove the two free integration constants in $\Phi(r)$ [26].

The brane-localized fields must also satisfy their own classical field equations,

$$\frac{\delta S_b}{\delta H} = 0, \quad (6.15)$$

and so for x -independent H eq. (6.14) should be supplemented with

$$H^\dagger H = \frac{1}{2\lambda}(\mu_H^2 - g\Phi_b). \quad (6.16)$$

This can be used to eliminate H from (6.14), to give

$$-2\pi\alpha\mathcal{A} + \lambda_{2\text{eff}}\Phi_b + \mu_{\Phi\text{eff}}^2 = 0, \quad (6.17)$$

where we define the ‘effective’ couplings

$$\lambda_{2\text{eff}} := \lambda_2 - \frac{g^2}{2\lambda}; \quad \mu_{\Phi\text{eff}}^2 := \mu_\Phi^2 + \frac{g\mu_H^2}{2\lambda}. \quad (6.18)$$

Divergences and classical brane renormalization

The complication of bulk divergences enters once eq. (6.13) is used to eliminate Φ_b . This diverges logarithmically near $r = 0$ due to the asymptotic limit $f \approx r$ there:

$$\Phi(r) = \mathcal{A} \left[\log(r/\hat{r}) + \text{nonsingular} \right] \quad (\text{as } r \rightarrow 0). \quad (6.19)$$

Because Φ diverges logarithmically as $r \rightarrow 0$, we first regularize by taking $r \rightarrow \epsilon \ll R$, and then renormalize by allowing the brane couplings to be ϵ -dependent in such a way that $\epsilon \rightarrow 0$ can be taken smoothly [18, 19]. Although unfamiliar in RS models, such classical divergences (and renormalizations) are generic to *any* theories with sources with two or more transverse dimensions (making RS models the exception, rather than the rule). Physically, these divergences arise from taking the source brane to be infinitely thin, and as such they can be lumped together with all of the other quantum ultraviolet (UV) effects that renormalizations of brane couplings would in any case have to encompass.

With this understanding the boundary condition (6.17) becomes

$$-2\pi\alpha\mathcal{A} + \lambda_{2\text{eff}}(\epsilon)\mathcal{A}F(\epsilon, \hat{r}) + \mu_{\Phi\text{eff}}^2(\epsilon) = 0, \quad (6.20)$$

and we require the singular form of the couplings $\lambda_{2\text{eff}}$ and $\mu_{\Phi\text{eff}}^2$ in order to determine how the near-brane boundary condition relates the integration constants \mathcal{A} and \hat{r} . The one condition that eq. (6.20) remain finite is insufficient in itself to fix the ϵ -dependence of all couplings, but these are easily determined by repeating the steps of [18, 19] and demanding the finiteness of a few other quantities. For completeness, one way of doing this is described Appendix D.1, which yields the same results as

earlier authors when restricted to the couplings considered there.

The result for the ϵ -dependence required of the brane couplings obtained in this way is simply summarized as follows,

$$\begin{aligned} \bar{\mu}_\Phi^2(\bar{r}) &= \frac{\mu_\Phi^2}{1 - \frac{\lambda_2}{2\pi\alpha} F(\epsilon, \bar{r})}; & \bar{g}(\bar{r}) &= \frac{g}{1 - \frac{\lambda_2}{2\pi\alpha} F(\epsilon, \bar{r})}; & \bar{\lambda}_2(\bar{r}) &= \frac{\lambda_2}{1 - \frac{\lambda_2}{2\pi\alpha} F(\epsilon, \bar{r})}; \\ \bar{\lambda}(\bar{r}) &= \lambda + \frac{1}{2} \left(\frac{g^2}{2\pi\alpha} \right) \frac{F(\epsilon, \bar{r})}{1 - \frac{\lambda_2}{2\pi\alpha} F(\epsilon, \bar{r})}; & \bar{\mu}_H^2(\bar{r}) &= \mu_H^2 - \left(\frac{gM^2}{2\pi\alpha} \right) \frac{F(\epsilon, \bar{r})}{1 - \frac{\lambda_2}{2\pi\alpha} F(\epsilon, \bar{r})}, \end{aligned} \quad (6.21)$$

where it is the renormalized ('barred') couplings that are held fixed as $\epsilon \rightarrow 0$. The associated RG equations can be found in eqs. (6.134), below. Here \bar{r} is an arbitrary renormalization scale, and the property $F(r, r) = 0$ ensures that the bare couplings may be interpreted as the renormalized couplings evaluated at $\bar{r} = \epsilon$. Given these expressions, the ϵ -dependence of the effective coupling combinations appearing in eq. (6.20) are easily read off:

$$\bar{\lambda}_{2\text{eff}}(\bar{r}) = \frac{\lambda_{2\text{eff}}}{1 - \frac{\lambda_{2\text{eff}}}{2\pi\alpha} F(\epsilon, \bar{r})}; \quad \bar{\mu}_{\Phi\text{eff}}^2(\bar{r}) = \frac{\mu_{\Phi\text{eff}}^2}{1 - \frac{\lambda_{2\text{eff}}}{2\pi\alpha} F(\epsilon, \bar{r})}. \quad (6.22)$$

Using these expressions to eliminate $\mu_{\Phi\text{eff}}^2$ and $\lambda_{2\text{eff}}$ from eq. (6.20) gives a result for \mathcal{A} that is finite when $\epsilon \rightarrow 0$,

$$2\pi\alpha \mathcal{A} = \frac{\mu_{\Phi\text{eff}}^2}{1 - \frac{\lambda_{2\text{eff}}}{2\pi\alpha} F(\epsilon, \hat{r})} = \frac{\bar{\mu}_{\Phi\text{eff}}^2(\bar{r})}{1 - \frac{\bar{\lambda}_{2\text{eff}}(\bar{r})}{2\pi\alpha} F(\bar{r}, \hat{r})} = \bar{\mu}_{\Phi\text{eff}}^2(\hat{r}), \quad (6.23)$$

where the second equality gives the required relation between \mathcal{A} and \hat{r} in terms of the renormalized coupling $\bar{\mu}_{\Phi\text{eff}}^2$ evaluated at an arbitrary scale \bar{r} . The third equality shows how this relation simplifies when expressed in terms of $\bar{\mu}_{\Phi\text{eff}}^2$ defined at the

renormalization scale \hat{r} . As these expressions make clear, the dependence of the right-side of the last equality on the arbitrary parameter \bar{r} is illusory. In what follows we will often choose the arbitrary renormalization point for which the answer is most condensed, at the expense of making a logarithmic dependence implicit.

As mentioned earlier, the boundary condition at the distant brane at $r = \pi R$ imposes a second relation between \mathcal{A} and \hat{r} , in general fixing both and so completely fixing the bulk field configuration [26]. For the present purposes we leave \hat{r} arbitrary, a placeholder for this faraway boundary condition. It is easy to track in what follows because it appears only through the function F , a dependence that is generically logarithmic and so quite weak.

With this understanding the bulk solution now becomes

$$\Phi(r) = \left(\frac{\bar{\mu}_{\Phi \text{ eff}}^2(\hat{r})}{2\pi\alpha} \right) F(r, \hat{r}), \quad (6.24)$$

which, when substituted into eq. (6.16) gives the Higgs expectation as

$$H^\dagger H = \frac{1}{2\lambda} \left(\mu_H^2 - g \Phi(\epsilon) \right) = \frac{1}{2\lambda} \left[\mu_H^2 - \left(\frac{g \bar{\mu}_{\Phi \text{ eff}}^2(\hat{r})}{2\pi\alpha} \right) F(\epsilon, \hat{r}) \right] = \frac{\bar{\mu}_H^2(\hat{r})}{2\lambda(\hat{r})}, \quad (6.25)$$

which uses eqs. (6.21). This is finite as $\epsilon \rightarrow 0$, as expected. The corresponding formula expressed in terms of renormalized couplings defined at a different scale is found simply by running them up or down according to (6.21).

Eq. (6.25) shows that it is the renormalized combination $\bar{\mu}_H^2$ that must be positive for H to become nonzero. Notice also that eq. (6.24) shows that it is nonzero $\bar{\mu}_{\Phi \text{ eff}}^2(\hat{r})$ that determines when $\mathcal{A} \neq 0$, and so whether Φ has a nontrivial bulk profile. Physically, this profile arises because $\bar{\mu}_{\Phi \text{ eff}}^2$ controls the linear couplings of Φ to the

brane, and having these nonzero precludes Φ 's near-brane derivative from vanishing.

6.2.3 Higgs-Bulk mixing

We next describe the fluctuations about this background solution, with a view towards identifying the extent to which the $H - \Phi$ couplings cause the Higgs particle to mix with KK Φ -modes in the bulk. We only track here the mixing in the $H - \Phi$ sector, ignoring in particular potential mixing with other bulk fields that might arise within applications where the scalar interacts significantly with other fields (like the metric or fluxes) that are involved in extra-dimensional stabilization. This is known in particular to be a real complication when Φ is the dilaton that arises as part of the 6D bulk supergravity multiplet [31].

To study fluctuations we expand the regularized action in powers of the fluctuation fields,

$$\Phi = \left(\frac{\bar{\mu}_{\Phi}^2(\hat{r})}{2\pi\alpha} \right) F(r, \hat{r}) + \phi(x, r, \theta); \quad H = \frac{1}{\sqrt{2}} \begin{pmatrix} 0 \\ v + h(x) \end{pmatrix}, \quad (6.26)$$

where $x = \{x^\mu\}$ and $v^2 = \bar{\mu}_H^2(\hat{r})/\bar{\lambda}(\hat{r}) = (246 \text{ GeV})^2$ is fixed from measurements of Fermi's constant, G_F , in muon decay. This gives the bulk action

$$S_B = - \int d^6x \sqrt{-\mathcal{G}} \left(\frac{1}{2} \mathcal{G}^{MN} \partial_M \phi \partial_N \phi \right), \quad (6.27)$$

while the on-brane potential of the scalar sector reads

$$U_b = T + \lambda v^2 h^2 + \lambda v h^3 + \frac{\lambda}{4} h^4 + \frac{\lambda_2}{2} \phi^2(0) + g v h \phi(0) + \frac{g}{2} h^2 \phi(0), \quad (6.28)$$

$$\begin{aligned}
\tilde{D}_k^\phi &= \text{---} \rightarrow \text{---} + \text{---} \rightarrow \text{---} \blacklozenge \text{---} \rightarrow \text{---} + \dots = \text{---} \bigcirc \text{---} \\
\langle hh^* \rangle &= \text{---} \rightarrow \text{---} + \text{---} \rightarrow \text{---} \bullet \text{---} \bigcirc \text{---} \bullet \text{---} \rightarrow \text{---} + \dots = \text{---} \bigcirc \text{---}
\end{aligned}$$

Figure 6.2: Perturbative calculation of the Green's function for the h operator. Dotted lines represent D_k^ϕ and dashed lines represent D_k^h as defined in the text. Circles are used for the $gvh\phi(0)$ vertex, diamonds represent a $\frac{1}{2}\lambda_2\phi^2(0)$ vertex and \tilde{D}_k^ϕ is the λ_2 -resummed Green's function for the bulk field, Fourier transformed in the brane directions but not in the extra dimensions.

where all of the above are 'bare' couplings. The rest of the Standard Model looks like it usually does, with h acting as the usual Higgs field.

Our goal is to compute the implications of the $gvh\phi(0)$ term that mixes the brane and bulk scalar degrees of freedom, and we do so in two ways. Although somewhat redundant, comparing both approaches provides insight and a check on our calculations.

Perturbative method

A straightforward way to approach Higgs-bulk mixing [12] is to regard the terms $\frac{1}{2}\lambda_2\phi^2(0)$ and $gvh\phi(0)$ as part of the interaction lagrangian so that the unperturbed system does not mix brane and bulk. The implications of mixing are then found by summing all possible types of insertions of the mixing interactions.

For instance, at tree level a calculation of the correlator $\langle hh^* \rangle_k$ requires summing over the diagrams of Fig. 6.2. Summing these graphs gives the following momentum-space result [20],

$$\langle hh^* \rangle_k = \frac{D_k^h [1 + i\lambda_2 D_k^\phi(0,0)]}{1 + [i\lambda_2 + (gv)^2 D_k^h] D_k^\phi(0,0)}, \quad (6.29)$$

This expression can alternatively be derived using a Schwinger-Dyson approach, as shown in Appendix D.2. The advantage of this approach is that it does not require λ_2 to be perturbatively small. In eq. (6.29), D_k^h is the momentum-space propagator of h in the unperturbed theory⁴

$$D_k^h = -\frac{i}{k^2 + 2\lambda v^2 - i\varepsilon}, \quad (6.30)$$

and $D_k^\phi(0,0)$ is the unperturbed propagator for the bulk field, Fourier transformed only in the four brane directions and with both extra-dimensional positions evaluated at the Higgs-brane position ($r = 0$).

The unperturbed bulk propagator satisfies

$$\left[-f k^2 + \frac{1}{f} \partial_\theta^2 + \partial_r (f \partial_r) \right] D_k^\phi(r, \theta; r', \theta') = i\delta(r - r')\delta(\theta - \theta'), \quad (6.31)$$

and it is useful when solving this to expand in a basis of unperturbed eigenmodes for \square_2 :

$$\phi(k, r, \theta) = \sum_{nl} \phi_{nl}(k) Z_{nl}(r, \theta), \quad (6.32)$$

where

$$\square_2 Z_{nl}(r, \theta) = \left[\frac{1}{f^2} \partial_\theta^2 + \frac{1}{f} \partial_r (f \partial_r) \right] Z_{nl}(r, \theta) = -M_{nl}^2 Z_{nl}(r, \theta). \quad (6.33)$$

Rotational invariance of the background further allows the separation of variables

$$Z_{nl}(r, \theta) = P_{nl}(r) e^{in\theta/\alpha}, \quad (6.34)$$

⁴Notice we use ϵ to denote the cutoff, while ε governs the poles of the Feynman propagator.

where n is an integer and the P_{nl} are the corresponding set of radial mode functions.⁵ Because these are unperturbed modes, they do not yet ‘know’ about the Higgs-bulk couplings, and so satisfy the comparatively simple near-brane Neumann conditions corresponding to no brane couplings,

$$(f\partial_r P_{nl})_{r=0,\pi R} = 0, \quad (6.35)$$

and satisfy the traditional Sturm-Liouville bulk normalization relations

$$2\pi\alpha \int_0^{\pi R} dr f P_{nl}^* P_{n'l'} = \delta_{ll'}. \quad (6.36)$$

The result that follows from using this expansion in (6.31) is

$$D_k^\phi(r, \theta; r', \theta') = -\frac{i}{2\pi\alpha} \sum_{nl} \frac{P_{nl}(r) P_{nl}^*(r')}{k^2 + M_{nl}^2 - i\varepsilon} e^{in(\theta-\theta')/\alpha}, \quad (6.37)$$

and, since only $n = 0$ modes survive as $r, r' \rightarrow 0$ (as is shown below), the required brane-to-brane propagator becomes

$$D_k^\phi(0, 0) = -\frac{i}{2\pi\alpha} \sum_l \frac{P_{0l}(0) P_{0l}^*(0)}{k^2 + M_{0l}^2 - i\varepsilon}. \quad (6.38)$$

Continuum limit

These expressions become particularly simple in the large-volume limit, where $|k^2 R^2| \gg 1$. In this case the discrete mode spacing is very small and the mode sum is well-approximated by a continuum momentum integral. This continuum limit is taken

⁵Do not confuse these with Legendre functions, despite the notation.

explicitly in Appendix D.3, starting from the discrete mode sum in a simple toy model, but the near-brane result can be obtained more simply by solving (6.31) directly for noncompact extra dimensions. This can be done explicitly near the branes, where $f \approx r$, since eq. (6.31) becomes the equation for a free 2D field in cylindrical coordinates, whose solution are given in terms of Bessel functions.

Demanding normalizability near $r = 0$ for the unperturbed functions, one finds

$$D_k^\phi(r, \theta; r', \theta') = -i \sum_{n=-\infty}^{\infty} \int \left(\frac{q \, dq}{2\pi\alpha} \right) \frac{e^{in(\theta-\theta')}}{k^2 + q^2 - i\varepsilon} J_{|n/\alpha|}(qr) J_{|n/\alpha|}(qr'). \quad (6.39)$$

Since only the $n = 0$ term contributes when evaluated at $r = r' = 0$, the near-brane limit becomes

$$D_k^\phi(0, 0) = \frac{-i}{4\pi\alpha} \int_0^\infty \frac{dq^2}{k^2 + q^2 - i\varepsilon}. \quad (6.40)$$

The integral in eq. (6.40) diverges logarithmically at large q , and once this is regularized with a cutoff $\Lambda = 1/\epsilon$ the result becomes

$$D_k^\phi(0, 0) = \frac{i}{4\pi\alpha} \log(k^2\epsilon^2). \quad (6.41)$$

The $i\varepsilon$ prescription tells us which branch of the logarithm should be used when k^2 is negative (*i.e.* k^μ is timelike), in which case

$$\log(k^2\epsilon^2) = \log(-k^2\epsilon^2) - i\pi. \quad (6.42)$$

Using this in the Higgs two-point function, and expressing the result in terms of

renormalized couplings gives the finite final (continuum) result

$$\langle hh^* \rangle_k = -i \left[k^2 + 2\bar{\lambda}(\bar{r})v^2 + \left(\frac{\bar{g}^2(\bar{r})v^2}{4\pi\alpha} \right) \frac{\log(k^2\bar{r}^2)}{1 - \left(\frac{\bar{\lambda}_2(\bar{r})}{4\pi\alpha} \right) \log(k^2\bar{r}^2)} \right]^{-1}, \quad (6.43)$$

where \bar{r} is the same arbitrary renormalization energy scale at which the renormalized couplings are also evaluated, and in we have used $F(r, r') = \log(r/r')$ appropriate for the large R limit. It is the implicit \bar{r} -dependence in these couplings that cancels the explicit dependence appearing in the logarithms, ensuring that \bar{r} does not contribute to physical quantities computed from $\langle hh^* \rangle_k$.

Direct mode diagonalization

We next provide an alternative derivation of the Higgs two-point function, which proceeds more directly by calculating $\langle hh^* \rangle_k$ explicitly by diagonalizing the KK and Higgs modes. This provides a more physical interpretation for the branch cut introduced into $\langle hh^* \rangle_k$ by the Higgs-bulk couplings, in terms of Higgs mixing with KK bulk states.

Propagation eigenstates are found by solving the field equations for h and ϕ , keeping track of the boundary conditions near the brane. In the present instance the relevant equations are the bulk scalar equation

$$(\square_4 + \square_2) \phi = \left[\partial_\mu \partial^\mu + \frac{1}{f^2} \partial_\theta^2 + \frac{1}{f} \partial_r (f \partial_r) \right] \phi = 0, \quad (6.44)$$

the (linearized) Higgs field equation on the brane,

$$-\partial_\mu \partial^\mu h + 2\lambda v^2 h + gv \phi(0) = 0, \quad (6.45)$$

and the near-brane boundary condition for ϕ ,

$$-2\pi\alpha (f\partial_r\phi)_{r=0} + gv h + \lambda_2 \phi(0) = 0. \quad (6.46)$$

As before we decompose the 6D scalar into a KK tower by expanding the solutions to eq. (6.44) in a basis of eigenfunctions of \square_2 ,

$$\phi(k, r, \theta) = \sum_{n\ell} \varphi_{n\ell}(k) \mathcal{Z}_{n\ell}(r, \theta), \quad (6.47)$$

with

$$\square_2 \mathcal{Z}_{n\ell}(r, \theta) = -M_{n\ell}^2 \mathcal{Z}_{n\ell}(r, \theta). \quad (6.48)$$

We use the indices $(n\ell)$ rather than (nl) here to emphasize that they run over a slightly different range, with ℓ including a value corresponding to h in the special case $n = 0$, in addition to the complete range of l for the unperturbed $n = 0$ KK modes. This change only happens for the $n = 0$ modes because only these mix nontrivially with the brane.

As for the unperturbed case, we write

$$\mathcal{Z}_{n\ell}(r, \theta) = \mathcal{P}_{n\ell}(r) e^{in\theta/\alpha}, \quad (6.49)$$

where n is an integer and the $\mathcal{P}_{n\ell}$ are the radial mode functions, satisfying

$$\left[M_{n\ell}^2 - \left(\frac{n}{\alpha f} \right)^2 + \frac{1}{f} \partial_r (f \partial_r) \right] \mathcal{P}_{n\ell} = 0. \quad (6.50)$$

In terms of the 4D modes $\varphi_{n\ell}$ and h , the ϕ and h field equations, eqs. (6.44) and

(6.45), are as for the unperturbed case,

$$\begin{aligned} \left[k^2 + M_{n\ell}^2 \right] \varphi_{n\ell} &= 0 \\ \left[k^2 + 2\lambda v^2 \right] h + \sum_{n\ell} \left[gv \mathcal{P}_{n\ell}(0) \right] \varphi_{n\ell} &= 0, \end{aligned} \quad (6.51)$$

but $\mathcal{P}_{n\ell}$ differs from $P_{n\ell}$ by satisfying the near-brane boundary condition, eq. (6.46), including the implications of the Higgs-bulk mixing,

$$gv h + \sum_{n\ell} \left[-2\pi\alpha (f\partial_r \mathcal{P}_{n\ell}) + \lambda_2 \mathcal{P}_{n\ell} \right]_{r=0} \varphi_{n\ell} = 0. \quad (6.52)$$

Using eqs. (6.51) to eliminate h and k^2 gives

$$h = \sum_{n\ell} \left[\frac{gv \mathcal{P}_{n\ell}(0)}{M_{n\ell}^2 - 2\lambda v^2} \right] \varphi_{n\ell}, \quad (6.53)$$

and allows (6.52) to be rewritten as a boundary condition purely for $\mathcal{P}_{n\ell}$:

$$\left[-2\pi\alpha (f\partial_r \mathcal{P}_{n\ell}) + \left(\lambda_2 - \frac{(gv)^2}{M_{n\ell}^2 - 2\lambda v^2} \right) \mathcal{P}_{n\ell} \right]_{r=0} = 0. \quad (6.54)$$

What is unusual about this boundary condition is the presence of $M_{n\ell}^2$, which makes it mode-dependent, at least for those modes⁶ for which it is satisfied with $\mathcal{P}_{n\ell}(0) \neq 0$. The presence of the unorthodox mode-dependent near-brane boundary conditions implies the eigenfunctions need not be orthogonal using the usual Sturm-Liouville (or Wronskian) inner product. Instead, as shown in detail in Appendix D.4, the natural inner product adapted to this boundary-value problem also involves some

⁶The only normalizable modes for which $\mathcal{P}_{n\ell}(0) \neq 0$ are those with $n = 0$, expressing conservation of angular momentum, as expected.

boundary dependence.

The resulting generalized orthonormality condition for this new inner product is

$$2\pi\alpha \int_0^{\pi R} dr f \mathcal{P}_s^* \mathcal{P}_t + \frac{(gv)^2 \mathcal{P}_s^*(0) \mathcal{P}_t(0)}{(M_s^2 - 2\lambda v^2)(M_t^2 - 2\lambda v^2)} = \delta_{st}, \quad (6.55)$$

where we collectively denote $s, t = \{n, \ell\}$. As shown in Appendix D.4, it is this modified boundary condition that ensures that the KK expansion of the action gives a quadratic action that is diagonal in the $\varphi_{n\ell}$. This property would be ruined in the present instance for an expansion using the unperturbed mode functions, $\phi = \sum_{nl} \phi_{nl} P_{nl}$ by the term $gv h \phi(0) = gv h \sum_{nl} \phi_{nl} P_{nl}(0)$ in the lagrangian, which causes bulk modes with $n = 0$ to mix with h . In Appendix D.5 we make this discussion explicit by solving the perturbed wavefunctions subject to this boundary condition in an illustrative toy model.

The complete mass eigenstates of the theory obtained including this mixing are related to the unperturbed states discussed earlier by a linear rotation, as follows:

$$h = \sum_s \mathcal{B}_s \varphi_s \quad \phi_i = \sum_s \mathcal{U}_{is} \varphi_s, \quad (6.56)$$

where the index i denotes $\{n, \ell\}$ in the same manner as s denotes $\{n, \ell\}$. Because only $n = 0$ modes mix with the brane, in practice $\mathcal{U}_{is} = \delta_{is}$ unless $n = 0$.

The quantity \mathcal{B}_s is of most interest, because it controls the two point function for the h field, which can be written

$$\langle h h^* \rangle_k = \sum_s |\mathcal{B}_s|^2 \langle \varphi_s \varphi_s^* \rangle_k = -i \sum_s \frac{|\mathcal{B}_s|^2}{k^2 + M_s^2 - i\varepsilon}. \quad (6.57)$$

Eq. (6.53) gives \mathcal{B}_s as

$$\mathcal{B}_s = \frac{gv\mathcal{P}_s(0)}{M_s^2 - 2\lambda v^2}, \quad (6.58)$$

and \mathcal{U}_{is} is found by using $\mathcal{P}_s(r) = \sum_i \mathcal{U}_{is} P_i(r)$ together with the normalization conditions, eqs. (6.36) and (6.55), respectively satisfied by P_i and \mathcal{P}_s . This gives

$$\sum_i \mathcal{U}_{is}^* \mathcal{U}_{it} + \mathcal{B}_s^* \mathcal{B}_t = \delta_{st}, \quad (6.59)$$

as well as the remaining unitarity conditions

$$\sum_s \mathcal{B}_s^* \mathcal{B}_s = 1, \quad \sum_s \mathcal{U}_{js} \mathcal{B}_s^* = 0 \quad \text{and} \quad \sum_s \mathcal{U}_{is} \mathcal{U}_{js}^* = \delta_{ij}. \quad (6.60)$$

The continuum (large R) limit

Although the formulae in §6.2.3 so far make no assumption about the relative size of λv^2 and the KK scale, $m_{KK}^2 \approx 1/R^2$, we pause here to display the simple result that obtains in the limit $\lambda v^2 \gg m_{KK}^2$ (appropriate to large-volume models, say) for which KK mode sums are more usefully cast as integrals [10, 16].

In this limit it is a good approximation to write the sum appearing in the two-point function as an integral

$$\langle hh^* \rangle_k = -i \sum_s \frac{|\mathcal{B}_s|^2}{k^2 + M_s^2 - i\epsilon} \approx -i \int dM^2 \frac{\rho_h(M^2)}{k^2 + M^2 - i\epsilon}, \quad (6.61)$$

which defines the spectral function, $\rho_h(M^2)$. The simplest way to obtain an expression for ρ_h is by using the explicit result for $\langle hh^* \rangle_k$ obtained above from the perturbative

calculation. To read off $\rho_h(M^2)$ from this calculation we employ unitarity, in the form

$$\pi\rho_h(M^2) = \text{Re} \langle hh^* \rangle_k \Big|_{k^2=-M^2}. \quad (6.62)$$

Using expression (6.43), and separating the real and imaginary parts of the logarithms, gives the finite result

$$\begin{aligned} \pi\rho_h(M^2) &= \frac{\bar{g}^2(\bar{r})v^2/4\alpha}{[M^2 - 2\bar{\lambda}(\bar{r})v^2]^2 + \pi^2 \left[\frac{\bar{\lambda}_2(\bar{r})}{4\pi\alpha} [M^2 - 2\bar{\lambda}(\bar{r})v^2] + \frac{\bar{g}^2(\bar{r})v^2}{4\pi\alpha} \right]^2} \Big|_{\bar{r}=1/M} \\ &= \frac{v^2\zeta(M^2)}{[M^2 - \Pi(M^2)]^2 + v^4\zeta^2(M^2)}, \end{aligned} \quad (6.63)$$

where

$$\zeta(M^2) := \frac{\bar{g}(\bar{r})/4\alpha}{\left[1 - \left(\frac{\bar{\lambda}_2(\bar{r})}{4\pi\alpha} \right) \log(M^2\bar{r}^2) \right]^2 + \left(\frac{\bar{\lambda}_2(\bar{r})}{4\alpha} \right)^2}, \quad (6.64)$$

and

$$\Pi(M^2) := 2\bar{\lambda}(\bar{r})v^2 + \left(\frac{\bar{g}^2(\bar{r})v^2}{4\pi\alpha} \right) \frac{\log(M^2\bar{r}^2) \left[1 - \left(\frac{\bar{\lambda}_2(\bar{r})}{4\pi\alpha} \right) \log(M^2\bar{r}^2) \right] - \frac{\pi\bar{\lambda}_2(\bar{r})}{4\alpha}}{\left[1 - \left(\frac{\bar{\lambda}_2(\bar{r})}{4\pi\alpha} \right) \log(M^2\bar{r}^2) \right]^2 + \left(\frac{\bar{\lambda}_2(\bar{r})}{4\alpha} \right)^2}. \quad (6.65)$$

For future reference we note here that many of the above expressions simplify if we make a specific choice, $\bar{r} = 1/M$, for the arbitrary renormalization scale, so that the $\log(M^2\bar{r}^2)$ terms disappear. In the present instance this leads to the simpler formulae

$$\zeta(M^2) = \frac{\bar{g}^2(\bar{r})/4\alpha}{1 + (\bar{\lambda}_2(\bar{r})/4\alpha)^2} \Big|_{\bar{r}=1/M}, \quad (6.66)$$

and

$$\Pi(M^2) = 2v^2 \left[\bar{\lambda}(\bar{r}) - \frac{\zeta(M)\bar{\lambda}_2(\bar{r})}{8\alpha} \right]_{\bar{r}=1/M}. \quad (6.67)$$

The weak-coupling limits of the spectral function are most easily seen using the second equality in eq. (6.63), together with the representation $\pi\delta(x) = \lim_{\zeta \rightarrow 0} \zeta/(x^2 + \zeta^2)$. This gives

$$\rho_h(M^2) \rightarrow \delta(M^2 - 2\lambda v^2), \quad (6.68)$$

both when $g \rightarrow 0$ and when $\lambda_2 \rightarrow \infty$, illustrating how the Standard Model is obtained in both of these limits.⁷ Although it is clear why this should hold when $g = 0$, it turns out also to hold when $\lambda_2 \rightarrow \infty$ because the boundary conditions, (6.46), imply in this case that the KK modes all vanish on the brane.

It is the two functions ζ and Π that control the phenomenology of Higgs-bulk mixing, as we now show.

6.3 Phenomenological implications

In this section we discuss the leading sources of constraint on the Higgs-bulk mixing just described. We separate the effects into three types: virtual effects from exchanging KK modes; real effects from KK modes in the final state; and changes to the relation between the Higgs mass and couplings (together with associated changes to the constraints from vacuum stability).

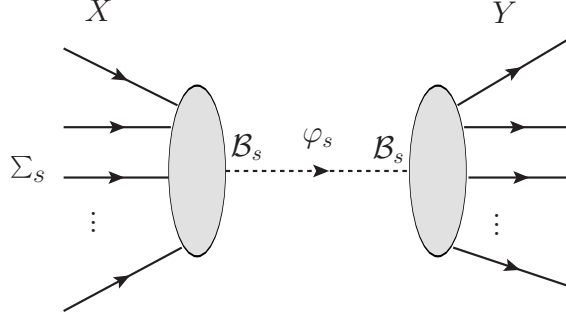


Figure 6.3: Scattering via virtual exchange of the Higgs-bulk tower. A factor of \mathcal{B}_s comes from the vertex between φ_s and both the initial and final state. All modes are summed over because any of the φ_s can mediate this interaction.

6.3.1 Virtual Higgs Exchange

Consider first a tree-level Standard Model parton process of the form $X \rightarrow h \rightarrow Y$, where an initial state X produces a virtual h that subsequently produces state Y , as in Fig. 6.3. The Standard Model amplitude for this process can be schematically written

$$\mathcal{M}^{SM}(X \rightarrow Y) = \mathcal{M}(X \rightarrow h) \langle hh^* \rangle_k^{SM} \mathcal{M}(h \rightarrow Y), \quad (6.69)$$

and so once h mixes with the KK tower this becomes

$$\begin{aligned} \mathcal{M}(X \rightarrow Y) &= \mathcal{M}(X \rightarrow h) \mathcal{M}(h \rightarrow Y) \sum_s |\mathcal{B}_s|^2 \langle \varphi_s \varphi_s \rangle_k \\ &= \mathcal{M}(X \rightarrow h) \mathcal{M}(h \rightarrow Y) \langle hh^* \rangle_k, \end{aligned} \quad (6.70)$$

where $k^\mu = p_X^\mu = p_Y^\mu$ represents the 4-momentum flowing down the Higgs line. That is, virtual effects of Higgs-bulk mixing exchange processes are found by using $\langle hh^* \rangle_k$ in place of the Standard Model Higgs propagator.

⁷We describe these limits in terms of bare couplings, since complications associated with divergences vanish in these limits, and the renormalized couplings $\bar{\lambda}$, \bar{g} and $\bar{\lambda}_2$ no longer run.

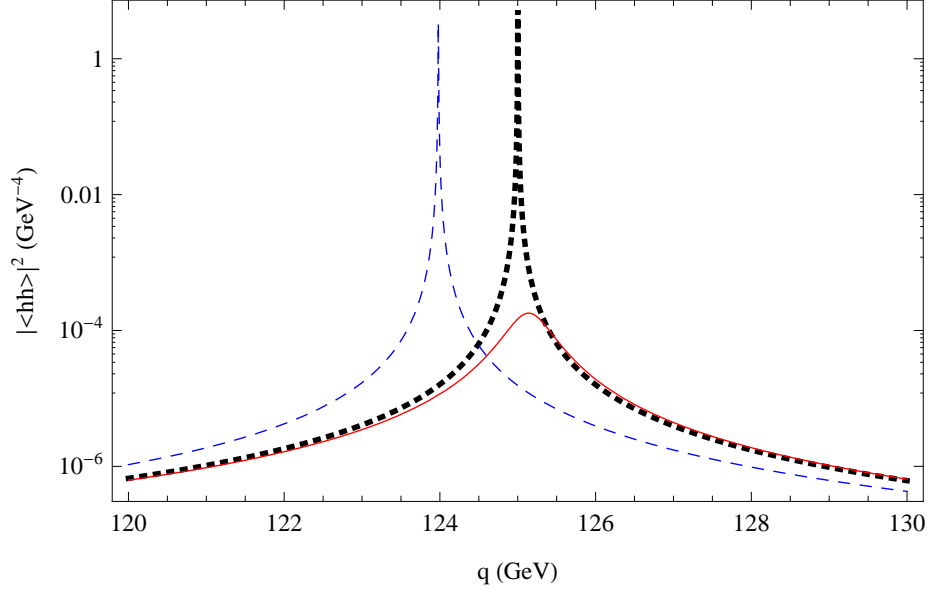


Figure 6.4: The lineshape, $|\langle hh^* \rangle_k|^2$, for the KK tower exchange with various values of $(\bar{\lambda}, \bar{\lambda}_2, \bar{g}, \alpha)$ evaluated at $\bar{r} = (125 \text{ GeV})^{-1}$. The dotted black line is the comparison lineshape for a Standard Model Higgs with mass, $m_h = 125 \text{ GeV}$ and a Standard Model width of $\Gamma_{SM} = 4 \text{ MeV}$. (In the Standard Model the Higgs coupling for this mass is $\bar{\lambda} = 0.1291$.) The dashed blue line shows a similarly narrow peak (chosen to lie near 124 GeV rather than 125 GeV to avoid clutter in the figure), obtained using $(\bar{\lambda}, \bar{\lambda}_2, \bar{g}, \alpha) = (0.127, 0, 0.0021, 0.8)$. The solid red line shows instead a broad peak at 125 GeV for an exaggerated choice of couplings $(\bar{\lambda}, \bar{\lambda}_2, \bar{g}, \alpha) = (0.16, 2, 0.35, 0.01)$.

Lineshape

Implications of this modification to Higgs exchange are easiest to study in the large-volume limit, for which the KK sums are well-approximated by integrals. In this case we may use eq. (6.43), which we rewrite in the Lorentzian form by separating the real and imaginary parts of the denominator

$$\langle hh^* \rangle_k = -i \left[\Pi(-k^2) + k^2 - iv^2 \zeta(-k^2) \right]^{-1}, \quad (6.71)$$

where the functions are, not surprisingly, the same functions as in §6.2.3.

Physical processes depend on the squared magnitude,

$$|\langle hh^* \rangle_k|^2 = \frac{1}{[\Pi(-k^2) + k^2]^2 + v^4 \zeta^2(-k^2)}, \quad (6.72)$$

which defines the resonant Higgs lineshape in the presence of mixing. A plot of this lineshape, and a comparison with its Standard Model counterpart, is given in Fig. 6.4, for several choices for the Higgs-bulk couplings.

The position of the resonant maximum occurs at

$$m_h^2 = \Pi(m_h^2) = v^2 \left[2\bar{\lambda}(\bar{r}) - \frac{\bar{g}^2(\bar{r}) \bar{\lambda}_2(\bar{r})}{(4\alpha)^2 + \bar{\lambda}_2^2(\bar{r})} \right]_{\bar{r}=1/m_h}, \quad (6.73)$$

where we have used the definitions of ζ and Π in eqs. (6.66) and (6.67). This suggests the definition

$$m_h^2 := 2\bar{\lambda}_{\text{eff}}(\bar{r})v^2 \Big|_{\bar{r}=1/m_h} \quad \text{with} \quad 2\bar{\lambda}_{\text{eff}}(\bar{r}) := 2\bar{\lambda}(\bar{r}) - \frac{\bar{g}^2(\bar{r}) \bar{\lambda}_2(\bar{r})}{(4\alpha)^2 + \bar{\lambda}_2^2(\bar{r})}. \quad (6.74)$$

It is the value of the renormalized couplings at the scale $\bar{r} = 1/m_h$ that is relevant to many physical quantities, such as the condition $\bar{\lambda}_{\text{eff}}(\bar{r} = 1/m_h) = 0.1291$ that is required to ensure a Higgs mass of 125 GeV. Because of this, in what follows a barred coupling without a specified renormalization scale is understood to be evaluated at $1/m_h$:

$$\bar{\lambda} = \bar{\lambda}(\bar{r}) \Big|_{\bar{r}=1/m_h}, \quad \bar{g} = \bar{g}(\bar{r}) \Big|_{\bar{r}=1/m_h}, \quad \text{and so on.} \quad (6.75)$$

Notice also that the condition $m_h = 125$ GeV imposes only a single relation amongst the couplings $\bar{\lambda}$, $\bar{\lambda}_2$ and \bar{g} , rather than fixing $\bar{\lambda}$ completely, as it would have done in the Standard Model. Fig. 6.5 plots the value predicted for $\bar{\lambda}$ as a function of \bar{g} for

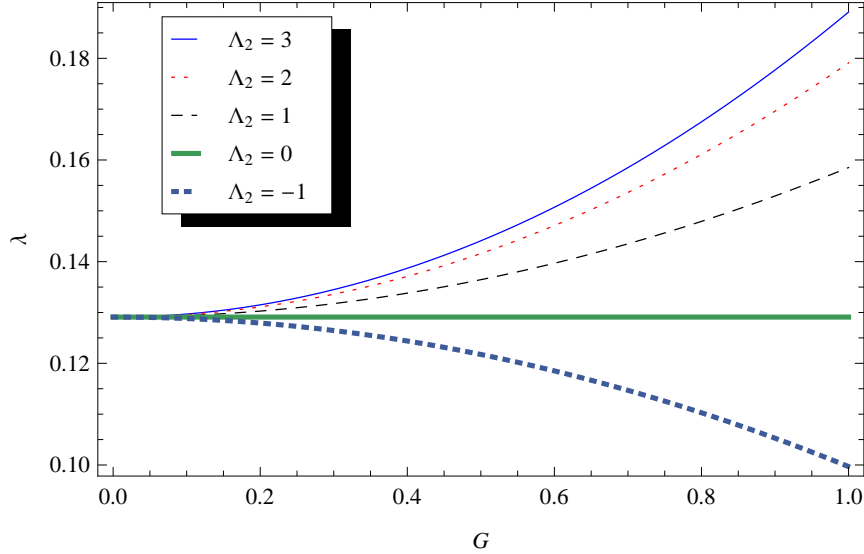


Figure 6.5: The Higgs quartic coupling $\bar{\lambda}$ required to ensure $m_h = 125$ GeV, as a function of the brane bulk mixing parameter $G = \bar{g}/\sqrt{\alpha}$ for various choices of the coupling parameter $\Lambda_2 = \bar{\lambda}_2/\alpha$ (as listed in the legend). The flat line $\bar{\Lambda}_2 = 0$ corresponds to the Standard Model value $\bar{\lambda} = 0.1291$. All couplings are renormalized and evaluated at a scale $\bar{r} = (125 \text{ GeV})^{-1}$.

various choices $\bar{\lambda}_2$, and we assume in what follows that $\bar{\lambda}$ is fixed in this way.

We see that the lineshape can resemble a single Higgs resonance despite its containing a sum over many KK states. Its width at its maximum is

$$m_h \Gamma_B := \zeta(m_h^2) v^2 = \frac{\bar{g}^2 v^2 / 4\alpha}{1 + (\bar{\lambda}_2 / 4\alpha)^2}. \quad (6.76)$$

This width is related by unitarity to the rate for invisible processes where the KK modes escape invisibly into the bulk, carrying with them missing energy. When Γ_B is sufficiently small, such as in the $g \rightarrow 0$ limit, its role in the unitarity argument is eventually replaced by the Standard Model Higgs decay width, Γ_{SM} , corresponding to the imaginary part of the usual Standard Model Higgs vacuum-polarization graphs.

This suggests the definition $\Gamma_h = \Gamma_B + \Gamma_{SM}$. However, because the Standard Model contribution is a loop effect it should only be kept in the special case where it dominates Γ_B at the peak of a narrow resonance. Given these considerations, we write the corrected Green's function

$$\langle hh^* \rangle'_k = -i [\Pi(-k^2) + k^2 - iv^2\zeta(-k^2) - im_h\Gamma_{SM}]^{-1}, \quad (6.77)$$

so that

$$|\langle hh^* \rangle'_k|^2 = \frac{1}{[\Pi(-k^2) + k^2]^2 + m_h [v^2\zeta(-k^2) + m_h\Gamma_{SM}]}. \quad (6.78)$$

Invisible width

In essence, mixing with the bulk introduces a new invisible channel into Higgs reactions while leaving unchanged the relative strength of all of the visible h couplings to other Standard Model particles. The exchange of the KK tower (instead of just the Higgs) suppresses the overall rates for observable Higgs-mediated processes, while preserving their relative frequency. The success of the Standard Model description of the resonance at 125 GeV, as seen by both CMS and ATLAS, therefore provides an immediate constraint on such mixing, in much the same way as it constrains a more conventional Higgs invisible width.

In the present context the nature of this constraint is easiest to see within the narrow-width approximation, which applies in the phenomenologically most relevant case where $m_h \gg \Gamma_B + \Gamma_{SM}$. In this case the resonant h autocorrelation becomes

$$|\langle hh^* \rangle'_k|^2 \approx \frac{\pi}{m_h [\Gamma_B + \Gamma_{SM}]} \delta(k^2 + m_h^2), \quad (6.79)$$

which neglects a factor $[1 - \Pi'(m_h^2)]^{-1}$. This factor can be dropped because

$$\Pi'(m_h^2) := \left(\frac{\partial \Pi}{\partial k^2} \right)_{k^2=-m_h^2} = \frac{\zeta(m_h^2) v^2}{\pi m_h^2} \left[\frac{1 - (\bar{\lambda}_2/4\alpha)^2}{1 + (\bar{\lambda}_2/4\alpha)^2} \right] \approx \mathcal{O} \left(\frac{\Gamma_B}{m_h} \right), \quad (6.80)$$

and so is similar in size to other contributions that have been neglected.

For comparison, the Standard Model Higgs distribution in the same narrow-width limit reads

$$|\langle hh^* \rangle_k|_{SM}^2 \approx \frac{\pi}{m_h \Gamma_{SM}} \delta(k^2 + m_h^2), \quad (6.81)$$

with m_h being the physical mass of the Higgs. In this limit the momentum dependence of the two results is identical, and the exchange of the KK tower just provides an overall suppression to the rates for Higgs-mediated processes by the factor

$$\mathcal{R} = \frac{\Gamma_{SM}}{\Gamma_B + \Gamma_{SM}}, \quad (6.82)$$

relative to the Standard Model.

The bound that follows for \mathcal{R} can be inferred using the results of extant global fits to the LHC data that were performed to constrain the branching ratio into invisible decays of an otherwise Standard Model-like Higgs. The corresponding narrow-width suppression for a conventional invisible decay width would be $\mathcal{R}_{\text{inv}} = \Gamma_{SM}/(\Gamma_{SM} + \Gamma_{\text{inv}}) = 1 - B_{\text{inv}}$, where B_{inv} is the branching fraction into invisible decays. Recent fits give an upper bound $B_{\text{inv}} \lesssim (0.3 - 0.64)$ at 95% CL [32, 33, 34, 35], where the range depends on precisely the priors used when performing the fit. (Ref. [33] finds $B_{\text{inv}} < 0.64$ using 15 signals from the Tevatron, Atlas and CMS, while ref. [32] finds the slightly stronger limit of $B_{\text{inv}} < 0.4$ at 95% CL using a different suite of 16 observables. The bound from ref. [35] is similar. Ref. [34] finds the strongest bound,

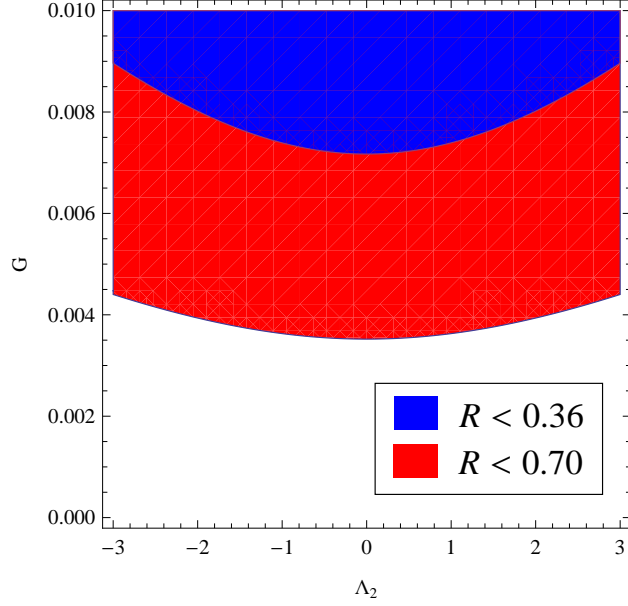


Figure 6.6: Bounds on $\Lambda_2 = \bar{\lambda}_2/\alpha$ and $G = \bar{g}/\sqrt{\alpha}$ from constraints on the invisible branching ratio of a Standard Model Higgs. The shaded region is excluded, for two sets of assumptions (described in the main text). Couplings are evaluated at a scale $\bar{r} = (125 \text{ GeV})^{-1}$.

$B_{\text{inv}} < 0.2$ using a smaller set of Higgs signals that are argued to be more sensitive.)

Taking the most conservative of these limits, we infer the constraint

$$\mathcal{R} \gtrsim 0.36. \quad (6.83)$$

The corresponding constraint in the $\bar{g} - \bar{\lambda}_2$ plane is plotted in Fig. 6.6, which also shows the result obtained from the more aggressive constraints. This plot shows that these global Higgs fits imply a conservative limit

$$\frac{\bar{g}}{\sqrt{\alpha}} \lesssim 0.007 \quad \text{for } \bar{\lambda}_2 = 0; \quad (6.84)$$

with weaker constraints on \bar{g} as $\bar{\lambda}_2$ increases. (This weakening of the \bar{g} constraint with

large $\bar{\lambda}_2$ is a general consequence of the decoupling of brane and bulk in the $\bar{\lambda}_2 \rightarrow \infty$ limit.) For comparison, Ref. [15] considered the phenomenological implications of the cubic vertex $\frac{1}{2}gh^2\phi(0)$ but neglected Higgs-bulk mixing and λ_2 . They found that $g = 0.18$ was accessible at the LHC with 100 fb^{-1} at 14 TeV in the $h\phi \rightarrow \gamma\gamma\phi$ channel.

Notice that Γ_B depends on the two variables \bar{g} and $\bar{\lambda}_2$ only through the combination $\zeta(m_h^2)$, and this is generally true (once m_h is fixed) for any observables for which the narrow-width approximation is justified. Whenever this is true it is more useful to quote the constraint directly on $\zeta(m_h^2)$, giving

$$\zeta(m_h^2) \lesssim 5 \times 10^{-5}. \quad (6.85)$$

Low-energy bounds

The effects of other virtual contributions of KK modes can be similarly computed given an expression for $\langle hh^* \rangle$. Important among these are constraints from low-energy precision measurements, such as the anomalous magnetic moment of the muon. By way of example we study this here for the large-volume limit where $\langle hh^* \rangle$ has a simple closed-form expression.

This section uses this calculation to conclude that these bounds are negligibly weak, in agreement with standard intuition for the large-volume case. This standard intuition starts from the observation that each KK mode couples with gravitational strength, and so it is only the enormous phase space for KK modes that can compensate for this suppression [10]. Bounds on extra dimensions from low-energy observables are usually weaker than those from colliders because, for low-energy processes,

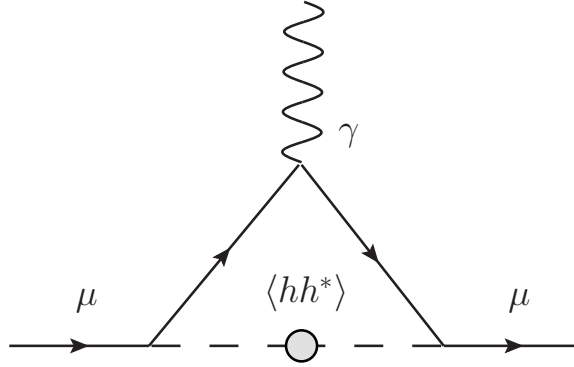


Figure 6.7: The Feynman graph corresponding to the one-loop correction to the muon anomalous magnetic moment in the Higgs-bulk mixing scenario.

only sub-TeV modes contribute, making the phase-space compensation incomplete and so insufficient to produce an observable result. Astrophysical energy-loss bounds on extra dimensions are an important exception to this intuition [36, 37, 38, 39], and we return to these below.

Fig. 6.7 displays the Feynman graphs whose evaluation gives the KK mode contribution to a fermion's anomalous magnetic moment. We estimate that the difference between this graph and the corresponding graph for a Standard Model Higgs is quite small, as it should be if we consider perturbing in small g , and brane-bulk mixing effects are negligible.

To see this, consider first the Higgs contribution from the analogous graph in the Standard Model. This evaluates to an anomalous fermion magnetic moment of size

$$a_h = \frac{y_f^2 m_f^2}{8\pi^2 m_h^2} \int_0^1 dx \frac{(x-2)x^2}{(1-x) + x^2(m_f^2/m_h^2)}, \quad (6.86)$$

where m_f is the fermion's mass and $y_f := m_f/v$ is its Higgs Yukawa coupling. The

regime of practical interest is $m_f \ll m_h$ and, because the integral diverges logarithmically near $x = 1$ when $m_f = 0$, the answer in this limit is dominated by

$$\begin{aligned} a_h &\approx \frac{y_f^2 m_f^2}{8\pi^2 m_h^2} \left[\log\left(\frac{m_f^2}{m_h^2}\right) + \frac{7}{6} + \dots \right] \\ &\approx -0.0021 \times 10^{-11} \quad (\text{muon}), \end{aligned} \quad (6.87)$$

where the numerical values assume the fermion is the muon. This is negligible in comparison to both the electroweak boson contributions and the experimental precision, which are of order a few 100×10^{-11} [40].

Repeating this exercise for the graph in Fig. 6.7 using the large-volume expression for $\langle hh^* \rangle_k$ allows us to estimate the difference between the Standard Model Higgs contribution a_h and the contribution from the whole KK tower a_B . We do not use $\langle hh^* \rangle'_k$ with the inclusion of the Standard Model Higgs width because it is a higher-loop effect, and for simplicity we assume $\lambda_2 = 0$. Therefore, accounting for the new propagator in the graph is accomplished by making the replacement

$$\frac{1}{k^2 + 2\lambda v^2} \rightarrow \frac{1}{k^2 + 2\bar{\lambda}(\bar{r})v^2 + \left(\frac{\bar{g}^2 v^2}{4\pi\alpha}\right) \log(k^2 \bar{r}^2)} \approx \frac{1}{k^2 + 2\bar{\lambda}(\bar{r})v^2} + \left(\frac{\bar{g}^2 v^2}{4\pi\alpha}\right) \frac{\log(k^2 \bar{r}^2)}{[k^2 + 2\bar{\lambda}(\bar{r})v^2]^2}, \quad (6.88)$$

where we write $\bar{g}(\bar{r}) = \bar{g}$ because it does not run in the limit of vanishing λ_2 .

Although the above propagator is only one term in the graph, which also contains a loop integral over k^2 , in order of magnitude, we estimate that the relative difference between the anomalous moment in the Higgs-bulk scenario and in the Standard Model is

$$\left| \frac{a_B - a_h}{a_h} \right| \approx \frac{\bar{g}^2}{8\pi\alpha\bar{\lambda}}, \quad (6.89)$$

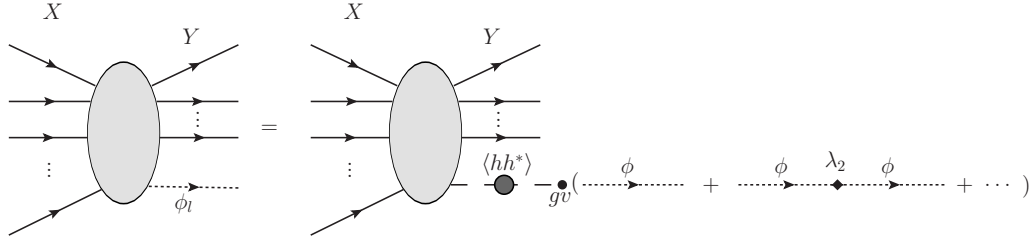


Figure 6.8: The tree level contribution to vector boson fusion with an invisible final state.

and so can be ignored given the strong constraints already found for \bar{g} .

6.3.2 Invisible final states

This section considers the implications of Higgs-bulk mixing for observables with Higgs-bulk final states, rather than simply as intermediate states. We first argue that these states are invisible and then relate their production rates in various channels to the analogous Standard Model Higgs production rate. Invisible states appear as missing energy at high-energy colliders, and we discuss Higgs-bulk mixing signals at both LEP and the LHC. We then turn to low-energy constraints on missing energy in astrophysical systems. We conclude that LEP provides weak bounds on the Higgs-bulk couplings, but astrophysical bounds are considerably stronger. We also provide a preliminary estimate of the reach at the LHC, beyond the constraints already discussed coming from the suppression of the rates for producing Standard Model particles.

Invisible-state production rates

Consider a process whereby the tower of φ_s states is produced through their overlap with h . For weak couplings the physics of this process resembles the physics of sterile

neutrinos, in that production and detection of the produced state occurs only because of the mixing with a weakly-interacting Standard Model particle. For weak couplings invisible processes are therefore described by requiring the amplitude for producing a state orthogonal to h ; that is, for being in one of the ‘flavour’ eigenstates, ϕ_i rather than a propagation eigenstate, φ_s .

We therefore consider the squared amplitude to produce a ϕ_i final state

$$|\mathcal{M}(X \rightarrow Y \phi_i)|^2 \approx |\mathcal{M}_{SM}(X \rightarrow Y h)|_{p_\phi}^2 |\mathcal{M}(h \rightarrow \phi_i)|_{p_\phi}^2, \quad (6.90)$$

where the first factor is the Standard Model result for Higgs production, but evaluated using p_ϕ , the momentum of the final state ϕ_i , which in practice amounts to replacing $m_h \rightarrow M_i$. The second factor can be understood in two ways. Formally, $\mathcal{M}(h \rightarrow \phi_i)$ is given in terms of $\langle h \phi^* \rangle_k$ by amputating the final unperturbed ϕ_i propagator and putting the correlation on shell (as usual) to obtain an amplitude with ϕ_i in the final state:

$$\mathcal{M}(h \rightarrow \phi_i) = \text{Amp} [\langle h \phi^*(0) \rangle_{k=p_\phi}] := \langle h \phi^*(0) \rangle_{k=p_\phi} [D_{k=p_\phi}^\phi]^{-1}. \quad (6.91)$$

As shown in Appendix D.2, the amputated $\langle h \phi^* \rangle_k$ correlation is given by

$$\text{Amp} [\langle h \phi^*(0) \rangle_{k=p_\phi}] = - \frac{i\bar{g}(\bar{r})v}{1 + i(\bar{\lambda}_2(\bar{r})/4\alpha)} \Big|_{\bar{r}=1/M_i} \langle h h^* \rangle_{k=p_\phi}. \quad (6.92)$$

where the renormalization point $\bar{r} = 1/M_i$ is chosen for notational convenience. Alternatively, the factorization in eq. (6.90) and the expression in eq. (6.92) can be derived by directly summing the graphs of Fig. 6.8. However, the virtue of using a

Schwinger-Dyson equation over the graphical methods is that it emphasizes that the result need not assume λ_2 is small.

Using this in eq. (6.90) then gives the general result

$$|\mathcal{M}(X \rightarrow Y \phi_i)|^2 \approx 4\alpha v^2 \zeta(M_i^2) |\langle h h^* \rangle_{k=p_\phi}|^2 |\mathcal{M}_{SM}(X \rightarrow Y h)|_{p_\phi}^2, \quad (6.93)$$

where $\langle h h^* \rangle_{k=p_\phi}$ is given explicitly in terms of the unperturbed h and ϕ propagators in earlier sections (*c.f.* eq. (6.29)).

In practical applications, it is the sum over modes' squared amplitudes (possibly weighting some other function O) that is relevant to a physical observable. That is,

$$\mathcal{O} = \sum_i |\mathcal{M}(X \rightarrow Y \phi_i)|^2 O(M_i^2). \quad (6.94)$$

This sum over bulk states, and the expression for $\langle h h^* \rangle_{k=p_\phi}$, both simplify considerably in the large-volume limit. In this limit we can also account for the on-resonance effects of decays into Standard Model particles, by using the large-volume expression for $\langle h h^* \rangle'_{k=p_\phi}$ in place of $\langle h h^* \rangle_{k=p_\phi}$. Then, the observable can be written in the simple resonant form

$$\mathcal{O} \approx \int dM^2 \Upsilon(M^2) O(M^2) |\mathcal{M}_{SM}(X \rightarrow Y h)|_{p_\phi}^2, \quad (6.95)$$

where

$$\Upsilon(M^2) := \frac{v^2 \zeta(M^2) / \pi}{[M^2 - \Pi(M^2)]^2 + [v^2 \zeta(M^2) + m_h \Gamma_{SM}]^2}. \quad (6.96)$$

In taking this continuum limit we use the fact that each mode has only a gravitational-strength coupling to the brane, due to the proportionality of each normalized mode

to $\mathcal{V}_2^{-1/2}$, where \mathcal{V}_2 is the extra-dimensional volume. Consequently, it is only the enormous phase space available at high energies that can compensate for the extremely feeble coupling of each mode, implying that it is only the density of states of the high-energy modes that is important. But the density of these modes does *not* depend on the details of the shape of the extra dimensions (unlike the density of states for the lowest-lying modes), which allows us to use the flat-space result appropriate to an extra-dimensional torus,

$$\frac{1}{\mathcal{V}_2} \sum_i I(M_i^2) \approx \int \frac{d^2p}{(2\pi\alpha)^2} I(p^2) = \int \frac{dM^2}{4\pi\alpha} I(M^2), \quad (6.97)$$

even for applications to more complicated geometries like spheres and rugby balls.

Missing energy at LEP

If the Higgs mixes significantly with invisible light states then these should have been produced at LEP, leading to a constraint on Higgs-bulk mixing. A convenient way to obtain this constraint is to use a particular search performed by the ALEPH, DELPHI, L3 and OPAL experiments at LEP II. These experiments have sought evidence for Z boson production in association with a Higgs that decays 100% invisibly while being produced with a Standard Model rate [41]. A combined analysis of each experiment's $\sqrt{s} = (200 - 209)$ GeV data has been used to place a lower bound on the mass of such a Higgs as $m_h \gtrsim 114.4$ GeV at 95% CL.

This is a convenient search for the present purposes for two reasons. First, the resulting bounds usefully constrain the cross section at these energies for generic electron positron annihilation into a Z boson plus missing energy, since it gives the

same signal; that is

$$\sigma_{\text{exp}}(e^+ e^- \rightarrow Z \cancel{E}_T) < \sigma_{SM}(e^+ e^- \rightarrow Zh) \Big|_{m_h=114 \text{ GeV}}, \quad (6.98)$$

where both sides are evaluated at $\sqrt{s} = 209 \text{ GeV}$. This is true so long as the selection efficiencies are similar for the new process and the Higgs process. Second, as we expect from the discussion in §6.3.2, the invisible cross section predicted from Higgs-bulk mixing shares enough of the features of the Standard Model cross section to allow a simple inference of the constraints.

Any of the ϕ_i states produced at LEP would appear as missing energy, so that the total missing energy cross section is the sum of the individual cross sections

$$\sigma(e^+ e^- \rightarrow Z \cancel{E}_T) = \sum_i \sigma(e^+ e^- \rightarrow Z \phi_i). \quad (6.99)$$

The total missing energy cross section is therefore a weighted sum of squared ϕ_i production amplitudes. Using the results of §6.3.2, we can write the cross section for the missing energy process in the form of an integral

$$\sigma(e^+ e^- \rightarrow Z \cancel{E}_T) = \int_0^{M_{\text{max}}^2} dM^2 \frac{\Upsilon(M^2)}{\mathcal{F}} \int \frac{d^3 \mathbf{p}_Z}{(2\pi)^3 2E_Z} \frac{d^3 \mathbf{p}_\phi}{(2\pi)^3 2E_\phi} |\mathcal{M}_{SM}|_{p_\phi}^2 (2\pi)^4 \delta^4(p_x - p_Z + p_\phi), \quad (6.100)$$

where the upper bound on integration $M_{\text{max}} = \sqrt{s} - m_Z$ with m_Z as the mass of the Z boson. This reflects the fact that only these modes are kinematically accessible. Additionally, $|\mathcal{M}_{SM}|_{p_\phi}^2 = |\mathcal{M}_{SM}(e^+ e^- \rightarrow Zh)|^2$ is the Standard Model Higgsstrahlung amplitude appropriately spin-summed/averaged, with the subscript, p_ϕ , reminding us that it is evaluated using the ϕ_i final-state four-momentum $p_\phi = (E_\phi, \mathbf{p}_\phi)$ where

$E_\phi^2 = \mathbf{p}_\phi^2 + M^2$. Here and in the following, \mathcal{F} is the usual initial-state-dependent flux factor associated with a cross section, p_x is the four-momentum of this initial state and $p_z = (E_z, \mathbf{p}_z)$ is the four-momentum of the Z boson.

The Standard Model Higgsstrahlung cross section can be written

$$\sigma_{SM}(e^+e^- \rightarrow Zh) = \frac{1}{\mathcal{F}} \int \frac{d^3\mathbf{p}_z}{(2\pi)^3 2E_z} \frac{d^3\mathbf{p}_h}{(2\pi)^3 2E_h} |\mathcal{M}_{SM}|_{p_h}^2 (2\pi)^4 \delta^4(p_x - p_z + p_h), \quad (6.101)$$

with $E_h^2 = \mathbf{p}_h^2 + m_f^2$ where $p_h = (E_h, \mathbf{p}_h)$, and $|\mathcal{M}_{SM}|^2$ is evaluated using the Higgs momentum p_h . We recognize the same expression in the missing energy cross section with the replacement $m_h \rightarrow M$. This allows the missing energy cross section to be rewritten as follows

$$\sigma(e^+e^- \rightarrow Z \cancel{E}_T) = \int_0^{M_{\max}^2} dM^2 \Upsilon(M^2) \sigma_{SM}(e^+e^- \rightarrow Zh) \Big|_{m_h=M}. \quad (6.102)$$

This expresses our missing-energy prediction in terms of the well-known Standard Model Higgsstrahlung cross section σ_{SM} , whose m_h - and \sqrt{s} -dependence is given by a standard result [42],

$$\sigma_{SM}(e^+e^- \rightarrow Zh) \propto \sqrt{J(m_h^2)} [J(m_h^2) + 12M_Z^2/s], \quad (6.103)$$

where $J(m^2) := (1 - m^2/s - M_Z^2/s)^2 - 4m^2 M_Z^2/s^2$ is the two-body phase-space function.

Using this, we may write the bound

$$\sigma(e^+e^- \rightarrow Z \cancel{E}_T) < \sigma_{\text{exp}}(e^+e^- \rightarrow Z \cancel{E}_T) < \sigma_{SM}(e^+e^- \rightarrow ZH) \Big|_{m_h=114 \text{ GeV}} \quad (6.104)$$

in the form

$$\int_0^{M_{\max}^2} dM^2 \Upsilon(M^2) \sqrt{J(M^2)} [J(M^2) + 12M_Z^2/s] < \sqrt{J(m_h^2)} [J(m_h^2) + 12M_Z^2/s] \Big|_{m_h=114 \text{ GeV}}, \quad (6.105)$$

where all other pre-factors in the cross-section formula cancel. The integral can be evaluated numerically to determine the allowed region of parameter space, with the result plotted in the $\bar{g} - \bar{\lambda}_2$ plane in Fig. 6.9. The result excludes an island in parameter space, and at first sight it might appear surprising that the bounds get weaker at large \bar{g} as well as at small \bar{g} . The weakening for large \bar{g} is a consequence of the resonant shape of $\Upsilon(M^2)$ together with the proximity of $\sqrt{s} - m_Z = 118$ GeV to the resonance's maximum, because $\Upsilon \propto 1/(\zeta v^2)$ when ζv^2 is bigger than both $M^2 - \Pi(M^2)$ and $m_h \Gamma_{SM}$. (A similar thing happens for bounds obtained for other observables dominated by the resonance, though the weakening of the constraints at large \bar{g} for these occurs for \bar{g} too large to justify our approximations, and so is not shown in the plots.)

The bounds obtained are clearly weaker than the LHC bounds on the Higgs invisible width discussed above (and the astrophysical bounds discussed below). So, although the issue of selection efficiency was ignored in arriving at these constraints, their weakness illustrates that a very large discrepancy in the two signals' selection efficiencies, that furthermore favours Higgs-bulk events, would have to exist for LEP bounds to become significant.

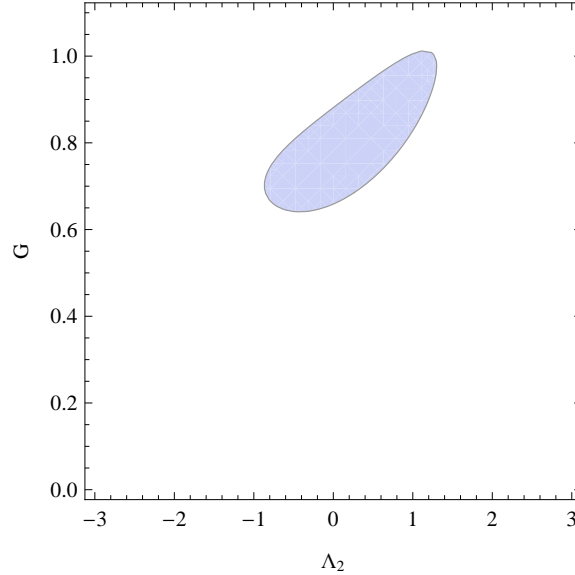


Figure 6.9: Constraints from LEP expressed in the Λ_2 - G plane (with $G = \bar{g}/\sqrt{\alpha}$ and $\Lambda = \bar{\lambda}_2/\alpha$) from LEP constraints. The small shaded region is excluded. All couplings are evaluated at a scale $\bar{r} = (125 \text{ GeV})^{-1}$

Missing energy at the LHC

The dominant production mechanisms for a 125 GeV Higgs at the LHC are gluon fusion $gg \rightarrow h$ through a top-quark loop and vector-boson fusion $qq \rightarrow qqh$. Additionally, the Higgsstrahlung process $q\bar{q} \rightarrow Vh$ provides a clean signal at the cost of a reduced cross section with respect to the other production channels.

These processes give rise to three different missing-energy signals for an invisible Higgs. At non-leading order, additional jets can radiate from coloured particle lines in gluon fusion, resulting in $j \cancel{E}_T$ and $jj \cancel{E}_T$ final states, the second of which is also attainable at leading order through vector boson fusion and Higgsstrahlung with a Z decaying hadronically. Alternatively, a Higgsstrahlung Z can decay leptonically, giving a signal $\ell^+\ell^- \cancel{E}_T$.

Missing energy rates from Higgs-bulk mixing at the LHC are also determined from the rate to produce ϕ_i final states. The arguments in §6.3.2 up to eq. (6.102) can be repeated for any of Higgs production processes at LHC, at least at parton-level, so that the missing energy, parton level cross section, $\hat{\sigma}$, is

$$\hat{\sigma}(X \rightarrow Y \cancel{E}_T) = \int_0^{M < \sqrt{\hat{s}} - m_Y} dM^2 \Upsilon(M^2) \hat{\sigma}_{SM}(X \rightarrow Y h) \Big|_{m_h=M}, \quad (6.106)$$

where \hat{s} is the parton-level center of mass energy squared, and m_Y is a placeholder for the region of M phase space denied to ϕ_i by the presence of the other final state particles. For example, if the final state particles associated with ϕ_i are all massless, $m_Y = 0$, and for Higgsstrahlung $m_Y = m_Z$ as in §6.3.2.

An important difference between the LHC rate and the rate at LEP is that the LHC is sufficiently energetic to probe the peak of $\Upsilon(M^2)$ that lies at m_h . This allows us to employ the narrow width approximation for $m_h \gg \Gamma_B + \Gamma_{SM}$, in which

$$\Upsilon(M^2) \approx \left[\frac{\Gamma_B}{\Gamma_B + \Gamma_{SM}} \right] \delta(M^2 - m_h^2), \quad (6.107)$$

where we have used the fact that $v^2 \zeta(m_h) = m_h \Gamma_B$. This simplifies the parton-level missing energy cross section

$$\hat{\sigma}(X \rightarrow Y \cancel{E}_T) = \left[\frac{\Gamma_B}{\Gamma_B + \Gamma_{SM}} \right] \hat{\sigma}_{SM}(X \rightarrow Y h). \quad (6.108)$$

One might worry that there are collisions where the initial state partons have small momentum fractions $x_{1,2}$, resulting in a small center of mass energy $\sqrt{\hat{s}} = \sqrt{x_1 x_2 \bar{s}}$. If $\sqrt{\hat{s}}$ is too small, then the integral over M^2 will not saturate the delta function

$\delta(M^2 - m_h^2)$. However, the resulting step function $\Theta(m_h + m_Y - \sqrt{\hat{s}})$ also appears in the Standard Model cross section where it encodes the threshold above which the Standard Model Higgs can be produced, and so we refrain from rewriting it. This calculation reveals that, in the narrow width limit, we expect the parton-level rate of producing an invisible Higgs to be suppressed relative to the Standard Model cross section by a factor of the invisible branching ratio $B = \Gamma_B/(\Gamma_B + \Gamma_{SM})$, as in other models with additional invisible Higgs decay channels.

The trivial mass and energy dependence of this factor allow us to convolve the parton distribution functions without complications. Furthermore, since it is only the modes near $M \approx m_h$ that contribute to the cross section in the narrow-width approximation, kinematic cuts will apply equally to single Higgs cross section and the Higgs-bulk cross section. Therefore, for a given production mechanism, the total missing energy proton-proton cross section at the LHC can be written

$$\sigma(pp \rightarrow Y \cancel{E}_T) = B \times \sigma_{SM}(pp \rightarrow Y h), \quad (6.109)$$

where $B = \Gamma_B/(\Gamma_B + \Gamma_{SM})$ as before, and $\sigma_{SM}(pp \rightarrow Y h)$ is the Standard Model production cross section at the LHC.

New-physics constraints and discovery estimates for a Higgs with invisible decay channels, specific to a given production channel are cast in terms of the quantity

$$\xi^2 := \left(\frac{\sigma_{BSM}}{\sigma_{SM}} \right) B_{\text{inv}}, \quad (6.110)$$

where σ_{BSM} is the production cross section of the proposed invisible Higgs, σ_{SM} is the Standard Model Higgs production cross section, and B_{inv} is the invisible branching

ratio predicted by new physics. Although these constraints envision a single Higgs state with new decay (and possibly production) modes, they apply equally well to Higgs-bulk production in the narrow width approximation, where we have $\sigma_{BSM} = \sigma_{SM}$ and $B_{inv} = B$ and so $\xi^2 = B$. The constraints and reach of LHC invisible-Higgs searches are readily translated into constraints on Higgs-bulk mixing (as in §6.3.1.)

Using the ATLAS monojet search at $\sqrt{s} = 7$ TeV with 1 fb^{-1} [43], the authors of Ref. [44] were able to bound $\xi^2 \lesssim 20$ for a 125 GeV Higgs-like particle. The updated CMS monjet data [45] with 4.7 fb^{-1} at 7 TeV was subsequently used [46] to tighten this constraint to $\xi^2 < 1.3$ at 95% C.L. and it was argued that the bound could be increased to $\xi^2 \lesssim 0.9$ with 15 fb^{-1} at 8 TeV. It is only once $\xi^2 < 1$ becomes possible that measurements become sensitive to Higgs-bulk mixing. However, part of this region is already accessible (and ruled out) by constraints from the LHC global fits discussed earlier, since they require $B_{inv} \lesssim 0.64$.

Nonetheless, higher integrated luminosity, and different channels, will allow Higgs-bulk mixing to be further probed. Ref. [47] estimates that the LHC with 20 fb^{-1} at 7 and 8 TeV can exclude invisible rates down to $\xi^2 \approx 0.4$ at 95% C.L. via the dijets plus missing energy signal. Finally, it was estimated that $\xi^2 \approx 0.25$ would be probed at 5σ by the LHC with 300 fb^{-1} at 14 TeV [48], also via dijets plus missing energy. Both of these studies also considered the LHC sensitivity to Higgsstrahlung process, where the Higgs is invisible and the Z decays leptonically, but found it to be a weaker probe of ξ^2 . Monojet searches were also concluded to be a weaker probe than vector boson fusion in ref. [47].

Astrophysical constraints

The new, invisible ϕ_i states can carry energy away from stars and supernovae. If the new emission process were too efficient, then it would conflict with the current understanding of stellar evolution. On this basis, it has been argued very generally [36] that any new energy loss channels in the sun must not exceed the solar energy loss rate $\dot{\mathcal{E}}_{\text{sun}} \approx 2 \text{ erg s}^{-1}\text{g}^{-1}$ and new channels in red giants and horizontal-branch stars cannot exceed $\dot{\mathcal{E}}_{\text{RG}} \approx 10 \text{ erg s}^{-1}\text{g}^{-1}$. Additionally, neutrino observations from SN1987a suggest that a new channel must not release energy at a rate exceeding the neutrino rate $\dot{\mathcal{E}}_{\text{SN}} \approx 10^{19} \text{ erg s}^{-1}\text{g}^{-1}$ during core collapse.

In this section, we consider a variety of ϕ emission processes in these settings and determine the strength of the corresponding bounds on Higgs-bulk mixing. Since the goal of this section is to estimate constraints, we make various simplifying assumptions and neglect the effects of dense media, interference effects from multiple scattering [36, 49] and the possibilities of trapping the KK modes inside of an astrophysical object, or of their decaying before exiting the astrophysical medium.

Electron-positron annihilation in supernovae

The temperature in the core of SN1987a $T_{\text{SN}} = (20 - 60) \text{ MeV}$ was high enough to produce electron-positron pairs. These pairs could have subsequently annihilated into an h state that then mixed over to a ϕ_i mode that carried energy away from the core. We calculate the associated energy loss rate for this simple process as an example to guide our discussion of astrophysics constraints on Higgs-bulk mixing.

The energy loss rate for this process is given by the sum of the individual ϕ_i

emission rates

$$\dot{\mathcal{E}} = \sum_i \dot{\mathcal{E}}_i. \quad (6.111)$$

where the emission rate to a single state ϕ_i is given by

$$\dot{\mathcal{E}}_i = \frac{1}{4\rho} \int \frac{d^3\mathbf{p}_1}{(2\pi)^3 2E_1} \frac{d^3\mathbf{p}_2}{(2\pi)^3 2E_2} \frac{d^3\mathbf{p}_\phi}{(2\pi)^3 2E_\phi} (f_1 f_2 E_\phi) |\mathcal{M}|_{p_\phi}^2 (2\pi)^4 \delta^4(p_1 + p_2 - p_\phi), \quad (6.112)$$

In the above equation $\rho = 3 \times 10^{14} \text{g cm}^{-3} \approx \Lambda_{QCD}^4$ is the density of the supernova core, $|\mathcal{M}|^2 = |\mathcal{M}(e^+e^- \rightarrow \phi_i)|^2$ is the spin-summed amplitude for the annihilation process, $p_{(1,2)}$ is the momentum of the initial state electron (positron) with energy $E_{(1,2)}$ and \mathbf{p}_ϕ is the momentum of the outgoing KK mode with energy E_ϕ . The occupation numbers $f_{(1,2)}$ are given by the Fermi-Dirac distribution for a relativistic electron (positron)

$$f_{(1,2)} = \frac{1}{e^{(E_{(1,2)} \mp \mu_e)/T} + 1}, \quad (6.113)$$

where $\mu_e \approx 345 \text{ MeV}$ is the chemical potential for the electron in the supernova core. Because the final state KK mode is assumed to escape, there is also no need for a Bose-Einstein final-state factor for it in the energy-loss rate. Eqs. (6.111) and (6.112) show that the total energy loss rate is a weighted sum of squared ϕ_i production amplitudes, so the results of §6.3.2 allow us to write the total energy loss rate in the form of an integral over M^2

$$\dot{\mathcal{E}} = \int_0^\infty dM^2 \frac{\Upsilon(M^2)}{4\rho} \int \frac{d^3\mathbf{p}_1}{(2\pi)^3 2E_1} \frac{d^3\mathbf{p}_2}{(2\pi)^3 2E_2} \frac{d^3\mathbf{p}_\phi}{(2\pi)^3 2E_\phi} (f_1 f_2 E_\phi) |\mathcal{M}_{SM}|_{p_\phi}^2 (2\pi)^4 \delta^4(p_1 + p_2 - p_\phi), \quad (6.114)$$

where $|\mathcal{M}_{SM}|^2 = |\mathcal{M}_{SM}(e^+e^- \rightarrow h)|^2$ is the spin-summed Standard Model Higgs amplitude squared.

As in §6.3.2 and §6.3.2, we could proceed by noting that the energy-loss rate can be written

$$\dot{\mathcal{E}} = \int_0^\infty dM^2 \Upsilon(M^2) \dot{\mathcal{E}}_{SM}(e^+e^- \rightarrow h) \Big|_{m_h=M}, \quad (6.115)$$

where $\dot{\mathcal{E}}_{SM}$ is the Standard Model Higgs emission rate, and it should be evaluated for a Higgs with mass $m_h = M$. However, since $\dot{\mathcal{E}}_{SM}$ is unknown, it is more straightforward to determine the total energy-loss rate via eq. (6.114), a task to which we now turn.

The spin-summed, squared, Standard Model amplitude is

$$|\mathcal{M}_{SM}(e^+e^- \rightarrow h)|^2 = 4(y_e^h)^2 E_1 E_2 (1 - \cos \theta_{12}), \quad (6.116)$$

where y_e^h is the Standard Model Higgs-electron Yukawa coupling, θ_{12} is the angle between the momentum vectors of the electron and positron, and the mass of the electron is neglected because $T_{SN} \gg m_e$. Using standard techniques to integrate phase space, we find

$$\dot{\mathcal{E}} = \frac{(y_e^h)^2}{64\pi^3 \rho} \int_0^\infty dE_1 dE_2 dM^2 \Upsilon(M^2) M^2 f_1 f_2 (E_1 + E_2) \Theta(4E_1 E_2 - M^2), \quad (6.117)$$

where Θ is a step function encoding the threshold above which a ϕ_i mode with mass M can be produced. This integral must be integrated numerically using the expression for $\Upsilon(M^2)$ in eq. (6.96).

The low-energy form of $\Upsilon(M^2)$ simplifies greatly if we specialize to $\lambda_2 = 0$, and consider the $\bar{g} \ll 1$ limit justified by existing constraints. First, eq. (6.64) gives $\zeta(M^2) = \bar{g}^2/4\alpha$ as constant. Additionally, assuming $\bar{g} \ll 1$ allow us to approximate eq. (6.65) as $\Pi(M^2) = m_h^2$. Finally, since $T_{SN}^2 \ll m_h^2$ we find that in these three limits

$\Upsilon(M^2)$ is a constant

$$\Upsilon(M^2) \approx \frac{\bar{g}^2 v^2}{4\pi\alpha m_h^4}, \quad (6.118)$$

where this approximation is better than 1% for $M < 1$ GeV and $\bar{g}/\alpha < 0.007$. This simplifies the total energy-loss rate to

$$\dot{\mathcal{E}} \approx \frac{(y_e^h)^2 T^5}{8\pi^3 \rho} \left(\frac{\bar{g}^2 v^2 T^2}{4\pi\alpha m_h^4} \right) \int_0^\infty dx dy \frac{(x+y)(xy)^2}{(e^{x-\mu_e/T} + 1)(e^{y+\mu_e/T} + 1)}, \quad (6.119)$$

where $x = E_1/T$ and $y = E_2/T$. This gives

$$\dot{\mathcal{E}} \approx \left(\frac{\bar{g}^2}{\alpha} \right) (4.4 \times 10^{17} \text{ erg s}^{-1} \text{g}^{-1}) T_{20}^7 \mathcal{I}(\mu_e/T), \quad (6.120)$$

where $T_{20} = T/(20 \text{ MeV})$ and \mathcal{I} is the integral factor in (6.119). It is exponentially sensitive to μ_e/T and ranges from 2×10^{-3} to 4.4 as temperature ranges from 20 to 60 MeV. However, even the most severe bound on Higgs-bulk mixing from electron-positron annihilation in SN1987a, which is found by assuming $T_{SN} = 60$ MeV, only constrains $\bar{g}/\sqrt{\alpha} \lesssim 0.05$, which is already ruled out (for $\bar{\lambda}_2 = 0$) by the LHC global-fit constraints in Fig. 6.6.

Stellar processes

Rather than calculating additional subdominant constraints on Higgs-bulk mixing, we next use existing constraints on the Yukawa coupling of a single light scalar ψ to estimate whether a given emission process will result in a significant bound. For example, the strongest stellar bound on the Yukawa coupling of a light scalar to nucleons, $y_N^\psi < 4.3 \times 10^{-11}$, comes from the Compton process $A\gamma \rightarrow A\psi$ in red

giants, where $A = \{^4\text{He}, p\}$ and the temperature of red giants is $T_{RG} \sim 10 \text{ keV}$ [36, 50]. The bound is derived by assuming that the light scalar couples only to nucleons, which is a good approximation to the Higgs-bulk mixing scenario since the ϕ_i states couple to the stellar constituents through the h state, and the Standard Model Higgs-nucleon Yukawa coupling is much larger than the electron Yukawa coupling $y_N^h \approx (340 \text{ MeV}/v) \gg y_e^h$ [51].

To estimate the energy loss rate for the Compton process $A \gamma \rightarrow A \phi$ in Higgs-bulk mixing, we write it the same form as eq. (6.115)

$$\dot{\mathcal{E}} = \int_0^\infty dM^2 \Upsilon(M^2) \dot{\mathcal{E}}_{SM}(A \gamma \rightarrow A h) \Big|_{m_h=M}, \quad (6.121)$$

where $\dot{\mathcal{E}}_{SM}$ is the Standard Model Higgs emission rate. In order of magnitude, we assume the Standard Model Higgs emission rate is related to the emission rate of a single light scalar ψ as follows

$$\dot{\mathcal{E}}_{SM}(A \gamma \rightarrow A h) \Big|_{m_h=M} \approx \left(\frac{y_N^h}{y_N^\psi} \right)^2 \dot{\mathcal{E}}_\psi(A \gamma \rightarrow A \psi) \Theta(T_{RG} - M), \quad (6.122)$$

where $\dot{\mathcal{E}}_\psi$ is the emission rate of a light scalar. We include a step function, Θ , to account for the fact that only Higgses of mass $M \lesssim T$ will have appreciable production rates. This follows from the fact that A is much heavier than the energy of the photon, so we can neglect its recoil and assume that the outgoing ϕ_i mode has the energy of the incoming photon $E_\phi \approx E_\gamma$. The emission rate for heavier ϕ_i modes is therefore suppressed by a Boltzmann factor $e^{-E_\gamma/T} \approx e^{-M/T} \ll 1$.

Using this approximation, and taking the $\lambda_2 = 0$, small \bar{g} , low-energy limits for $\Upsilon(M^2)$ in eq. (6.118) then gives an order of magnitude estimate for the Higgs-bulk

energy loss rate in terms of the ψ emission rate

$$\dot{\mathcal{E}} = \left(\frac{\bar{g}^2 v^2 T_{RG}^2}{4\pi\alpha m_h^4} \right) \left(\frac{y_N^h}{y_N^\psi} \right)^2 \dot{\mathcal{E}}_\psi(A\gamma \rightarrow A\psi). \quad (6.123)$$

This allows the bound on y_N^ψ to be translated into a bound on Higgs-bulk mixing (with $\lambda_2 = 0$)

$$\frac{\bar{g}^2 v^2 T_{RG}^2 (y_N^h)^2}{4\pi\alpha m_h^4} \lesssim (4.3 \times 10^{-11})^2, \quad (6.124)$$

from which it is estimated that even the tightest constraint $g/\sqrt{\alpha} \lesssim 0.8$ from stellar physics is subdominant to constraints from LHC global fits in Fig 6.6. For completeness, we note that there are similar constraints on the Yukawa coupling of a light scalar to nucleons from the Compton process in the sun, and the bremsstrahlung process $Ae \rightarrow Ae\psi$ in the sun and red giants [50], but none of these are estimated to give improved bounds on Higgs-bulk mixing.

Photon annihilation

Photon annihilation is a relevant process in both stars and supernovae. However, the Standard Model Higgs couples to photons through W and heavy quark loops, and so must the KK modes. For processes like photon annihilation $\gamma\gamma \rightarrow h$, in which the photons and Higgs are all on shell, the effect of these loops is well captured by the following effective Lagrangian [42]

$$\mathcal{L} = - \sum_{\ell} c_\gamma F_{\mu\nu} F^{\mu\nu} h \quad \text{with} \quad c_\gamma \approx \frac{\alpha_{em}}{6\pi v}. \quad (6.125)$$

We estimate that

$$|\mathcal{M}_{SM}(\gamma\gamma \rightarrow h)|^2 \approx \left(\frac{\alpha_{em}^2 T}{6\pi v y_e^h}\right)^2 |\mathcal{M}_{SM}(e^+ e^- \rightarrow h)|^2, \quad (6.126)$$

from which it follows that energy loss rate from photon annihilation is less than the rate from electron-positron annihilation, in stars and supernovae, and therefore gives a negligible bound.

Nucleon-bulk bremsstrahlung in supernovae

In addition to the bounds from the sun and red giants, there is a similar bound on the nucleon Yukawa coupling of a light scalar from SN1987a data $y_N^\psi \leq 4 \times 10^{-11}$ that follows from considering the nucleon bremsstrahlung process $NN \rightarrow NN\psi$ [52] and assuming $T_{SN} = 60$ MeV. This can be used to estimate the constraint coming from the energy loss process $NN \rightarrow NN\phi$. Although this upper limit is similar to the stellar bounds on the same coupling, it provides a much more stringent constraint on Higgs-bulk mixing because the supernova core is much hotter than red giants, thereby enhancing the Higgs-bulk energy loss rate by a factor $T_{SN}^2/T_{RG}^2 \sim 10^6$. Generalizing eq. (6.123) to bulk-nucleon bremsstrahlung, we expected a constraint $\bar{g}/\sqrt{\alpha} \lesssim 10^{-4}$ if the supernova temperature is assumed to be $T_{SN} = 60$ MeV, which is dominant to all other constraints discussed so far.

In order to confirm this estimate, we calculate the energy loss rate in the one pion exchange approximation, using the following interactions

$$\mathcal{L} = -ig_{\pi NN}\bar{N}\gamma_5 N \pi^0 - y_n^h h \bar{N}N, \quad (6.127)$$

where N represents the neutron, π^0 the neutral pion, and $g_{\pi NN} \approx 13$ phenomenologically. This approximation is known to overestimate the rate of axion and KK graviton bremsstrahlung, where it can be tested against model-independent calculations [53]. Since model-independent methods are not applicable to scalar radiation via a Yukawa coupling [54], the emission rate and associated bound are just crude estimates. We are content to further simplify the calculation by neglecting bremsstrahlung from protons, because the proton fraction in the supernova core is small, and by neglecting the Higgs-pion coupling, which is a dimension-5 operator. We also neglect a suppression due to multiple scattering effects [49] that is expected to reduce the emission rates of scalars in nucleon bremsstrahlung by as much as a factor of 5 [54].

The total energy loss rate for this process is given by

$$\dot{\mathcal{E}} = \int_0^\infty dM^2 \frac{\Upsilon(M^2)}{4\rho} \int \prod_{j=1,\dots,4} \left(\frac{d^3\mathbf{p}_j}{(2\pi)^3 2E_j} \right) \frac{d^3\mathbf{p}_\phi}{(2\pi)^3 2E_\phi} [f_1 f_2 (1-f_3)(1-f_4) E_\phi] \\ \times |\mathcal{M}_{SM}|_{p_\phi}^2 (2\pi)^4 \delta^4(p_1 + p_2 - p_3 - p_4 - k), \quad (6.128)$$

where $|\mathcal{M}_{SM}|^2 = |\mathcal{M}_{SM}(NN \rightarrow NNh)|^2$ is the spin-summed Standard Model Higgs amplitude squared, p_j represent the neutron four-momenta, and everything else maintains its old definition, except that it is now appropriate to use Maxwell-Boltzmann distributions for the non-relativistic neutrons with number density n_N

$$f_j = \frac{n_N}{2} \left(\frac{2\pi}{m_N T} \right)^{3/2} \exp \left(-\frac{\mathbf{p}_j^2}{2m_N T} \right), \quad (6.129)$$

and in the phase space measures $E_j \rightarrow m_N$, where m_N is the nucleon mass.

We proceed by calculating the spin-summed Standard Model Higgs amplitude $|\mathcal{M}_{SM}|^2$. There are 8 relevant diagrams for this process, four of which can be found

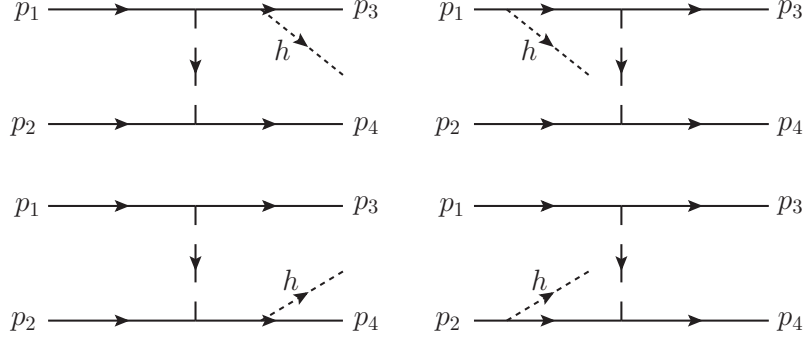


Figure 6.10: The four uncrossed graphs for Higgs-nucleon bremsstrahlung.

in Fig. 6.10. The other four correspond to the crossed analogues of those listed. In the nonrelativistic limit $|\mathbf{p}_j| \ll m_N$, and we assume the relevant KK modes are much lighter than the neutron $M \ll m_N$. In this limit, the squared, summed matrix element reads

$$|\mathcal{M}_{SM}|^2 = \frac{8(y_N^h)^2 g_{\pi NN}^4}{m_N^2} \left[\left(\frac{|\mathbf{k}|^2}{|\mathbf{k}|^2 + m_\pi^2} \right)^2 + \left(\frac{|\mathbf{l}|^2}{|\mathbf{l}|^2 + m_\pi^2} \right)^2 + \frac{|\mathbf{k}|^2 |\mathbf{l}|^2 - 2(\mathbf{k} \cdot \mathbf{l})^2}{(|\mathbf{k}|^2 + m_\pi^2)(|\mathbf{l}|^2 + m_\pi^2)} \right], \quad (6.130)$$

where $\mathbf{k} = \mathbf{p}_2 - \mathbf{p}_4$, $\mathbf{l} = \mathbf{p}_2 - \mathbf{p}_3$. The individual terms in the square brackets are $\mathcal{O}(1)$ since $|\mathbf{k}|, |\mathbf{l}| \sim \sqrt{m_N T} \approx m_\pi$ so that we approximate the matrix element as a constant [36]

$$|\mathcal{M}_{SM}|^2 \approx \frac{8(y_N^h)^2 g_{\pi NN}^4}{m_N^2}. \quad (6.131)$$

We evaluate the phase space integral in the non-degenerate limit. Although the neutrons in a supernova core are somewhat degenerate, in more detailed calculations of scalar-nucleon bremsstrahlung [54], the non-degenerate limit approximated the full emission rate well for moderate supernova temperatures $T_{SN} \gtrsim 20$ MeV. In this limit

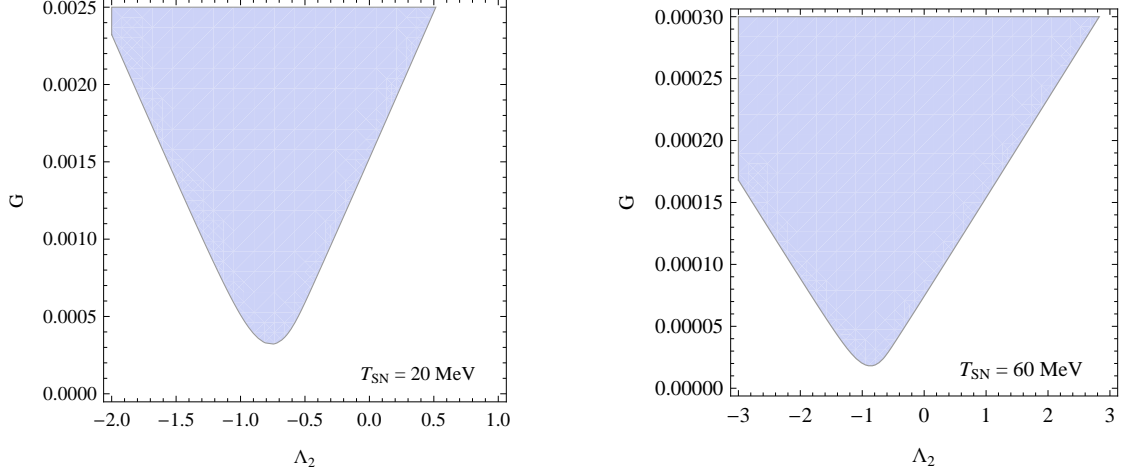


Figure 6.11: Constraints on Higgs-bulk mixing from bulk-nucleon bremsstrahlung in SN1987a. The left panel shows the constraints obtained assuming $T_{SN} = 20$ MeV and the right panel shows the analogous constraints assuming $T_{SN} = 60$ MeV. Couplings are evaluated at $1/\bar{r} = m_h = 125$ GeV.

we neglect the blocking factors $1 - f_{3,4} \approx 1$, and after integrating over phase space we find

$$\begin{aligned} \dot{\mathcal{E}} &= \frac{n_N^2 (y_n^h)^2 g_{\pi NN}^4 T^{7/2}}{128 \pi^{7/2} M_n^{9/2} \rho} \int_0^\infty dx dy dz \Upsilon(zT^2) x e^{-y-x} (y^2 + xy)^{1/2} (x^2 - z)^{1/2} \theta(x^2 - z) \\ &\approx \frac{n_N^2 (y_n^h)^2 g_{\pi NN}^4 T^{7/2}}{128 \pi^{7/2} M_n^{9/2} \rho} \int_0^\infty dx \int_0^{x^2} dz \Upsilon(zT^2) x e^{-x} (1 + x\pi/4)^{1/2} (x^2 - z)^{1/2}, \quad (6.132) \end{aligned}$$

where $x = E_\phi/T$, $z = M^2/T^2$ and the approximation made in the second line is good to within 2.2% [36]. This integral can be evaluated numerically, and the allowed region of parameter space from SN1987a constraints is plotted in Fig. 6.11.

This somewhat crude calculation and the associated bounds verify that bulk-nucleon bremsstrahlung in SN1987a is likely the strongest constraint on Higgs-bulk

mixing and, for $T_{SN} = 60$ MeV, gives $\bar{g}/\sqrt{\alpha} \lesssim 10^{-4}$ when $\lambda_2 = 0$, as estimated. However, since we neglected many effects that might suppress energy loss rate, and SN1987a bounds from nucleon bremsstrahlung are at best order of magnitude estimates, we assume the $T_{SN} = 20$ MeV bounds in order to be conservative.

6.3.3 Mass-coupling relations and vacuum stability

A great virtue of the Standard Model Higgs is the tight connection between the strength of its coupling to a particle and that particle's mass. In particular, knowledge of the mass of the Higgs itself reveals the strength of its self-coupling. Although it is not yet possible to directly measure this self-coupling, it plays a role in how couplings run at higher energies and so indirectly constrains the possibilities for UV physics.

These constraints differ in the presence of Higgs-bulk mixing, because this mixing changes the relation between the Higgs mass and its self-coupling. Furthermore, brane-bulk interactions quite generally introduce a new source of running for brane-localized interactions. Both of these observations work to change the nature of the constraints on UV physics.

There are generically two kinds of UV constraints that arise for Higgs couplings: ‘vacuum stability’ [55] and ‘triviality’ [56]. The first of these demands that the relevant quartic coupling of the Higgs potential not run to negative values. The second demands that any Landau poles (where the running couplings diverge) not arise at too low an energy. The depth of one's worry about these bounds depends fairly strongly on the depth of one's convictions as to how far this running can be trusted before some at-present-unknown UV physics intervenes. In the present instance triviality turns out to provide a fairly strong constraint on the brane-bulk coupling $\bar{\lambda}_2$.

To see how Higgs-bulk mixing changes things, we briefly restate the two sources of running. For the Standard Model Higgs self-coupling, one-loop renormalization — including the Higgs, top quark and the gauge bosons in the loop — gives the following beta function for $\bar{\lambda}$ [57]

$$\left(\mu \frac{d\bar{\lambda}}{d\mu}\right)_{SM} := \beta_{SM} \approx \frac{3}{4\pi^2} \left[\bar{\lambda}^2 + \bar{\lambda} y_t^2 - y_t^4 - \frac{\bar{\lambda}}{8} (3g_2^2 + g_1^2) + \frac{1}{64} (3g_2^4 + 2g_2^2 g_1^2 + g_1^4) \right], \quad (6.133)$$

where $y_t = m_t/v$ is the top-quark Yukawa coupling, and g_1 and g_2 are (respectively) the $U(1)_Y$ and $SU(2)_L$ gauge couplings, with the mass of the W and Z bosons given by $m_W^2 = g_2^2 v^2$ and $m_Z^2 = \frac{1}{4} (g_2^2 + g_1^2) v^2$ at tree-level, as usual. To these must be added the new Higgs-bulk contributions to the UV running of brane couplings, and writing $\mu d/d\mu = -f(\bar{r}) d/d\bar{r}$ these are given by

$$\begin{aligned} \left(\mu \frac{d\bar{\mu}_\Phi^2}{d\mu}\right)_B &= \frac{\bar{\lambda}_2 \bar{\mu}_\Phi^2}{2\pi\alpha}; & \left(\mu \frac{d\bar{g}}{d\mu}\right)_B &= \frac{\bar{g} \bar{\lambda}_2}{2\pi\alpha}; & \left(\mu \frac{d\bar{\lambda}_2}{d\mu}\right)_B &= \frac{\bar{\lambda}_2^2}{2\pi\alpha} \\ \left(\mu \frac{d\bar{\lambda}}{d\mu}\right)_B &= \frac{\bar{g}^2}{4\pi\alpha}; & \left(\mu \frac{d\bar{\mu}_H^2}{d\mu}\right)_B &= \frac{\bar{g} \bar{\mu}_\Phi^2}{2\pi\alpha}; & \left(\mu \frac{d\bar{T}}{d\mu}\right)_B &= \frac{\bar{\mu}_\Phi^4}{4\pi\alpha}. \end{aligned} \quad (6.134)$$

where a derivation can be found in Appendix D.1.

We've seen that ζ and $\bar{\lambda}_{\text{eff}}$ are two combinations of these couplings appear quite frequently in Higgs observables. Eqs. (6.134) imply these couplings satisfy

$$\left(\mu \frac{d\zeta}{d\mu}\right)_B = \left(\frac{\zeta \bar{\lambda}_2}{\pi\alpha}\right) \frac{1}{1 + (\bar{\lambda}_2/4\alpha)^2}, \quad (6.135)$$

and

$$\left(\mu \frac{d\bar{\lambda}_{\text{eff}}}{d\mu}\right)_B = \left(\frac{\zeta}{\pi}\right) \frac{1 - (\bar{\lambda}_2/4\alpha)^2}{1 + (\bar{\lambda}_2/4\alpha)^2}. \quad (6.136)$$

Notice that there is no requirement that $\bar{\lambda}_2$ be small, so we need not expand the

denominator in these expressions.

Triviality

An example of a solution to eqs. (6.134) is

$$\bar{g}(\mu) = \frac{\bar{g}(m_h)}{1 - \frac{\bar{\lambda}_2(m_h)}{2\pi\alpha} \log(\mu/m_h)}, \quad (6.137)$$

where we show the running relative to the Higgs mass scale, $\mu = m_h$. This shows how strongly the running depends on the coupling $\bar{\lambda}_2$. The triviality bound comes from demanding that couplings like \bar{g} remain within the perturbative regime throughout the energy ranges of interest. In particular, we require that the Landau pole (where $\bar{g} \rightarrow \infty$ and so $\bar{\lambda}_2(m_h) \log(\mu/m_h) = 2\pi\alpha$), not occur within this energy range.

Notice that the Landau pole arises for scales $\mu < m_h$ whenever $\bar{\lambda}_2 < 0$, but occurs for $\mu > m_h$ when $\bar{\lambda}_2 > 0$. If we demand no such pole at energies below 1 TeV then we must therefore require $\bar{\lambda}_2$ to lie in the range

$$0 \leq \Lambda_2 = \frac{\bar{\lambda}_2}{\alpha} \lesssim 3, \quad (6.138)$$

as indicated in Fig. 6.1. The upper limit becomes smaller if no Landau pole is allowed for energies above 1 TeV. This represents a significant constraint since none of our results required perturbing in $\bar{\lambda}_2$, and so were not restricted *a priori* to small $\bar{\lambda}_2$.

Vacuum stability

The vacuum-stability bound demands that $\bar{\lambda}$ remains positive as it is extrapolated into the UV (at least up to the point where any new UV physics intervenes to change

how things run). In the Standard Model this provides the strongest constraint for light Higgs masses, for which $\bar{\lambda}$ must be small. In this case, neglecting $\bar{\lambda}$ in its RG equation gives

$$\left(\mu \frac{d\bar{\lambda}}{d\mu}\right)_{SM} \approx \frac{3}{4\pi^2} \left[-y_t^4 + \frac{1}{64} (3g_2^4 + 2g_2^2 g_1^2 + g_1^4) \right], \quad (6.139)$$

and the constraint arises because the dominant term is negative, eventually driving $\bar{\lambda}$ negative.

The presence of Higgs-bulk mixing can change this constraint in at least three ways, two of which act to weaken the vacuum stability constraint. It first does so by moving the starting point for $\bar{\lambda}$ to more positive values. That is, the condition $m_h = 125$ GeV implies $\bar{\lambda}_{\text{eff}}(m_h) = 0.1291$ and so

$$\bar{\lambda}(m_h) = 0.1291 + \frac{\bar{g}^2(m_h)\bar{\lambda}_2(m_h)}{(4\alpha)^2 + \bar{\lambda}_2^2(m_h)}, \quad (6.140)$$

rather than simply $\bar{\lambda}(m_h) = 0.1291$, as would have been the case for the Standard Model. Because the triviality bound requires $\bar{\lambda}_2 > 0$ we see that the presence of bulk couplings moves the initial condition, $\bar{\lambda}(m_h)$, to more positive values.

The second change is to the RG equations governing the running of $\bar{\lambda}$. Including both the contributions from the bulk and from Standard Model loops, we have

$$\left(\mu \frac{d\bar{\lambda}}{d\mu}\right)_B = \beta_{SM} + \frac{\bar{g}^2}{4\pi\alpha}, \quad (6.141)$$

where β_{SM} represents the contribution of eq. (6.133). This shows that the bulk couplings always make $d\bar{\lambda}/d\mu$ more positive, and make it more difficult for $\bar{\lambda}$ to become

negative at higher energies.

Finally, the third way Higgs-bulk mixing changes the logic of these bounds is by providing new UV physics, beyond which a naive extrapolation using the renormalization group need not apply. Perhaps the most dramatic way this might happen can be seen in the large-volume case, for which the KK scale is much smaller than the Higgs mass. In this kind of scenario the extra-dimensional Newton constant is much smaller than the 4D Planck mass, and all extrapolations must break down at the mass scale associated with the extra-dimensional Newton constant due to the intervention of the UV physics (perhaps string theory) that is required to unitarize gravitational interactions.

Ultraviolet Fixed point for λ

The new, positive bulk contribution to the beta function also allows $\bar{\lambda}$ to reach an ultraviolet fixed point. Demanding the vanishing of eq. (6.141) at some UV scale μ gives

$$\frac{\bar{g}^2(\mu)}{\alpha} \approx -\frac{3}{\pi} \left[\bar{\lambda}^2 + \bar{\lambda} y_t^2 - y_t^4 - \frac{\bar{\lambda}}{8} (3g_2^2 + g_1^2) + \frac{1}{64} (3g_2^4 + 2g_2^2 g_1^2 + g_1^4) \right]. \quad (6.142)$$

To approximate the numerical value of this expression we evaluate the gauge couplings, top Yukawa coupling and Higgs quartic coupling at the weak scale, which is justified by their weak running and the proximity of μ to the electroweak scale. (A scale much higher than the weak scale would exceed the extra-dimensional gravity scale, as discussed above.) We also approximate $\bar{\lambda}(m_h) = 0.1291 + \mathcal{O}(\bar{g}^2(m_h)) \approx 0.1291$ and so we find that $\bar{g}(\mu)/\sqrt{\alpha} \approx 0.4$ is required to obtain a UV fixed point.

This condition can be run down to the Higgs mass scale using eq. (6.137), which

gives

$$\frac{\bar{g}(m_h)}{\sqrt{\alpha}} = \frac{\bar{g}(\mu)}{\sqrt{\alpha}} \left[1 - \frac{\bar{\lambda}_2(m_h)}{2\pi\alpha} \log(\mu/m_h) \right]. \quad (6.143)$$

Since constraints on Higgs bulk mixing restrict $\bar{g}(m_h)/\sqrt{\alpha} \ll \bar{g}(\mu)/\sqrt{\alpha} \approx 0.4$, the value of $\bar{\lambda}_2(m_h)$ required to attain a UV fixed point is given approximately by the vanishing of eq. (6.143). Choosing $\bar{\lambda}_2(m_h)$ in this way also ensures a Landau pole at μ , and so we conclude that the UV fixed point for $\bar{\lambda}$ and Landau pole are approximately coincident.

6.4 Conclusion

In summary, this paper examines the phenomenological implications of Higgs mixing with a bulk scalar field within an extra-dimensional brane-world scenario with the Standard Model localized on a brane. We focus in particular on the *Higgs portal*: the dimensionless couplings that can exist in such a scenario between a brane-localized Standard Model Higgs and a bulk scalar field if there are precisely two extra dimensions. We have a variety of motivations for studying this problem, with the main one being the requirement for such couplings in the recently discovered mechanism [22] for stabilizing two dimensions at naturally large values (through a manner similar to the Goldberger-Wise mechanism [21] with one extra dimension).

In a nutshell, we find that the Higgs portal causes the Higgs to mix with KK modes of the bulk scalar, generically leading to new channels for emitting missing energy in processes that can lead to Higgs emission. This can give observable signals at the LHC that strongly resemble the phenomenology of a Higgs with a branching ratio to an invisible decay channel. Unlike Higgs-curvature mixing, or bulk emission by

a Higgs (through the trilinear $hh\phi$ coupling), Higgs-bulk mixing through the extra-dimensional portal can give rise to an appreciable energy-loss rate in supernovae, leading to significant constraints on their couplings. As shown in Fig. 6.1, although strong, these constraints need not preclude an observable signal for an invisible Higgs ‘decay’ channel at the LHC.

In more detail, we find:

- *The strongest constraints come from nucleon bremsstrahlung in SN1987a:* the phase space made available by the high temperature of the supernova, the appreciable Higgs coupling to nucleons, and the strongly coupled nature of nucleon interactions makes this a very strong bound, as we expect from experience with graviton emission in extra dimensional models. However, the one pion exchange approximation we employ is known to overestimate the emission rate, the temperature of the supernova core is uncertain and our calculation assumes the non-degenerate limit, which overestimates the rate at small temperatures [54]. Furthermore, the neglected effect of multiple scatterings will decrease the emission rate. Therefore we conservatively estimate bounds assuming $T_{SN} = 20$ MeV, which gives the dominant bound $\bar{g}/\sqrt{\alpha} \lesssim 1.5 \times 10^{-3}$ (or $\zeta \lesssim 5.6 \times 10^{-7}$) when $\bar{\lambda}_2 = 0$.
- *LHC global fits:* the LHC can indirectly probe an invisible Higgs. An additional, invisible width suppresses Higgs signals, and too large a suppression would be in tension with the Standard-Model-like strength of signals currently being observed at the LHC. Global fits to the Tevatron and LHC Higgs data currently imply bounds $B_{inv} < (0.3 - 0.64)$ the most conservative of which imposes $\bar{g}/\sqrt{\alpha} \lesssim 0.007$ (or $\zeta \lesssim 5 \times 10^{-5}$), a bound subdominant to the SN1987a

bound. If more LHC data were to begin favouring a universal suppression to Higgs signals, then this would suggest an invisible Higgs width, possibly from Higgs-bulk mixing.

- *Invisible final states at the LHC:* the LHC can also directly search for invisible Higgs decays. The LHC will be most sensitive to the $2j + \cancel{E}_T$ signal from vector boson fusion into an invisible Higgs. Current searches are only sensitive to invisible Higgs cross sections roughly equal to the Standard Model cross section. However, at design energy and 300 fb^{-1} of integrated luminosity, it was estimated that this channel would allow the 5σ discovery of an invisible Higgs with Standard Model production cross section and an invisible branching ratio as small as $B_{\text{inv}} \approx 0.25$. With a more modest 20 fb^{-1} of luminosity at 7 and 8 TeV, the LHC should be able to rule out $B_{\text{inv}} \lesssim 0.4$ at 95% C.L. In both cases, there are regions of allowed parameter space that predict these branching ratios.
- *Additional cubic interaction:* Higgs-bulk mixing also predicts a cubic Higgs-Higgs-bulk interaction $\frac{1}{2}gh^2\phi(0)$. This interaction was studied in [15] in the context of the $h\phi \rightarrow \gamma\gamma\phi$ final state before the discovery of the new 125 GeV Higgs-like resonance, and without λ_2 and Higgs-bulk mixing effects. It was concluded that the LHC can probe down to $g = 0.18$ with 100 fb^{-1} at 14 TeV. The possibility of large λ_2 and a $h\phi \rightarrow b\bar{b}\phi$ final state through this interaction make the $\gamma\gamma\cancel{E}_T$ and $b\bar{b}\cancel{E}_T$ signals worth investigating as a probe of Higgs-bulk physics. The observation of an invisible Higgs width consistent with an increased rate in one or both of these channels would provide strong evidence of Higgs-bulk mixing.

- *Beyond the large-volume limit:* we present constraints and signals in the large-volume limit, but expect the the phenomenology to change a great deal if the volume were not large, so that $m_h \lesssim m_{KK}$. A single state in the diagonal KK tower would be identified as the 125 GeV resonance, and the spacing of nearby states would be governed by R^{-1} . There is no reason to believe that the main signals of large R Higgs-bulk mixing – invisible final states and suppressed Higgs production rates – would persist, and the astrophysical bounds would no longer apply to the much heavier states of this scenario. This scenario might resemble Higgs-radion mixing in Randall-Sundrum models, and we regard its exploration to be worth pursuing.
- *Future colliders:* although we refrained from discussing these in any detail, a future muon collider running at $\sqrt{s} = m_h$ with 0.5 fb^{-1} of data and beam energy resolution of 0.01% (0.003%) could directly probe the Higgs width to within 0.85 MeV (0.30 MeV) [58]. A future linear collider with an integrated luminosity of 250 fb^{-1} at 250 GeV would be able to constrain the Higgs invisible branching ratio to less than a few % [59]. This would correspond to the $B = 0.03$ line in Fig. 6.1.

In short, mixing through the Higgs-bulk portal provides a particular example of what detailed Higgs studies might ultimately tell us about the nature of vacuum energetics. We hope that this is the path Nature chooses, and that the Higgs is shown to have exotic invisible properties, rather than persisting in having invisible exotic properties.

Acknowledgements

We thank Hugo Beauchemin, Leo van Nierop, Brian Shuve, Matt Williams and Itay Yavin for useful discussions.

Bibliography

- [1] G. Aad *et al.* [ATLAS Collaboration], “Observation of a new particle in the search for the Standard Model Higgs boson with the ATLAS detector at the LHC,” *Phys. Lett. B* **716** (2012) 1 [arXiv:1207.7214 [hep-ex]];
- S. Chatrchyan *et al.* [CMS Collaboration], “Observation of a new boson at a mass of 125 GeV with the CMS experiment at the LHC,” *Phys. Lett. B* **716** (2012) 30 [arXiv:1207.7235 [hep-ex]].
- [2] J. M. Maldacena, “The large N limit of superconformal field theories and supergravity,” *Adv. Theor. Math. Phys.* **2** (1998) 231 [*Int. J. Theor. Phys.* **38** (1999) 1113] [hep-th/9711200];
- S. S. Gubser, I. R. Klebanov and A. M. Polyakov, “Gauge theory correlators from non-critical string theory,” *Phys. Lett. B* **428** (1998) 105 [hep-th/9802109];
- E. Witten, “Anti-de Sitter space and holography,” *Adv. Theor. Math. Phys.* **2** (1998) 253 [hep-th/9802150].
- [3] S. Weinberg, “Implications of Dynamical Symmetry Breaking,” *Phys. Rev. D* **13** (1976) 974;
- L. Susskind, “Dynamics of Spontaneous Symmetry Breaking in the Weinberg-Salam Theory,” *Phys. Rev. D* **20** (1979) 2619.
- [4] E. Farhi and L. Susskind, “Technicolor,” *Phys. Rept.* **74** (1981) 277.
- [5] J. Wess and B. Zumino, *Nucl. Phys. B* **70** (1974) 39;
- E. Witten, “Dynamical Breaking of Supersymmetry,” *Nucl. Phys. B* **188**

- (1981) 513;
- S. Dimopoulos and H. Georgi, “Softly Broken Supersymmetry and SU(5),” Nucl. Phys. B **193** (1981) 150.
- [6] H. P. Nilles, “Supersymmetry, Supergravity and Particle Physics,” Phys. Rept. **110** (1984) 1.
- H. E. Haber and G. L. Kane, “The Search for Supersymmetry: Probing Physics Beyond the Standard Model,” Phys. Rept. **117** (1985) 75.
- [7] C. P. Burgess, J. Matias and F. Quevedo, “MSLED: A Minimal supersymmetric large extra dimensions scenario,” Nucl. Phys. B **706** (2005) 71 [arXiv:hep-ph/0404135];
- J. Matias and C. P. Burgess, “MSLED, neutrino oscillations and the cosmological constant,” JHEP **0509** (2005) 052 [arXiv:hep-ph/0508156].
- [8] D. V. Volkov and V. P. Akulov, “Is the Neutrino a Goldstone Particle?,” Phys. Lett. B **46** (1973) 109;
- E. A. Ivanov and A. A. Kapustnikov, “General Relationship Between Linear And Nonlinear Realizations Of Supersymmetry,” J. Phys. A **11** (1978) 2375;
- E. A. Ivanov and A. A. Kapustnikov, “The Nonlinear Realization Structure Of Models With Spontaneously Broken Supersymmetry,” J. Phys. G **8** (1982) 167;
- S. Samuel and J. Wess, “A Superfield Formulation Of The Nonlinear Realization Of Supersymmetry And Its Coupling To Supergravity,” Nucl. Phys. B **221** (1983) 153.
- J. Bagger and J. Wess, “Partial Breaking Of Extended Supersymmetry,” Phys. Lett. B **138** (1984) 105;
- J. Hughes and J. Polchinski, “Partially Broken Global Supersymmetry and the Superstring,” Nucl. Phys. B **278** (1986) 147.
- [9] L. Randall, R. Sundrum, “A Large Mass Hierarchy from a Small Extra Dimension” Phys. Rev. Lett. **83** (1999) 3370 [hep-ph/9905221];

- “An Alternative to Compactification” *Phys. Rev. Lett.* **83** (1999) 4690 [hep-th/9906064].
- [10] N. Arkani-Hamed, S. Dimopoulos and G. R. Dvali, “The hierarchy problem and new dimensions at a millimeter,” *Phys. Lett. B* **429** (1998) 263 [arXiv:hep-ph/9803315];
- I. Antoniadis, N. Arkani-Hamed, S. Dimopoulos and G. R. Dvali, “New dimensions at a millimeter to a Fermi and superstrings at a TeV,” *Phys. Lett. B* **436** (1998) 257 [arXiv:hep-ph/9804398].
- [11] F. Coradeschi, S. De Curtis, D. Dominici, J. R. Pelaez, “Modified spontaneous symmetry breaking pattern by brane-bulk interaction terms,” *JHEP* **0804**, 048 (2008). [arXiv:0712.0537 [hep-th]].
- [12] G. F. Giudice, R. Rattazzi and J. D. Wells, “Graviscalars from higher dimensional metrics and curvature Higgs mixing,” *Nucl. Phys. B* **595**, 250 (2001) [hep-ph/0002178];
- D. Dominici and J. F. Gunion, “Invisible Higgs Decays from Higgs Graviscalar Mixing,” *Phys. Rev. D* **80**, 115006 (2009) [arXiv:0902.1512 [hep-ph]].
- [13] E. Dudas, C. Papineau and V. A. Rubakov, “Flowing to four dimensions,” *JHEP* **0603** (2006) 085 [hep-th/0512276];
- [14] C. P. Burgess, C. de Rham and L. van Nierop, “The Hierarchy Problem and the Self-Localized Higgs,” *JHEP* **0808** (2008) 061 [arXiv:0802.4221 [hep-ph]].
- [15] P. H. Beauchemin, G. Azuelos and C. P. Burgess, “Dimensionless coupling of bulk scalars at the LHC,” *J. Phys. G G* **30**, N17 (2004) [hep-ph/0407196];
- G. Azuelos, P. H. Beauchemin and C. P. Burgess, “Phenomenological constraints on extra dimensional scalars,” *J. Phys. G G* **31**, 1 (2005) [hep-ph/0401125].
- [16] N. Arkani-Hamed, S. Dimopoulos and G. R. Dvali, “Phenomenology, astrophysics and cosmology of theories with submillimeter dimensions and TeV scale quantum gravity,” *Phys. Rev. D* **59**, 086004 (1999) [hep-ph/9807344];
- G. F. Giudice, R. Rattazzi and J. D. Wells, “Quantum gravity and extra dimensions at high-energy colliders,” *Nucl. Phys. B* **544**, 3 (1999) [hep-ph/9811291];

- T. Han, J. D. Lykken and R. -J. Zhang, “On Kaluza-Klein states from large extra dimensions,” *Phys. Rev. D* **59**, 105006 (1999) [hep-ph/9811350].
- [17] K. Lanczos, *Phys. Z.* **23** (1922) 239–543; *Ann. Phys.* **74** (1924) 518–540;
- C.W. Misner and D.H. Sharp, “Relativistic Equations for Adiabatic, Spherically Symmetric Gravitational Collapse” *Phys. Rev.* **136** (1964) 571–576;
- W. Israel, “Singular hypersurfaces and thin shells in general relativity” *Nuov. Cim.* **44B** (1966) 1–14; *errata Nuov. Cim.* **48B** 463.
- [18] C. P. Burgess, D. Hoover, C. de Rham and G. Tasinato, “Effective Field Theories and Matching for Codimension-2 Branes,” *JHEP* **0903** (2009) 124 [arXiv:0812.3820 [hep-th]];
- A. Bayntun, C.P. Burgess and L. van Nierop, “Codimension-2 Brane-Bulk Matching: Examples from Six and Ten Dimensions,” *New J. Phys.* **12** (2010) 075015 [arXiv:0912.3039 [hep-th]];
- [19] W. D. Goldberger and M. B. Wise, “Renormalization group flows for brane couplings,” *Phys. Rev. D* **65** (2002) 025011 [hep-th/0104170];
- T. Kobayashi, “UV caps, IR modification of gravity, and recovery of 4D gravity in regularized braneworlds,” *Phys. Rev. D* **78** (2008) 084018 [arXiv:0806.0924 [hep-th]].
- [20] C. de Rham, “The Effective field theory of codimension-two branes,” *JHEP* **0801**, 060 (2008) [arXiv:0707.0884 [hep-th]];
- C. de Rham, “Classical renormalization of codimension-two brane couplings,” *AIP Conf. Proc.* **957** (2007) 309 [arXiv:0710.4598 [hep-th]].
- [21] W. D. Goldberger and M. B. Wise, “Modulus stabilization with bulk fields”, *Phys. Rev. Lett.* **83** (1999) 4922-4925 [arXiv:hep-ph/9907447]
- [22] C. P. Burgess and L. van Nierop, “Large Dimensions and Small Curvatures from Supersymmetric Brane Back-reaction,” *JHEP* **1104** (2011) 078 [arXiv:1101.0152 [hep-th]].
- [23] H. Nishino and E. Sezgin, *Phys. Lett.* **144B** (1984) 187; “The Complete N=2, D = 6 Supergravity With Matter And Yang-Mills Couplings,” *Nucl. Phys.* **B278** (1986) 353;

- S. Randjbar-Daemi, A. Salam, E. Sezgin and J. Strathdee, “An Anomaly Free Model in Six-Dimensions” *Phys. Lett.* **B151** (1985) 351.
- [24] A. Salam and E. Sezgin, “Chiral Compactification On Minkowski X S^{*2} Of $N=2$ Einstein-Maxwell Supergravity In Six-Dimensions,” *Phys. Lett. B* **147** (1984) 47.
- [25] Y. Aghababaie, C.P. Burgess, S. Parameswaran and F. Quevedo, “Towards a Naturally Small Cosmological Constant from Branes in 6D Supergravity” *Nucl. Phys.* **B680** (2004) 389–414, [hep-th/0304256].
- [26] C. P. Burgess, D. Hoover and G. Tasinato, “UV Caps and Modulus Stabilization for 6D Gauged Chiral Supergravity,” *JHEP* **0709** (2007) 124 [arXiv:0705.3212 [hep-th]];
- C. P. Burgess and L. van Nierop, “Bulk Axions, Brane Back-reaction and Fluxes,” *JHEP* **1102** (2011) 094 [arXiv:1012.2638 [hep-th]];
- [27] C. P. Burgess, “Supersymmetric large extra dimensions and the cosmological constant: An update,” *Annals Phys.* **313** (2004) 283 [arXiv:hep-th/0402200];
- “Towards a natural theory of dark energy: Supersymmetric large extra dimensions,” *AIP Conf. Proc.* **743** (2005) 417 [arXiv:hep-th/0411140].
- [28] C. P. Burgess and D. Hoover, “UV sensitivity in supersymmetric large extra dimensions: The Ricci-flat case,” *Nucl. Phys. B* **772** (2007) 175 [hep-th/0504004];
- D. Hoover and C. P. Burgess, “Ultraviolet sensitivity in higher dimensions,” *JHEP* **0601** (2006) 058 [hep-th/0507293];
- C. P. Burgess, D. Hoover, G. Tasinato, “Technical Naturalness on a Codimension-2 Brane,” *JHEP* **0906** (2009) 014. [arXiv:0903.0402 [hep-th]];
- M. Williams, C. P. Burgess, L. van Nierop and A. Salvio, “Running with Rugby Balls: Bulk Renormalization of Codimension-2 Branes,” arXiv:1210.3753 [hep-th];
- C. P. Burgess, L. van Nierop, S. Parameswaran, A. Salvio and M. Williams, “Accidental SUSY: Enhanced Bulk Supersymmetry from Brane Back-reaction,” arXiv:1210.5405 [hep-th].
- [29] F. Leblond, *Phys. Rev. D* **64**, 045016 (2001) [hep-ph/0104273].

- [30] G. W. Gibbons, R. Guven and C. N. Pope, “3-branes and uniqueness of the Salam-Sezgin vacuum,” *Phys. Lett. B* **595** (2004) 498 [hep-th/0307238];
- Y. Aghababaie *et al.*, “Warped brane worlds in six dimensional supergravity,” *JHEP* **0309** (2003) 037 [hep-th/0308064];
- C. P. Burgess, F. Quevedo, G. Tasinato and I. Zavala, “General axisymmetric solutions and self-tuning in 6D chiral gauged supergravity,” *JHEP* **0411** (2004) 069 [hep-th/0408109];
- S. L. Parameswaran, G. Tasinato and I. Zavala, “The 6D SuperSwirl,” *Nucl. Phys. B* **737** (2006) 49 [arXiv:hep-th/0509061];
- H. M. Lee and C. Ludeling, “The general warped solution with conical branes in six-dimensional supergravity,” *JHEP* **0601** (2006) 062 [arXiv:hep-th/0510026];
- A. J. Tolley, C. P. Burgess, D. Hoover and Y. Aghababaie, “Bulk singularities and the effective cosmological constant for higher co-dimension branes,” *JHEP* **0603** (2006) 091 [hep-th/0512218];
- A. J. Tolley, C. P. Burgess, C. de Rham and D. Hoover, “Scaling solutions to 6D gauged chiral supergravity,” *New J. Phys* **8** (2006) 324 [arXiv:0608.083 [hep-th]];
- A. J. Tolley, C. P. Burgess, C. de Rham and D. Hoover, “Exact Wave Solutions to 6D Gauged Chiral Supergravity,” *JHEP* **0807** (2008) 075 [arXiv:0710.3769 [hep-th]];
- M. Minamitsuji, “Instability of brane cosmological solutions with flux compactifications,” *Class. Quant. Grav.* **25** (2008) 075019 [arXiv:0801.3080 [hep-th]].
- [31] C. P. Burgess, C. de Rham, D. Hoover, D. Mason and A. J. Tolley, “Kicking the rugby ball: Perturbations of 6D gauged chiral supergravity,” *JCAP* **0702**, 009 (2007) [hep-th/0610078];
- S. L. Parameswaran, S. Randjbar-Daemi and A. Salvio, “General Perturbations for Braneworld Compactifications and the Six Dimensional Case,” *JHEP* **0903**, 136 (2009) [arXiv:0902.0375 [hep-th]];

- [32] P. P. Giardino, K. Kannike, M. Raidal and A. Strumia, “Reconstructing Higgs boson properties from the LHC and Tevatron data,” *JHEP* **1206**, 117 (2012) arXiv:1203.4254 [hep-ph].
- [33] J. R. Espinosa, M. Muhlleitner, C. Grojean and M. Trott, “Probing for Invisible Higgs Decays with Global Fits,” *JHEP* **1209**, 126 (2012) arXiv:1205.6790 [hep-ph].
- [34] D. Carmi, A. Falkowski, E. Kuflik, T. Volansky and J. Zupan, “Higgs After the Discovery: A Status Report,” *JHEP* **1210**, 196 (2012) arXiv:1207.1718 [hep-ph].
- [35] B. A. Dobrescu and J. D. Lykken, “Coupling spans of the Higgs-like boson,” arXiv:1210.3342 [hep-ph].
- [36] G. G. Raffelt, “Stars as laboratories for fundamental physics: The astrophysics of neutrinos, axions, and other weakly interacting particles,” Chicago, USA: Univ. Pr. (1996)
- [37] S. Hannestad and G. G. Raffelt, “Stringent neutron star limits on large extra dimensions,” *Phys. Rev. Lett.* **88** (2002) 071301 [arXiv:hep-ph/0110067];
- “New supernova limit on large extra dimensions,” *Phys. Rev. Lett.* **87** (2001) 051301 [arXiv:hep-ph/0103201].
- [38] S. Cullen and M. Perelstein, “SN1987A constraints on large compact dimensions,” *Phys. Rev. Lett.* **83** (1999) 268 [arXiv:hep-ph/9903422];
- V. D. Barger, T. Han, C. Kao and R. J. Zhang, “Astrophysical constraints on large extra dimensions,” *Phys. Lett. B* **461** (1999) 34 [arXiv:hep-ph/9905474];
- [39] D. Atwood, C. P. Burgess, E. Filotas, F. Leblond, D. London and I. Maksymyk, “Supersymmetric large extra dimensions are small and/or numerous,” *Phys. Rev. D* **63** (2001) 025007 [arXiv:hep-ph/0007178];
- [40] J. P. Miller, E. de Rafael and B. L. Roberts, “Muon (g-2): Experiment and theory,” *Rept. Prog. Phys.* **70**, 795 (2007) [hep-ph/0703049].
- [41] [LEP Higgs Working for Higgs boson searches and ALEPH and DELPHI and CERN-L3 and OPAL Collaborations], “Searches for invisible Higgs bosons: Preliminary combined results using LEP data collected at energies up to 209-GeV,” hep-ex/0107032.

- [42] See, for example, C. P. Burgess, J. Matias and M. Pospelov, “A Higgs or not a Higgs? What to do if you discover a new scalar particle,” *Int. J. Mod. Phys. A* **17**, 1841 (2002) [hep-ph/9912459];
- J. R. Ellis, M. K. Gaillard and D. V. Nanopoulos, “A Phenomenological Profile of the Higgs Boson,” *Nucl. Phys. B* **106**, 292 (1976).
- [43] G. Aad *et al.* [ATLAS Collaboration], “Search for new phenomena with the monojet and missing transverse momentum signature using the ATLAS detector in $\sqrt{s} = 7$ TeV proton-proton collisions,” *Phys. Lett. B* **705**, 294 (2011) [arXiv:1106.5327 [hep-ex]] and ATLAS-CONF-2011-096 updates.
- [44] C. Englert, J. Jaeckel, E. Re and M. Spannowsky, “Evasive Higgs Maneuvers at the LHC,” *Phys. Rev. D* **85**, 035008 (2012) [arXiv:1111.1719 [hep-ph]].
- [45] S. Chatrchyan *et al.* [CMS Collaboration], “Search for dark matter and large extra dimensions in monojet events in pp collisions at $\sqrt{s} = 7$ TeV,” *JHEP* **1209**, 094 (2012) [arXiv:1206.5663 [hep-ex]] and CMS-PAS-EXO-11-059 updates.
- [46] A. Djouadi, A. Falkowski, Y. Mambrini and J. Quevillon, “Direct Detection of Higgs-Portal Dark Matter at the LHC,” arXiv:1205.3169 [hep-ph].
- [47] Y. Bai, P. Draper and J. Shelton, “Measuring the Invisible Higgs Width at the 7 and 8 TeV LHC,” *JHEP* **1207**, 192 (2012) [arXiv:1112.4496 [hep-ph]].
- [48] D. Ghosh, R. Godbole, M. Guchait, K. Mohan and D. Sengupta, “Looking for an Invisible Higgs Signal at the LHC,” arXiv:1211.7015 [hep-ph].
- [49] G. Raffelt and D. Seckel, “Multiple scattering suppression of the bremsstrahlung emission of neutrinos and axions in supernovae,” *Phys. Rev. Lett.* **67**, 2605 (1991).
- [50] J. A. Grifols, E. Masso and S. Peris, “Energy Loss From The Sun And Red Giants: Bounds On Short Range Baryonic And Leptonic Forces,” *Mod. Phys. Lett. A* **4**, 311 (1989).
- [51] See, for example, C. P. Burgess, M. Pospelov and T. ter Veldhuis, “The Minimal model of nonbaryonic dark matter: A Singlet scalar,” *Nucl. Phys. B* **619**, 709 (2001) [hep-ph/0011335].
- [52] N. Ishizuka and M. Yoshimura, “Axion And Dilaton Emissivity From Nascent Neutron Stars,” *Prog. Theor. Phys.* **84**, 233 (1990).

- [53] C. Hanhart, D. R. Phillips and S. Reddy, “Neutrino and axion emissivities of neutron stars from nucleon-nucleon scattering data,” *Phys. Lett. B* **499**, 9 (2001) [astro-ph/0003445];
- C. Hanhart, D. R. Phillips, S. Reddy and M. J. Savage, “Extra dimensions, SN1987a, and nucleon-nucleon scattering data,” *Nucl. Phys. B* **595**, 335 (2001) [nucl-th/0007016].
- [54] D. Arndt and P. J. Fox, “Saxion emission from SN1987A,” *JHEP* **0302**, 036 (2003) [hep-ph/0207098].
- [55] S. Weinberg, “Mass of the Higgs Boson,” *Phys. Rev. Lett.* **36** (1976) 294;
- A. D. Linde, “Dynamical Symmetry Restoration and Constraints on Masses and Coupling Constants in Gauge Theories,” *JETP Lett.* **23**, 64 (1976) [*Pisma Zh. Eksp. Teor. Fiz.* **23**, 73 (1976)].
- [56] B. Grzadkowski and M. Lindner, “Stability Of Triviality Mass Bounds In The Standard Model,” *Phys. Lett. B* **178** (1986) 81;
- M. Luscher and P. Weisz, “Scaling Laws and Triviality Bounds in the Lattice ϕ^4 Theory. 1. One Component Model in the Symmetric Phase,” *Nucl. Phys. B* **290** (1987) 25;
- “Scaling Laws and Triviality Bounds in the Lattice ϕ^4 Theory. 2. One Component Model in the Phase with Spontaneous Symmetry Breaking,” *Nucl. Phys. B* **295** (1988) 65.
- [57] S. Dawson, “Introduction to electroweak symmetry breaking,” [hep-ph/9901280];
- T. P. Cheng, E. Eichten and L. -F. Li, “Higgs Phenomena in Asymptotically Free Gauge Theories,” *Phys. Rev. D* **9**, 2259 (1974).
- [58] T. Han and Z. Liu, “Direct Measurement of the Higgs Boson Total Width at a Muon Collider,” arXiv:1210.7803 [hep-ph].
- [59] H. Baer *et al.* “Physics at the International Linear Collider.” Physics Chapter of the ILC Detailed Baseline Design Report. Preliminary Version: Draft of January 22, 2013. <http://lcsim.org/papers/DBDPhysics.pdf>
- [60] C. P. Burgess and L. van Nierop, “Technically Natural Cosmological Constant From Supersymmetric 6D Brane Backreaction,” arXiv:1108.0345 [hep-th].

[61] J. W. Chen, M. A. Luty and E. Ponton, “A Critical cosmological constant from millimeter extra dimensions” JHEP **0009**(2000)012 [arXiv:hep-th/0003067];

F. Leblond, R. C. Myers and D. J. Winters, “Consistency conditions for brane worlds in arbitrary dimensions,” JHEP **0107** (2001) 031 [arXiv:hep-th/0106140];

S. M. Carroll and M. M. Guica, “Sidestepping the cosmological constant with football-shaped extra dimensions,” [hep-th/0302067].

Chapter 7

Summary and outlook

This thesis addressed naturalness issues within the standard models of particle physics and cosmology. The two issues of interest were the electroweak hierarchy problem and the cosmological constant problem. Both of these conundrums stem from the observed smallness of a physical quantity within the Standard model, and the fact that the physical quantity in question is controlled by a dimensionful parameter in the theory that is supposed to be sensitive to UV physics. More precisely, the electroweak hierarchy problem is the statement that the observed Higgs mass is far below the mass scale of any new physics, despite the expectation that heavy particles should contribute to the coupling of the $H^\dagger H$ operator at low energies. Similarly, the cosmological constant problem is associated with the constant part of the Standard Model Lagrangian, c_0 , which is expected to be large at low energies since it receives contributions from every Standard Model particle and any heavier particles. The issue is that the 4D curvature of the universe – which is linked to c_0 , at least in the Standard Model – is observed to be set by sub-eV scale physics. The first chapter outlined how neither of these scenarios can be considered natural, and quickly described how

braneworld models with large extra dimensions can alleviate these problems in a way that is consistent with current observational limits.

The second chapter illustrated more concretely how the 4D curvature of the universe can be calculated in extra-dimensional braneworld models, and highlighted that bulk scale invariance can be used to ensure a vanishing 4D curvature for any value of c_0 , at least in the absence of branes. Breaking the connection between c_0 and the observed small curvature would be progress towards solving the cosmological constant problem. However, when branes are added to the system, it is their direct contributions and their back-reaction effects that become the leading terms in the 4D curvature, and these might be as large as c_0 . As this chapter explained, branes complicate the story, because different technical difficulties stand in the way of fully understanding their back-reaction and stress-energy.

The subsequent chapters, 3 and 4, dealt with these issues. Branes in a higher-dimensional system were replaced with vortices, which are smooth, stable, localized field configurations that can be represented by branes at low energies. The vortices served as an unambiguous UV completion of branes whose behaviour was analyzed analytically and numerically. The back-reaction and stress-energy of vortices was calculated, and the pointlike limit of these results was used to determine the correct treatment of branes. It was shown that scale invariant branes/vortices do not source any 4D curvature, and this becomes a problem since vanishing curvature in this case is ensured by having a zero mode run away to infinity. So called decoupled branes and/or vortices were identified, for which scale invariance is broken, but only by the higher-order localized flux term in the brane lagrangian. This chapter concluded by describing why decoupled branes are a promising solution to the cosmological

constant problem, since scale breaking through the localized brane flux term appears to predict a 4D curvature that is suppressed by the size of the extra dimensions, while also stabilizing the runaway zero mode.

The fifth chapter examined the issues of zero mode stabilization and 4D curvature in the 4D effective theory of these models that is relevant at energies below the Kaluza-Klein scale. Scale breaking branes in a scale invariant bulk were shown to be described by an effective 4D theory with a single scalar field, the zero mode, that is subject to a potential $U(\varphi) = e^{2\varphi} F(\varphi)$. This potential was calculated as a function of brane parameters in the UV theory, and a number of phenomenologically interesting potentials were investigated, including potentials that can generate exponentially large extra dimensions from natural UV parameters, and potentials coming from branes that are perturbatively close to being scale invariant. The latter class of potentials generically give 4D curvatures that are suppressed by the small quantity that measures the deviation from scale invariance. The chapter concluded with comments on the viability of these potentials in a realistic setting that includes the Standard Model and quantum corrections.

A robust property of the models with stabilized extra dimensions is a coupling between a bulk scalar and the brane. The list of relevant interactions between the Standard Model brane and a bulk scalar is short, and these interactions were investigated phenomenologically in the sixth chapter. Constraints were placed on the strength of the Higgs-bulk mixing interaction which gives rise to phenomena like a modified invisible Higgs width, missing energy signals at colliders, energy loss in stars. Furthermore, renormalizing the divergences associated with Higgs-bulk mixing require the couplings in the Higgs potential to run classically, which improve vacuum

stability. Finally, it was shown that Higgs-bulk mixing might be among the first hints of extra dimensions, since the allowed parameter space will be probed at the LHC and proposed future colliders.

The final verdict on large extra dimensions as a solution to electroweak hierarchy problem is one of optimism. This thesis showed that there are straightforward mechanisms to generate extra dimensions that are large enough to help solve the electroweak hierarchy problem. There are robust, testable signals of these mechanisms, such as the invisible Higgs signals presented in this thesis. Though an anomalous invisible Higgs signal alone would not be enough to prove the existence of large extra dimensions, their discovery would merit a more concerted theoretical investigation into stabilization and Higgs-bulk mixing. For example, it might be possible to relate the desired size of the extra dimensions to the strength of Higgs-bulk coupling. However, at present, there are no theoretical estimates of the size of the Higgs-bulk couplings, despite the fact that this thesis presented fully functional mechanisms for stabilizing the size of the extra dimensions, from which such an estimate might be made. If modified invisible Higgs phenomena were observed, it would be very compelling if these observations were made at values that were favoured by extra-dimensional stabilization.

Solving the cosmological constant problem with large extra dimensions is arguably more difficult. The most promising prospects presented in the body of the thesis require the Standard Model to couple to a scalar field in a scale invariant way, which is a scenario that is accompanied by its own cabal of phenomenological issues. In any case, even the suppression of the 4D curvature below the particle physics scale is more progress than most models can claim, and there are a number of interesting

directions for future work, such as systems where the requirement of scale invariant brane tension might not require the Standard Model to couple to a scalar field.

The tools presented in this thesis can be used to attack other problems in particle physics and cosmology. A pressing issue that was almost entirely ignored here is the nature of dark matter. However, there are extra dimensional models of dark matter that bear a striking resemblance to some of the models studied here. For example, dynamical dark matter [1], is a proposal that suggests dark matter is composed of a bulk scalar living in large extra dimensions that couples to a brane with the same couplings as were considered in the Higgs-bulk mixing chapter. There are also popular models of dark matter with a hidden sector, and the portal between the Standard Model and this sector is gauge kinetic mixing [2]. There is an extra-dimensional analogue of this coupling, $F_Y^{\mu\nu} \mathcal{A}_{\mu\nu}$ that constitutes a dimension-5 operator. In the same way that the Higgs-bulk portal was special because it was the unique relevant interaction between the Standard Model and a bulk scalar field, this interaction is the most relevant interaction between the standard model and a bulk gauge field. This operator would provide a means for the photon and Z boson to escape into the bulk and some of the associated phenomena include light shining through walls [3], as the photon oscillates into the bulk then returns, and a modified invisible Z width [4], which is highly constrained and very testable.

Finally, the techniques employed in this thesis lay the groundwork for understanding the effective description of localized sources, and the back-reaction of higher codimension sources on bulk fields. This technology might find use in any number of places, for example to confront problems in high energy physics like monopole catalysis [5], or perhaps to better understand the physics biological membranes.

Bibliography

- [1] K. R. Dienes and B. Thomas, “Dynamical Dark Matter: I. Theoretical Overview,” *Phys. Rev. D* **85**, 083523 (2012) [arXiv:1106.4546 [hep-ph]].
- [2] N. Arkani-Hamed, D. P. Finkbeiner, T. R. Slatyer and N. Weiner, “A Theory of Dark Matter,” *Phys. Rev. D* **79**, 015014 (2009) [arXiv:0810.0713 [hep-ph]].
- [3] J. Redondo and A. Ringwald, “Light shining through walls,” *Contemp. Phys.* **52**, 211 (2011) [arXiv:1011.3741 [hep-ph]].
- [4] K. A. Olive *et al.* [Particle Data Group Collaboration], “Review of Particle Physics,” *Chin. Phys. C* **38**, 090001 (2014).
- [5] C. G. Callan, Jr., “Monopole Catalysis of Baryon Decay,” *Nucl. Phys. B* **212**, 391 (1983).

Appendix A

Appendix for Chapter 3

A.1 Stress-energy conservation

The matter field equations always guarantee the matter stress energy is covariantly conserved, $\nabla_M T^{MN} = 0$. For the geometries of interest this has one nontrivial component, $\nabla_M T^{M\rho} = 0$, which implies

$$\left(BW^d T^\rho{}_\rho \right)' = BW^d \left(\frac{B'}{B} T^\theta{}_\theta + \frac{W'}{W} T^\mu{}_\mu \right). \quad (\text{A.1})$$

A useful way to rewrite this multiplies by B and adds $BB'W^d T^\rho{}_\rho$ to both sides, so

$$\left(B^2 W^d T^\rho{}_\rho \right)' = BW^d \left[B' (T^\theta{}_\theta + T^\rho{}_\rho) + \frac{BW'}{W} T^\mu{}_\mu \right], \quad (\text{A.2})$$

or

$$\left[\sqrt{-g} B(\mathcal{Z} - \mathcal{X}) \right]' = -\sqrt{-g} \left[2B' \mathcal{X} + \frac{dBW'}{W} \varrho \right]. \quad (\text{A.3})$$

When applied to a vortex on flat space — for which $W = B' = 1$ and the constraint (3.26) implies $\mathcal{Z} - \mathcal{X} = 0$ outside the vortex — integrating eq. (A.3) over the vortex reduces to the simple statement

$$\langle \mathcal{X} \rangle_v \Big|_{\text{flat}} = \langle L_{\text{pot}} - L_{\text{gge}} \rangle_v \Big|_{\text{flat}} = 0, \quad (\text{A.4})$$

a result that may also be derived as the vortex equation of motion corresponding to extremizing the flat-space action against rigid rescalings.

A.2 Approximate near-vortex solutions

For the purposes of matching the bulk integration constants to the vortex properties we are most interested in the form of the solutions very near to, but outside of, the vortex sources. We start by recapping the form of the bulk solutions very close, but outside of, a small vortex.

Asymptotic forms

Near the branes it is possible to expand the solutions in powers of ρ/r_B , where ρ denotes proper distance in the bulk geometry from the vortex. Writing, as before, the metric in the form

$$ds^2 = W^2(\rho) \check{g}_{\mu\nu} dx^\mu dx^\nu + d\rho^2 + B^2(\rho) d\theta^2, \quad (\text{A.5})$$

we seek near-vortex solutions to the Einstein equations of the form

$$\begin{aligned} W &= W_0 \left(\frac{\rho}{r_B}\right)^w + W_1 \left(\frac{\rho}{r_B}\right)^{w+1} + W_2 \left(\frac{\rho}{r_B}\right)^{w+2} + \dots, \\ B &= B_0 \left(\frac{\rho}{r_B}\right)^b + B_1 \left(\frac{\rho}{r_B}\right)^{b+1} + B_2 \left(\frac{\rho}{r_B}\right)^{b+2} + \dots, \end{aligned} \quad (\text{A.6})$$

and so on. The special case of flat space in polar coordinates corresponds to $w = 0$ and $b = 1$, without the need for higher powers of ρ/r_B .

The leading powers, w and b , are constrained by the leading terms in the expansion of the field equations around the vortex position, $\rho = 0$. The source terms on the RHS of the Einstein equations in the bulk involve Λ and $\check{L}_A = \frac{1}{2}(Q/W^d)^2$, which vary respectively like ρ^0 and $(\rho/r_B)^{-2dw}$ as $\rho \rightarrow 0$. By comparison, as $\rho \rightarrow 0$ the curvature on the LHS of the Einstein equation are

$$\begin{aligned} \mathcal{R}_{(d)} - \frac{\check{R}}{W^2} &= d \left[(d-1) \left(\frac{W'}{W}\right)^2 + \left(\frac{W''}{W} + \frac{B'W'}{BW}\right) \right] \\ &= d \left\{ (d-1) \left(\frac{w}{\rho}\right)^2 + \left[\frac{w(w-1)}{\rho^2} + \frac{bw}{\rho^2} \right] \right\} \left[1 + \mathcal{O}\left(\frac{\rho}{r_B}\right) \right] \\ &= dw \left(\frac{dw+b-1}{\rho^2}\right) \left[1 + \mathcal{O}\left(\frac{\rho}{r_B}\right) \right]. \end{aligned} \quad (\text{A.7})$$

Assuming $w < 1$ — so that $\check{R}/W^2 \propto (\rho/r_B)^{-2w}$ is subdominant to the $1/\rho^2$ term explicitly displayed (a result justified below) — we see that the $(\mu\nu)$ Einstein equation implies $w(dw+b-1) = 0$. Similarly,

$$\mathcal{R}^{\theta}_{\theta} = \frac{B''}{B} + d \left(\frac{B'W'}{BW}\right) = \frac{b(dw+b-1)}{\rho^2} \left[1 + \mathcal{O}\left(\frac{\rho}{r_B}\right) \right], \quad (\text{A.8})$$

implies $b(dw + b - 1) = 0$, and

$$\mathcal{R}^\rho_\rho = \frac{B''}{B} + d\left(\frac{W''}{W}\right) = \frac{b(b-1) + dw(w-1)}{\rho^2} \left[1 + \mathcal{O}\left(\frac{\rho}{r_B}\right)\right], \quad (\text{A.9})$$

Besides the trivial special case ($w = b = 0$) we see that the vanishing of the $1/\rho^2$ terms in the field equations implies the following two Kasner conditions:

$$dw + b = 1, \quad (\text{A.10})$$

and

$$dw^2 + b^2 = 1. \quad (\text{A.11})$$

The last of these in turn implies w and b must reside within the intervals

$$|w| \leq \frac{1}{\sqrt{d}} \quad \text{and} \quad |b| \leq 1, \quad (\text{A.12})$$

which shows in particular why $1/W^2 \propto (\rho/r_B)^{-2w}$ is less singular than $1/\rho^2$, as assumed above. The Kasner conditions, eqs. (A.10) and (A.11) have precisely two solutions: either $w = 0$ and $b = 1$ (as is true for the rugby-ball solutions described above) or $dw = 1$ and $b = 0$.

Appendix B

Appendix for Chapter 4

B.1 Scaling and the suppression of $\langle \mathcal{X}_{\text{loc}} \rangle$

We here derive a useful integral identity that is satisfied by the vortex solutions in the limit where gravitational back-reaction is neglected so the vortex is in flat space. It is this identity that underlies the small size of vortex integrals like $\langle \mathcal{X}_{\text{loc}} \rangle$ encountered in the main text.

The starting point is the observation that the static vortex solution minimizes the energy (or negative action)

$$\begin{aligned} I &= \int d^2y \sqrt{-g} (L_\phi + L_\Psi + V_b + L_A + L_Z + L_{\text{mix}}) \\ &= 2\pi \int_0^\infty \sqrt{-g} \left[\frac{1}{2\kappa^2} g^{mn} \partial_m \phi \partial_n \phi + V_B(\phi) \right. \\ &\quad \left. + \frac{1}{2} g^{mn} (\partial_m \Psi \partial_n \Psi + e^2 \Psi^2 Z_m Z_n) + \frac{\lambda}{4} e^{q\phi} (\Psi^2 - v^2)^2 \right. \\ &\quad \left. + \frac{1}{4} e^{-\phi} A_{mn} A^{mn} + \frac{1}{4} e^{p\phi} Z_{mn} Z^{mn} + \frac{1}{2} \varepsilon e^{r\phi} Z_{mn} A^{mn} \right], \end{aligned}$$

and observes that this is stationary with respect to arbitrary variations of the matter fields (without also varying the metric), due to their field equations. In particular it is invariant under rescalings of the form $\phi(y) \rightarrow \phi(\sqrt{s} y)$, $\Psi(y) \rightarrow \Psi(\sqrt{s} y)$ and so on.

Now, suppose the metric g_{mn} also satisfies $g_{mn}(\sqrt{s} y) = s g_{mn}(y)$, such as is true for the case of a locally flat metric, $g_{mn} dy^m dy^n = d\rho^2 + \alpha^2 \rho^2 d\theta^2$ under the rescaling $\rho \rightarrow \sqrt{s} \rho$. Since I is invariant under *arbitrary* coordinate transformations, $y^m \rightarrow \xi^m(y)$, in the 2D directions, provided *both* the matter fields and metric transform, the stationarity of I with respect to redefinitions $\phi(y) \rightarrow \phi(\sqrt{s} y)$ (for all matter fields) is equivalent (for 2D metrics with conformal Killing vectors) to stationarity with respect to the rescaling $g_{mn} \rightarrow s g_{mn}$ without also performing the coordinate rescaling.

Under the rescaling $g_{mn} \rightarrow s g_{mn}$ we have $\sqrt{-g} \rightarrow s\sqrt{-g}$ and so (assuming all fields vary and point only in the transverse dimensions)

$$\begin{aligned} I &= \int d^2y \sqrt{-g} (L_\phi + L_\Psi + V_b + L_A + L_Z + L_{\text{mix}}) \\ &\rightarrow \int d^2y \sqrt{-g} \left[L_\phi + L_\Psi + s(V_B + V_b) + \frac{1}{s}(L_A + L_Z + L_{\text{mix}}) \right], \end{aligned} \quad (\text{B.13})$$

and so the stationarity condition becomes

$$\begin{aligned} 0 &= \left(\frac{dI}{ds} \right)_{s=1} = \int d^2y \sqrt{-g} \left[(V_B + V_b) - (L_A + L_Z + L_{\text{mix}}) \right] \\ &= \int d^2y \sqrt{-g} \left[(V_B + V_b) - (\check{L}_A + \check{L}_Z) \right] \\ &= \int d^2y \sqrt{-g} \mathcal{X}. \end{aligned} \quad (\text{B.14})$$

The claim is that this equation is an automatic consequence of the matter equations of

motion, and expresses the balancing of pressures (on average) in the radial directions for a stable vortex configuration.

The same arguments apply equally well for an isolated $Q = 0$ vortex for which L_ϕ and \check{L}_A are negligible in I , in which case eq. (B.14) reduces to

$$0 = \int d^2y \sqrt{-g} (V_b - \check{L}_z) = \int d^2y \sqrt{-g} \mathcal{X}_{\text{loc}}. \quad (\text{B.15})$$

In the special BPS case examined in the body this is not only true on average but is also locally true, following directly from eq. (4.112).

Notice that the way it has been derived shows that eq. (B.14) is a statement about the vanishing of the extra-dimensional components of the stress energy, as is made more explicit in the previous appendix. It need not hold once the metric back-reaction is turned on, but the vanishing of the flat-space result leads to the exact result being is smaller than might otherwise have been expected.

Appendix C

Appendix for Chapter 5

C.1 Scale invariant solutions

In this appendix we present the details of well-known solutions that exist when the branes are scale invariant. We first describe the Salam-Sezgin solution that applies when there are no branes, and we then show how this solution generalizes to the rugby ball solution in the case where the branes are identical, scale invariant, and supersymmetric.

C.1.1 Salam-Sezgin solution

In the absence of branes, it is consistent to assume a trivial warp factor $W = 1$ and no dilaton profile $\phi' = 0$. The second of these conditions is satisfied as long as the source terms in the dilaton field equation vanish

$$\square\phi = e^\phi \left[\left(\frac{2g_R^2}{\kappa^4} \right) - \frac{1}{2}Q^2 \right] = 0, \quad (\text{C.16})$$

where we eliminate the bulk field strength in terms of Q using $A_{\rho\theta} = QB e^\phi$. The constant Q is fixed below by flux quantization and for generic values of Q the above equation is only solved by taking the runaway solution: $\phi \rightarrow -\infty$. The exception is if flux quantization returns the specific Salam-Sezgin value, $Q = \pm Q_s := \pm 2g_R/\kappa^2$, in which case (C.16) is solved for any constant: $\phi = \varphi$.

With this choice of Q , the bulk metric function satisfies the field equation

$$\frac{B''}{B} = -\frac{e^\varphi}{L_s^2}, \quad (\text{C.17})$$

where $L_s = r_B = \kappa/2g_R$. The solution is

$$B_s = r_B e^{-\varphi/2} \sin(\rho e^{\varphi/2}/r_B), \quad (\text{C.18})$$

and we conclude that the extra dimensions are spherical with proper radius $\ell_s^2 = r_B^2 e^{-\varphi}$.

Consistency requires verifying the flux-quantization condition returns $Q = Q_s$. To check we evaluate

$$\frac{N}{g_A} = \int_0^{\ell_s} d\rho A_{\rho\theta} = Q \int_0^{\ell_s} d\rho B e^\phi = \left(\frac{Q}{Q_s}\right) \frac{1}{g_R}, \quad (\text{C.19})$$

where g_A is the gauge coupling of the background gauge field (which in principle could differ from g_R if this field gauges a group other than the R -symmetry for which g_R is the coupling). We see that only the supersymmetric choices $g_A = g_R$ and $Q/Q_s = N = \pm 1$ are consistent with $\phi = \varphi$ being a finite constant, and because $Q = \pm Q_s$ the value, φ , remains undetermined by the field equations.

C.1.2 Supersymmetric rugby ball

Many of the nice properties of the Salam-Sezgin solution are preserved if identical, scale invariant, supersymmetric branes are added to the system, with action

$$S_{\text{branes}} = - \sum_v \int_{\Sigma_v(u)} d^4u \sqrt{-\gamma} \left(T - \frac{1}{4!} \zeta \varepsilon^{\mu\nu\lambda\rho} F_{\mu\nu\lambda\rho} \right), \quad (\text{C.20})$$

where $\Sigma_v(u)$ denotes the worldsheet of each brane, parameterized by the four coordinates u^μ . By assumption T and ζ are the same for both branes and independent of the dilaton (as required for the branes not to break the classical bulk scale invariance). These choices are necessary if the branes are not to source gradients of the warp factor or dilaton, making it still consistent to assume $W = 1$ and $\phi' = 0$.

As before, the condition of constant ϕ requires bulk sources in the dilaton field equation to vanish, and so flux quantization must return the same value for Q as in the Salam-Sezgin solution: $\bar{Q} = \pm Q_s = \pm 2g_R/\kappa^2$. This choice of Q also preserves the radius of the extra dimensions so the rugby ball metric function is solved by

$$B = \alpha L_s e^{-\varphi/2} \sin(\rho e^{\varphi/2}/L_s). \quad (\text{C.21})$$

Note the presence of the constant α in this solution, which physically represents a conical singularity at the poles of the sphere with defect angle $\delta = 2\pi(1 - \alpha)$. This differs from the Salam-Sezgin value, $\alpha_s = 1$, because the presence of branes modifies the boundary condition of the bulk metric function B at the position of the branes to satisfy

$$B'(y_v) = \alpha = 1 - \frac{\kappa^2 T}{2\pi}, \quad (\text{C.22})$$

where the sign assumes the derivative is in the direction away from the brane and T is the brane's tension. Nonzero defect angles make the bulk resemble a rugby ball rather than a sphere.

The other effect of the branes is to introduce a localized piece of $A_{\rho\theta}$ at the brane positions, and this modifies the flux-quantization condition (C.19) to become

$$\frac{N}{g_A} = \int_0^{\ell_s} d\rho A_{\rho\theta} = Q \int d\rho B e^\phi - \frac{1}{2\pi} \sum_v \zeta, \quad (\text{C.23})$$

showing that $\zeta/2\pi$ describes that amount of the total gauge flux that is localized in this way. Evaluating as before gives

$$\frac{N}{g_A} = \frac{\alpha}{g_R} \left(\frac{Q}{Q_s} \right) - \frac{1}{2\pi} \sum_v \zeta = \frac{1}{g_R} \left(\frac{Q}{Q_s} \right) \left(1 - \frac{\kappa^2 T}{2\pi} \right) - \frac{1}{2\pi} \sum_v \zeta, \quad (\text{C.24})$$

which shows how the brane-localized flux compensates for the reduction of bulk volume caused by the defect angles.

Flux quantization is only consistent with constant ϕ if it returns $Q = \pm Q_s$. Having source branes can allow this if T and ζ are related by

$$\kappa^2 T = \mp g_R \sum_v \zeta = \mp 2g_R \zeta, \quad (\text{C.25})$$

in addition to the bulk conditions $g_A = g_R$ and $N = \pm 1$. This brane condition also turns out to be required by demanding supersymmetry not be broken by the presence of the branes, showing how supersymmetry again ensures the value $Q = Q_s$ required for a flat potential that does not determine the value $\phi = \varphi$.

C.2 Linearized solutions

We now assume that the branes are perturbatively close to the identical, scale-invariant supersymmetric ones just described. However, the perturbations we consider to the tension and localized flux need not respect scale invariance and can differ at each brane

$$\zeta_v = \zeta_0 + \delta\zeta_v(\phi) \quad \text{and} \quad T_v = T_0 + \delta T_v(\phi), \quad (\text{C.26})$$

where T_0 and ζ_0 satisfy (C.25).

We track the effects of these perturbations on the the bulk fields by solving the entire set of field equations, including the equations for warping, the dilaton profile, and flux quantization, at linear order in the perturbations. When the brane perturbations break scale invariance, we also solve for the stabilized value of the zero mode, $\varphi = \varphi_*$, to linear order. We also calculate the 4D effective potential for φ at the linearized level, and show how it reproduces this stabilized value of the zero mode computed with the full 6D theory.

Full field equations

We first present the set of field equations and boundary conditions to be solved.

Because of the scale invariance of the unperturbed theory it is useful to switch to the following scale invariant variables

$$b := e^{\phi/2} B \quad \text{and} \quad d\sigma = e^{\phi/2} d\rho. \quad (\text{C.27})$$

With these the undifferentiated dilaton only appears in the field equations through scale-breaking terms. Since these terms are by assumption perturbatively small,

we can simply replace the dilaton factor ϕ appearing there with the zero mode φ . These variables also simplify the linearization of the scale invariant terms in the field equations since the background dilaton solution reads $\bar{\phi}' = 0$ (where bars denote background quantities). Additionally, the equations simplify if we rewrite the warp factor as

$$W^4 = e^\omega, \quad (\text{C.28})$$

so we can perturb around the background solution $\bar{\omega} = 0$. In these new variables the background of the bulk metric function simplifies to $\bar{b} = \bar{\alpha}\bar{L}\sin(\sigma/\bar{L})$, with $\bar{\alpha}$ determined by $\kappa^2 T_0$ and $\bar{L} = L_s = r_B$.

Since our interest is in computing the shape of the zero-mode potential we also follow Refs. [6] of chapter 5 and add a stabilizing current to the bulk action

$$\Delta S_J = - \int d^6x \sqrt{-g} J = - \int d^4x \int d\theta \int d\sigma J b e^{\omega-\phi}. \quad (\text{C.29})$$

Choosing J appropriately allows us to investigate values of φ away from the minimum of the potential while still solving all of the field equations. In particular, we read the equation that would have determined the stabilized value $\varphi = \varphi_*$ as instead to be solved for $J(\varphi)$, allowing us to trace the shape of the effective potential for φ . Then, $\varphi = \varphi_*$ corresponds to $J = 0$.

To solve for the perturbations to the bulk metric function and warp factor, we desire two linear combinations of the Einstein equations (4.13) - (4.15) in chapter 4 that contain second derivatives of the metric fields, and no factors of the 4D curvature.

The first of these reads

$$\left[e^\omega \left(b' - \frac{1}{2} b \phi' \right) \right]' = -\kappa^2 b e^\omega \left(\frac{3Q^2}{4} e^{-2\omega} + \frac{g_R^2}{\kappa^4} + \frac{1}{2} J e^{-\phi} \right), \quad (\text{C.30})$$

and is to be solved for b . (From here on primes on bulk fields denote differentiation with respect to σ rather than ρ .) The other relevant Einstein equation is

$$\omega'' + \omega' \phi' + \frac{(\omega')^2}{4} - \frac{\omega' b'}{b} = -(\phi')^2, \quad (\text{C.31})$$

and this is to be solved for ω . In these variables the dilaton field equation similarly reads

$$(b e^\omega \phi')' = \kappa^2 b e^\omega \left(\frac{2g_R^2}{\kappa^4} - \frac{Q^2}{2} e^{-2\omega} \right), \quad (\text{C.32})$$

and flux quantization (for $N = 1$ and $g_A = g_R$) can be written as

$$\frac{1}{g_R} = Q \int d\sigma b e^{-\omega} - \frac{1}{2\pi} \sum_v \zeta_v. \quad (\text{C.33})$$

Finally, we rewrite the boundary conditions in the new variables, to get

$$[b \phi']_{\sigma_v} = \frac{\kappa^2}{2\pi} [T'_v + Q \zeta'_v]_{\sigma_v}, \quad (\text{C.34})$$

and

$$\left[1 - \left(b' - \frac{1}{2} b \phi' \right) \right]_{\sigma_v} = \frac{\kappa^2}{2\pi} [T_v]_{\sigma_v}, \quad (\text{C.35})$$

where σ_v are the brane positions and the signs are such that the derivatives of b and ϕ are in the direction away from the branes. In general the right-hand side of these boundary conditions generically diverge as $\sigma \rightarrow \sigma_v$. As shown explicitly in the

examples of Appendix C.3 this divergence can (and must) be renormalized into the parameters describing the brane-bulk couplings.

Linearized field equations

The perturbations we consider to the tension and localized flux need not respect scale invariance, by depending nontrivially on the dilaton, and they can differ at each brane

$$\zeta_v = \zeta_0 + \delta\zeta_v(\phi) \quad \text{and} \quad T_v = T_0 + \delta T_v(\phi). \quad (\text{C.36})$$

The supersymmetric solutions are relatively simple because gradients in the warp factor and dilaton are absent: $\bar{\omega} = 0$ and $\bar{\phi}' = 0$. This need no longer be true given any asymmetry in the brane perturbations, and so to linearized order these bulks fields instead satisfy

$$\omega(\sigma) = \delta\omega(\sigma) \quad \text{and} \quad \phi'(\sigma) = \delta\phi'(\sigma), \quad (\text{C.37})$$

where primes again denote differentiation with respect to σ . These changes feed into the Einstein equations that govern the bulk metric function and the flux quantization condition that governs the size of Q , so

$$b(\sigma) = \bar{b}(\sigma) + \delta b(\sigma) \quad \text{and} \quad Q = \bar{Q} + \delta Q. \quad (\text{C.38})$$

To solve for the field perturbations, we now linearize the full field equations around the supersymmetric rugby ball case. This gives the following Einstein equation for

the metric function

$$\delta b'' + \bar{b}' \delta \omega' - \frac{1}{2} (\bar{b} \delta \phi')' = -\frac{\bar{b}}{\bar{L}^2} \left[\frac{\delta b}{\bar{b}} + \frac{3}{2} (\delta q - \delta \omega) + \frac{1}{2} \kappa^2 \bar{L}^2 J e^{-\phi} \right], \quad (\text{C.39})$$

where $\delta q = \delta Q / \bar{Q}$. We also have the linearized dilaton field equation

$$(\bar{b} \delta \phi')' = \frac{\bar{b}}{\bar{L}^2} (\delta \omega - \delta q). \quad (\text{C.40})$$

Inserting this into the Einstein equation gives

$$\delta b'' + \bar{b}' \delta \omega' = -\frac{\bar{b}}{\bar{L}^2} \left[\frac{\delta b}{\bar{b}} + 2(\delta q - \delta \omega) + \frac{1}{2} \kappa^2 \bar{L}^2 J e^{-\phi} \right]. \quad (\text{C.41})$$

The linearized field equation for the warp factor simplifies a great deal

$$\bar{b} \delta \omega'' - \bar{b}' \delta \omega' = 0. \quad (\text{C.42})$$

The linearized boundary conditions reduce to

$$[\bar{b} \delta \phi']_{\bar{\sigma}_v} = \frac{\kappa^2}{2\pi} \left[\delta T'_v + \bar{Q} \delta \zeta'_v \right]_{\bar{\sigma}_v}, \quad (\text{C.43})$$

and

$$\left[\delta b' + \frac{1}{2} \bar{b} \delta \phi' \right]_{\bar{\sigma}_v} = -\frac{\kappa^2}{2\pi} \left[\delta T_v \right]_{\bar{\sigma}_v}, \quad (\text{C.44})$$

where $\bar{\sigma}_v = \{0, \pi \bar{L}\}$ are the unperturbed values of the brane positions, and again the sign assumes derivatives are directed away from the branes. Finally, combining the two boundary conditions gives an expression for the near-source derivative of the bulk

metric function

$$[\delta b']_{\bar{\sigma}_v} = -\frac{\kappa^2}{2\pi} \left[\delta T_v - \frac{1}{2} \delta T'_v - \frac{1}{2} \bar{Q} \delta \zeta'_v \right]_{\bar{\sigma}_v}. \quad (\text{C.45})$$

In many of the above results we use the useful property of the unperturbed solution that $\kappa^2 \bar{Q}^2 \bar{L}^2 = 1$.

Linearized solutions

The linearized field equations can all be solved analytically. Inserting the background solution into (C.42) and integrating gives the following general solution for the warp factor

$$\delta\omega = \omega_0 + \omega_1 \cos z, \quad (\text{C.46})$$

with $z := \sigma/\bar{L}$ and ω_0 and ω_1 both integration constants.

Absorbing the constant ω_0 into a rescaling of the 4D coordinates and using the result in the linearized dilaton equation (C.40) then gives

$$\partial_z (\sin z \partial_z \delta\phi) = (\omega_1 \cos z - \delta q) \sin z, \quad (\text{C.47})$$

whose integral yields

$$\sin z \partial_z \delta\phi = -\frac{\omega_1}{2} \cos^2 z + \delta q \cos z + \phi_1, \quad (\text{C.48})$$

where ϕ_1 is another integration constant. Integrating again gives the full solution for the dilaton,

$$\phi = \bar{\phi} + \delta\phi = \varphi - \frac{\omega_1}{2} \cos z + \left(\phi_1 - \frac{\omega_1}{2} \right) \log[\tan(z/2)] + \delta q \log(\sin z). \quad (\text{C.49})$$

The constant part of the dilaton profile, φ , need not be perturbatively small so in ϕ -dependent expressions that are already perturbatively small, like $Je^{-\phi}$, we can make the replacement $\phi \rightarrow \varphi$. This allows us to rewrite the Einstein equation (C.41) as

$$\partial_z^2 \delta b = -\delta b - 2\bar{\alpha}\bar{L} \left[\delta q + \delta j(\varphi) \right] \sin z + 3\bar{\alpha}\bar{L}\omega_1 \cos z \sin z, \quad (\text{C.50})$$

where

$$\delta j(\varphi) := \frac{1}{4}\kappa^2\bar{L}^2 J e^{-\varphi}. \quad (\text{C.51})$$

The general solution to this field equation is given by

$$\delta b = \bar{\alpha}\bar{L} \left[b_0 \cos z + b_1 \sin z + (\delta q + \delta j)z \cos z - \omega_1 \sin z \cos z \right], \quad (\text{C.52})$$

where b_0 and b_1 are integration constants. We are free to shift the radial coordinate to ensure $\delta b(0) = 0$ and thereby set $b_0 = 0$.

Changes in geometry

The points σ_v where the metric function vanishes define the brane positions. These are also perturbed relative to the background value $\sigma_v = \bar{\sigma}_v + \delta\sigma_v$ and we can solve for these perturbations by linearizing $b(\sigma_v) = 0$, which gives

$$0 = \delta b(\bar{\sigma}_v) + \delta\sigma_v [\partial_{\sigma} \bar{b}]_{\bar{\sigma}_v} = \delta b(\bar{\sigma}_v) + \bar{\alpha}\delta\sigma_v. \quad (\text{C.53})$$

This shows that the choice $b_0 = 0$ ensures that that one of the branes is always located at the origin $b(\sigma_0) = 0$ at linear order. At the other pole, near $\bar{\sigma}_\pi = \pi\bar{L}$, we instead

find the following shift

$$\frac{\delta\sigma_\pi}{\pi\bar{L}} = \delta q, \quad (\text{C.54})$$

which shows how the backreaction can change the proper distance between the branes.

The change in scale invariant k -volume, defined as

$$\widehat{\Omega}_k := 2\pi \int d\rho BW^k e^\phi = 2\pi \int d\sigma b e^{k\omega/4}, \quad (\text{C.55})$$

is given to linear order by the following expression

$$\delta\widehat{\Omega}_k = 2\pi \int_0^{\pi\bar{L}} d\sigma \delta b + \frac{2\pi k}{4} \int_0^{\pi\bar{L}} d\sigma \bar{b} \delta\omega. \quad (\text{C.56})$$

Evaluating the integral using the explicit solutions derived above gives

$$\frac{\delta\widehat{\Omega}_k}{4\pi\bar{\alpha}\bar{L}^2} = \frac{1}{2} \int_0^\pi dz \left[b_1 \sin z + (\delta q + \delta j) z \cos z \right] = b_1 - \delta q - \delta j, \quad (\text{C.57})$$

where the integral over $\delta\omega$ vanishes because it is odd on the interval of integration.

We learn the perturbation to the volume is independent of warping to linear order and is determined by the integration constants.

Boundary conditions and integration constants

We next determine these integration constants in terms of the assumed brane perturbations, δT_v and $\delta\zeta_v$, using the near-brane boundary conditions. We first evaluate the combined boundary condition (C.45) using (C.52) at both branes to get the following

relation between integration constants and brane parameters

$$b_1 + \delta q + \delta j - \omega_1 e^{i\nu} = -\frac{\kappa^2}{2\pi\bar{\alpha}} \left[\delta T_\nu - \frac{1}{2} \delta T'_\nu - \frac{1}{2} \bar{Q} \delta \zeta'_\nu \right]_{\bar{\sigma}_\nu}, \quad (\text{C.58})$$

where we use $\nu = \{0, \pi\}$ as an index to represent the branes located near $z = 0$ and $z = \pi$, and the explicit sign $e^{i\nu}$ appears because the boundary conditions assume a radial coordinate that increases away from the brane (so the radial derivative in the boundary condition is $-d/d\sigma$ near $\sigma = \pi\bar{L}$). The dilaton boundary condition (C.43) similarly evaluates using the dilaton solution in (C.48), to give

$$\delta q + \left(\phi_1 - \frac{\omega_1}{2} \right) e^{i\nu} = \frac{\kappa^2}{2\pi\bar{\alpha}} \left[\delta T'_\nu + \bar{Q} \delta \zeta'_\nu \right]_{\bar{\sigma}_\nu}. \quad (\text{C.59})$$

The integration constant controlling the gradient in W is fixed by the difference between the (C.58) at $\nu = 0$ and $\nu = \pi$ in terms of brane differences

$$\omega_1 = \frac{\kappa^2}{2\pi\bar{\alpha}} \left(\delta T_{\text{dif}} - \frac{1}{2} \delta T'_{\text{dif}} - \frac{1}{2} \bar{Q} \delta \zeta'_{\text{dif}} \right), \quad (\text{C.60})$$

where $\delta T_{\text{dif}} = \frac{1}{2}(\delta T_{\nu=0} - \delta T_{\nu=\pi})$ and so on. Using this in the difference between the two versions of (C.59) similarly determines the gradient of ϕ by fixing

$$\phi_1 = \frac{\kappa^2}{2\pi\bar{\alpha}} \left(\frac{1}{2} \delta T_{\text{dif}} + \frac{3}{4} \delta T'_{\text{dif}} + \frac{3}{4} \bar{Q} \delta \zeta'_{\text{dif}} \right). \quad (\text{C.61})$$

The remaining integration constants are found by summing rather than subtracting boundary conditions, and the two versions of (C.59) sum to give δq in terms of brane averages

$$\delta q = \frac{\kappa^2}{2\pi\bar{\alpha}} \left(\delta T'_{\text{avg}} + \bar{Q} \delta \zeta'_{\text{avg}} \right), \quad (\text{C.62})$$

where $\delta T_{\text{avg}} = \frac{1}{2}(\delta T_{v=0} + \delta T_{v=\pi})$ and so on. This expression can be used in conjunction with (C.58) to solve for the last integration constant, b_1 , and we find

$$b_1 + \delta j = -\frac{\kappa^2}{2\pi\bar{\alpha}} \left(\delta T_{\text{avg}} + \frac{1}{2}\delta T'_{\text{avg}} + \frac{1}{2}\bar{Q}\delta\zeta'_{\text{avg}} \right). \quad (\text{C.63})$$

These four conditions completely fix the integration constants, ϕ_1 , ω_1 , b_1 and δq in terms of the brane parameters, the stabilizing current J and φ (which to this point remains arbitrary).

A final relation comes from the linearized flux-quantization condition,

$$0 = 4\pi\alpha\bar{L}^2\delta Q + \bar{Q}\delta\hat{\Omega} - \sum_v \delta\zeta_v, \quad (\text{C.64})$$

which we use to determine J in terms of brane properties and φ . To this end we use the linearized volume change in (C.57) to fix b_1

$$b_1 = \frac{\kappa^2}{2\pi\bar{\alpha}} (\bar{Q}\delta\zeta_{\text{avg}}), \quad (\text{C.65})$$

where we have used $\kappa^2\bar{L}^2\bar{Q}^2 = 1$ to write the linearized flux quantization condition in this suggestive manner. Combining (C.63) with (C.65) gives a solution for the stabilizing current

$$\delta j = \frac{1}{4}\kappa^2\bar{L}^2 J e^{-\varphi} = -\frac{\kappa^2}{2\pi\bar{\alpha}} \left(\delta T_{\text{avg}} + \bar{Q}\delta\zeta_{\text{avg}} + \frac{1}{2}\delta T'_{\text{avg}} + \frac{1}{2}\bar{Q}\delta\zeta'_{\text{avg}} \right). \quad (\text{C.66})$$

Setting $J = 0$ in this gives the stabilized value, $\varphi = \varphi_*$, of the zero mode entirely in terms of the brane parameters.

The effective potential

We now construct the effective potential of the 4D theory using the ancillary current J , and verify that it is minimized by the condition (C.66). The addition of ΔS_J to the bulk action gives rise to a corresponding term in the effective theory. To identify how the current contributes to the effective theory we note that it can be treated like a novel contribution to the 6D potential

$$\Delta V_B = J. \quad (\text{C.67})$$

Using this in (??) shows that the presence of a stabilizing current in the 6D theory can be captured by shifting the overall potential in the 4D theory as follows

$$\Delta U = \frac{1}{2} e^{2(\varphi - \varphi_*)} \langle J \rangle = \frac{1}{2} e^{2(\varphi - \varphi_*)} \int d^2 y \sqrt{\hat{g}_2} J e^{-\phi}. \quad (\text{C.68})$$

To the linear order of interest this gives

$$\Delta U = 2\pi \bar{\alpha} \bar{L}^2 e^{2(\varphi - \varphi_*)} J e^{-\varphi}, \quad (\text{C.69})$$

where the dependence on φ only appears in the exponential factors. The presence of this additional term in the 4D theory modifies the field equation for the zero mode

$$\frac{\partial U}{\partial \varphi} + 2\pi \bar{\alpha} \bar{L}^2 e^{2(\varphi - \varphi_*)} J e^{-\varphi} = 0. \quad (\text{C.70})$$

Since J is a known function of φ this can be read as a differential equation for the

potential which is solved by

$$U(\varphi) = -2\pi\bar{\alpha}L^2 e^{-2\varphi_*} \int d\tilde{\varphi} J e^{\tilde{\varphi}}. \quad (\text{C.71})$$

This can be combined to with (C.66) to determine the potential in terms of brane perturbations

$$U(\varphi) = 4e^{-2\varphi_*} \int d\tilde{\varphi} e^{2\tilde{\varphi}} \left(\delta T_{\text{avg}} + \bar{Q} \delta \zeta_{\text{avg}} + \frac{1}{2} \delta T'_{\text{avg}} + \frac{1}{2} \bar{Q} \delta \zeta'_{\text{avg}} \right). \quad (\text{C.72})$$

It is possible to directly integrate this expression to find the linearized potential

$$U(\varphi) = 2 e^{2(\varphi - \varphi_*)} \left[\delta T_{\text{avg}} + \left(\frac{2g_R}{\kappa^2} \right) \delta \zeta_{\text{avg}} \right], \quad (\text{C.73})$$

where we have used $\bar{Q} = 2g_R/\kappa^2$. There is no background contribution to the potential because it vanishes identically in the supersymmetric case around which we are perturbing.

This potential agrees with the linearization of the potential found by dimensional reduction in §5.3.4 of the main text, and correctly predicts that the energy is perturbed by $\sum_v \delta T_v$ at linear order when the brane tension is perturbed in a way that vanishes when the brane perturbations are scale invariant and supersymmetric. Furthermore, minimizing the potential for general brane perturbations gives the same condition on the zero mode as (C.66) gives when $J = 0$, and this confirms that the effective potential reproduces the stabilization of the zero mode that was derived in the 6D theory.

C.3 Examples of stabilization

We now investigate simple examples of zero mode stabilization by choosing explicit forms for the ϕ -dependence of the brane perturbations. In all cases, we imagine the ϕ -dependence of the brane appears predominantly in the flux perturbation, since we expect this choice to help suppress vacuum energies, as in (5.34). In many cases we find that exponentially large extra dimensions and suppressed curvatures can be obtained if there is a hierarchy between the size of the brane perturbations.

Along the way, we also illustrate how classical renormalization of brane parameters can be used to absorb divergences that arise when the brane is treated as an idealized, infinitely thin source. The procedure renders finite physical observables like the value of the zero mode, and the potential at its minimum.

Flux with linear ϕ -dependence

We now investigate simple example in which the the branes are perturbed identically, with the following properties

$$\delta T_v = \tau \quad \text{and} \quad \delta \zeta_v = \lambda \phi. \quad (\text{C.74})$$

This choice of identical brane perturbations immediately gives

$$\phi_1 = \omega_1 = 0. \quad (\text{C.75})$$

Note that this greatly simplifies the solution for the dilaton

$$\phi = \varphi + \delta q \log(\sin z). \quad (\text{C.76})$$

The remaining unknown integration constant can be calculated from (C.62) and it gives $\delta q = \lambda g_R / \pi \bar{\alpha}$. Inserting this into (C.66) and setting $J = 0$ gives an equation to be solved for the value of the zero mode

$$0 = 2\lambda g_R \varphi_\star + \left(\frac{2\lambda^2 g_R^2}{\pi \bar{\alpha}} \right) \log(\epsilon / \bar{L}) + \kappa^2 \tau + \lambda g_R. \quad (\text{C.77})$$

Note that we have regularized the $\lim_{\sigma \rightarrow 0} \log[\sin(\sigma / \bar{L})]$ divergence with the finite expression $\log(\epsilon / \bar{L})$. However, the divergence as $\epsilon \rightarrow 0$ must be absorbed into the brane couplings such that physical quantities are finite.

In general, divergences associated with brane terms that are linear in a bulk scalar can be absorbed by renormalizing the ϕ -independent part of the brane tension [13]. This case is no different, and the observables of the theory can be made finite if we renormalize the tension as follows

$$\kappa^2 \tau(\bar{r}) = \kappa^2 \tau - \left(\frac{2\lambda^2 g_R^2}{\pi \bar{\alpha}} \right) \log(\epsilon / \bar{r}). \quad (\text{C.78})$$

In particular, this renormalization gives a finite expression for the value of the zero mode

$$\varphi_\star = - \left[\frac{\kappa^2 \tau(\bar{r})}{2\lambda g_R} \right] - \frac{1}{2} - \left(\frac{\lambda g_R}{\pi \bar{\alpha}} \right) \log(\bar{r} / \bar{L}). \quad (\text{C.79})$$

For convenience, we can choose the renormalization scale $\bar{r} = \bar{L}$ to eliminate the logarithmic term and this gives

$$\varphi_\star = - \left[\frac{\kappa^2 \tau(\bar{L})}{2\lambda g_R} \right] - \frac{1}{2}. \quad (\text{C.80})$$

Note that the limit $\lambda \rightarrow 0$ sends to zero mode to the expected runaway value $\varphi_\star \rightarrow$

$-\infty$. Also note that the value of the zero mode comes to us as the ratio of two small, dimensionless numbers $\kappa^2\tau(\bar{L})$ and λg_R but can itself be made large if $\lambda g_R \ll \kappa^2\tau(\bar{L})$. Because the proper volume of extra dimensions is controlled by $\ell^2 = r_B^2 e^{-\varphi_\star}$, a large negative value of the zero mode gives large extra dimensions. Furthermore, this choice does not invalidate the assumed perturbativity of $\kappa^2\bar{Q}\delta\zeta \approx \lambda g_R\varphi \approx \kappa^2\tau(\bar{L}) \ll 1$ near the minimum of the potential, and so the approximate, linearized potential is valid in this region.

We can therefore calculate this potential, and using (C.73) gives

$$U(\varphi) = \frac{2e^{2(\varphi-\varphi_\star)}}{\kappa^2} \left[\kappa^2\tau + 2\lambda g_R\varphi + \left(\frac{2\lambda^2 g_R^2}{\pi\bar{\alpha}} \right) \log(\epsilon/\bar{L}) \right]. \quad (\text{C.81})$$

Again, the logarithmic divergence of the scalar field has been regularized with a finite regulator ϵ . Conveniently, though not surprisingly, this divergence can be renormalized into the tension to yield a finite potential

$$U = \frac{2e^{2(\varphi-\varphi_\star)}}{\kappa^2} [\kappa^2\tau + 2\lambda g_R\phi(\bar{\sigma}_0)] = \frac{2e^{2(\varphi-\varphi_\star)}}{\kappa^2} [\kappa^2\tau(\bar{L}) + 2\lambda g_R\varphi], \quad (\text{C.82})$$

where we have chosen the renormalization scale $\bar{r} = \bar{L}$ so that the finite logarithms are all implicit. Minimizing this potential reproduces the solution for the zero mode in (C.80) as it should. Finally, the value of the potential at the minimum is

$$U_\star = -2\tau \left(\frac{\lambda g_R}{\kappa^2\tau} \right). \quad (\text{C.83})$$

In the parameter range $\kappa^2\tau(\bar{L})/\lambda g_R \gg 1$ that gives large dimensions, the vacuum energy is suppressed relative to the naive expectation 2τ .

Flux quadratic in ϕ

We now consider the case in which the perturbation to the localized flux is quadratic in ϕ

$$\delta T_v = \tau \quad \text{and} \quad \delta \zeta_v = m \phi^2. \quad (\text{C.84})$$

We again make the simplifying assumption of identical branes and this gives $\phi_1 = \omega_1 = 0$ so that $\phi = \delta q \log(\sin z) + \varphi$. Inserting this into (C.62) allows us to rewrite it as follows

$$\delta q = \frac{2mg_R}{\pi\bar{\alpha}} [\delta q \log(\epsilon/\bar{L}) + \varphi], \quad (\text{C.85})$$

where the logarithmic divergence of the dilaton is ϵ -regularized in the same way as before. This equation can be used to solve for δq in terms of the zero mode

$$\pi\bar{\alpha}\delta q = \frac{2mg_R\varphi}{1 - \frac{2mg_R}{\pi\bar{\alpha}} \log(\epsilon/\bar{L})}. \quad (\text{C.86})$$

When the brane has a quadratic coupling to a bulk scalar field, the associated divergences can be absorbed into the renormalization of this coupling's coefficient [13, 29]. In the present case this amounts to renormalizing m as follows

$$m(\bar{r}) = \frac{m}{1 - \frac{2mg_R}{\pi\bar{\alpha}} \log(\bar{\epsilon}/\bar{r})}. \quad (\text{C.87})$$

This gives a finite value for the δq as a function of the zero mode $\pi\bar{\alpha}\delta q = 2gm(\bar{L})\varphi$ because it absorbs the divergences associated with evaluating the dilaton profile at the brane positions $m\phi(\bar{\sigma}_0) = m(\bar{L})\varphi$.

The condition on the zero mode in (C.66) is also finite after renormalization and

appropriately linearizing ϕ^2 . It reads

$$0 = \kappa^2\tau + 2g_R m(\bar{L})\varphi_\star + 2g_R m(\bar{L})\varphi_\star^2. \quad (\text{C.88})$$

This can alternatively be derived by minimizing the linearized and renormalized potential

$$U(\varphi) = \frac{2e^{2(\varphi-\varphi_\star)}}{\kappa^2} [\kappa^2\tau + 2g_R m\phi^2(\bar{\sigma}_v)] = \frac{2e^{2(\varphi-\varphi_\star)}}{\kappa^2} [\kappa^2\tau + 2g_R m(\bar{L})\varphi^2], \quad (\text{C.89})$$

where we have used $m\phi^2(\bar{\sigma}_v) = m(\bar{L})\varphi\phi = m(\bar{L})\varphi^2$ to linear order. The solution for the zero mode reads

$$\varphi_\star = \frac{1}{2} \left(\pm\sqrt{1+2t} - 1 \right) \quad (\text{C.90})$$

where $t = -\kappa^2\tau/gm(\bar{L})$. There are real roots when $t \geq -1/2$ and they are both negative unless $t > 0$ at which point one of them switches sign. The concavity of the potential at the extrema is proportional to $gm(\bar{L})\left(\varphi_\star + \frac{1}{2}\right) = \pm gm(\bar{L})\sqrt{1+2t}$. So if there are extrema, one of them is always a minimum and the other is always a maximum. The minimum can occur at the more negative root if $gm(\bar{L})$ is also negative.

If we assume $t \gg 1$ then the stabilized value of the zero mode is dominated by the root of the large ratio t as follows

$$\varphi_\star = \pm \sqrt{\left| \frac{\kappa^2\tau}{2g_R m(\bar{L})} \right|}, \quad (\text{C.91})$$

and the negative solution can be a minimum if $g_R m(\bar{L}) < 0$. This would also require $\kappa^2\tau > 0$ if $t > 0$ is to be satisfied. If the stabilized value of φ_\star is chosen to be large

and negative, then the extra dimensions have exponentially large radius as suggested by the leading order result $\ell^2 = r_B^2 e^{-\varphi_\star}$.

Finally, the value of the potential at this minimum can be written as follows

$$U_\star = - \left(\frac{4g_R}{\kappa^2} \right) m(\bar{L})\varphi_\star = -2\tau \sqrt{\frac{2|g_R m(\bar{L})|}{\kappa^2 \tau}}. \quad (\text{C.92})$$

Similar to the linear case, this vacuum energy is suppressed relative to the naive expectation 2τ , though the suppression here is weaker because it is sensitive to the root of the hierarchy in the brane perturbations.

Appendix D

Appendix for Chapter 6

D.1 Floating Brane Renormalization

Here we consider a theory that is sourced by a “floating” codimension-1 brane at $r = \bar{r}$, that can be dimensionally reduced to a codimension-2 brane. The properties of the floating brane are fixed by demanding that the solution to the field equations for $r \geq \bar{r}$ matches the regularized solution. The dependence on some cutoff (say ϵ) will be eliminated when the bare couplings c are traded for the coupling constants of the floating brane \bar{c} . It is in this sense that \bar{r} can be thought of as a subtraction scale, and \bar{c} can be thought of as the renormalized couplings.

After dimensional reduction to codimension-2, we assume the floating brane has the form

$$\bar{S}_b = - \int d^4x \left(\bar{T} - \bar{\mu}_H^2 H^\dagger H + \bar{\lambda} (H^\dagger H)^2 + \bar{\mu}_\Phi^2 \Phi_{\bar{r}} + \frac{1}{2} \bar{\lambda}_2 \Phi_{\bar{r}}^2 + \bar{g} H^\dagger H \Phi_{\bar{r}} \right), \quad (\text{D.93})$$

where $\Phi_{\bar{r}} = \Phi(x, \bar{r})$ and the theta dependence has been integrated out. Varying the

action gives two boundary field equations

$$-2\pi\alpha (f\partial_r\Phi)_{r=\bar{r}} + \bar{g}H^\dagger H + \bar{\lambda}_2\Phi_{\bar{r}} + \bar{\mu}_\Phi^2 = 0; \quad H^\dagger H = \frac{1}{2\lambda} (\bar{\mu}_H^2 - \bar{g}\Phi_{\bar{r}}), \quad (\text{D.94})$$

in direct analogy with the boundary field equations in §6.2.2. These equations should be read as fixing the floating brane couplings, since we have demanded that Φ and H solve the regularized field equations and so their functional form is already fixed. For a given value of \bar{r} , the floating brane couplings will have to be chosen appropriately, and will change with a change in \bar{r} . However, since \bar{r} is arbitrary, this change in the couplings cannot have any effect on physical quantities, such as $H^\dagger H$. For example, changes in (D.94) under a change in \bar{r} should vanish, giving

$$\begin{aligned} H^\dagger H \partial_{\bar{r}} \bar{g} + \Phi(\bar{r}) \partial_{\bar{r}} \bar{\lambda}_2 + \bar{\lambda}_2 \partial_{\bar{r}} \Phi(\bar{r}) + \partial_{\bar{r}} \bar{\mu}_\Phi^2 &= 0 \\ 2H^\dagger H \partial_{\bar{r}} \bar{\lambda} - \partial_{\bar{r}} \bar{\mu}_H^2 + \Phi(\bar{r}) \partial_{\bar{r}} \bar{g} + \bar{g} \partial_{\bar{r}} \Phi(\bar{r}) &= 0, \end{aligned} \quad (\text{D.95})$$

where we have used the fact that $\partial_{\bar{r}}(f\partial_r\Phi)_{r=\bar{r}} = (\partial_r f \partial_r \Phi)_{r=\bar{r}} = 0$ by the bulk equation of motion (6.11), and $\partial_{\bar{r}}(H^\dagger H) = 0$ because it is a physical quantity that should not depend on \bar{r} . We premultiply both equations by $f(\bar{r})$ to facilitate the use of the relation

$$f(\bar{r}) \partial_{\bar{r}} \Phi(\bar{r}) = (f\partial_r\Phi)_{r=\bar{r}} = \frac{1}{2\pi\alpha} (\bar{\mu}_\Phi^2 + \bar{\lambda}_2\Phi(\bar{r}) + \bar{g}H^\dagger H). \quad (\text{D.96})$$

Substituting this into (D.95) and equating powers of Φ and $H^\dagger H$ yields the following RG equations

$$\partial_{\bar{F}} \bar{\mu}_\Phi^2 = -\frac{\bar{\lambda}_2 \bar{\mu}_\Phi^2}{2\pi\alpha}; \quad \partial_{\bar{F}} \bar{g} = -\frac{\bar{g} \bar{\lambda}_2}{2\pi\alpha}; \quad \partial_{\bar{F}} \bar{\lambda}_2 = -\frac{\bar{\lambda}_2^2}{2\pi\alpha};$$

$$\partial_{\bar{F}}\bar{\lambda} = -\frac{\bar{g}^2}{4\pi\alpha}; \quad \partial_{\bar{F}}\bar{\mu}_H^2 = \frac{\bar{g}\bar{\mu}_\Phi^2}{2\pi\alpha}; \quad \partial_{\bar{F}}\bar{T} = -\frac{\bar{\mu}_\Phi^4}{4\pi\alpha}, \quad (\text{D.97})$$

where we have used $f(\bar{r})\partial_{\bar{r}} = \partial_{\bar{F}}$. The solutions can be found in (6.21). Although not explicitly derived in this section, for completeness the RG equation for \bar{T} is listed here.

D.2 Schwinger-Dyson equation

In this Appendix we derive the relation of eq. (6.92),

$$[\text{Amp}\langle h\phi^*(0)\rangle_k]^* = \text{Amp}\langle\phi(0)h^*\rangle_k = -\frac{i\bar{g}(\bar{r})v\langle hh^*\rangle_k}{1 - i(\bar{\lambda}_2(\bar{r})/4\alpha)} \Big|_{\bar{r}^2 = -1/k^2}, \quad (\text{D.98})$$

relating the amputated mixed $h - \phi$ propagator to the $h - h$ autocorrelation, and the relation of eq. (6.43)

$$\langle hh^*\rangle_k = \frac{D_k^h[1 + i\lambda_2 D_k^\phi(0, 0)]}{1 + [i\lambda_2 + (gv)^2 D_k^h] D_k^\phi(0, 0)}, \quad (\text{D.99})$$

that gives the dressed two point function h , and largely controls the phenomenology of Higgs-bulk mixing.

Our goal is to compute relations amongst the four correlation functions of interest, given by

$$\begin{aligned} \langle hh^*\rangle_k &:= G_{hh}(k), & \langle h\phi^*(y)\rangle_k &:= G_{h\phi}(k; y), \\ \langle\phi(y)h^*\rangle_k &:= G_{\phi h}(k; y) & \text{and} & \quad \langle\phi(y)\phi^*(y')\rangle_k := G_{\phi\phi}(k; y, y'), \end{aligned} \quad (\text{D.100})$$

where $G_{h\phi}(k; y) = G_{\phi h}^*(k; y)$. In these expressions y^m denotes the spatial coordinates

in the two extra dimensions while k^μ is the Fourier transform variable in the four on-brane directions.

The most direct way to obtain the desired relations is to express the Higgs-bulk interactions as delta-function localized terms in the lagrangian density, following arguments made in the appendix of ref. [14].¹ The starting point is the field equations for linearized fluctuations

$$\begin{aligned}\sqrt{\mathcal{G}_2}(\square_4 + \square_2)\phi - \left[\lambda_2 \phi + gv h\right] \delta^2(y) &= 0 \\ \square_4 h - 2\lambda v^2 h - gv \phi(0) &= 0.\end{aligned}\tag{D.101}$$

which imply the following equations for the propagators

$$\begin{aligned}\sqrt{\mathcal{G}_2}(-k^2 + \square_2)G_{\phi\phi}(k; y, y') - \left[\lambda_2 G_{\phi\phi}(k; 0, y') + gv G_{h\phi}(k; y')\right] \delta^2(y) &= i\delta^2(y - y') \\ \sqrt{\mathcal{G}_2}(-k^2 + \square_2)G_{\phi h}(k; y) - \left[\lambda_2 G_{\phi h}(k; 0) + gv G_{hh}(k)\right] \delta^2(y) &= 0 \\ (k^2 + 2\lambda v^2)G_{hh}(k) + gv G_{\phi h}(k; 0) &= -i \\ (k^2 + 2\lambda v^2)G_{h\phi}(k; y) + gv G_{\phi\phi}(k; 0, y) &= 0.\end{aligned}\tag{D.102}$$

By contrast, the unperturbed propagators in the absence of Higgs-bulk couplings satisfy

$$\begin{aligned}\sqrt{\mathcal{G}_2}(-k^2 + \square_2)D_k^\phi(y, y') &= i\delta^2(y - y') \\ (k^2 + 2\lambda v^2)D_k^h &= -i.\end{aligned}\tag{D.103}$$

¹A disadvantage of the delta-function formulation is the requirement to deal with expressions like $f(x)\delta(x)$, with $f(x) \rightarrow \infty$ as $x \rightarrow 0$. This requires a more careful treatment of regularization and renormalization, along the lines of the codimension-one formulation used in the main text, but in the present instance leads to the same conclusions.

We use the first of eqs. (D.103) to solve the second of eqs. (D.102), leading to

$$\begin{aligned} G_{\phi h}(k; y) &= -i \int d^2 y' D_k^\phi(y, y') \left[\lambda_2 G_{\phi h}(k; 0) + gv G_{hh}(k) \right] \delta^2(y') \\ &= -i D_k^\phi(y, 0) \left[\lambda_2 G_{\phi h}(k; 0) + gv G_{hh}(k) \right], \end{aligned} \quad (\text{D.104})$$

and this, when specialized to $y = 0$, in turn implies

$$G_{\phi h}(k; 0) = -i D_k^\phi(0, 0) \left[\lambda_2 G_{\phi h}(k; 0) + gv G_{hh}(k) \right], \quad (\text{D.105})$$

which may be solved to give

$$G_{\phi h}(k; 0) = -i \left[\frac{gv G_{hh}(k)}{1 + i\lambda_2 D_k^\phi(0, 0)} \right] D_k^\phi(0, 0). \quad (\text{D.106})$$

The overall factor of $D_k^\phi(0, 0)$ is removed when the external ϕ -line is amputated, and for the denominator we use the continuum result, eq. (6.41), to evaluate $D_k^\phi(0, 0)$,

$$D_k^\phi(0, 0) = \frac{i}{4\pi\alpha} \left[\log(-k^2 \epsilon^2) - i\pi \right], \quad (\text{D.107})$$

and renormalize the divergence into the brane couplings, \bar{g} and $\bar{\lambda}_2$, using eqs. (6.21). Eq. (D.98) then follows by choosing the renormalization point so that $k^2 \bar{r}^2 = 1$ and the logarithms vanish.

We can also use the second of eqs. (D.103) to solve the third of eqs. (D.102), giving

$$G_{hh}(k) + igv G_{\phi h}(k; 0) D_k^h = D_k^h \quad (\text{D.108})$$

To solve for $G_{hh}(k)$ we substitute eq. (D.106) into the above expression, which can

be rearranged to give eq. (D.99) as desired.

D.3 Toy model: unperturbed modes

In this appendix we explicitly take the continuum limit of (6.38) to arrive at eq. (6.40). This is accomplished in a toy model in which the extra dimensions are a flat disc: $f(r) = r$ for $0 \leq r \leq \pi R$. We can explicitly solve the wavefunctions on this background, which allows for a straightforward move to the large R limit, although the results are true for all R .

Using eq. (6.34) in eq. (6.33) on the disc geometry gives the field equation for the $n = 0$ wavefunctions

$$\left[M_{0l}^2 + \frac{1}{r} \partial_r (r \partial_r) \right] P_{0l} = 0, \quad (\text{D.109})$$

with the following boundary conditions

$$(r \partial_r P_{0l})_{r=0, \pi R} = 0, \quad (\text{D.110})$$

and normalization conditions

$$2\pi\alpha \int_0^{\pi R} dr r P_{0l}^* P_{0l'} = \delta_{ll'}. \quad (\text{D.111})$$

The properly normalized solutions and eigenvalue conditions read

$$P_{0l}(r) = \frac{1}{\sqrt{\pi^3 \alpha R^2}} \left(\frac{J_0(M_{0l} r)}{J_0(M_{0l} \pi R)} \right) \quad \text{with} \quad J_1(\pi R M_{0l}) = 0, \quad (\text{D.112})$$

where J_0 is the zeroth Bessel function of the first kind. The brane-to-brane propagator

is given by

$$D_k(\epsilon, 0) = \sum_l \left(\frac{-i}{k^2 + M_{0l}^2 - i\epsilon} \right) \frac{J_0(\epsilon M_{0l})}{J_0^2(\pi R M_{0l}) \pi^3 \alpha R^2}, \quad (\text{D.113})$$

since $J_0(0) = 1$. Using the fact that $J_0(x) \rightarrow \sqrt{\frac{2}{\pi x}}$ for large x gives

$$D_k(\epsilon, 0) = \sum_l \left(\frac{-i}{k^2 + M_{0l}^2 - i\epsilon} \right) \frac{J_0(\epsilon M_{0l}) M_{0l}}{2\pi \alpha R}. \quad (\text{D.114})$$

Sums over closely spaced modes in d dimensions can be replaced by integrals as follows

$$\frac{1}{\Omega^d} \sum_{\vec{n}} f_{\vec{n}} \rightarrow \int \frac{d^d M}{(2\pi)^d} f(M), \quad (\text{D.115})$$

where, in this case, the sum is over the radial index, so the conversion is one-dimensional. Using $\Omega^d = 2\pi R$ for the diameter of the disc is gives

$$D_k^\phi(\epsilon, 0) = \frac{-i}{2\pi \alpha} \int_0^\infty dq \frac{q J_0(\epsilon M)}{k^2 + q^2 - i\epsilon}. \quad (\text{D.116})$$

The integral can be computed

$$D_k^\phi(\epsilon, 0) = \frac{-i}{2\pi \alpha} K_0 \left(\sqrt{k^2} \epsilon \right), \quad (\text{D.117})$$

where K_0 is the zeroth modified bessel function. For small arguments $K_0(x) \rightarrow -\log(x/2) + \gamma$ so the divergent part of the brane-to-brane propagator reads

$$D_k^\phi(\epsilon, 0) = \frac{i}{4\pi \alpha} \log(k^2 \epsilon^2), \quad (\text{D.118})$$

in agreement with eq. (6.41).

D.4 Beyond Sturm Liouville

In this Appendix we describe how the Sturm-Liouville orthogonality conditions generalize to the case of interest in the main text, for which the boundary conditions differ for different modes.

For the present purposes the eigenvalue condition for the mode functions $\xi_n(x)$ has the general form

$$\partial_x [p(x)\partial_x \xi_n] - q(x)\xi_n + \lambda_n w(x)\xi_n = 0, \quad (\text{D.119})$$

in an interval $x_0 \leq x \leq x_1$, with p, q, w known real functions and λ_n the corresponding eigenvalue. The unusual part relative to Sturm-Liouville problems of childhood days is that they satisfy n -dependent boundary conditions at the edges of the domain of interest:

$$\left[J_b(\lambda_n - K_b)p \partial_x \xi_n + (\lambda_n - L_b)\xi_n \right]_{x=x_b} = 0, \quad (\text{D.120})$$

where J_b, K_b, L_b are again known coefficients. These boundary conditions ruin the orthonormality of the mode functions under the usual inner product,

$$\int_{x_0}^{x_1} dx w(x) \xi_m^* \xi_n \neq \delta_{mn}, \quad (\text{D.121})$$

which in turn ruins the diagonalization of the 4D action once decomposed in terms of these modes.

To identify how the inner product must generalize in order to maintain orthogonality with the new boundary conditions we follow standard steps. First multiply eq. (D.119) by ξ_m then subtract the complex conjugate of the same equation with

($m \leftrightarrow n$) and integrate the result over x . This yields

$$(\lambda_m - \lambda_n) \int_{x_0}^{x_1} dx w(x) \xi_m^* \xi_n = \left[p (\xi_m^* \partial_x \xi_n - \xi_n \partial_x \xi_m^*) \right]_{x_0}^{x_1}, \quad (\text{D.122})$$

which would vanish for the usual Sturm-Liouville boundary conditions. However, with the n -dependent boundary conditions of the form (D.120) we instead have

$$(\lambda_m - \lambda_n) \int_{x_0}^{x_1} dx w(x) \xi_m^* \xi_n = (\lambda_m - \lambda_n) \sum_b (-1)^{1-b} \left(\frac{L_b - K_b}{J_b} \right) \frac{\xi_m^*(x_b) \xi_n(x_b)}{(\lambda_n - K_b)(\lambda_m - K_b)} \neq 0. \quad (\text{D.123})$$

What allows us to devise an inner product with respect to which the modes are automatically orthogonal is the property that the n -dependence of the boundary conditions is linear in λ_n , since this ensures both sides of eq. (D.123) depend on n through their common factor of $(\lambda_m - \lambda_n)$. This suggests defining the following inner product

$$\langle \xi_m, \xi_n \rangle = \int_{x_0}^{x_1} dx w(x) \xi_m^* \xi_n + \sum_b (-1)^{1-b} \left(\frac{L_b - K_b}{J_b} \right) \frac{\xi_m^*(x_b) \xi_n(x_b)}{(\lambda_m - K_b)(\lambda_n - K_b)},$$

since eq. (D.123) then shows that the boundary conditions imply modes with different eigenvalues are automatically orthogonal, and so a basis of eigenmodes can be chosen to be orthonormal: $\langle \xi_m, \xi_n \rangle = \delta_{mn}$.

In the dimensional-reduction problem the constants J_b, K_b, L_b are read from the brane action, and so are the quantities that appear in the quadratic lagrangian once bulk fields are decomposed in terms of these mode functions. This ensures that the action diagonalizes as it would have done for a standard KK decomposition without

endpoints.

For example, for the zero modes in the brane bulk mixing scenario we send $x \rightarrow r$ and $n, m \rightarrow s, t$ and use $p(r) = 2\pi\alpha f(r)$, $q(r) = 0$ and $w(r) = 2\pi\alpha f(r)$. We replace the eigenvalues with the KK masses $\lambda_\ell = M_{0\ell}^2$. There is only one brane at $r_0 = 0$ and (neglecting subscripts) it gives $J = -1/\lambda_2$, $K = 2v^2\lambda$ and $L = 2v^2\lambda + (gv)^2/\lambda_2$ so that the inner product reads

$$\langle \mathcal{P}_s, \mathcal{P}_t \rangle = 2\pi\alpha \int_0^{\pi R} dr f \mathcal{P}_s^* \mathcal{P}_t + \frac{(gv)^2 \mathcal{P}_s^*(0) \mathcal{P}_t(0)}{(M_s^2 - 2\lambda v^2)(M_t^2 - 2\lambda v^2)}, \quad (\text{D.124})$$

and the orthonormality relationship (6.55) in the text follows.

Diagonalization of the quadratic action

We now show that in the case of interest in the main text, this modified inner product is just what is required to diagonalize the quadratic action, including the Higgs-bulk mixing terms. For simplicity, we only include the $n = 0$ modes, but the extension to any $n \neq 0$ level of the KK tower follows readily. We still use $s = \{n, \ell\}$ with the understanding that $n = 0$.

In terms of KK modes the the bulk action (6.27) reads

$$\begin{aligned} S_B = & -2\pi\alpha \int d^4x \int dr \sum_{s,t} (f \mathcal{P}_s^* \mathcal{P}_t) \left[\frac{1}{2} \partial_\mu \varphi_s \partial^\mu \varphi_t \right] \\ & -2\pi\alpha \int d^4x \int dr \sum_{s,t} (f \partial_r \mathcal{P}_s^* \partial_r \mathcal{P}_t) \left[\frac{1}{2} \varphi_s \varphi_t \right], \end{aligned} \quad (\text{D.125})$$

where terms have been organized into their r -dependent parts, which are in round brackets, and their x -dependent parts, which are in square brackets. They have also

been written on separate lines for organizational purposes. Integrating the second term by parts gives

$$\begin{aligned}
S_B &= -2\pi\alpha \int d^4x \int dr \sum_{s,t} (f\mathcal{P}_s^* \mathcal{P}_t) \left[\frac{1}{2} \partial_\mu \varphi_s \partial^\mu \varphi_t \right] \\
&\quad + 2\pi\alpha \int d^4x \int dr \sum_{s,t} (\mathcal{P}_t \partial_r f \partial_r \mathcal{P}_s^*) \left[\frac{1}{2} \varphi_s \varphi_t \right] \\
&\quad + 2\pi\alpha \int d^4x \sum_{s,t} (f\mathcal{P}_t \partial_r \mathcal{P}_s^*)_{r=0} \left[\frac{1}{2} \varphi_s \varphi_t \right], \tag{D.126}
\end{aligned}$$

where the term on the bottom line is a boundary term, and it is assumed that the other boundary term for the faraway brane vanishes by the boundary conditions, or is cancelled by the faraway brane's action. The bulk equation of motion (6.50) allows the second line to be combined with the first as follows

$$\begin{aligned}
S_B &= -2\pi\alpha \int d^4x \int dr \sum_{s,t} (f\mathcal{P}_s^* \mathcal{P}_t) \left[\frac{1}{2} \partial_\mu \varphi_s \partial^\mu \varphi_t + \frac{1}{2} M_s^2 \varphi_s \varphi_t \right] \\
&\quad + 2\pi\alpha \int d^4x \sum_{s,t} (f\mathcal{P}_t \partial_r \mathcal{P}_s^*)_{r=0} \left[\frac{1}{2} \varphi_s \varphi_t \right]. \tag{D.127}
\end{aligned}$$

The integration over the radial coordinate can be completed using the orthonormality relationship (6.55) so that the bulk action contributes three terms to the dimensionally reduced Lagrangian that will be called $\mathcal{L}_{1,2,3}$

$$\begin{aligned}
\mathcal{L}_1 &= - \sum_s \left[\frac{1}{2} \partial_\mu \varphi_s \partial^\mu \varphi_s + \frac{1}{2} M_s^2 \varphi_s^2 \right] \\
\mathcal{L}_2 &= \sum_{s,t} \frac{(gv)^2 \mathcal{P}_s(0) \mathcal{P}_t(0)}{(M_s^2 - 2\lambda v^2)(M_t^2 - 2\lambda v^2)} \left[\frac{1}{2} \partial_\mu \varphi_s \partial^\mu \varphi_t + \frac{1}{2} M_s^2 \varphi_s \varphi_t \right] \\
\mathcal{L}_3 &= 2\pi\alpha \sum_{s,t} (f\mathcal{P}_t \partial_r \mathcal{P}_s^*)_{r=0} \left[\frac{1}{2} \varphi_s \varphi_t \right]. \tag{D.128}
\end{aligned}$$

The first line is a canonically normalized KK tower of scalar fields with masses M_s , which is the desired final result. The second and third term are cancelled by terms in the brane action as will be shown explicitly. For example, writing the h kinetic and mass term in terms of eigenstates φ_s and then combining them with \mathcal{L}_2 gives

$$\mathcal{L}_2 + \mathcal{L}_h = \mathcal{L}_2 - \frac{1}{2} \partial_\mu h \partial^\mu h - \lambda v^2 h^2 = \sum_{s,t} \frac{(gv)^2 \mathcal{P}_s(0) \mathcal{P}_t(0)}{(M_t^2 - 2\lambda v^2)} \left[\frac{1}{2} \varphi_s \varphi_t \right], \quad (\text{D.129})$$

while \mathcal{L}_3 and the brane mass term for ϕ give

$$\mathcal{L}_3 + \mathcal{L}_\phi = \mathcal{L}_3 - \frac{1}{2} \lambda_2 \phi^2(0) = \sum_{s,t} \mathcal{P}_t(0) (2\pi \alpha f \partial_r \mathcal{P}_s(0) - \lambda_2 \mathcal{P}_s(0)) \left[\frac{1}{2} \varphi_s \varphi_t \right], \quad (\text{D.130})$$

which is identical to (D.129) once the boundary condition (6.54) is employed. Finally the mixing term gives

$$\mathcal{L}_{h\phi} = -gvh\phi(0) = -2 \sum_{s,t} \frac{(gv)^2 \mathcal{P}_s(0) \mathcal{P}_t(0)}{(M_t^2 - 2\lambda v^2)} \left[\frac{1}{2} \varphi_s \varphi_t \right], \quad (\text{D.131})$$

so that $\mathcal{L}_2 + \mathcal{L}_3 + \mathcal{L}_\phi + \mathcal{L}_h + \mathcal{L}_{h\phi} = 0$ and the dimensionally reduced theory is the KK tower of massive scalar fields found in \mathcal{L}_1 .

D.5 Solving for the KK mode functions

In this appendix we solve the $n = 0$ perturbed wavefunctions $\mathcal{P}_{0\ell}$ for $f(r) = r$, and $0 < r < \pi R$ with Dirichlet boundary conditions at $r = \pi R$. In this geometry the general solution can be written in terms of Bessel functions

$$\mathcal{P}_{0\ell}(r) = N_\ell \left[\frac{\pi}{2} Y_0(rM_{0\ell}) + D_\ell J_0(rM_{0\ell}) \right], \quad (\text{D.132})$$

where N_ℓ are normalization constants, D_ℓ are integration constants and the factor of $\pi/2$ is chosen for convenience. It is straightforward to impose Dirichlet BCs at $r = \pi R$, which imply

$$D_\ell = -\frac{\pi Y_0(\pi R M_{0\ell})}{2 J_0(\pi R M_{0\ell})}. \quad (\text{D.133})$$

Imposing the UV boundary condition, on the other hand, is more complicated. This is because of the UV divergences we expect in this theory. Near the origin, the relevant Bessel functions behave like

$$\begin{aligned} Y_0(x) &\approx \frac{2}{\pi} [\ln(x/2) + \gamma] \\ Y_1(x) &\approx -\frac{2}{\pi} \frac{1}{x} \\ J_0(0) &= 1 \\ J_1(0) &= 0. \end{aligned} \quad (\text{D.134})$$

So, as in the vacuum solutions, the boundary condition near the brane diverges, and must be regulated and renormalized. We cut off the boundary condition at $r = \epsilon$ and find

$$D_\ell = \frac{2\pi\alpha}{\beta_\ell} - \log(\epsilon M_{0\ell}/2) - \gamma \quad \text{with} \quad \beta_\ell = \lambda_2 + \frac{(gv)^2}{M_{0\ell}^2 - 2v^2\lambda}. \quad (\text{D.135})$$

We can rewrite this boundary condition in terms of the renormalized quantities of (6.21), rendering it finite and cutoff-independent

$$D_\ell = \frac{2\pi\alpha}{\bar{\beta}_\ell(\bar{r})} - \log(\bar{r} M_{0\ell}/2) - \gamma \quad \text{with} \quad \bar{\beta}_\ell(\bar{r}) = \bar{\lambda}_2(\bar{r}) + \frac{\bar{g}^2(\bar{r})v^2}{M_{0\ell}^2 - 2v^2\bar{\lambda}(\bar{r})}. \quad (\text{D.136})$$

Equating the two expressions for D_i yields an eigenvalue equation for the M_ℓ^2 masses

$$-\frac{\pi Y_0(\pi R M_{0\ell})}{2 J_0(\pi R M_{0\ell})} = \frac{2\pi\alpha}{\beta_\ell(\bar{r})} - \log(\bar{r} M_{0\ell}/2) - \gamma, \quad (\text{D.137})$$

which is, unfortunately, quite difficult to solve.

The normalization condition for the perturbed wavefunctions reads

$$2\pi\alpha \int_{\epsilon}^{\pi R} r dr \mathcal{P}_{0\ell}^2(r) + \frac{(gv)^2 \mathcal{P}_{0\ell}^2(0)}{(M_{0\ell}^2 - 2v^2\lambda)^2} = 1. \quad (\text{D.138})$$

We break this calculation into parts. First, we calculate the integral

$$\int_{\epsilon}^{\pi R} r dr \mathcal{P}_{0\ell}^2(r) = N_\ell^2 \int_{\epsilon}^{\pi R} r dr \left[\frac{\pi}{2} Y_0(r M_{0\ell}) + D_\ell J_0(r M_{0\ell}) \right]^2 := N_\ell^2 I_\ell. \quad (\text{D.139})$$

Using the identity

$$\frac{d}{dx} \left[\frac{1}{2} x^2 (Z_0^2(x) + Z_1^2(x)) \right] = x Z_0^2(x), \quad (\text{D.140})$$

for any function Z_0 that satisfies Bessel's equation, we can write

$$\begin{aligned} I_\ell &= \frac{1}{M_{0\ell}^2} \left[\frac{1}{2} x^2 \left(\frac{\pi}{2} Y_0(x) + D_\ell J_0(x) \right)^2 + \frac{1}{2} x^2 \left(\frac{\pi}{2} Y_1(x) + D_i J_1(x) \right)^2 \right]_{\epsilon M_{0\ell}}^{\pi R M_{0\ell}} \\ &= \frac{1}{2} \pi^2 R^2 \left[\left(\frac{\pi}{2} Y_0(\pi R M_{0\ell}) + D_i J_0(\pi R M_{0\ell}) \right)^2 + \left(\frac{\pi}{2} Y_1(\pi R M_{0\ell}) + D_i J_1(\pi R M_{0\ell}) \right)^2 \right] - \frac{1}{2 M_{0\ell}^2}, \end{aligned}$$

where the second term follows from taking the $\epsilon \rightarrow 0$ limit. Using the boundary

condition (D.133) gives

$$I_\ell = \frac{1}{2} \frac{\pi^2 R^2}{J_0^2(\pi R M_{0\ell})} \left(\frac{\pi}{2} Y_1(\pi R M_{0\ell}) J_0(\pi R M_{0\ell}) - \frac{\pi}{2} Y_0(\pi R M_{0\ell}) J_1(\pi R M_{0\ell}) \right)^2 - \frac{1}{2M_{0\ell}^2}. \quad (\text{D.141})$$

Bessel functions obey the following identity

$$\frac{\pi}{2} Y_1(\pi R M_i) J_0(\pi R M_i) - \frac{\pi}{2} Y_0(\pi R M_i) J_1(\pi R M_i) = -\frac{1}{\pi R M_i}, \quad (\text{D.142})$$

so that

$$I_\ell = \frac{1}{2M_{0\ell}^2} \left(\frac{1}{J_0^2(\pi R M_{0\ell})} - 1 \right). \quad (\text{D.143})$$

Now we move to the second term in (D.138), which is equal to \mathcal{B}_ℓ^2 . Using the $r = 0$ boundary condition allows us to write

$$\mathcal{B}_\ell = \frac{gv\mathcal{P}_{0\ell}(0)}{M_{0\ell}^2 - 2v^2\lambda} = \frac{2\pi\alpha gv [r\partial_r\mathcal{P}_{0\ell}]_{r=0}}{(M_{0\ell}^2 - 2v^2\lambda)\lambda_2 + (gv)^2} = \frac{2\pi\alpha gv N_\ell}{(M_{0\ell}^2 - 2v^2\lambda)\lambda_2 + (gv)^2}, \quad (\text{D.144})$$

which can be inserted into (D.138) to give the following equation

$$N_\ell^{-2} = 2\pi\alpha \left[\frac{1}{2M_{0\ell}^2} \left(\frac{1}{J_0^2(\pi R M_{0\ell})} - 1 \right) + \frac{2\pi\alpha (gv)^2}{[\lambda_2 (M_{0\ell}^2 - 2v^2\lambda) + (gv)^2]^2} \right]. \quad (\text{D.145})$$

From the above normalization we find the mixing coefficients

$$\mathcal{B}_\ell^{-2} = 1 + \frac{1}{2M_{0\ell}^2} \left(\frac{1}{J_0^2(\pi R M_{0\ell})} - 1 \right) \frac{[\lambda_2 (M_{0\ell}^2 - 2v^2\lambda) + (gv)^2]^2}{2\pi\alpha (gv)^2}. \quad (\text{D.146})$$

Note that the mixing coefficients vanish as $g \rightarrow 0$ or $\lambda_2 \rightarrow \infty$ unless $M_i^2 = 2v^2\lambda$.